Molecular Mechanisms Driving the Initiation of an Inflammatory Response in Human Lamina Propria Cells – Impact of mTOR Pathway Activation

Dissertation

To Fulfill the
Requirements for the Degree of
"doctor rerum naturalium" (Dr. rer. nat.)

Submitted to the Council of the Faculty
of Biology and Pharmacy
of the Friedrich Schiller University Jena

by Dipl. - Biol. Judith Gras

born on 14.12.1986 **in** Lahnstein

Reviewer

(1) Prof. Dr. Axel A. Brakhage, Jena

(2) Prof. Dr. Peter F. Zipfel, Jena

(3) Prof. Dr. Britta Siegmund, Berlin

Date of Disputation: 09.09.2016

Summary

Inflammatory bowel diseases (IBD) comprise a group of disorders that involve acute and relapsing stages of intestinal inflammation. The pathogenesis of IBD is associated with a mucosal barrier defect and the infiltration of pro-inflammatory immune cells into the lamina propria (LP). Under homeostatic conditions, intestinal resident LP cells have been shown to be hyporesponsive towards bacterial antigens. Currently, little is known about the molecular mechanisms that initially lead to the onset of an inflammatory response in these cells. This thesis aimed towards a better understanding of these initial mechanisms by utilizing a human *ex vivo* intestinal organ culture model, the so-called loss of epithelial layer (LEL) model.

In this model, normal human colonic mucosa is subjected to EDTA treatment, thereby detaching the epithelial layer from the underlying LP. The thus created barrier defect is associated with the induction of a global inflammatory response in resident LP cells, as could be shown by global gene expression profile analysis and subsequent quantitative gene expression analysis of approx. 590 immune-system related genes in LP cells isolated by laser-capture microdissection. Furthermore, a significant overlap to a published gene expression profile of total mucosa biopsies of ulcerative colitis (UC) patients demonstrated the physiological relevance of the inflammatory response initiated in the LEL model. Additionally, the expression of several genes induced in the LEL model are linked to single-nucleotide polymorphism loci enriched in IBD patients. In order to identify pathways, biological functions and potential upstream regulators associated with the observed inflammatory response, a bioinformatic analysis via Ingenuity Pathway Analysis (IPA) of the global gene expression profiles was performed. An enrichment of growth factors and translation specific kinases among upstream regulators predicted by IPA, suggested the induction of protein synthesis in LP cells at the onset on inflammation.

Supporting these *in silico* findings, a rapid upregulation of protein translation in LP cells after the onset of inflammation was detected *in situ* by utilizing Ortho-propargyl-

puromycin (OPP) Click-It technology®. Remarkably and in contrast to nonstimulated peripheral blood mononuclear cells, no detectable protein synthesis levels were observed in the mucosa under homeostatic conditions.

The upregulation of protein synthesis in LP cells at the onset of inflammation was subsequently shown to be associated with the activation of the mammalian target of rapamycin (mTOR) pathway as indicated by an increase in Ser235/236 phosphorylation levels of the mTOR downstream target ribosomal protein S6 (RPS6) in OPP^+ LP cells including macrophages. This finding could be further validated by inhibition experiments employing the mTOR inhibitor Torin1, which led to a significant decrease of $RPS6^{Ser235/236}$ phosphorylation in these macrophages *in situ* as well as in emigrated myeloid cells and a marked decrease in protein synthesis *in situ*.

Finally, secretion of the chemokines CCL2, CCL19, CCL22 and CXCL1 by LP cells was decreased in the presence of Torin1 as measured by Luminex® multiplex analysis of LEL organ culture supernatants. These results suggest a participation of the mTOR pathway in the recruitment of leukocytes to the intestinal mucosa during the initial phase of intestinal inflammation. Furthermore, the concomitant inhibition of IL-18 as well as the increase of MIF and M-CSF secretion by Torin1 support the notion that mTOR is involved in - and potentially coordinates - multiple aspects of the initial inflammatory response of LP cells such as the induction of inflammasome activation (IL-18), the differentiation of macrophages (M-CSF), and the restriction of MIF-induced pro-inflammatory processes.

In summary, the results in this thesis led to the following conclusions: The LEL model was shown to represent a physiological relevant tool to study molecular mechanisms driving the initial onset of an intestinal inflammatory response in resident LP cells. The onset of the observed global inflammatory response after LEL was shown to be regulated by the mTOR pathway, which modulated the secretion of inflammatory mediators. The findings of this thesis therefore suggest the mTOR pathway as a potential target in IBD therapy.

Zusammenfassung

Chronisch-entzündliche Darmerkrankungen (CED) zeichnen sich durch rezidivierende und kontinuierliche Entzündungen des Darmes aus. Die Pathogenese dieser Erkrankungen wird mit einem Barrieredefekt der intestinalen Mukosa und der Infiltration von pro-inflammatorischen Immunzellen in die Lamina Propria (LP) assoziiert. Residente LP Zellen hingegen besitzen unter homöostatischen Bedingungen einen anergen Phänotyp und zeichnen sich durch ihre Hyporesponsivität gegenüber bakteriellen Antigenen und Nahrungsantigenen aus. Die molekularen Mechanismen, die an der initialen inflammatorischen Antwort in diesen Zellen beteiligt sind, sind derzeit noch weitgehend unbekannt und wurden daher in der vorliegenden Arbeit mittels eines humanen, intestinalen Organkultur-Modells untersucht.

In diesem sogenannten 'loss of epithelial layer (LEL)'-Modell wird gesunde humane Mukosa des Kolons *ex vivo* mit EDTA behandelt. Dies führt zu der Ablösung der Epithelzellschicht von der darunterliegenden LP. Der so ausgelöste Barrieredefekt geht mit der Induktion einer globalen inflammatorischen Antwort daher, wie globale sowie quantitative Genexpressionsanalysen von laser-mikrodissezierter LP zeigen konnten. Die physiologische Relevanz dieser Antwort wurde nachfolgend anhand der signifikanten Übereinstimmung mit einem publizierten Genexpressionsprofil von Mukosa-Biopsien von Colitis Ulcerosa (CU) Patienten bestätigt. Außerdem war im LEL-Model die Expression mehrerer Gene hochreguliert, welche mit CED assoziierten Einzelnukleotid-Polymorphismus Loci verknüpft sind.
Mit dem Ziel, Signaltransduktionswege, biologische Funktionen sowie potentielle übergeordnete Regulatoren zu detektieren, welche für die initiale inflammatorische Antwort von Bedeutung sind, wurde anschließend eine bioinformatische Analyse der globalen Genexpressionsprofile durch die Software 'Ingenuity Pathway Analysis' duchgeführt. Eine Anreicherung von Wachstumsfaktoren und Translations-spezifischen Kinasen, innerhalb der Gruppe der bioinformatisch vorhergesagten übergeordneten Regulatoren, wies nachfolgend auf die Induktion der Proteinsynthese in LP Zellen zu Beginn der

inflammatorischen Antwort hin.

Diese *in silico* vorhergesagte Induktion der Proteinsynthese zu Beginn der inflammatorischen Antwort konnte anschließend mittels Ortho-Propargyl-Puromycin (OPP) Click-It® Technologie in u.a. $CD68^+$ Makrophagen der LP *in situ* nachgewiesen werden. Unter homöostatischen Bedingungen war in der Mukosa - im Gegensatz zu ruhenden Leukozyten des peripheren Blutes - unter den angewandten experimentellen Bedingungen keine Proteinsynthese nachweisbar.

Die Induktion der Proteinsynthese war assoziiert mit der Aktivierung des mTOR (mammalian target of rapamycin) Signalweges, wie durch die Induktion der Ser235/236 Phosphorylierung des mTOR Zielproteins ribosomales protein S6 (RPS6) in u.a. $CD68^+$ Makrophagen zu Beginn der inflammatorischen Antwort mittels Immunfluoreszenzanalyse gezeigt werden konnte. Inhibitionsexperimente mit dem mTOR Inhibitor Torin1 bestätigten die Kontrolle der $RPS6^{Ser235/236}$ Phosphorylierung durch den mTOR Signalweg. Darüber hinaus konnte nachgewiesen werden, dass die beobachtete Hochregulation der Proteinsynthese in LP Zellen, wie z.B. Makrophagen, in großen Anteilen durch mTOR vermittelt wird.

Die vielseitige funktionelle Bedeutung der mTOR Aktivierung für die Induktion der inflammatorischen Antwort konnte anhand von Überständen des LEL-Modells in Luminex® Multiplex Analysen gezeigt werden. So wies die erniedrigte Sekretion der Chemokine CCL2, CCL19, CCL22 und CXCL1 in Gegenwart von Torin1 einerseits auf die Bedeutung des mTOR Signalweges für die Kontrolle der Rekrutierung peripherer Leukozyten zur intestinalen Mukosa hin. Andererseits konnte durch die gleichzeitige Torin1 vermittelte Inhibition der Sekretion von IL-18 sowie der Steigerung der MIF- als auch M-CSF-Sekretion gezeigt werden, dass mTOR außerdem in die Induktion der Inflammasom-Aktivierung (IL-18), die Differenzierung von Makrophagen (M-CSF) sowie die Restriktion von MIF-induzierten pro-inflammatorischen Prozessen involviert ist.

Die Resultate dieser Arbeit führen zu folgenden Schlussfolgerungen: Das LEL Modell ist ein adäquates und physiologisch relevantes Modell, um molekulare Mechanismen zu untersuchen, die der initialen inflammatorischen Antwort in residenten LP Zellen zu-

grunde liegen. Der mTOR Signalweg ist an dieser initialen inflammatorischen Antwort durch die Kontrolle der Sekretion von inflammatorischen Mediatoren durch LP Zellen beteiligt. Die Erkenntnisse dieser Arbeit legen daher den mTOR Signalweg als potentiellen Ansatzpunkt in der zukünftigen Therapie von CED nahe.

Abbreviations

4E-BP1	Eukaryotic initiation factor 4E (eIF-4E) binding protein-1
ABX	Antibiotics
adj.P.Val	Adjusted P Value
AF	Alexa Fluor
AMPK	5' adenosine monophosphate-activated protein kinase
bp	base pair
CCL	Chemokine (C-C motif) ligand
CD	Crohn's disease
CD[n]	Cluster of differentiation i.e. 14
CED	Chronisch-Entzündliche Darmerkrankungen
CU	Colitis Ulcerosa
DC	Dendritic cells
DNA	Deoxyribonucleic acid
DSS	Dextran sodium sulphate
DTT	1,4-dithiothreitol
ECM	Extracellular matrix
EDTA	Ethylenediaminetetraacetic acid
eIF	Eukaryotic translation initiation factor
EtOH	Ethanol
FACS	Fluorescence activated cell sorting
FCS	Fetal calf serum
FFPE	Formalin fixed paraffin embedded
FMO	Fluorescence minus one
FSC	Forward scatter
GWAS	Genome-wide association study
HBSS	Hanks' Balanced Salt Solution
IBD	Inflammatory bowel disease
IFN	Interferon
Ig	Immunglobulin
IKBKB	Inhibitor of nuclear factor-κ B kinase-β)
IL	Interleukin
IPA	Ingenuity Pathway Analysis
LEL	Loss of epithelial layer
LEL-M	Loss of epithelial layer - mucosa
LMD	Laser-capture microdissection
logFC	Log 2 fold change
LP	Lamina propria
LPMC	Lamina propria mononuclear cells

LPS	Lipopolysaccharide
M-CSF	Macrophage - colony stimulating factor
MFI	Mean fluorescence intensity
MIF	Macrophage migration inhibitory factor
MME	Metalloelastase
MMP	Matrix metalloproteinase
mRNA	messenger ribonucleic acid
mTOR	Mammalian target of rapamycin
mTORC	mTOR complex
NC	Normal colon
Obs.	Observation
OPP	Ortho-propargyl-puromycin
PAMP	Pathogen-associated molecular pattern
PBMC	Peripheral blood mononuclear cells
PBS	Phosphate-buffered saline
PCR	Polymerase chain reaction
PI3K	Phosphatidylinositol-4,5-bisphosphate 3-kinase
PRR	Pattern recognition receptor
R	Replicate
Raptor	Regulatory associated protein of MTOR
Rictor	Rapamycin-insensitive companion of MTOR
RIN	RNA integrity number
ROI	Region of interest
RPMI	Roswell Park Memorial Institute
RPS6	Ribosomal protein S6
S6K	Ribosomal protein S6 kinase
SA-Cy3	Streptavidin - cyanine 3
SNP	Single-nucleotide polymorphism
SSC	Sideward scatter
TBS	Tris-buffered saline
TGF	Transforming growth factor
TH	Threshold
TLR	Toll like receptor
TM	Total mucosa
TNF	Tumor necrosis factor
TNBS	2,4,6-Trinitrobenzenesulfonic acid
TOP	Terminal oligopyrimidine
UC	Ulcerative colitis
VEGF	Vascular endothelial growth factor
WG-DASL	Whole-Genome cDNA-mediated Annealing, Selection, extension, and Ligation

List of Figures

List of Tables

Table of contents

1. Introduction

1.1. The immune system of the human intestine

The intestine represents the largest compartment of the immune system and contains higher numbers of immune cells than any other tissue. It is also the human organ that harbours the largest number of bacteria: With a number as high as 10^{13}-10^{14}, the intestine contains more bacteria than the total cell number of the human body, with an increasing bacterial diversity and number from small to large intestine [Xu and Gordon, 2003; Sekirov *et al.*, 2010]. In spite of the close proximity of both immune cells and commensal bacteria as well as dietary antigens, the intestine normally remains in a homeostatic state. Even more so, reduced numbers and/or diversity of microbiota are associated with a variety of diseases ranging from psychiatric conditions to metabolic disease, allergy and autoimmunity [Belkaid and Hand, 2014]. Although the mechanisms that ensure the maintenance of the homeostatic state are still not completely understood, one main factor is thought to be the mucosal barrier between bacteria of the lumen and immune cells in the mucosa. A disrupted barrier has been associated with the manifestation of chronic inflammatory bowel disease (IBD) [Turner, 2009].

1.1.1. The intestinal mucosa

In order to explain the mechanisms that are currently thought to ensure and maintain intestinal homeostasis, first, a short overview will be given over the structure and the functions of the intestine and the intestinal mucosa. The human gut is divided into the small and large intestine, the former being further regionally differentiated as duodenum (closest to stomach), jejunum and ileum, while the large intestine consists of

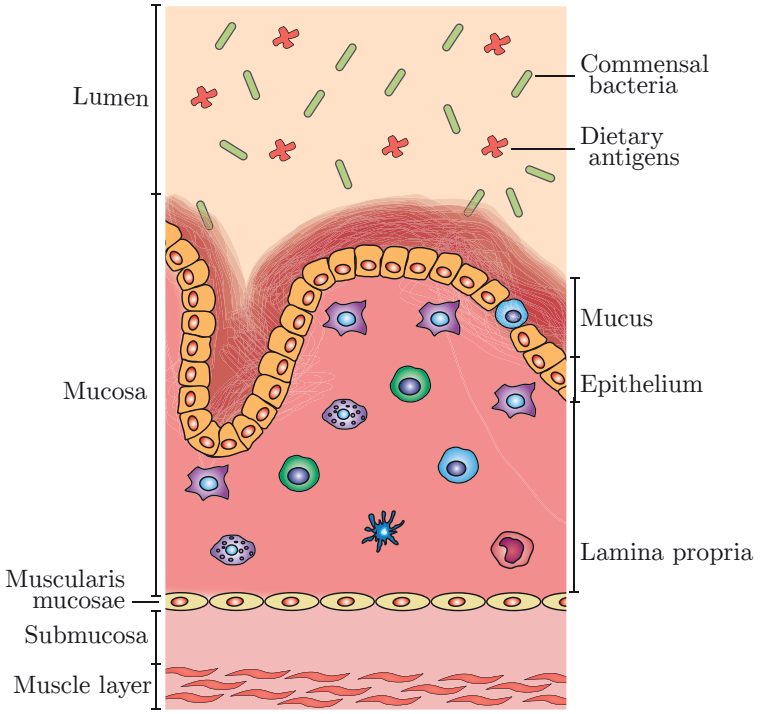

Figure 1.1.: *The mucosa of the large intestine.* The lamina propria hosts a variety of immune cells including dendritic cells (DC), macrophages, T cells, B cells and eosinophils. Figure was created based on Mowat and Agace [2014].

caecum (closest to ileum), ascending, transverse and descending colon and finally rectum. Whereas the main function of the small intestine is the disintegration and absorption of nutrients, the large intestine mediates water absorption and processing of nondigestable material.

Most immunological processes occur in the mucosa, the multi-levelled layer of the gastrointestinal tract which borders the gut lumen. The luminal side of the small and large intestine of the mucosa is covered with an unicellular epithelial layer, which is adjacent to the lamina propria (LP), loose-connected tissue that hosts most immune cells. Beneath the LP is the muscularis mucosae (a thin muscle layer), which is located next to the submucosa and the muscle layer (Mowat and Agace [2014]; for a schematic figure of the mucosa of the large intestine, see Figure 1.1).

The unicellular epithelial layer at the luminal side of the small intestinal mucosa forms finger-like projections with LP in their core. These so-called 'villi' extend into the lumen and increase the surface area of digestively active epithelium. In addition, epithelial invaginations that extend into the mucosa are defined as 'crypts' [Peterson and Artis,

2014]. Stem cells at the base of these crypts enable the constant renewal of the intestine: the turnover of the human duodenum is thought to take 1.50 (±2.90, N=3) days, whereas it takes 4.12 (±1.32, N=53) days in the human colorectal region [Darwich *et al.*, 2014].

The majority of epithelial cells of the small intestine are enterocytes, however, additionally, also Paneth cells (which secrete antimicrobial peptides into the lumen), goblet cells and neuroendocrine cells are present. In the large intestine, the unicellular epithelium layer only contains crypts but no villi and therefore is relatively flat. Furthermore, Paneth cells are absent; however, the large intestine does contain more goblet cells than the small intestine [Peterson and Artis, 2014].

The mucosal barrier

Goblet cells constitutively secrete highly glycosylated mucins (e.g. MUC2) into the lumen, together forming a thick layer called 'mucus'. Whereas the mucus of the murine small intestine only has one layer, the mucus of both murine and human large intestine consists of two distinct layers [Gustafsson *et al.*, 2012]. Studies performed in the murine system demonstrated that the outer layer is inhabited by a distinctive microbial population of commensal bacteria, whereas the inner layer is nearly sterile [Li *et al.*, 2015]. Additionally, the outer layer contains soluble IgA, which is constantly secreted by LP plasma cells. The mucus thus represents the first important barrier between luminal bacteria and LP immune cells [Johansson *et al.*, 2013]. In accordance, MUC2-deficient mice are known to spontaneously develop colitis [Van der Sluis *et al.*, 2006].

The most efficient mucosal barrier however is provided by the epithelial cell membrane, which is impenetrable to most hydrophilic solutes in the absence of specific transporters. In conformity, epithelial layer damage induced by toxins as secreted by the pathogenic bacterium *Clostridium difficile* [Riegler *et al.*, 1995] is associated with a pronounced barrier loss. With an intact epithelial cell layer, however, the paracellular pathway between epithelial cells is controlled by tight and adherens junctions [Diamond, 1977; Turner, 2009]. The selective permeability of tight junctions is known to be regulated by cy-

tokines, such as tumor necrosis factor (TNF)-α and interferon (IFN)-γ and dysregulated expression of these cytokines is linked to diseases associated with barrier dysfunction such as IBD [Baert *et al.*, 1999].
Beneath the mucosal barrier provided by mucus and the epithelial layer, the LP hosts a variety of immune cells which will be described in detail in the following section.

1.2. Immune cells in the lamina propria during homeostasis

Resident LP cells include immune cells such as dendritic cells, macrophages, T cells, B cells, eosinophils, mast cells and stromal cells such as fibroblasts [Mowat and Agace, 2014]. Intestinal immune cells in contrast to their relatives of the peripheral blood are generally understood to have a decreased activation ability, a characteristic that is thought to aid in the maintenance of intestinal homeostasis.

1.2.1. Lymphocytes

Lymphocytes constitute one of the largest populations of immune cells in the intestinal mucosa. They consist of T cells, B cells, and innate lymphoid cells. Like all other intestinal immune cells, lymphocytes are confined to the mucosa under homeostatic conditions. A notable exception is a population of $CD8^+$ intraepithelial lymphocytes, which are located at the basement membrane between enterocytes.

Findings of our group and others could show that the ability of T lymphocytes to mount an adaptive immune response is seriously compromised under homeostatic conditions. Activation of T cells through the T cell receptor (TCR) are strongly inhibited by several local mechanisms, keeping the LP T cells in a hyporesponsive state [Sido *et al.*, 2008, 2000; Qiao *et al.*, 1991, 1993; Pirzer *et al.*, 1990; De Maria *et al.*, 1993]. At the same time, LP T cells sensitively respond to CD2 ligation, an antigen-independent pathway of T cell activation [Meuer *et al.*, 1984; Hunig *et al.*, 1987; Braunstein *et al.*, 2008], or CD28 co-stimulation, producing significantly higher amounts of cytokines than

peripheral blood lymphocytes [Liu *et al.*, 2001; Boirivant *et al.*, 1996]. This specialised differentiation state of LP T cells likely contributes to the maintenance of intestinal homeostasis by preventing a chronic inflammatory response to the large number of antigens present in close proximity in the gut lumen.

Unlike most healthy tissues, the normal LP contains large numbers of IgA producing plasma cells. A small fraction of plasma cells produce IgM. Through the constant secretion of IgA into the gut lumen, plasma cells contribute to the mucosal barrier by protecting the epithelium from pathogens [Brandtzaeg and Johansen, 2005].

1.2.2. Myeloid cells

There are several different cell types of non-lymphoid immune cells localized in the intestinal LP such as DCs, macrophages, eosinophils and mast cells. One focus of this study is the characterization of an inflammatory response in macrophages. This population will therefore be described in detail in this section.

Macrophages

In mice, the large intestine contains one of the largest pools of mononuclear phagocytes in the body with macrophages representing one of the most abundant fraction of leukocytes in the healthy intestinal LP [Lee *et al.*, 1985; Mowat and Agace, 2014]. Human intestinal tissue resident macrophages are - in contrast to murine macrophages - not able to proliferate and their life span is currently unknown [Smythies *et al.*, 2006; Jenkins *et al.*, 2011]. In mice, Bain *et al.* [2014] could show, that macrophages are constantly replenished by circulating monocytes every three to four days.

Interestingly, in both humans and mice, their abundance seems to correlate with the increase of the bacterial load in the lumen from proximal to distal gastrointestinal tract and thus, macrophages are found to be most prominent represented in the colon [Nagashima *et al.*, 1996; Denning *et al.*, 2011; Sekirov *et al.*, 2010]. Especially in the human colon, $CD68^+$ macrophages have been shown to be localized directly beneath

the epithelial surface and thereby are in very close proximity to the massive load of bacterial antigens in the lumen [Mahida *et al.*, 1989].

Under homeostatic conditions, intestinal macrophages have been shown to be hyporesponsive towards pathogen-associated molecular pattern (PAMP) stimulation, which is thought to be achieved by their relatively low expression of pattern recognition receptors, Fc and complement receptors compared to the expression in peripheral blood mononuclear cells (PBMC). Among other potential factors, this anergic phenotype is thought to evolve by TGF-β mediated downregulation of nuclear factor (NF)-κ B proteins in bone-marrow derived, pro-inflammatory macrophages previously recruited from the periphery via locally produced IL-8 and TGF-β [Smythies *et al.*, 2010, 2005; Qiao *et al.*, 1996; Hausmann *et al.*, 2002]. This hyporesponsive phenotype is generally thought to contribute to the maintenance of homeostasis.

1.3. Intestinal inflammation

As described in the last sections, in the past many studies have established mechanisms such as the mucosal barrier and the hyporesponsive phenotype of LP immune cells as key factors in the maintenance of intestinal homeostasis despite the close proximity of immune cells and microbiota as well as dietary antigens in the gut. In contrast, little is known about the ability of the intestine to mount an immediate inflammatory response i.e. after pathogenic infection as well as the factors that - under certain conditions - lead to the perseverance of inflammation and culminate in the manifestation of chronic inflammatory bowel diseases (IBD).

Acute intestinal inflammation is most often caused by infection with enteric pathogens and can lead to clinical symptoms such as bloody diarrhoea, abdominal pain and fever. Most of these enteric infections are 'self-limited' and require little or no medical attention, although they can be fatal in some cases. Morphologically, the mucosa of these patients often shows an acute or mixed inflammatory immune cell infiltration into the LP. At their onset, acute and chronic inflammation histologically share many

common features. However, in contrast to patients with later-stage IBD, the mucosa of patients with acute self-limiting colitis normally shows an intact crypt architecture, although the surface epithelium is often damaged [Lamps, 2015].

Chronic inflammatory bowel diseases (IBD) comprise two clinical phenotypes: Ulcerative colitis (UC) and Crohn's Disease (CD). These two diseases have a pattern of chronic relapsing and remitting intestinal inflammation, whose pathogenesis has been shown to be closely associated with a mucosal barrier defect and infiltration of LP immune cells [Pastorelli *et al.*, 2013]. Whereas UC is normally limited to the colon and rectum with inflammatory infiltrates being confined to the mucosa, the manifestation of CD can occur in the whole gastrointestinal tract, although ileum and colon are most frequently involved. Additionally, inflammation in CD can extend throughout the intestinal wall. Clinically, both UC and CD patients among other symptoms suffer from severe diarrhoea, bloody stools, ulcers as well as fibrosis, the latter being more prominent but not exclusively present in CD patients [Hendrickson *et al.*, 2002; Gordon *et al.*, 2014]. In accordance with the resembling disease presentation of both phenotypes, a global gene expression analysis showed that gene expression patterns in chronic inflamed mucosa compared to healthy mucosa are remarkably similar between CD and UC [Granlund *et al.*, 2013].
Although knowledge regarding the pathogenesis of IBD is limited, an aberrant reaction of the intestinal immune system to luminal antigens and barrier dysfunctions have been implicated. Moreover, a statistical enrichment of single-nucleotide polymorphisms (SNPs) in patients has been associated with IBD. Many of the detected loci were associated with both disease types. Interestingly, risk alleles at two CD loci, PTPN22 and NOD2, show protective effects in UC and may reflect some of the biological differences between both diseases [Jostins *et al.*, 2012].
Given the little insight into the etiology of IBD, treatment for IBD patients is mostly symptomatic. It includes lifestyle alterations, medical management and surgical interventions. In addition to the administration of broad anti-inflammatory medication, an antibody against TNF-α is able to restore the epithelial barrier in IBD with highest efficiency in CD patients. However, after an initial success in treating the symptoms of IBD, some patients develop anti-drug antibodies and require increasing doses or the

switch to a different TNF-α antibody [Scott and Lichtenstein, 2016].
As of today, IBDs are incurable diseases. To develop more suitable treatment options, investigations to enhance our understanding of the origins of intestinal inflammation is essential.

1.3.1. Models to study intestinal inflammation

Currently, more than 70 distinct genetically engineered mouse models exist in which intestinal inflammation develops spontaneously [Mizoguchi *et al.*, 2016]. Additionally, several murine models employ chemical agents to induce experimental colitis. The most widely used model employing a chemical agent is probably the dextran sodium sulphate (DSS) - induced colitis model. Here, the uptake of 3-10 % DSS via the drinking water leads to extensive epithelial damage in the colon within six to ten days. The developed symptoms imitate to some extent the symptoms of UC, including diarrhoea, rectal bleeding and weight loss [Okayasu *et al.*, 1990]. Another chemically induced colitis model, the TNBS model, mimics some of the symptoms of CD. In this model, intrarectal administration of 2,4,6-trinitrobenzene sulfonic acid (TNBS), a substance which renders self-proteins immunogenic to the immune system by haptenation, causes a massive mucosal inflammation involving a dense infiltration of T cells and macrophages throughout the entire wall of the large intestine. This is accompanied by progressive weight loss, bloody diarrhea, rectal prolapse and large bowel wall thickening [Neurath *et al.*, 2000]. TNBS-induced colitis is also used to study fibrosis [Loeuillard *et al.*, 2014].
In addition to the murine models described above, several groups have successfully established "humanized mice" by establishing a human microbiome in germ-free mice [Rongvaux *et al.*, 2014].

In comparison to the huge availability of murine models, intestinal models of the human system are scarce. Most human studies focus on the analysis of chronic stages of intestinal inflammation comparing biological processes as occurring in normal mucosa with those occurring at relapsed or remitting stages of IBD. Tissue of acute /self-limiting intestinal inflammation is usually not available, as neither endoscopy nor surgery is re-

quired as part of the diagnostic procedure or treatment follow-up, respectively.
The study of acute intestinal inflammation is mainly performed *in vitro* employing epithelial cell lines or *ex vivo* by the isolation of intestinal LP cells through the removal of the epithelial layer via treatment with the Ca^{2+}-chelator ethylenediaminetetraacetic acid (EDTA) and subsequent enzymatic digestion of mucosal tissue [Rogler *et al.*, 1998]. Rarely, organ cultures are employed for the study of intestinal inflammatory responses. Mahida *et al.* [1997] developed a model to study the migratory behaviour of intestinal immune cells after epithelial barrier defects. In this model, mucosa resectates were denuded of the epithelium by treatment with EDTA in order to mimic epithelial damage occurring *in vivo*. After culture of the remaining mucosa, lymphocytes, macrophages and eosinophils migrated out of the LP via tunnels of the extracellular matrix.

1.3.2. Macrophages in intestinal inflammation

Given the focus of this thesis, the knowledge regarding intestinal macrophages in intestinal inflammation, based on murine and human models, will be summarized in this section.
Despite the hyporesponsive, $CD14^{low}$ phenotype, that intestinal macrophages display under homeostatic conditions, they have been implicated to play an important role in intestinal inflammation: For one, CD patients show a strong mucosal infiltration of $CD14^{hi}$ macrophages [Autschbach *et al.*, 2002]. Moreover, intestinal macrophages in patients with acute inflammation (acute appendicitis and acute diverticulitis) as well as IBD patients have been shown to express increased levels of TREM-1. This increased TREM-1 expression by macrophages in IBD patients has been further linked to an enhanced secretion of pro-inflammatory cytokines such as TNF, IL-6, IL-8, IL-1β as well as the chemokine CCL2, thus further demonstrating the impact of these cells on intestinal inflammation [Schenk *et al.*, 2007].

In mice as well as humans, it has been proposed, that during intestinal inflammation, PBMC are recruited to the intestinal inflammatory site [Bain *et al.*, 2014; Thiesen *et al.*, 2014]. However, whether (and if so, how) previously anergic tissue resident macrophages

are able to differentiate into the observed proinflammatory phenotype in inflammation or if the inflammatory response is entirely mediated by fully responsive recruited PBMC is still unclear.

In addition to their proinflammatory role, intestinal macrophages have also been implicated in anti-inflammatory processes such as tissue remodelling and wound healing [Kühl *et al.*, 2015]. Expression of MMP2, which takes part in the breakdown of the extracellular matrix (ECM), has been shown to be expressed in tissue resident macrophages and is increased in the mucosa of fibrotic CD patients [Kirkegaard *et al.*, 2004; Bailey *et al.*, 2012]. Moreover, mannose receptor CD206 expressing wound-healing macrophages are increased in the injured mucosa of UC patients [Martinez *et al.*, 2013; Cosin-Roger *et al.*, 2013].

In accordance with the differential role of macrophages in intestinal inflammation, it should be noted, that in contrast to the earlier M1/M2 dogma of macrophages, which distinguished them into an either distinct pro- (M1) or anti-inflammatory (M2) type, recent work showed that macrophages display a great extent of plasticity and their phenotype can vary greatly dependent on stimuli and milieu [Xue *et al.*, 2014].

1.4. Protein synthesis in inflammation

A coordinated and dynamic regulation of gene and protein expression levels is essential for the induction and resolution of a healthy inflammatory response. For instance, the activation of PRRs in response to microbial infection triggers signalling cascades and consequent activation of certain transcription factors, culminating in the differential regulation of hundreds of genes involved in antimicrobial defense, phagocytosis, cell migration, tissue repair and the regulation of adaptive immunity [Carpenter *et al.*, 2014]. Defects in these control mechanisms may result in a failure to resolve the inflammatory response and thus contribute to the development and progression into chronic inflammatory diseases [Mazumder *et al.*, 2010].

The following section first gives an overview of the knowledge regarding regulation of protein synthesis in inflammation in general, before explicitly focusing on regulation of protein synthesis in the intestine in subsection 1.4.2.

Regulation of gene expression at the level of translation offers several benefits over transcriptional control: Post-transcriptional regulation can be rapidly activated based on existing mRNAs without the need of prior transcription. Additionally, it can be quickly reversed by e.g. phosphorylation events that lead to the activation or deactivation of specific regulatory factors. There are several post-transcriptional regulation pathways regulating gene expression in innate immunity such as mRNA splicing, mRNA polyadenylation, mRNA stability and protein translation - all of which have been shown to be implicated in regulating the strength and duration of inflammatory processes. Upon bacterial challenge *in vitro*, almost one fifth of genes that are expressed in dendritic cells undergo alternative splicing, some of them known to participate in antimicrobial defense [Rodrigues *et al.*, 2013]. Furthermore, when human monocytes are stimulated with the toll like receptor 4 (TLR4) ligand lipopolysaccharide (LPS) and IFN-γ, the polyadenylation machinery favours proximal poly(A) site use in terminal exons that contain two or more poly(A) sites. This leads to a global shortening of key regulatory elements such as microRNA target sites and stability mediating AU-rich elements [Sandberg *et al.*, 2008].

Eukaryotic protein translation is generally cap-dependent and involves the following steps: Initiation, elongation, termination and ribosomal degradation. The rate-limiting step of translation is the initiation step and thus makes it a sensitive and efficient anchor point for regulation. In accordance, most known regulatory mechanisms control the initiation step, in which the small ribosome subunit is recruited to the 5' end of mRNA, causing the assembly of the complete ribosome that subsequently begins polypeptide synthesis. The recruitment of the small ribosome subunit depends on the assembly of the eukaryotic translation initiation factor 4F (eIF4F) complex at the 5' cap structure of mRNA. This complex consists of the three initiation factors eIF4F, eIF4G and eIF4A. To achieve eIF4F complex assembly, eIF4E binds to the 5' cap of mRNA and then recruits eIF4G and eIF4A. The inhibitory 4E-binding protein 1 (4E-BP1) controls eIF4F complex assembly by inhibiting the binding of eIF4G to eIF4E. Phosphorylation of 4E-BP1 leads to its dissociation from eIF4E, thus allowing the recruitment of eIF4G and

eIF4A [Pestova *et al.*, 2001]. The phosphorylation of 4E-BP1 is known to be regulated by the mTOR pathway.

1.4.1. The mTOR pathway

The mammalian target of rapamycin (mTOR) pathway is known to upregulate anabolic processes such as protein and lipid synthesis while inhibiting autophagy. It thus represents a key regulator of cell size and proliferation. Its dysregulation has been implicated in the pathogenesis of several diseases including diabetes, fibrosis and cancer [Ma and Blenis, 2009; Laplante and Sabatini, 2012].

Several findings implicate a role of mTOR in innate immunity: TLR ligands have been shown to activate mTOR in human monocytes, macrophages and DCs. After LPS stimulation, murine macrophages and DCs massively increase protein synthesis, a process that is largely dependent on the PI3K-mTORC1 pathway [Lelouard *et al.*, 2007; Ivanov and Roy, 2013].

mTOR is an atypical serine/threonine protein kinase and a member of the phosphoinositide 3-kinase (PI3K)-related kinase family. Together with several proteins mTOR forms two distinct complexes, known as mTORC1 (see Figure 1.2) and mTORC2. mTORC1 contains mTOR, raptor (regulatory associated protein of mTOR) as well as LST8 (lethal with SEC13 protein 8) and has been shown to directly regulate translation in mammals via its two main downstream targets 4E-BP1 and the 40S ribosomal protein S6 kinases (S6Ks) [Jacinto and Hall, 2003].

mTORC1 exhibits phosphotransferase activity that is activated by the GTP-bound form of the small G protein RHEB (Ras homologue enriched in brain) after translocation of mTOR to the lysosome in response to amino acids. Activated mTOR can also be found in the cytoplasm, nucleus and mitochondrium, although the functional significance of these localisations are still under investigation [Betz and Hall, 2013]. RHEB itself is negatively regulated by a tumor suppressor heterodimer of tuberous sclerosis 1 (TSC1) and 2 (TSC2), which converts RHEB into its inactive GDP-bound form.

mTORC1 was shown to be regulated by several pathways as the PI3K-AKT, Ras-ERK (extracellular signal-regulated kinase) and Wnt signaling pathway by the inibition of the

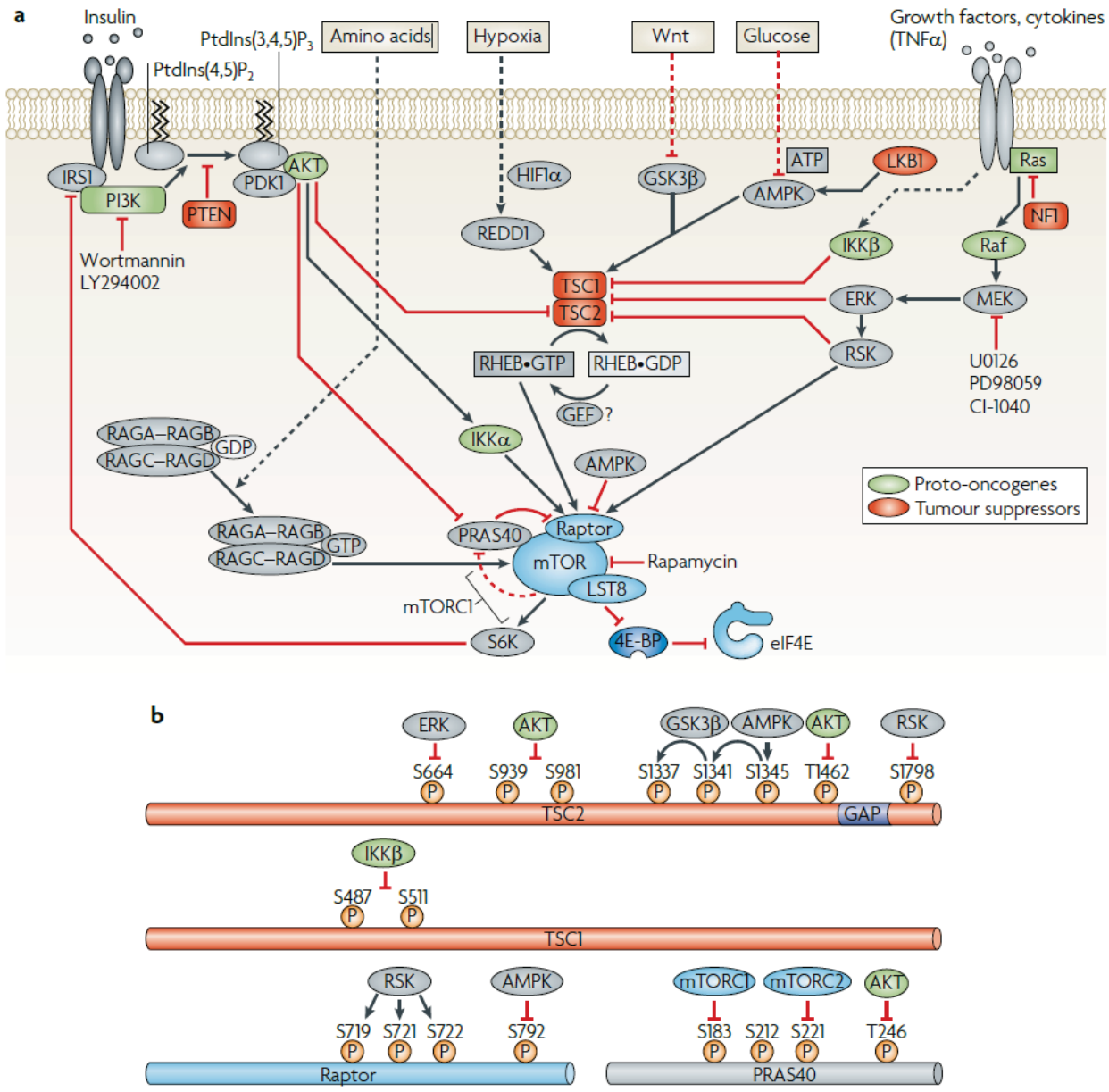

Figure 1.2.: *mTORC1 signaling.* GEF, guanine nucleotide-exchange factor; HIF1α, hypoxia-inducible factor 1α; IRS1, insulin receptor substrate 1; NF1, neurofibromin 1; PDK1, phosphoinositide-dependent kinase 1; PtdIns, phosphatidylinositol; PTEN, phosphatase and tensin homologue; REDD1, protein regulated in development and DNA damage response 1 (also known as DDIT4) [Ma and Blenis, 2009]

TSC1-TSC2 complex [Shaw and Cantley, 2006; Inoki *et al.*, 2006].
Additionally, several factors are known to influence mTORC1 activity: Among others, amino acids, glucose, insulin and growth factors are known to activate mTORC1. Furthermore, mTORC1 can also be stimulated by cytokines such as TNF-α. It has been recently shown, that the inhibitor of NF-κB kinase-β(IKKβ), a main downstream kinase in the TNF-α signaling pathway, can activate mTORC1 via TSC1 inhibition by phosphorylation [Lee *et al.*, 2007].
In contrast, hypoxia is known to negatively regulate mTORC1 activity. Moreover, mTORC1 is suggested to sense an inadequate supply of cellular energy and suppress the energy-consuming protein synthesis under starvation conditions. Recent studies have proposed the AMP-activated protein kinase (AMPK) as one of the 'energy sensors' for mTORC1 that leads to mTOR deactivation under conditions that increase intracellular levels of AMP to limit ATP-consuming functions of the cell [Hahn-Windgassen *et al.*, 2005; Gwinn *et al.*, 2008] .

The mTORC2 complex contains mTOR, LST8, rictor (rapamycin independent companion of mTOR) and SIN1 (stress-activated protein kinase-interacting protein 1). Similar to mTORC1, it can be activated by growth factors and PI3K/Akt signaling. Functionally, mTORC2 is involved in cytoskeletal organization and - through the activation of the kinases SGK1 and Akt - in the regulation of cell survival and proliferation [Ma and Blenis, 2009].

Apart from its well described impact on the regulation of eIF4F assembly, mTOR on the one hand is known to stimulate the translation of 'eIF4E-sensitive' mRNA through mechanisms that yet remain elusive. On the other hand, mTOR controls the expression of so-called TOP mRNAs. These mRNAs have a terminal oligopyrimidine (TOP) tract at their 5' end and are very sensitive towards mTOR inhibitors [Nandagopal and Roux, 2015].
There are several inhibitors available for studying downstream effector functions of mTOR. mTOR was originally named after its sensivity towards the antifungal compound rapamycin that led to its original detection. Rapamycin (synonym: sirolimus)

shows anti-proliferative and immunosuppressive characteristics [Chang *et al.*, 1991] and is clinically i.e. utilized as base therapy in the prophylaxis of acute renal transplant rejection [Groth *et al.*, 1999]. Additionally, sirolimus-coated stents efficiently prevent restenosis [Sousa *et al.*, 2001, 2005].
On the molecular level, rapamycin is only able to inhibit mTORC1, whereas mTORC2 is insensitive to treatment with this drug (at least under short-term treatment). Additionally, recent findings have demonstrated that rapamycin is not able to fully inhibit mTORC1 [Feldman *et al.*, 2009]. In contrast, another mTOR inhibitor, Torin1, which was used in this study, is able to inhibit both mTORC1 and mTORC2 activity [Thoreen *et al.*, 2012, 2009].

1.4.2. Protein synthesis in the intestine

As mentioned before, the intestinal immune cells of the LP are known to be hyporesponsive towards PAMPs under homeostatic conditions, thus the upregulation of protein synthesis to bacterial stimuli under physiological conditions as described above seems unlikely.
Currently, little is known about the regulation of protein synthesis in the human intestine, regardless whether concerning the protein synthesis ratio compared to other organs or changes occurring between homeostatic and inflamed mucosa. This lack of knowledge is likely due to methodological difficulties in measuring protein synthesis tissue specifically. In rats, McNurlan *et al.* [1979] predicted the amount of protein synthesized in the small intestine, utilizing a flooding technique involving a bolus of L-[1-13C]leucine. He observed that the intestine makes up 14 % and the liver 12 % of total protein synthesis of the whole body and found that protein synthesis rates of the small intestine was reduced 30 % after two days of starvation. Heys *et al.* [1992] were able to show via leucine uptake, that daily protein synthesis rates in colorectal mucosa from IBD patients (with five patients diagnosed with UC and one with CD) were raised 2.6 fold in comparison to normal mucosa (N=10). In comparison, the levels in malignant colorectal cancer were raised 2.3 fold and 3.9 fold in benign tumors of the rectum. Remarkably, protein synthesis in the liver of IBD patients was raised 1.7 fold compared to benign diseases such as

chronic cholecystitis or benign colonic tumors. Importantly, so far, no data is available regarding the compartment-specific protein synthesis in the human colonic LP, neither under homeostatic nor under inflammatory conditions.

1.5. Aim of thesis

Inflammatory bowel diseases (IBD) define a group of chronic inflammatory diseases of the intestinal tract that affect five million people worldwide. They are associated with a mucosal barrier defect and the dysregulated, chronic activation of resident lamina propria (LP) immune cells, that under homeostatic conditions have a high tolerance towards bacterial and dietary antigens. However, little is known about the molecular mechanisms underlying the onset of the initial acute inflammatory response in LP cells. A better understanding of these initial processes will help to determine the factors that eventually lead to a chronic manifestation of the inflammation.

To study early intestinal inflammation, I employed the 'loss of epithelial layer' (LEL) model, a human organ culture model, in which an EDTA-mediated barrier defect in colonic mucosa is associated with the activation of resident LP cells.

In this thesis, I sought to understand the molecular mechanisms underlying the initiation of acute intestinal inflammation in resident LP cells by the following concept:

(1) Characterization of the inflammatory response of LP cells as induced in the LEL model by conducting global gene expression analysis and subsequent validation of the physiological relevance of the inflammatory response.

(2) Identification of biological processes involved in the initiation of an inflammatory response in LP cells by performing bioinformatic analysis of the obtained global gene expression profiles.

(3) Evaluation of global translation levels in LP cells in the LEL model *in situ*.

(4) Investigation of the mTOR pathway with regard to its role in the observed induction of protein synthesis.

(5) Examination of the contribution of the mTOR pathway to the induction of inflammatory effector molecules in LP cells.

2. Material and Methods

2.1. Tissue samples

Patient material was obtained in collaboration with the departments of surgery at the University Hospital Heidelberg, the hospital Salem in Heidelberg as well as the St. Vincentius Hospital in Speyer. Gut specimen were derived from patients undergoing resection due to localized colon cancer. Colonic mucosa, localized near the resection margin and declared as healthy by a pathologist, was dissected from the surgical specimen and immediately subjected to the experimental procedures. Exclusion criteria for this study were the presence of multiple metastasis, diabetes, IBD, diverticulitis/diverticulosis or previous chemo- or radiotherapy treatment. Biopsies were obtained from patients undergoing routine colonoscopy. All human studies were approved by the ethics committee of the University of Heidelberg (ethical votes S-024/2003 and S-390/2015) and performed in accordance with the principles laid down in the Declaration of Helsinki. Written informed consent was obtained from the patients. Patients taking part in this study had an average age of 72 $\pm$ 8.11 years.

2.2. The LEL model

The dissected mucosa (see section 2.1) was washed for 1.5 h using RPMI/ABX medium at 4°C under constant shaking with changes of medium every 20 min at 4°C (for composition of all used solutions in this section, see Table 2.1). Mucosa was then washed once in ice-cold HBSS/ABX for 10 min. Mucus was removed via treatment with 1 mM 1,4-dithiothreitol (DTT, Roche AG, Karlsruhe) dissolved in HBSS/ABX for 15 min followed by washing the explant with HBSS/ABX twice for 5 min each. The epithelial

Component	Company	Conc.	Volume	Solution 1	2	3
RPMI 1640 Medium	Life Technologies, Paisley, UK	-	500 ml	x		x
HBSS w/o Ca^{2+}, Mg^{+}	Life Technologies	-	500 ml		x	
Penicillin / Streptomycin	Life Technologies	10000 IE/ml	5 ml	x	x	x
Fungizone	Life Technologies	250 μg/ml	5 ml	x	x	x
Ciprobay	Bayer Pharma AG, Berlin, DE	2 mg/ml	2,5 ml	x	x	x
Gentamicin	Life Technologies	50 mg/ml	500 μl	x	x	x
Cotrim	Ratiopharm GmbH, Ulm, DE	96 mg/ml	500 μl	x	x	x
Fetal Calf Serum (FCS)	Pan Biotech GmbH, Aidenbach, DE	100%	50 ml			x
L-Glutamine	Life Technologies	200 mM	5 ml			x

Table 2.1.: *Composition of media and salt solutions in the LEL model.* Solution 1 is stated as RPMI/ABX, solution 2 as HBSS/ABX and solution 3 as RPMI/ABX + 10 % FCS in the text.

layer was subsequently removed by treating the explant three times with 0.7 mM EDTA (Merck KGaA, Darmstadt, pH 7.3 - 7.35, dissolved in HBSS/ABX) for 30 min each with intermittent 10 min HBSS/ABX washing steps at 37°C under constant shaking. After washing for four times 10 min each with HBSS/ABX, the tissue was transfered to medium consisting of RPMI/ABX + 10 % FCS for 12 h over night at 37°C. For an image depicting the main steps of the LEL model, see Figure 3.1 on page 36.

At specific time points, size standardized tissue punches were collected from mucosa as described in Table 2.2.

2.2.1. Inhibitors

For experiments with inhibitors, the LEL model was performed using small jars. After 20 min of washing, standardized 0.8 cm punches were made and distributed into jars (max four punches were put into one jar) containing 7 ml of the appropriate solution (same

ID	DTT	EDTA	Add. treatment before collection	t collection
TM 0 h	-	-	-	0 h
TM 2 h	x	-	10 min HBSS/ABX	2 h
LEL - M 3 h	x	1 x	10 min HBSS/ABX	3 h
LEL - M 4 h	x	2 x	10 min HBSS/ABX	4 h
LEL - M 5 h	x	3 x	2 x 10 min HBSS/ABX	5 h
TM 5 h	-	-	RPMI/ABX + 10% FCS (37°C)	5 h
LEL - M 17 h	x	3 x	RPMI/ABX + 10% FCS (37°C)	17 h
TM 17 h	-	-	RPMI/ABX + 10% FCS (37°C)	17 h

Table 2.2.: *Samples collected at different time points during the LEL model.* At indicated time point of collection, samples were either flash frozen in liquid nitrogen and stored at -80°C, transferred to 4% formalin or subjected to additional treatment (see subsection 2.2.2). TM: Total mucosa; LEL-M: Loss of epithelial layer - mucosa.

as described in the standard protocol) with or without addition of specified inhibitors. Torin1 (Merck KGaA, Darmstadt) was employed at a concentration of 250 nM or 1 μM. Cycloheximide (Merck KGaA) was used at concentrations 10 μg/ml or 100 μg/ml. Inhibitors were present at all times during performance of the LEL model.

2.2.2. Detection of protein synthesis *in situ* via Click-It® technology

A way to study protein synthesis *in situ* is the so called Click-It® technology (Life Technologies), where the alkyne analog of puromycin, Ortho-Propargyl-Puromycin (OPP) is rapidly incorporated into newly synthesized proteins by binding covalently to nascent polypeptide chains, a reaction which can subsequently be detected by a copper(1)-catalyzed azide-alkyne cycloaddition [Liu *et al.*, 2012]. The technology has so far only been used in animal models and in this thesis was established for the human system by utilizing the LEL model.

Briefly, at specified time points (see Table 2.2), tissue samples were incubated with 20 μM OPP in RPMI/ABX medium + 10% FCS at 37°C for 30 min (or RPMI/ABX medium + 10% FCS w/o OPP as a control). Tissue samples were then rinsed briefly in HBSS/ABX and transferred immediately to 4 % PBS-buffered methanol-free formalin for subsequent preparation of formalin fixed-paraffin embedded (FFPE) samples and sectioning (see

section 2.6). For subsequent slide preparation followed by immunofluorescent detection of OPP incorporation, see subsection 2.7.2.

2.3. Sample collection for gene expression analysis

2.3.1. Laser-capture microdissection

A powerful method to isolate specific areas from heterogeneous tissue, such as the intestinal mucosa, is laser-capture microdissection (LMD) of tissue sections transferred to 1.0 PEN (D) MembraneSlides (Carl Zeiss, Oberkochen, Germany). After specifying the desired area on the section using a microscope linked to a computer, a connected laser melts the membrane of the selected area and with a single laser impulse catapults it into a collection tube for subsequent lysis and RNA isolation. Using this approach, the lamina propria was isolated from the mucosa at four time points throughout the LEL model: TM 0 h, TM 5 h, LEL-M 5 h and LEL-M 17 h (see Table 2.2).
For global gene expression analysis, following preparation of 12 μm cryosections at -25°C, sections were directly covered with DTT (1 mg/ml) and incubated in solution for 5 min. Slides were then transfered to a cuvette containing 100 % EtOH (-25°C).
Immediately before LMD using a PALM MicroBeam LMD (Carl Zeiss), sections were counterstained at 4°C by successively immersing slides in cuvettes containing Cresyl Violet acetate (Sigma-Aldrich, Munich, Germany; 0.1 % in EtOH, 15 s), 100 % EtOH (10 s, two changes) and xylene (10 s). Slides were then incubated in another change of xylene for 5 min. Finally, slides were allowed to air-dry for 5 min.
LMD was performed for 1 h using the 10 x magnification of the microscope. For subsequent lysis, 50 μl of RLT buffer from the Qiagen RNeasy Kit including DTT (20 mM in 1 ml) and glycogen (1.14 %) were added to the tube containing the LMD sample and then vortexed vigorously for 30 s followed by a 5 min incubation step and repeated vortexing. The lysates were then stored in -80°C until RNA isolation.
Samples prepared for nCounter experiments were obtained similarly as described above, however, 8 μm cryosections were made in order to better detect underlying epithelial cells and prevent epithelial contamination observed in the WG-DASL Assay. Slides were

immersed in 4°C acetone instead of xylene to allow protein isolation (data not shown in thesis).

2.3.2. RNA isolation

RNA Isolation of LMD samples was performed using the RNeasy Kit (Qiagen N.V., Venlo, NL) following the manufacturer's instructions for microdissected cryosections with minor changes.

Briefly, LMD samples in RLT buffer were placed in a 37°C heatblock until thawed. RNA was precipitated by adding 1 Vol 70 % EtOH to the LMD sample. The precipitated RNA of the thoroughly resuspended sample was then bound to the membrane of a RNeasy MinElute Spin column by centrifugation for 15 s at 8,000 g at room temperature (if not stated otherwise, these configurations were used for all further steps). Samples with a total volume exceeding column capacity (700 μl) were pooled by repeating precipitation and binding steps reusing the same RNeasy MinElute Spin Column. Flowthrough was discarded after each step in the protocol until elution. After a washing step with 350 μl RW1 buffer, residual DNA was removed by a DNase treatment (10 μl DNase + 70 μl RDD buffer), which was terminated after 15 min by adding 350 μl RW1 buffer and a consequent centrifugation step. Chaotropic salts were removed by the addition of 500 μl RPE buffer. After centrifugation, 500 μl 80% EtOH were added to the column and centrifuged for 2 min at 8,000 g. The column was then allowed to air-dry by centrifuging with an open lid for 5 min at 16,000 g. RNA was finally eluted from the RNeasy MinElute Spin column by adding 12 μl of RNase-free water directly to the center of the spin column membrane. After centrifugation for 1 min at 16,000 g, the elute was again added to the membrane to increase the RNA harvest and eluted again by centrifuging for 4 min at 16,000 g. The RNA eluate was stored at -80°C after taking a separate aliquot for evaluation of RNA integrity.

2.3.3. RIN evaluation

RNA quality was analyzed via a 2100 bioanalyzer (Agilent Technologies Inc., Santa Clara, USA) using the RNA integrity number (RIN) software tool as indicator for the

intactness of the RNA. A RIN of 10 equals totally intact and a RIN of 0 totally degraded RNA [Schroeder *et al.*, 2006]. To qualify for downstream experiments, the RIN had to be at least 3. For a representative example of electropherograms of bioanalyzer analysis from samples obtained at different time points during the course of one experiment, please see page A-4 in the appendix.

2.4. Gene expression analysis

2.4.1. WG-DASL Assay

Global gene expression analysis of samples microdissected at the timepoints TM 0 h, LEL-M 5 h and LEL-M 17 h during the LEL model was performed using the Whole-Genome cDNA-mediated Annealing, Selection, extension, and Ligation (WG-DASL) Assay (Illumina, San Diego, CA, USA). In this assay, after conversion of total RNA to cDNA using biotinylated oligo (dT) and random nonamer primers, the biotinylated cDNA is annealed to the DASL Assay Pool probe groups. The probe sets consist of an upstream and a downstream oligo, each containing a gene-specific sequence and a universal PCR primer sequence at its 5' or 3' end, respectively. After the hybridization of the upstream oligo to the targeted cDNA site, it extends and ligates to its corresponding downstream oligo to create a PCR template which can be amplified with universal PCR primers. For the final analysis of gene expression, the resulting PCR products are hybridized to the HumanHT-12 v4 Expression BeadChip [April *et al.*, 2009]. The probe groups of the WG-DASL Assay only span 50 base pairs (bp), which makes this assay compatible with partially degraded RNA. For further details to the assay, please see Table 2.3. Sample RNA concentrations were adjusted to the sample with the lowest RNA amount according to bioanalyzer evaluation. The analysis was performed by the Genomics and Proteomics Core Facility of the German Cancer Research Center (DKFZ), Heidelberg, Germany.

2.4.2. nCounter Assay

The nCounter Assay from Nanostring was chosen as method of choice for validation of the WG-DASL Assay using the prebuilt Immunology Panel which consists of 594 genes, as it was the most appropriate available panel based on the focus of this thesis. In this assay, the RNA target molecule is directly hybridized with a reporter probe that carries a universal fluorescent barcode and a capture probe that contains a biotin moiety which immobilizes the hybridized complex on a cartridge for subsequent data collection [Reis *et al.*, 2011; Veldman-Jones *et al.*, 2015]. As the WG-DASL Assay, this method is compatible with partially degraded RNA because of the short probe span of 50 bp. However, in contrast to the WG-DASL Assay, the nCounter analysis requires no cDNA synthesis or preamplification, thus providing quantitiative information of transcript levels. For more details on the nCounter Assay and a direct comparison to the WG-DASL Assay, see Table 2.3.

Samples collected at the time points TM 0 h, TM 5 h, LEL-M 5 h and LEL-M 17 h were adjusted to the sample with the lowest RNA amount according to bioanalyzer evaluation before submission to the assay. The analysis was performed by the nCounter Core Facility of the Institute of Human Genetics in Heidelberg, Germany.

	WG-DASL (Illumina)	nCounter (Nanostring)
Analyzed genes	$\sim$ 29.000	594 (Immunology Panel)
Compatibility with degraded RNA	yes	yes
Probe length	50 bp	50 bp
Minimum RNA input	200 ng	100 ng
cDNA synthesis	yes	**no**
Preamplification	yes	**no**
Hybridization	on Chip	solution-based
Fold Change Sensitivity	1.5-2	1.67

Table 2.3.: *Comparison of the WG-DASL (Illumina) and nCounter (Nanostring) Assay.* [April *et al.*, 2009; Reis *et al.*, 2011]

2.5. Bioinformatic analysis on gene expression data

The normalization, calculation of differentially expressed genes and heatmap generation of the WG-DASL Assay data was performed by Maria Dinkelacker of the Bioinformatic Division of the DKFZ. She continued to support the author in all other bioinformatic analyses described in this section (which were performed by the author). If not stated otherwise, all bioinformatic analyses were performed in **R** version 3.2.3 [R Core Team, 2015]. For base operations and plots, the packages dplyr v0.4.3 [Wickham and Francois, 2015], ggplot2 v2.0.0 [Wickham, 2009] and data.table v1.9.6 [Dowle *et al.*, 2015] were used.

2.5.1. Normalization WG-DASL Assay

Rawdata was preprocessed with genome studio V2011.1 from Illumina and then read into **R**. Subsequent analysis of data was performed using the following packages: Biobase v2.30.0 [Huber *et al.*, 2015], limma v3.26.5 [Ritchie *et al.*, 2015], lumi v2.18.0 [Du *et al.*, 2008] with database lumiHumanAll.db$_1$.22.0. Annotation of data was performed using nuID1 from the limma package. After background correction (using the method 'normexp'), a quantile normalization was performed and values were log2 transformed. Boxplots before and after normalization can be found on page A-5 in the appendix.

2.5.2. Normalization nCounter Assay

nCounter Assay normalization was performed using the package NanoStringNorm 1.1.21 [Waggott *et al.*, 2012]. As in total, two cartridges from two different lots were run, a Lot-to-Lot calibration was performed during normalization of raw data according to the recommendation of the Nanostring tech support team (see Table 2.4). The resulting normalized counts were log2 transformed. Besides static plots that were part of the NanoStringNorm package (data not shown), boxplots of expression values indicated the legitimation of this approach (see page A-7 in the appendix).

	Normalization via	SOP	Accounts for	Option 'NanoStringNorm' package
1.	Positive controls	y	Technical variation	geo.mean
2.	Calibration of cartridges	n	Lot-to-Lot variation	-
3.	Negative controls	y	Background noise	mean.2sd
4.	Housekeeping genes	y	RNA input variation	housekeeping.geo.mean

Table 2.4.: *Worfklow normalization nCounter via 'NanoStringNorm' package [Waggott* et al.*, 2012].* Raw data of both cartridges was used as initial input and normalized together. Calibration was performed by first calculating the gene-wise geometric mean of the 1^{st} cartridge (geomean1) and 2^{nd} cartridge (geomean2). The calibration factor was defined as geomean1/geomean2 and multiplied with each positive control normalized gene count of the 2^{nd} cartridge. Housekeeping genes *ABCF1*, *ALAS1*, *G6PD*, *RPL19*, *TBP* were selected based on lowest % CV and a low, medium or high gene expression as recommended. Options chosen within the package were the default options/methods as recommended by Nanostring and package developers [Waggott *et al.*, 2012]. SOP: Standard operation procedure for normalization of nCounter Assays; y: yes; n: no

2.5.3. Heatmaps

Heatmaps for expression data of both WG-DASL and nCounter Assay were generated using the package Heatplus v2.16.0 [Ploner, 2012] after performing z-score transformation. Samples were sorted by highest variance and clustering calculated using Eucledian distance metrics. For the WG-DASL Assay, only the 1000 genes with the highest variance were plotted.

2.5.4. Analysis of differential gene expression and inter-assay comparisons

For both WG-DASL and nCounter assays, differential expression was calculated by the test implemented in the limma package and P values adjusted for multiple testing by the method of Benjamini and Hochberg [1995]. Differential expressed genes for observations LEL-M 5 h vs. TM 0 h (Obs.1), LEL-M 17 h vs. TM 0 h (Obs.2), LEL-M 17 h vs. LEL-M 5h (Obs.3) as well as TM 5 h vs. TM 0 h (nCounter Assay only, Obs.4) were

defined as having an adj.P.Val below 0.05 and a log 2 fold change (logFC) $\geq |1|$.

Venn diagrams

To create Venn diagrams, the package VennDiagram v1.6.16 was used [Chen, 2012]. For optimal comparison of WG-DASL and nCounter data, only genes present in both datasets (mapped by Gene symbol annotation) were included in the analysis (565 genes).

Comparison of WG-DASL Assay and UC vs. NC dataset

For comparison between the LEL model (WG-DASL Assay) and UC vs. NC (normal colon) data set [Granlund *et al.*, 2013], genes were mapped by EntrezID annotation (the only annotation present for the UC vs. NC dataset) which led to an overlap of 18,047 genes. Within these common genes, a cut off of an adj.P.Val of < 0.01 and a logFC $\geq |1|$ was applied for both datasets to obtain lists of the differentially regulated genes. Subsequently, lists were generated, which contained the overlaps of up- and downregulated genes between both assays.
In collaboration with Maria Dinkelacker, random sampling of the same number of overlapping genes from all available genes on either array were generated for 1000 replications, and an empirical P value for the number of genes in the intersection was calculated. As no single random replicate had the same or a higher number of genes in the intersection of both data sets, the P value was given as P.Val < 0.001.

Comparison of WG-DASL Assay with IBD associated SNP loci

For detection of IBD associated SNP loci [Jostins *et al.*, 2012] near keygenes that were upregulated in the LEL model but not in UC patient data, again a cut off of an adj.P.Val < 0.01 and a logFC $\geq |1|$ for both datasets was applied. Comparison analysis was done based on Gene ID annotation. Prior to analysis, the UC vs. NC dataset was Gene ID annotated by using the package mygene v1.6.0 [Mark *et al.*, 2014].

2.5.5. Ingenuity Pathway Analysis

Pathway analysis of the WG-DASL Assay was performed with the software Ingenuity Pathway Analysis (IPA, Qiagen) using content version 26127183. For analysis, the values for Obs.1, 2 and 3, as calculated in subsection 2.5.4, including adj.P.Val, logFC and average expression were uploaded into IPA. All datasets were then filtered for an adj.P.Val < 0.05 and a logFC $\geq |1|$, after which a core analysis was performed with each filtered dataset. Data from the subunits 'Canonical Pathways', 'Diseases & Functions' and 'Upstream Analysis' was then further analyzed in **R**. For all subunits, data related to 'Cancer', 'Disease' or 'Development' was filtered out. Cut-offs were set to an adj.P.Val < 0.05 and a z-score $\geq |2|$.

2.6. Preparation of FFPE samples and sectioning

Samples as obtained at time points indicated in Table 2.2 were subsequently transferred to histology cassettes and fixed after an user-optimized short-fixation perfusion protocol with solutions and times as stated in Table 2.5. A rotary microtome (Leica, Nussloch) was used to subsequently prepare 2 μm tissue sections.

Solution	Incubation time
4 % formalin (in PBS)	24 h
70 % EtOH	$\leq$ 48 h
95 % EtOH	20 min
abs. EtOH	20 min
abs. EtOH/ abs. Acetone (1:1)	20 min
abs. Acetone	30 min
Paraffin (65 °C)	40 min

Table 2.5.: *Short-fixation perfusion protocol.* 4 % PBS-buffered methanol-free formalin was prepared from a 16 % stock solution (Life Technologies). Apart from incubation in paraffin, all steps were performed at room temperature. After procedure as described in this table, tissue samples were placed into with molten paraffin filled metal molds and orientated as desired after which the mold was placed on a cold plate. Paraffin blocks were then stored at 4°C.

2.7. Immunfluorescence imaging

2.7.1. Antibodies

Detailed information to primary and secondary antibodies used for immunofluorescence staining can be found in Table 2.6.

Antigen	Clone	Species	Company	Dilution
4E-BP1-p (Thr37/46)	236B4	rIgG	Cell Signaling	1:1600
anti-active Caspase 3	polyclonal	rIgG	Abcam	1:20
CD14	SP192	rIgG	Abcam	1:50
CD3	SP7	rIgG	DCS	1:50
CD68	EBM11	mIgG1	Dako	1:50
CD68 (FFPE)	PG-M1	mIgG3	Dako	1:50
IgA	polyclonal	rIgG	Dako	1:1000
mTOR	7C10	rIgG	Cell Signaling	1:50
mTOR-p (Ser2448)	49F9	rIgG	Cell Signaling	1:50
RPS6	5G10	rIgG	Cell Signaling	1:50
RPS6-p (Ser235/236)	D57.2.2E	rIgG	Cell Signaling	1:400
Directed against	**Host**	**Label**	**Company**	**Dilution**
mouse	sheep	Biotin	Amersham	1:600
mouse	donkey	AF488	Jackson ImmunoRes.	1:800
rabbit	donkey	Biotin	Jackson ImmunoRes.	1:800
rabbit	donkey	AF488	Jackson ImmunoRes.	1:800
biotin	-	SA-Cy3	Jackson ImmunoRes.	1:1000

Table 2.6.: *Primary and secondary antibodies used in immunofluorescence experiments.* All primary antibodies were directed against human antigens. Company informations: Cell Signaling (Cambridge, UK), Abcam (Cambridge, UK), Dako (Glostrup, Denmark), Jackson ImmunoResearch Laboratories, Inc. (West Grove, PA, USA), Amersham plc (Little Chalfont, UK). AF: Alexa Fluor, SA: Streptavidin.

2.7.2. FFPE sections

Tissue sections on slides were deparaffinized and rehydrated by immersing them into xylene (two changes), 100 % EtOH (two changes), 95 % EtOH, 75 % EtOH and H_2O (two changes) for 5 min each. Subsequently, heat mediated antigen retrieval was performed by incubating the slides in citrate buffer pH 6 (DCS diagnostics GmbH&Co.KG)

at 120°C in a pressure cooker for 5 min. Slides were then rinsed in H_2O. To block the ability of eosinophils to bind fluorochromes and thus generating a false-positive signal, sections were incubated with 0.1 g Chromotrope2R (Sigma-Aldrich) in 1% phenol for 1 h [Floyd *et al.*, 1983; Patterson *et al.*, 1989]. Subsequently, they were permeabilized and blocked by incubating them with an antibody diluent (DCS diagnostics GmBH&Co.KG) for 10 min.

For Click-It® detection, sections were at this point incubated with the Click-It® Reaction Cocktail (including Alexa Fluor 647 picocyl azide) for 30 min at room temperature.

The sections were then incubated with a primary antibody for 1 h or with antibody diluent as a negative control. The sections were subsequently stained with the appropriate secondary antibodies, either labeled with biotin or a fluorochrome, for 30 min. Subsequently, the sections were incubated with SA-Cy3 (1:1000) and nuclear mask stain (1:2000, Life Technologies) for 30 min. The slides were then mounted with cover slips using ProLong Diamond AntiFade Mountant (Life Technologies). In between steps, slides were washed with Tris-buffered saline (TBS).

2.7.3. Frozen sections

After generation of 8 μm sections, slides were immediately immersed in a -20°C cold methanol-acetone (1:1) solution and incubated for 1 min in order to preserve phosphorylation of proteins in cryo sections. The slides were then transferred to TBS. Endogenous biotin was blocked with the Avidin/Biotin Blocking Kit (Vector Laboratories Inc, Burlingame, CA, USA). Slides were then permeabilized and blocked by incubating them with an antibody diluent (DCS diagnostics GmBH&Co.KG) for 10 min. The primary antibody was incubated over night at 4°C and additionally for 1 h at room temperature. All other steps were performed as described for FFPE sections.

2.7.4. PBMC

Peripheral blood mononuclear cells (PBMC) were obtained by Ficoll-Hypaque (GE Healthcare) density gradient centrifugation. After resuspension in RPMI medium + 10 % FCS (+ Penicillin/ Streptomycin and L-Glutamine (see Table 2.1); from now on referred to as RPMI/PS + 10 % FCS), 4 * 10^5 cells/well were transferred to Poly-L-Lysin coated LapTek Chambers (Corning, Kaiserslautern, Germany) and allowed to adhere and regain resting conditions for 24 h at 37°C in a CO_2 incubator. 30 min prior to assessment of protein synthesis by OPP treatment (20 μM), the medium in two wells was exchanged to HBSS/ABX and 0.7 mM EDTA in HBSS/ABX, respectively, while 100 μg/ml cycloheximide was added to a third well as a negative control for protein synthesis. In the case of the wells that received prior HBSS or EDTA treatment and one additional well, OPP treatment was performed diluted in RPMI/ABX + 10 % FCS to mimic conditions as employed in the LEL model, whereas the other wells were incubated in RPMI/PS + 10 % FCS. As a background control, OPP was omitted in one additional well. After incubation with OPP for 30 min, cells were fixed using 4% methanol-free PBS buffered formalin for 12 min at 37°C. Cells were then permeabilized with 0.25 % Triton X-100 (Sigma-Aldrich) for 10 min. OPP Click-It® detection, nuclear stain and mounting (after removal of chamber) was performed as described in subsection 2.7.2, except for using phosphate-buffered saline (PBS) as a washing buffer.

2.7.5. Semi-quantification of the OPP Click-It® images

Semi-quantitative analysis of OPP Click-It® positive cells was performed using ImageJ 1.50e with a self-written macro (for complete script, see page A-8 in the appendix). After selecting the image of the time point with the strongest fluorescent OPP Click-It® signal, the lamina propria was manually selected and all other areas removed by the function 'clear outside'. An optimal minimal pixel threshold was then set for the AF647 (Click-It®) channel, so that after conversion into a binary image in combination with the function 'watershed', distinction of single cells was still possible. With the 'measure particles' function, OPP Click-It® positive cells were defined by having a pixel area size of 10-200 pixel (edges were excluded) and added to the region of interest (ROI)

manager. To confirm that the selection contained actual cells (and as such contained nuclei), an overlay of the selection with the DAPI channel was performed. Subsequently, the intensity of OPP Click-It® positive cells in the original AF647 channel was measured using the elements in the ROI manager. This resulted in a min, max, mean intensity and the sum of intensity for each measured cell. To quantify the overall cell number, the function 'Find Maxima' was applied to the DAPI channel with a noise tolerance of 450 (edges were excluded). The threshold defined for the image with the apparently most intense OPP Click-It® positive cells was used for all other analyzed images. To identify the OPP Click-It® intensity of specific cell populations, the threshold for the channel containing the cell population specific stain was defined. Subsequently, the resulting selection was overlaid over the AF647 (OPP Click-It®) channel. Further quantification was performed as described above.

2.8. Flow cytometry analysis of emigrated LP cells

Flow cytometric analysis was performed in collaboration with Dr. Anne-Kristin Heninger, who established the protocol and performed all steps after permeabilization as well as the analysis of collected data. Emigrated lamina propria cells, treated with 250 nM Torin1, 1 μM Torin1 or 10 μg/ml cycloheximide during the LEL-model were at LEL-M 17 h analyzed for the presence of phosphorylated proteins by flow cytometry. As a control, untreated, unstimulated PBMC, stained immediately after isolation from peripheral venous blood by density centrifugation over Ficoll-Hypaque, were used.
In order to determine the phosphorylation state of mTOR downstream targets in a cell-type specific manner, fluorochrome labelled antibodies recognizing (1) the B cell markers CD19 or CD20 (2) the myeloid cell markers CD14, CD33 or CD66b (see Table 2.7 on page 34) were added to the culture and incubated at 37°C for 20 min. Subsequently, cells were fixed at 37°C for 12 min by adding pre-warmed 4% PFA/PBS to the culture medium at a ratio of 1:1 for a final concentration of 2% PFA in the culture. Immediately after fixation, cells were harvested, washed 1x in FACS buffer (25 mM NaN_3, 50 mM EDTA, 4 mM $NaHCO_3$, 1% FCS in PBS) and 1x in PBS, permeabilized (-20°C BD Biosciences Phosflow Perm Buffer III) for 30 min on ice and

stored at -20°C until further processing.

Permeabilized cells were washed 3x with FACS buffer and divided into two tubes/ condition. One tube was stained with phospho-4E-BP1$^{Thr37/46}$ and phospho-RPS6$^{Ser235/236}$ and the other tube was stained with phospho-mTOR^{Ser2448} and phospho-Akt^{Ser473} for 60 min at room temperature. Fluorochrome-labelled antibodies recognizing the pan-leukocyte marker CD45, the T cell-specific receptor CD3 or the myeloid marker HLA-DR were added simultaneously (see Table 2.7). The secondary antibody donkey anti-rabbit AF488 (see Table 2.6) was used at 1:200 to label phospho-mTOR^{Ser2448} in a subsequent staining step for 20 min on ice. After staining, cells were washed with FACS buffer and acquired on a BD LSRFortessa flow cytometer equipped with FACS Diva 8 software. Doublets and clumps were excluded based on SSC-A vs. SSC-W and FSC-A vs. FSC-H plots. An unstained control was used to detect auto-fluorescence. At least 50,000 gated events were acquired for each sample and analyzed using FlowJo 2 software version 10.0.8 (TreeStar, Inc., Ashland, USA). Expression of suface receptors and phosphorylation state of mTOR downstream targets as well as mTOR^{Ser2448} was assessed by determining the MFI of relevant fluorochromes. A FMO (fluorescence minus one) control was used to determine the background MFI in the absence of the phospho-specific antibody. Lamina propria myeloid cells were identified as CD45$^+$ lineage$^-$ (i.e. CD3/19/20/66b$^-$), CD33$^+$HLA-DR$^+$ cells. Within the LP myeloid cell population, CD14$^+$ macrophages were distinguished from CD14$^-$ dendritic cells.

2.9. Luminex® multiplex analysis

For Luminex® multiplex analysis, size standardized punches, collected at indicated timepoints, were incubated in RPMI/ABX medium + 10% FCS with or without inhibitors for 1 h (12 h for LEL-M 17 h) at 37°C. Supernatants were collected and after cell removal by centrifugation flash frozen in liquid nitrogen and stored at -80°C until analysis. Luminex® multiplex analysis was performed using customized screening assays (for analytes CCL19, CCL2, CCL22, CD14, CD163, CXCL1, CXCL8, ICAM-1, IL-18, M-CSF, MIF, MMP12) or high-sensitivity performing assays (for analytes IL-1β, IL-6, TNF-

Antigen	Clone	Label	Company	Dilution
CD19	HIB19	APC-H7	BD Biosciences	1:5.5
CD20	L27	APC-H7	BD Biosciences	1:5.5
CD14	MϕP9	V450	BD Biosciences	1:5.5
CD33	P67.6	PE	BD Biosciences	1:3
CD66b	80H3	APC-AF750	Beckman Coulter	1:5.5
4E-BP1-p (Thr37/46)	236B4	AF647	Cell Signaling	1:50
RPS6-p (Ser235/236)	D57.2.2E	AF488	Cell Signaling	1:25
mTOR-p (Ser2448)	49F9	-	Cell Signaling	1:50
Akt-p (Ser473)	M89-61	AF700	BD Biosciences	1:10
CD45	HI30	AF700	BioLegend	1:56
CD3	SK7	PerCP	BD Biosciences	1:16
HLA-DR	G46-6	V500	BD Biosciences	1:25

Table 2.7.: *Antibodies used for surface stain in flow cytometry analysis of emigrated LPMC and PBMC.* All primary antibodies were directed against human antigens. Company information: BD Biosciences (Heidelberg, Germany), Beckman Coulter (Brea, CA, USA).

α, VEGF) from R&D systems (Minneapolis, MN, USA) and a Bio-Rad Luminex 100 (Bio-Rad Laboratories, Inc., Hercules, CA, USA). The Luminex® multiplex analysis itself was performed in collaboration with Dr. Niels Halama, National Center for Tumor Diseases (NCT), Heidelberg.

3. Results

3.1. The loss of epithelial layer (LEL) model

Epithelial layer damage represents an early hallmark of acute and chronic intestinal inflammation and has been shown to coincide with the induction of an inflammatory response in resident lamina propria (LP) cells. However, little information is available regarding molecular mechanisms driving the activation of the normally hyporesponsive phenotype of LP immune cells.

Recent work from our group introduced the loss of epithelial layer (LEL) model (Figure 3.1) as a helpful tool to study molecular mechanisms underlying an acute inflammatory response in the intestine. Initial observations indicated that release of mucus and epithelial cells from normal human colonic mucosa by DTT and EDTA treatment resulted in the upregulation of transcript levels of inflammatory markers such as *IL6*, *IL8*, *IL1B*, *TNFA*, *INFG*, *IL23A* and *CCL2* in resident LP cells.
To determine, whether these initially analyzed inflammation markers correspond to the initiation of a global inflammatory response and to further investigate the dimensions and details of this event, global gene expression analysis was performed employing mucosa samples taken at different time points during the LEL model.

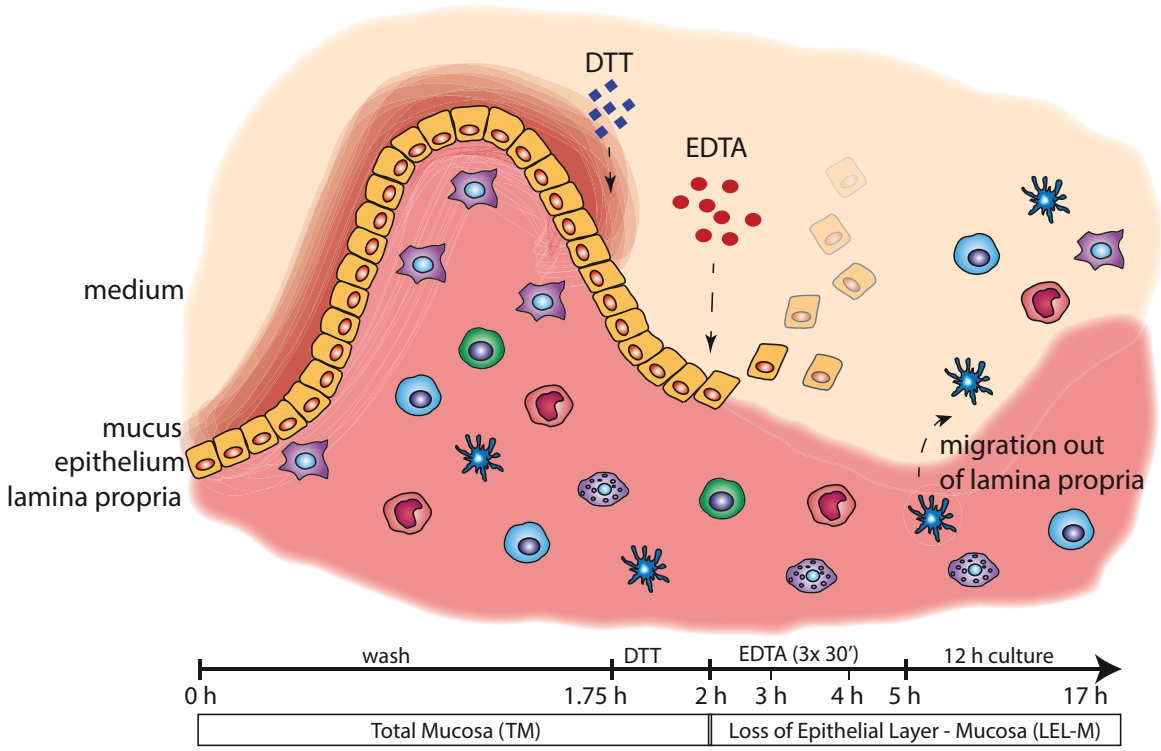

Figure 3.1.: *The loss of epithelial layer (LEL) model.* Healthy total mucosa (TM) from patients undergoing surgery for colon cancer is dissected from the surgical specimen (TM 0 h) and submitted to extensive washing. Mucus is removed by DTT treatment (TM 2 h). Subsequently, the mucosa is subjected to three consecutive 0.7 mM EDTA treatments with intermittent washing steps (LEL-M = 3 h, 4 h, 5 h), leading to the detachment of the epithelial layer from the underlying LP. After LEL, cells migrate out of the LP. The LEL is followed by a 12 h culture (LEL-M 17 h). For detailed information regarding tissue sample collection, see Table 2.2 on page 20. Image of model was created based on Mowat and Agace [2014].

3.2. Global gene expression analysis indicates the initiation of an inflammatory response in the LEL model

With the objective of investigating mechanisms associated with the induction of inflammation specifically in LP cells, laser-capture microdissection (LMD) was employed to isolate the latter cell population from total mucosa prior to culturing (TM 0 h),

after LEL (LEL-M 5 h) as well as after 12 h of subsequent culture (LEL-M 17 h, see Figure 3.1).
To assess homeostatic gene expression levels in order to subsequently determine differential gene expression under inflammatory conditions, most approaches as input either use (1) entire biopsies or (2) LP cells isolated via EDTA treatment and subsequent enzymatic digestion from normal, uninflamed TM. However, method (1) includes all layers of the mucosa and the LP cells from method (2) express inflammatory markers that are not detected under homeostatic conditions *in situ* (unpublished data). Taken these findings into consideration, LMD, a superior method to accurately assess the resting state of LP cells and their subsequent activation after onset of inflammation, was chosen for the first time.

After LMD and RNA isolation, all tissue samples showed signs of degradation with a RNA integrity number (RIN) ranging between 3.5 and 7 (for representative electropherograms of RNA quality assessment, see page A-4 in the appendix). Given the low RNA integrity, samples were analyzed using the whole genome cDNA-mediated Annealing, Selection, extension and Ligation (WG-DASL) assay from Illumina, an array-based method that allows the expression profiling of partially degraded RNA by using probe-groups that only span 50 bps.
For further details regarding the WG-DASL Assay and its bioinformatic normalization, see subsection 2.4.1 on page 23 and 2.5.1 on page 25, respectively.
Hierarchical clustering analysis of the quantile normalized microarray data sets demonstrated a clear distinction between TM and LEL-M samples by two separate clusters and a further distinction between LEL-M samples by a subcluster of LEL-M 17 h samples (Figure 3.2). The color distribution in the heatmap of the same figure, indicating the relative gene expression, is very similar between replicates of one time point. These results demonstrate the reproducibility of the gene expression results obtained in the four replicate experiments.

After defining significantly differentially regulated genes by an absolute log 2 fold change (logFC) ≥ 1 and an Benjamini-Hochberg adj.P.Val < 0.05, 2171 genes were differentially

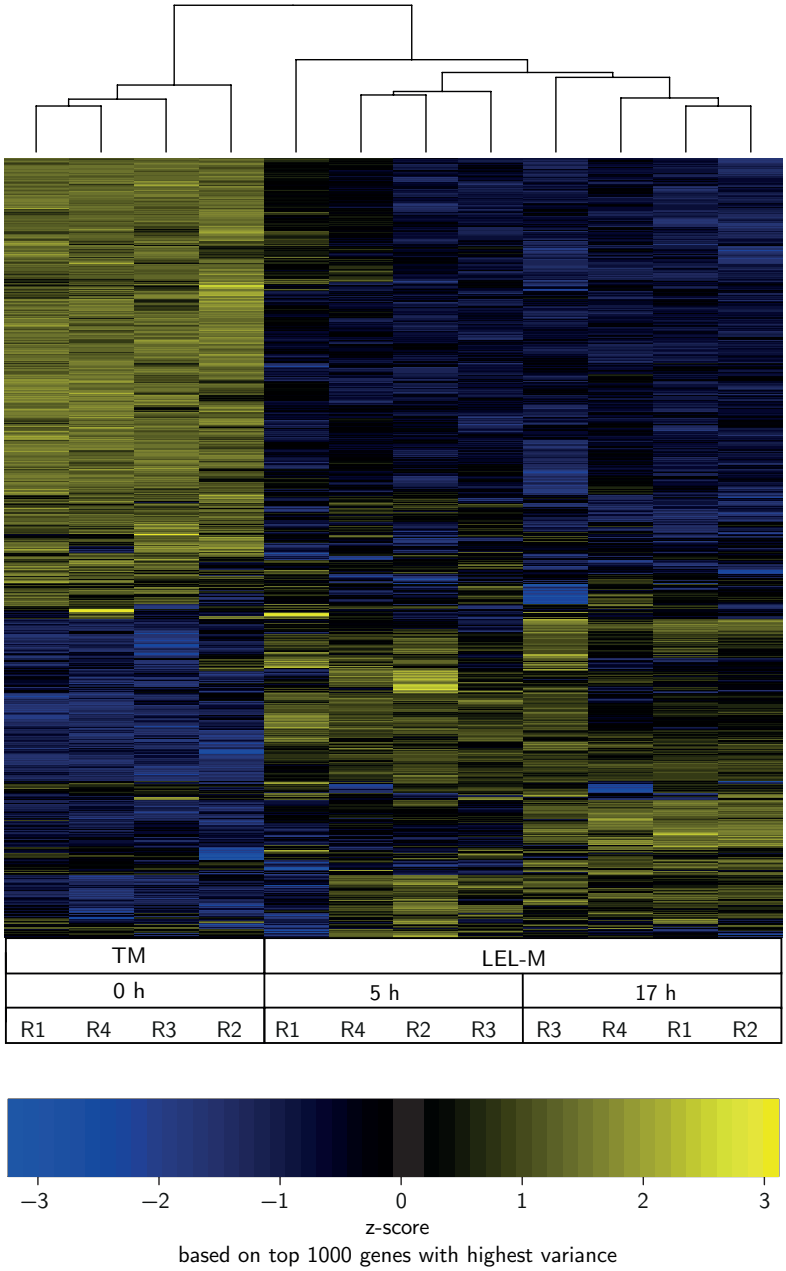

Figure 3.2.: *Expression profile of WG-DASL gene expression data.* Shown is a heatmap based on z-score transformed expression values of the top 1000 genes (sorted by highest variance of the WG-DASL Assay dataset for the time points TM 0 h, LEL-M 5 h and LEL-M 17 h). Columns have been reordered by hierarchical clustering (complete linkage, Euclidean distance metrics). Colors indicate z-score values as shown in the scale legend. Shown data was obtained in four independent experiments (R1-R4) with tissue samples collected at different time points within one experiment being obtained from the same specimen.

expressed for Observation (Obs.)1: LEL-M 5 h vs. TM 0 h, whereas 3100 genes were differentially regulated for Obs. 2: LEL-M 17 h vs. TM 0 h. Both observations showed a similar ratio of upregulated vs. downregulated genes (having a small tendency towards downregulated genes). Notably, only 178 genes were differentially expressed for Obs. 3: LEL-M 17 h vs. LEL-M 5 h, indicating a rapid upregulation of most differentially regulated genes immediately after LEL. An overview over numbers of up- and downregulated genes between time points is given in Table 3.1.

adj.P.Val cut-off	Direction of regulation	**Obs.1** LEL-M (5 h) vs. TM (0 h)	**Obs.2** LEL-M (17 h) vs. TM (0 h)	**Obs.3** LEL-M (17 h) vs. LEL-M (5 h)
0.05	↑	1046	1525	110
	↓	1125	1575	68
0.01	↑	380	741	3
	↓	517	916	0

Table 3.1.: *Differential gene expression in the LEL model (WG-DASL Assay).* Numbers indicate the absolute quantities of genes with an logFC $\geq |1|$ and an Benjamini-Hochberg adj.P.Val < 0.05 (0.01) for indicated observations. ↑: upregulated, ↓: downregulated.

As could be expected from previous qRT-PCR experiments of our group, inflammatory genes such as *CSF3*, *IL6*, *CXCL2* and *IL8* were among the top upregulated genes, with the expression of all four genes being significantly increased for both Obs.1 and 2. Additionally, the upregulation of other inflammatory genes such as *MMP10*, *IRF7*, *IL11*, *IL22*, *IL24*, *SERPINA3*, *CCL21* and *CXCL2* indicated the initiation of a global inflammatory response (Figure 3.3).

Overall, for the limited number of genes shown in Figure 3.3, the expression of many genes was significantly differentially regulated for both observations, while only gene *RERGL* was solely significant for Obs.1. However, several genes were only significantly differentially expressed for Obs.2 (i.e. *IL11*, *IL22*, *MME* (also known as *MMP12*), *MMP3*, *IL24*), thus showing a progression of the inflammatory response over the course of the LEL model.

At least some of these downregulated genes represent epithelium specific genes such as Kreatin 20 (KRT20) and Polymeric immunoglobulin receptor (PIGR), reflecting a degree of epithelial cell contamination of the microdissected LP compartment (page A-6 in the appendix). This was not preventable, as emerging crypts are not always morphologically distinguishable from the LP in a given tissue section.
The full lists of all up- and downregulated genes for Obs.1, 2 and 3 of the WG-DASL Assay can be found on pages A-22 ff. in the appendix.

In summary, the results of the microarray analysis showed the upregulation of expression of genes involved in the initiation of an inflammatory response in the LEL model immediately after the loss of the epithelial layer (LEL-M 5 h). This inflammatory response is still present at LEL-M 17 h. Furthermore, the differential regulation of certain genes for Obs.2 but not Obs.1 indicate a progression of the inflammatory response from LEL-M 5 h to LEL-M 17 h.

3.3. Validation of global gene expression data by quantitative gene expression analysis using the nCounter system

Before taking further analysis steps, the microarray results were validated via nCounter technology (Nanostring, Seattle, WA, USA) by using the Human Immunology v2 kit, consisting of 594 immunology-related human genes and 15 internal reference genes. At the time of analysis, this kit among other predefined nCounter gene expression codesets comprised the most comprehensive set of immune system associated genes.
In contrast to the WG-DASL Assay, the nCounter technology does not include a preamplification step and thus can be seen as a more quantitative approach. As the nCounter system like the WG-DASL Assay uses probes that only span 50 bps, this technology is compatible with partially degraded RNA. For more details to the nCounter Assay and a detailed comparison to the WG-DASL Assay, see subsection 2.4.2

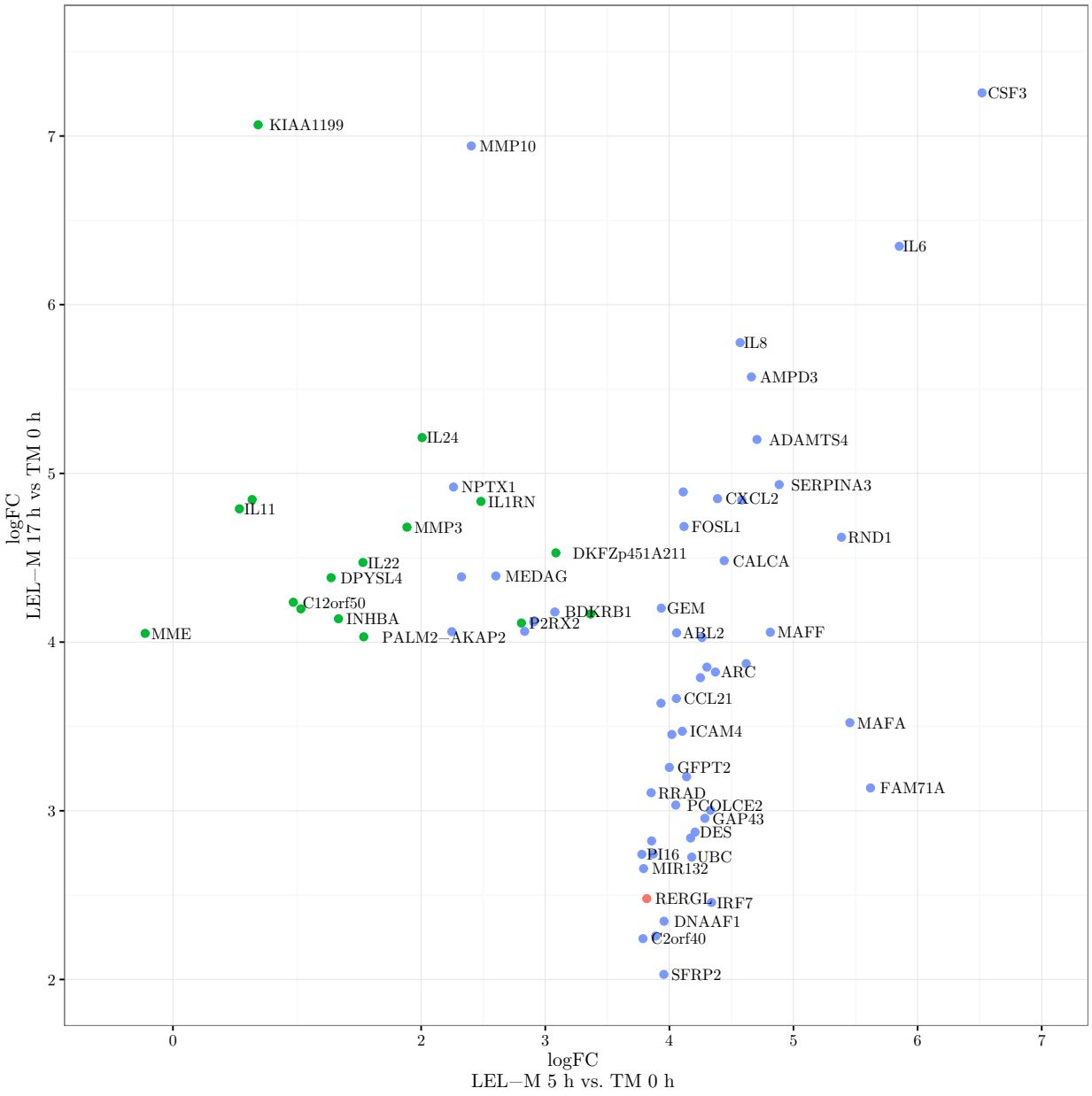

Figure 3.3.: *Top 50 upregulated genes in the LEL model (WG-DASL Assay).* Blue dots indicate that the upregulation of the associated gene was significant (adj.P.Val < 0.05) for both observations (Obs.1: LEL-M 5 h vs. TM 0 h, Obs.2: LEL-M 17 h vs. 0 h), while red dots indicate significance only for Obs.1 and green dots for Obs.2, respectively. Where two logFC values are too close to each other to produce two readable gene names, only one gene name is indicated randomly.

on page 24.
Again, LP samples were collected by LMD at time points TM 0 h, TM 5 h, LEL-M 5 h and LEL-M 17 h. Samples were obtained by four independent experiments. TM 5 h was included in the nCounter Assay as a control for time-dependent, but LEL independent upregulation of genes. This timepoint was omitted in the WG-DASL Assay in favor of analyzing four replicates for each of the three time points investigated, as the WG-DASL Assay has a capacity of 12 samples per run and possesses a limited inter-assay quantification ability (due to its preamplification step).
For details regarding normalization of the nCounter Assay, see subsection 2.5.2 on page 25.

In accordance with the WG-DASL Assay, hierarchical cluster analysis of the obtained nCounter expression data sets demonstrated a clear distinction between TM and LEL-M samples by two separate clusters as well as between LEL-M samples by two second level clusters (Figure 3.4). In contrast to this differentiation, the similarity of gene expression between TM time points was shown by their absent distinction from each other. These results, together with the color distribution in the heatmap, demonstrate the reproducibility of the nCounter gene expression results obtained in the four independent experiments.

Table 3.2 shows the absolute numbers of significantly differentially regulated genes (logFC $\geq |1|$, adj.P.Val < 0.05): For Obs.1, 248 genes were differentially expressed. This number decreased to 225 for Obs.2. Obs.3 yielded 87 differentially expressed genes. Notably, in total mucosa, following 5 h of culture (TM 5 h) when compared to TM prior to culturing (TM 0 h), the expression of only two genes, the chemokine family members *CXCR4* (logFC = 2.12) and *PPBP* (also known as *CXCL7*, logFC = -2), changed significantly. In accordance with the high resemblance of the gene expression profile between TM 0 h and TM 5 h, there was a high amount of similarity of differentially expressed genes for Obs.1 and LEL-M 5 h vs. TM 5 h (Obs.4).

Many of the top upregulated genes in the nCounter Assay as i.e. *IL6*, *IL8*, *CXCL2*

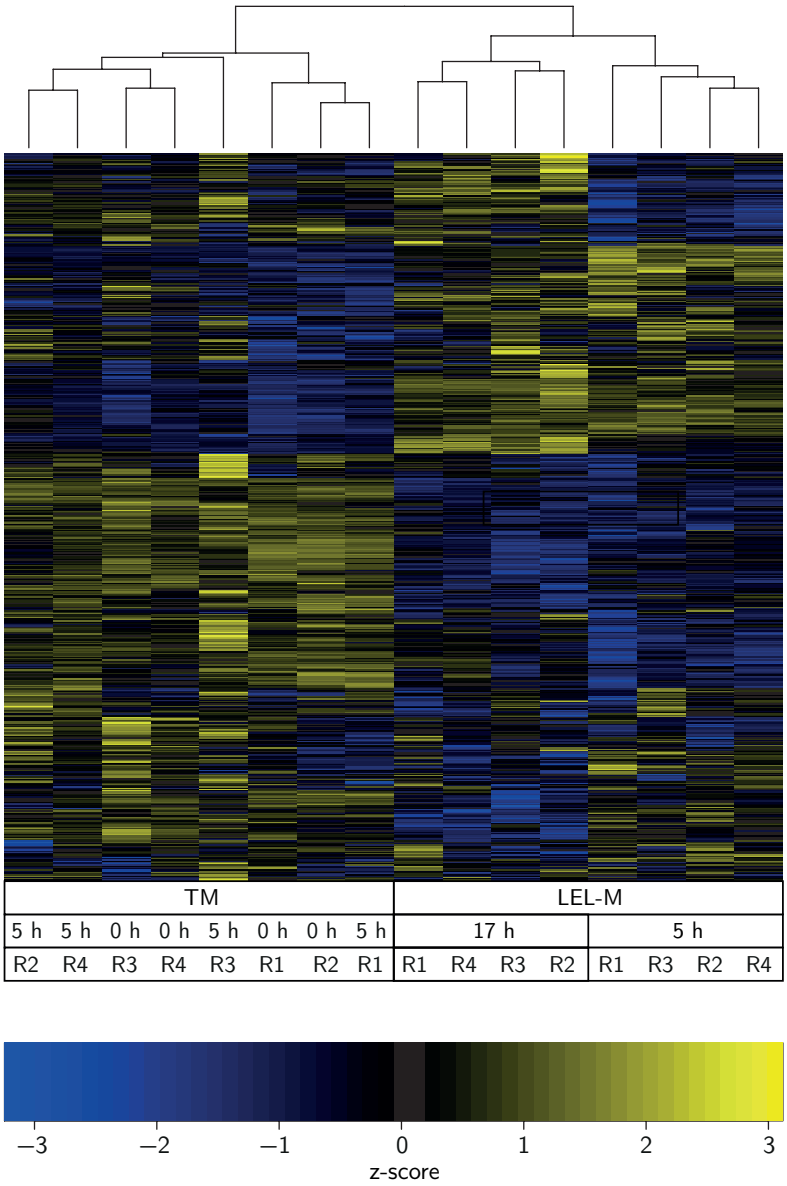

Figure 3.4.: *Expression profile of nCounter gene expression data.* Shown is a heatmap based on z-score transformed expression values of all 579 genes of the nCounter dataset for the time points TM 0 h, TM 5 h, LEL-M 5 h and LEL-M 17 h. Columns have been reordered by hierarchical clustering (complete linkage, Euclidean distance metrics). Colors indicate z-score values as shown in the scale legend. Shown data was obtained in four independent experiments (R1-R4), with tissue samples collected at different time points within one experiment being obtained from the same specimen.

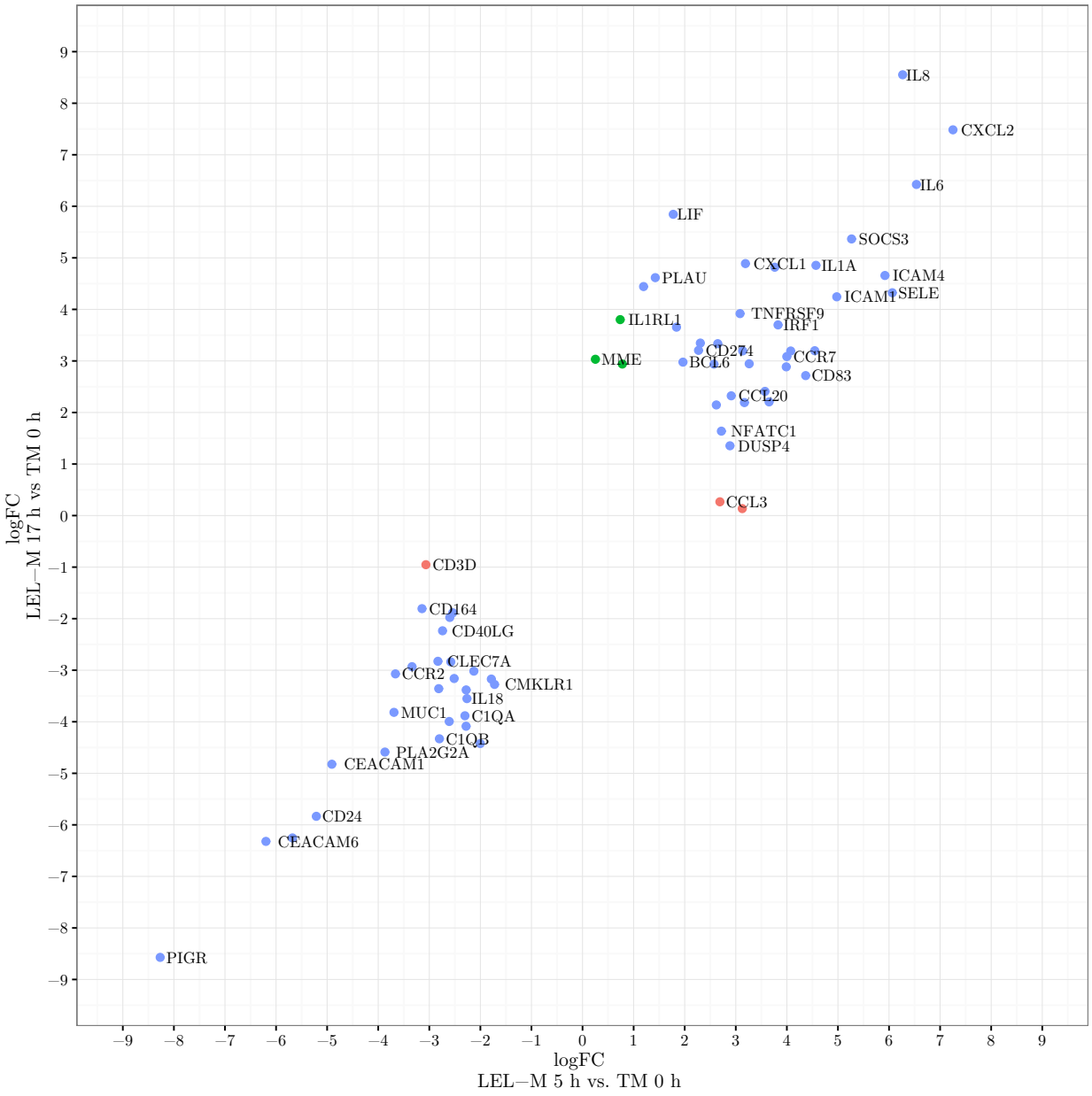

Figure 3.5.: *Top 50 differentially regulated genes in the LEL model (nCounter Assay).* Blue dots indicate that the upregulation of the associated gene was significant (adj.P.Val < 0.05) for both observations (Obs.1: LEL-M 5 h vs. TM 0 h, Obs.2: LEL-M 17 h vs. 0 h), while red dots indicate significance only for Obs.1 and green dots for Obs.2, respectively. Where two or more logFC values were too close to each other to produce readable gene names, only one gene name is indicated randomly.

adj.P.Val cut-off	Direction of regulation	**Obs.1** LEL-M (5 h) vs. TM (0 h)	**Obs. 2** LEL-M (17 h) vs. TM (0 h)	**Obs.3** LEL-M (17 h) vs. LEL-M (5 h)	**Obs.4** LEL-M (5 h) vs. TM (5 h)
0.05	↑	93	95	47	78
	↓	155	130	40	141
0.01	↑	68	74	11	57
	↓	123	93	4	88

Table 3.2.: *Differential gene expression in the LEL model (nCounter Assay).* Numbers indicate the absolute quantities of significantly differentially regulated genes for indicated time point comparisons. logFC $\geq |1|$, Benjamini-Hochberg adj.P.Val as indicated. ↑: upregulated, ↓: downregulated.

and *ICAM4* were also among the top upregulated genes of the WG-DASL Assay (see Figure 3.5 and Figure 3.3). The full lists of all significantly differentially expressed genes for Obs.1, 2 and 4 can be found on pages A-37 ff. in the appendix.
A comparison between both assays based on 565 common genes revealed a strong overlap between assays (Figure 3.6). For Obs.1, 71 % of upregulated genes in the WG-DASL Assay were also upregulated in the nCounter Assay, which increased to 96 % for downregulated genes. For Obs.2, this corresponded to an overlap of 80 % for upregulated and 89 % for downregulated genes, respectively. Importantly, except gene ATP-binding cassette sub-family B member 1 (*ABCB1*), which was downregulated in the nCounter Assay, but upregulated in the WG-DASL Assay for Obs.1, no genes were regulated in opposite directions between assays. A list of the genes that were unidirectionally regulated in both assays can be found on page A-52 and A-53 in the appendix. Notably and in line with the results of the WG-DASL Assay (Figure 3.3), most overlapping genes present for Obs.1 were also present for Obs.2, whereas overlapping genes for Obs.2 had a tendency to be differentially expressed only for that observation.

In summary, based on 565 common genes, the high overlap in up- and downregulated genes detected in the two different assays validated the initiation of the inflammatory response and furthermore the characteristics (based on differentially regulated genes) of this response in the LEL model at onset of inflammation.

(A) Obs.1

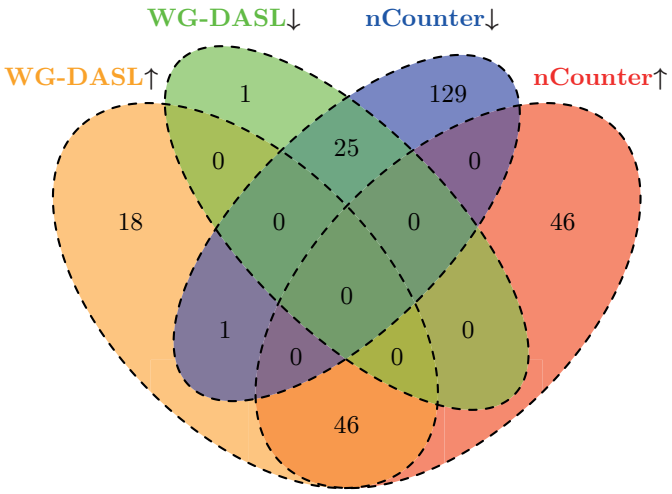

(B) Obs.2

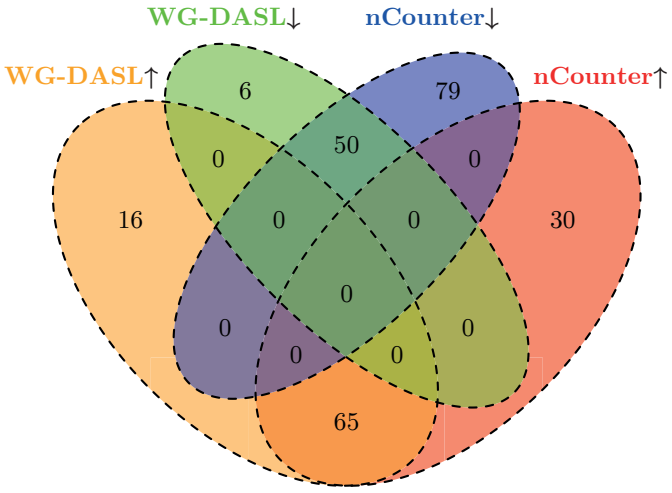

Figure 3.6.: *Gene expression overlap between WG-DASL and nCounter Assay.* Upregulated (↑) and downregulated (↓) genes were defined by an logFC $\geq |1|$ and an adj.P.Val < 0.05. The comparison includes only the common 565 genes between assays (mapped by Gene ID annotation); (A) Obs.1, LEL-M 5 h vs. TM 0 h: In total, 16% and 43 % of common genes were differentially regulated in the WG-DASL and nCounter Assay, respectively. (B) Obs.2, LEL-M 17 h vs. TM 0 h: In total, 23% and 40 % of common genes were differentially regulated in the WG-DASL and nCounter Assay, respectively.

3.4. The LEL model reflects inflammatory processes as observed in intestinal inflammation *in vivo*

Following validation of the results of the WG-DASL Assay, I next determined whether the LEL model reflects inflammatory processes as observed in intestinal inflammation *in vivo*. For that purpose, the WG-DASL data sets of differentially regulated genes in the LEL model were compared to a published analysis. In this publication, mucosa samples from ulcerative colitis (UC) patients were compared to healthy mucosa samples [Granlund *et al.*, 2013].

The published analysis consists of several datasets, comparing colonic mucosa samples from 20 healthy controls (NC, normal colon) and 37 patients with active UC. It has to be taken into consideration, that in contrast to the LMD LP samples collected during the LEL model, the samples of this analysis consisted of total mucosa. To be able to compare the datasets, genes analyzed in both datasets were matched via EntrezID annotation (being the only annotation given for the UC vs. NC dataset). This procedure resulted in 18,047 common genes. Out of these common genes, a total of 733 genes were significantly differentially regulated in the WG-DASL Assay for Obs.1 with an increase to 1310 genes for Obs.2, whereas 725 genes were differentially regulated in the UC vs. NC dataset (adj.P.Val < 0.01).

The comparison of the expression of the common genes revealed a partial overlap between the UC dataset and the LEL model, as can be seen in Figure 3.7. Based on the differentially regulated genes in the LEL model, there was an 12 % overlap between datasets in the upregulated genes for both Obs.1 and Obs.2, whereas the overlap in downregulated genes decreased from 26 % to 21% for Obs.1 to Obs.2. Notably, 16 genes (4 % of 434 genes) that were downregulated in the LEL model for Obs.1, were upregulated in the UC dataset, a number that increased to 31 (4 % of 736 genes) for Obs.2, whereas no genes were upregulated in the WG-DASL Assay, but downregulated in the UC vs. NC data set for Obs.1 and only 3 genes 0.4 % for Obs.2. A table with all overlapping or differing genes can be found on pages A-54 to A-56 in the appendix.

Generating 1000 random lists to exclude a false-positive overlap based on coincidence, the overlap between both datasets was significant with an adj.P.Val of < 0.001, thus indicating the physiological relevance of the LEL model.

Based on the assumption, that the LEL model reflects a 'normal' acute inflammatory response in contrast to the pathological chronic response seen in IBD patients, I next compared genes that were near single-nucleotide polymorphisms (SNP) associated with IBD as predicted by genome wide association studies (GWAS, Jostins *et al.* [2012]) with the WG-DASL dataset. For Obs.1, I found 16 and for Obs.2 27 genes that were upregulated in the LEL model, but not in the UC vs. NC dataset [Granlund *et al.*, 2013]. A table of all identified genes and their corresponding SNPs can be found on page A-57 in the appendix.

In summary, on a gene expression level, the LEL model partially reflects inflammatory processes as observed in chronic intestinal inflammation *in vivo*.

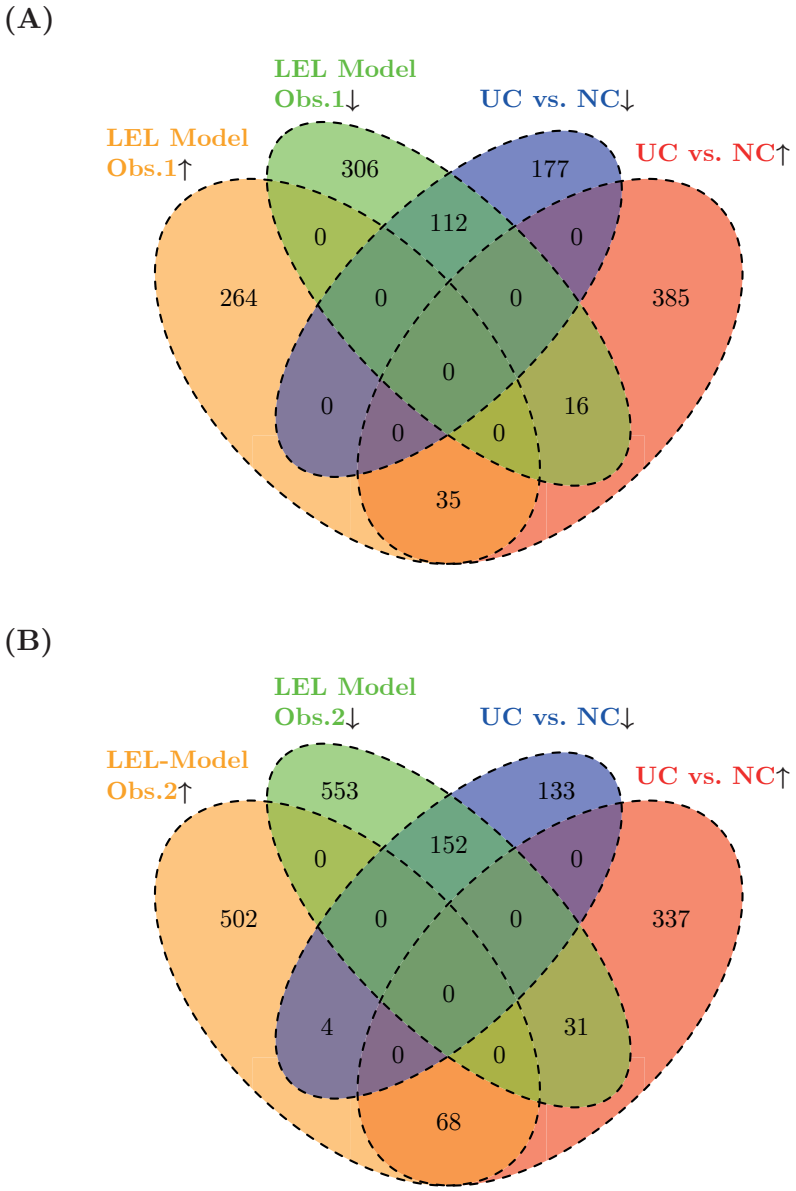

Figure 3.7.: *Gene expression overlap between the LEL model and UC vs. NC dataset.* Overlap of upregulated (↑) and downregulated (↓) genes is based on 18,047 common genes between WG-DASL Assay (LEL model) and UC vs. NC dataset [Granlund *et al.*, 2013] for (A) Obs.1 (B) Obs.2. Cut offs: LogFC $\geq |1|$; adj.P.Val < 0.01. NC: normal colon; UC: Ulcerative colitis

3.5. Bioinformatic analysis indicates an initiation of protein synthesis at the onset of inflammation in the LEL model

In order to search for potential biological processes as well as upstream regulators associated with the induction of an intestinal inflammatory response in the LEL model, I next analyzed the WG-DASL data using the software Ingenuity Pathway Analysis (IPA), a well known tool for pathway analysis. Further details regarding data input and analysis can be found in subsection 2.5.5 on page 28.
As expected, many of the identified canonical pathways and biological functions predicted to be activated were related to inflammation as i.e. 'IL-6 Signaling', 'Acute Phase Response Signaling', 'IL-8 Signaling' or 'Leukocyte Extravasation Signaling' (Table 3.3), 'adhesion of blood cells', 'stimulation of cells' and 'chemotaxis' (Table 3.4). IPA also allows the prediction of upstream regulators and their activation state. This analysis is based on (1) the overlap of differentially expressed genes in the dataset with known target molecules of the particular upstream regulator and (2) the differential expression of these target molecules in the dataset, respectively. In order to be predicted as an upstream regulator, the gene encoding the upstream regulator does not have to be differentially expressed in the dataset itself. The molecule types with the highest predicted numbers of upstream regulators for both Obs.1 and Obs.2 were 'transcription regulator', 'cytokine', 'kinase', 'other' and 'growth factor' (Table 3.5).

In search for potential mechanisms underlying intestinal inflammation, I observed that predicted pathways such as 'FGF signaling' or 'PI3K/Akt signaling' are involved in translational control. This finding was supported by predicted biological functions as 'cell proliferation', known to depend on ongoing protein synthesis and 'phosphorylation of protein', a function that is known to positively control the activation state of many translation regulators. Among predicted upstream regulators, the predominance of activated growth factors as well as kinases involved in translation such as EIF2AK2

and EIF2AK3 pointed toward the upregulation of translation. In contrast, known translation inhibitors such as microRNAs were consistently predicted to be inhibited.

		Obs.1 LEL-M 5 h vs. TM 0 h			Obs.2 LEL-M 17 h vs. TM 0 h		
	Ingenuity Canonical Pathway	z-score	% OL	-(log P.Val)	z-score	% OL	-(log P.Val)
1	Dendritic Cell Maturation	2.86	14.1	2.33	1.77	18.5	3.04
2	IL-1 Signaling	2.84	16.5	2.20	2.84	16.0	1.17
3	HMGB1 Signaling	2.56	19.2	4.06	3.40	22.5	3.97
4	Acute Phase Response Signaling	2.45	16.0	3.28	3.29	19.9	3.69
5	IL-6 Signaling	2.20	21.6	5.28	3.65	25.9	5.61
6	Protein Kinase A Signaling	2.14	11.7	2.05	0.47	13.6	1.49
7	B Cell Activating Factor Signaling	2.12	22.5	2.39	2.24	15.0	0.61
8	iNOS Signaling	2.12	20.5	2.10	1.63	19.1	1.26
9	FGF Signaling	1.94	15.3	1.72	1.70	19.1	1.96
10	p38 MAPK Signaling	1.88	20.5	4.71	2.35	22.2	3.75
11	PI3K/AKT Signaling	1.81	14.6	1.98	2.24	18.8	2.43
12	LPS/IL-1 Mediated Inhibition of RXR Function	1.73	15.5	3.68	2.07	23.6	7.85
13	4-1BB Signaling in T Lymphocytes	1.67	32.3	3.96	2.12	29.0	2.43
14	IL-8 Signaling	1.21	10.3	0.78	2.27	16.0	1.86
15	Leukocyte Extravasation Signaling	2.14	10.1	0.74	2.20	16.2	2.07
16	Ceramide Signaling	1.90	12.5	0.95	2.14	17.9	1.54
17	Oncostatin M Signaling		8.82	0.28	2.12	23.5	1.65
18	Wnt/Ca+ pathway	2.83	14.3	1.09	1.51	18.6	1.37
1	PPAR Signaling	-3.15	18.3	2.91	-3.67	25.8	4.60
2	PPARα/RXRα Activation	-2.98	14.0	2.30	-4.38	16.4	2.01
3	Aldosterone Signaling in Epithelial Cells	-2.12	18.4	4.47	-2.12	14.2	1.06
4	LXR/RXR Activation	-1.71	19.0	4.00	-3.16	25.8	6.07
5	Eicosanoid Signaling	-1.63	18.8	2.31	-2.33	19.5	1.96

Table 3.3.: *IPA Pathway Analysis of LEL model gene expression data (WG-DASL Assay).* Cut-Off: Fisher's exact T test adjusted -(log P.Val) overlap of 1.3 ($\equiv$ to 0.05) for at least one observation. % OL indicates overlap between known members of specified pathway and differentially regulated genes in dataset. Rank in table was firstly defined by z-score of significant pathways for Obs.1 and secondly z-score for Obs.2. A table including all significantly enriched pathways for all observations w/o z-score cut-off can be found on page A-58 ff. in the appendix.

	Biological Function	Obs.1 LEL-M 5 h vs. TM 0 h z-score	Obs.1 LEL-M 5 h vs. TM 0 h adj.P.Val	Obs.2 LEL-M 17 h vs. TM 0 h z-score	Obs.2 LEL-M 17 h vs. TM 0 h adj.P.Val
1	cell survival	3.46	6.3E-11	2.91	2.8E-17
2	function of blood cells	3.16	4.9E-10	2.35	5.1E-19
3	survival of organism	3.06	8.1E-15	2.04	4.6E-22
4	function of leukocytes	3.02	2.6E-11	1.95	1.5E-19
5	cell viability	2.98	6.3E-11	2.78	7.5E-18
6	adhesion of blood cells	2.96	1.3E-06		
7	stimulation of cells	2.90	1.2E-08	2.52	9.1E-16
8	function of phagocytes	2.68	1.3E-08	1.88	4.3E-17
9	homeostasis of blood cells	2.40	7.0E-09	2.79	2.1E-12
10	homeostasis of leukocytes	2.39	1.0E-08	2.72	2.9E-12
11	cellular homeostasis	2.39	1.9E-19	3.08	1.2E-21
12	Lymphocyte homeostasis	2.39	7.3E-09	2.72	1.4E-12
13	function of mononuclear leukocytes	2.38	3.1E-07		
14	recruitment of cells	2.38	1.3E-10	2.03	2.4E-20
15	cell movement	2.21	1.1E-21	2.10	4.8E-39
16	invasion of cells	2.01	2.0E-14	2.94	1.5E-26
17	chemotaxis	1.89	6.4E-11	2.28	1.5E-20
18	homing of cells	1.87	8.3E-12	2.25	1.1E-21
19	chemotaxis of cells	1.77	1.7E-10	2.08	1.2E-19
20	cell movement of muscle cells	1.74	1.4E-07	2.44	1.3E-10
21	proliferation of cells	1.70	1.8E-24	2.11	5.4E-47
22	binding of DNA	1.65	2.8E-08	2.49	3.6E-10
23	ion homeostasis of cells	1.49	2.6E-09	2.07	7.3E-11
24	organization of cytoplasm			2.73	9.9E-11
25	organization of cytoskeleton			2.67	1.8E-10
26	growth of plasma membrane projections			2.37	7.8E-10
27	function of antigen presenting cells			2.25	1.8E-13
28	phosphorylation of protein			2.22	1.6E-11
29	adhesion of connective tissue cells			2.04	4.9E-10
1	organismal death	-5.73	1.6E-15	-5.52	1.4E-23
2	morbidity or mortality	-5.30	4.3E-16	-5.30	1.4E-24
3	Edema	-2.86	6.8E-11	-2.66	5.1E-12
4	oxidation of fatty acid	-2.24	1.3E-07		
5	oxidation of lipid	-2.17	1.2E-08		

Table 3.4.: *IPA Biological Functions in the LEL model (WG-DASL Assay).* Shown are IPA annotated biological functions with an absolute z-score of ≥ 2 (in at least one observation) and a Fisher's exact T-test adjusted P Value < 0.05. Rank in table was defined by z-score in Obs.1 and secondly in Obs.2. A list with all significantly enriched biological functions for all observations w/o z-score cut-off can be found on page A-62 ff. in the appendix.

	Molecule Type	LEL-M 5 h vs. TM 0 h All	+	-	LEL-M 17 h vs. TM 0 h All	+	-	LEL-M 17 h vs. LEL-M 5 h All	+	-
1	complex	20	19	1	23	20	3	1	1	0
2	cytokine	43	42	1	47	45	2	6	5	1
3	enzyme	19	12	7	18	12	6	0	0	0
4	g-protein coupled receptor	6	6	0	6	6	0	0	0	0
5	group	31	28	3	32	29	3	3	3	0
6	growth factor	27	27	0	22	21	1	1	1	0
7	ion channel	3	1	2	4	2	2	0	0	0
8	kinase	40	38	2	44	42	2	1	1	0
9	ligand-dependent nuclear receptor	3	1	2	2	1	1	1	1	0
10	mature microRNA	1	0	1	4	0	4	0	0	0
11	microRNA	6	0	6	4	0	4	0	0	0
12	other	28	24	4	38	29	9	1	1	0
13	peptidase	4	4	0	7	7	0	0	0	0
14	phosphatase	5	1	4	4	1	3	0	0	0
15	transcription regulator	63	46	17	76	53	23	1	1	0
16	translation regulator	0	0	0	1	1	0	0	0	0
17	transmembrane receptor	26	23	3	29	25	4	2	1	1
18	transporter	4	3	1	5	4	1	1	0	1

Table 3.5.: *IPA Upstream Regulator prediction in the LEL model (WG-DASL Assay).* Shown is the summary of the numbers of predicted upstream regulators (categorized by molecule type and observation) that had an absolute z-score ≥ 2 and a Fisher's exact T-test adjusted P.Val. < 0.05. A full list of members of the molecule type and their predicted activation can be found on page A-67 ff. in the appendix. +: upstream regulators predicted to be activated; -: upstream regulators predicted to be inhibited.

3.6. Protein synthesis is rapidly upregulated at the onset of intestinal inflammation

Given (1) the bioinformatic prediction of an upregulation of protein synthesis in the LEL model and (2) lack of information on the regulation of protein synthesis in LP cells in intestinal inflammation, I next investigated whether protein synthesis was upregulated in the LEL model at the onset of inflammation.

One way to study protein synthesis *in situ* is the so called Click-It® technology, where the alkyne analog of puromycin, Ortho-Propargyl-Puromycin (OPP), is rapidly

incorporated into newly synthesized proteins by binding covalently to nascent polypeptide chains, a reaction which can subsequently be detected by a copper(1)-catalyzed azide-alkyne cycloaddition. This method has so far only been applied in cell culture experiments and animal models and was in the context of this thesis established for human intestinal tissue. Please note, that if not specifically indicated otherwise, all immunohistochemical stainings in this thesis were performed on formalin fixed paraffin embedded (FFPE) tissue sections.

Remarkably, no OPP uptake and thereby protein synthesis was detectable in either untreated total mucosa (0, 5 or 17 h) or DTT treated mucosa (TM 2 h) under the experimental conditions employed (Figure 3.8). In contrast to TM mucosa, LEL mucosa showed high levels of protein synthesis, which were visible immediately after the first EDTA treatment (LEL-M 3 h), where approx. 5 % of all LP cells were OPP^+, increased to approx. 20 % at LEL-M 5 h and to 25 % at LEL-M 17 h. For details to semi-quantitative analysis of OPP^+ cells, see subsection 2.7.5 on page 31.

It is important to mention that in PBMCs, while they showed constitutive levels of protein synthesis without the need for stimulation, treatment with EDTA did not lead to an upregulation of protein synthesis (see page A-16 in the appendix). Additionally, while tissue samples were routinely incubated in RPMI medium for OPP treatment, incubation of LEL-M 5 h samples in HBSS, to rule out starvation effects, led to similar results (data not shown).
To further exclude that the lack of protein synthesis as seen in TM 0 h samples was caused by side-effects of surgery, Click-It® technology was performed on colon biopsies from patients undergoing colonoscopy for colon cancer screening. In line with the findings in TM 0 h samples, no constitutive protein synthesis was detected in these samples (data not shown).

In order to identify the cell types showing enhanced protein synthesis in the LEL model, immunohistochemical analysis was performed. This revealed that $CD68^+$ macrophages were among OPP^+ cells (Figure 3.10). Remarkably, IgA^+ cells were the cell population

that did show the most intense OPP signal, while there was no protein synthesis detectable in $CD3^+$ T cells (see page A-17 and A-18 in the appendix). Other cell populations were not investigated.

In summary, these findings show that the induction of the inflammatory response in the LEL model was associated with the rapid upregulation of protein synthesis in LP cells including macrophages and IgA^+ cells.

3.7. The mTOR pathway is upregulated in $CD68^+OPP^+$ macrophages at the onset of inflammation

Regulation of protein synthesis is commonly associated with mTOR. The previously performed IPA analysis identified upstream and downstream members of the mTOR pathway in the top list of predicted pathways (PI3K/AKT signaling, see Table 3.3) and predicted upstream regulators (EIF4E, see page A-9 in the appendix). To investigate the role of the mTOR pathway in the LEL model, I first examined the expression of mTOR via immunofluorescence. Indeed, mTOR was found to be strongly expressed in $CD68^+OPP^+$ macrophages over the whole duration of the LEL model (Figure 3.9). Given the high intensity of the mTOR signal in macrophages, all other cells appeared $mTOR^-$ under the employed settings. Immunofluorescent staining of frozen sections showed that $CD68^+$ macrophages did express phospho-$mTOR^{Ser2448}$ throughout the model (see page A-13 in the appendix).
Interestingly, both mTOR and phospho-$mTOR^{Ser2448}$ are concentrated in granular structures in LP cells under homeostatic conditions (TM 0h). However, following LEL, mTOR remained localized in these granular structures, although a distinct reduction of these structures was observed, while phospho-$mTOR^{Ser2448}$ revealed a more diffuse, cytoplasmic staining pattern. Investigations to further characterize the subcellular localization of mTOR, which has been tightly linked to its activation status [Betz and Hall, 2013], are ongoing.

(A)

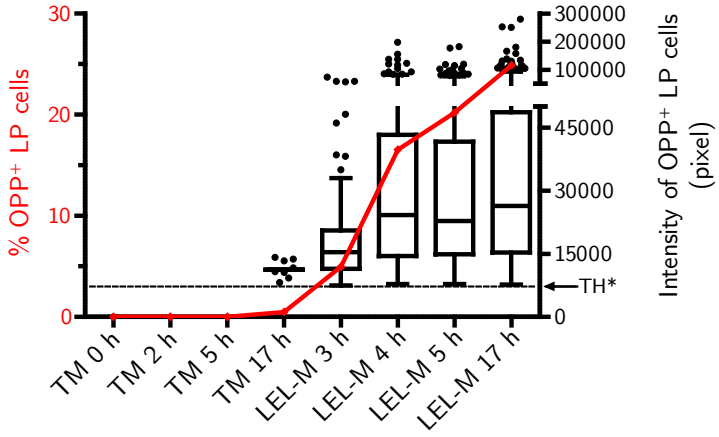
% OPP+ LP cells
30
20
10
0
300000
200000
100000
45000
30000
15000
0
TH*
Intensity of OPP+ LP cells (pixel)
TM 0 h
TM 2 h
TM 5 h
TM 17 h
LEL-M 3 h
LEL-M 4 h
LEL-M 5 h
LEL-M 17 h

(B)

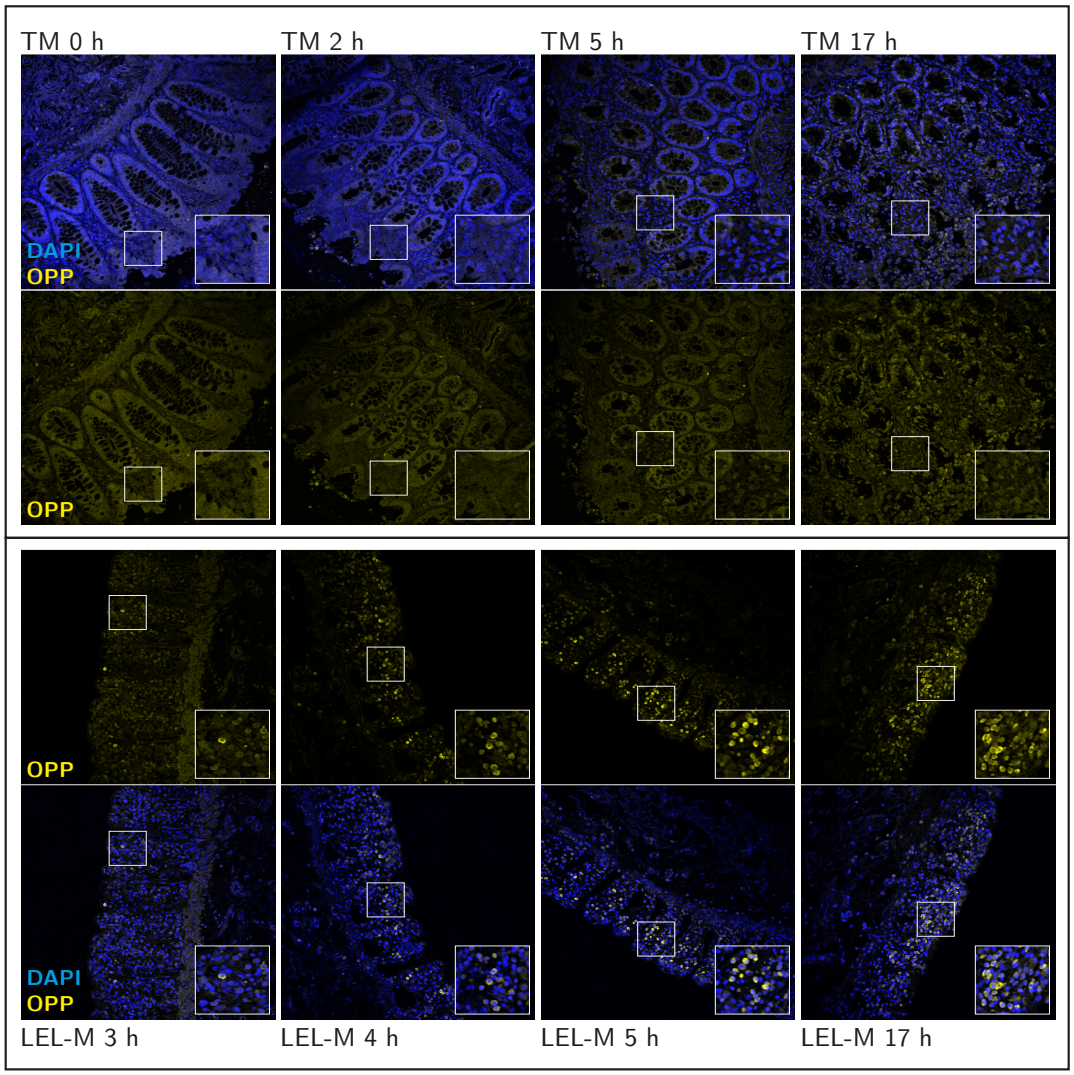
TM 0 h
TM 2 h
TM 5 h
TM 17 h
DAPI
OPP
OPP
OPP
DAPI
OPP
LEL-M 3 h
LEL-M 4 h
LEL-M 5 h
LEL-M 17 h

In accordance with mTOR expression, ribosomal protein S6 (RPS6), a known mTORC1 downstream target, was expressed constitutively throughout the LEL model (see page A-16 in the appendix). Phosphorylation of RPS6$^{Ser235/236}$ however was only upregulated after induction of inflammation by LEL, having its strongest expression at LEL-M 4 h and showed a partial overlap with the OPP Click-It® signal. Among cells that were strongly positive for phospho-RPS6$^{Ser235/236}$ were also CD68^{+}OPP^{+} macrophages (Figure 3.10).
In line with phosphorylation of RPS6$^{Ser235/236}$, phospho-Akt^{Ser473} expression in cryo sections was only detectable after the onset of inflammation, but not in homeostatic, total mucosa (see page A-14 in the appendix).

Taken together, the results indicated that the upregulation of protein synthesis is associated with the upregulation of the mTOR pathway at the onset of inflammation.

Figure 3.8. *(preceding page)*: *Mucosal protein synthesis in the LEL model.* Rate of protein synthesis was determined via OPP Click-It® technology. Results shown are from one representative experiment out of three independent experiments. (A) Percentage of OPP^{+} LP cells (red, left y-axis) and their pixel intensities shown as a Tukey boxplot (right y-axis) as determined by semi-automated particle analysis (for details see subsection 2.7.5 on page 31). A total of 1710 (± 351) cells were analyzed on average (using two images from distant section regions). All images were taken with the same microscope settings using a 20x objective. (B) Immunofluorescent images used for semi-quantification of protein synthesis rates (one of two analyzed images) is shown per time point). *TH, Minimum pixel threshold for analysis

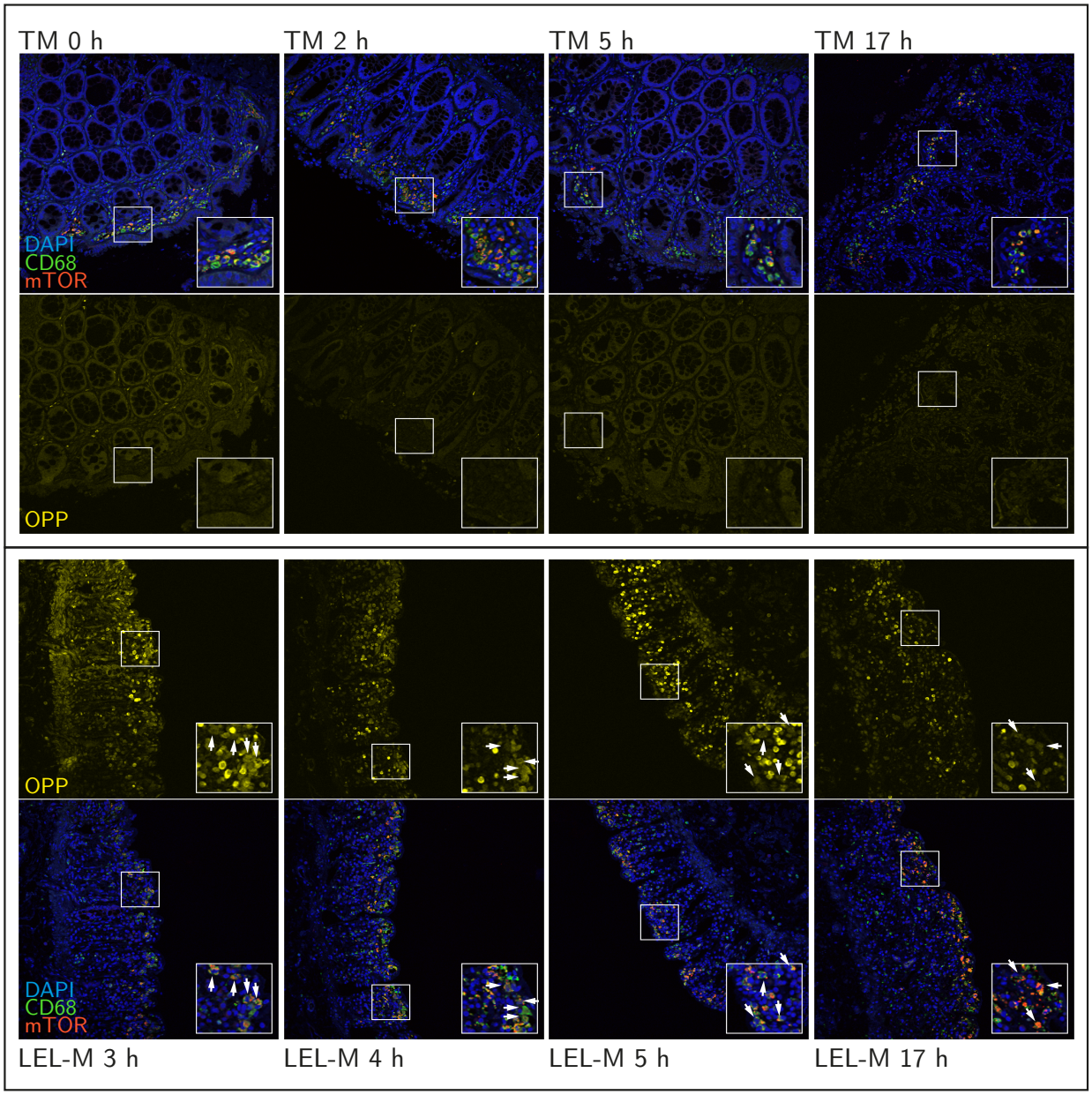

Figure 3.9.: *mTOR expression in CD68$^+$ macrophages and its correlation to protein synthesis in the LEL model.* Rate of protein synthesis was determined via OPP Click-It® technology. Results shown are from one representative experiment out of three independent experiments.

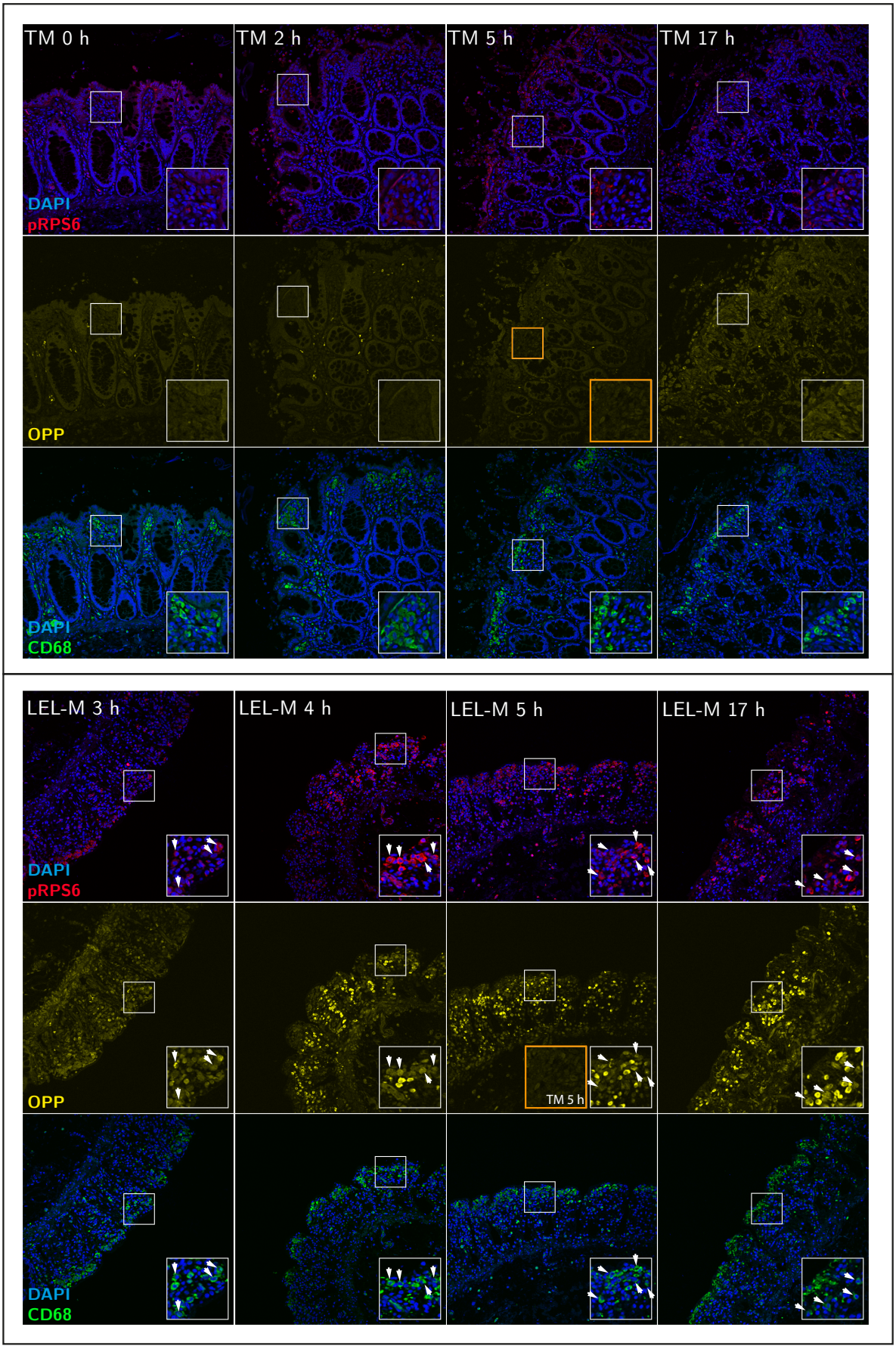
TM 0 h
TM 2 h
TM 5 h
TM 17 h
DAPI
pRPS6
OPP
DAPI
CD68
LEL-M 3 h
LEL-M 4 h
LEL-M 5 h
LEL-M 17 h
DAPI
pRPS6
OPP
TM 5 h
DAPI
CD68

3.8. Upregulation of protein synthesis in CD68$^+$ macrophages at the onset of inflammation is controlled by mTORC1

Given the parallel upregulation of both protein synthesis and activation of the mTOR downstream targets at the onset of inflammation, I next wanted to determine if the protein synthesis was actually controlled by the mTOR pathway. The LEL model was therefore performed in the presence of the mTORC1/2 inhibitor Torin1. The translation elongation inhibitor cycloheximide was employed as a control. 250 nM Torin1 were able to partially inhibit protein synthesis as indicated by a reduced OPP incorporation into these cells as well as by an approx. 30 % decrease in overall percentage of OPP$^+$ cells (Figure 3.11).

Importantly, Torin1 significantly inhibited protein translation in CD68$^+$ macrophages but not in IgA$^+$ cells (see Figure 3.12 as well as page A-17 in the appendix). As expected, RPS6 phosphorylation$^{Ser235/236}$ was inhibited in LP cells including CD68$^+$ macrophages following Torin1 treatment, confirming that this phosphorylation event is regulated by the mTOR kinase in the experimental system employed (Figure 3.12). In contrast, overall RPS6 expression levels were not much affected by treatment with this inhibitor, indicating that the decrease in RPS6$^{Ser235/236}$ phosphorylation was not a consequence of weaker RPS6 expression itself (see page A-16 in the appendix).

In summary, these findings suggest that the observed upregulation of protein synthesis at the onset of inflammation is partially controlled by the activation of the mTOR pathway.

Figure 3.10. *(preceding page)*: *mTORC1 target phospho-RPS6 expression in CD68$^+$ macrophages and its correlation to protein synthesis in the LEL model.* Rate of protein synthesis was evaluated via OPP Click-It® technology. Results shown are from one representative experiment out of three independent experiments.

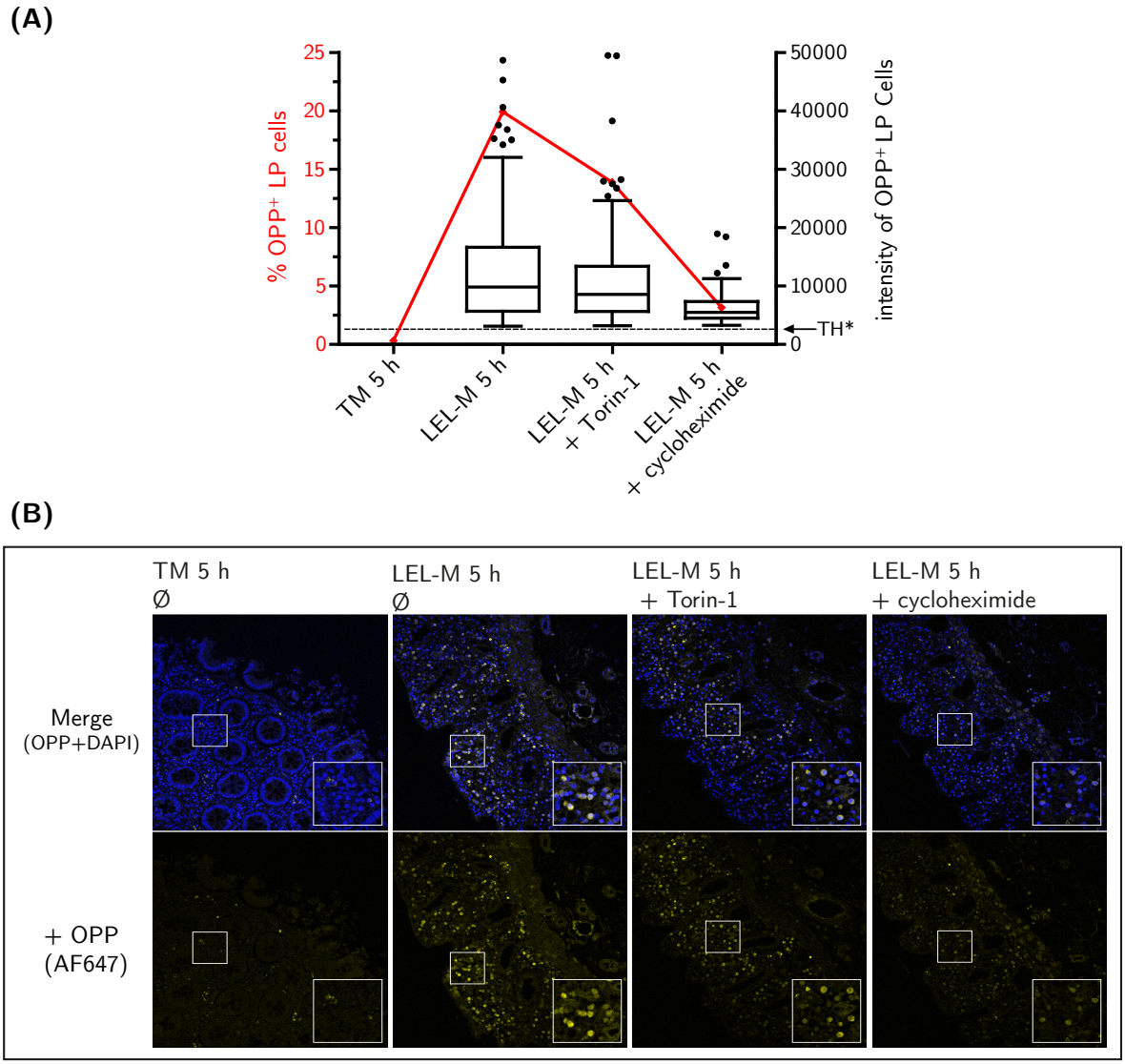

Figure 3.11.: *Impact of mTOR on regulation of protein synthesis in the LEL model.* The LEL model was performed in the absence or constant presence of the mTORC1/2 inhibitor Torin1 (250 nM) or cycloheximide (100 μg/ml). The rate of protein synthesis was evaluated at indicated time points via OPP Click-It® technology. Results shown are from one representative experiment out of three independent experiments. (A) Percentage of OPP$^+$ LP cells (red, left y-axis) and their pixel intensities shown as a Tukey boxplot (right y-axis). A small percentage of false-positive cells (indicated by negative controls w/o OPP) was subtracted as background. Remaining percentage of OPP$^+$ cells in timepoint TM 5 h was only 0.36% and therefore not plotted on boxplot. On average, 1690 ($\pm$ 297) cells were analyzed per time point. (B) Immunofluorescent images used for semi-quantification (one of two analyzed images is shown per time point). The corresponding negative controls can be found on page A-19 in the appendix.

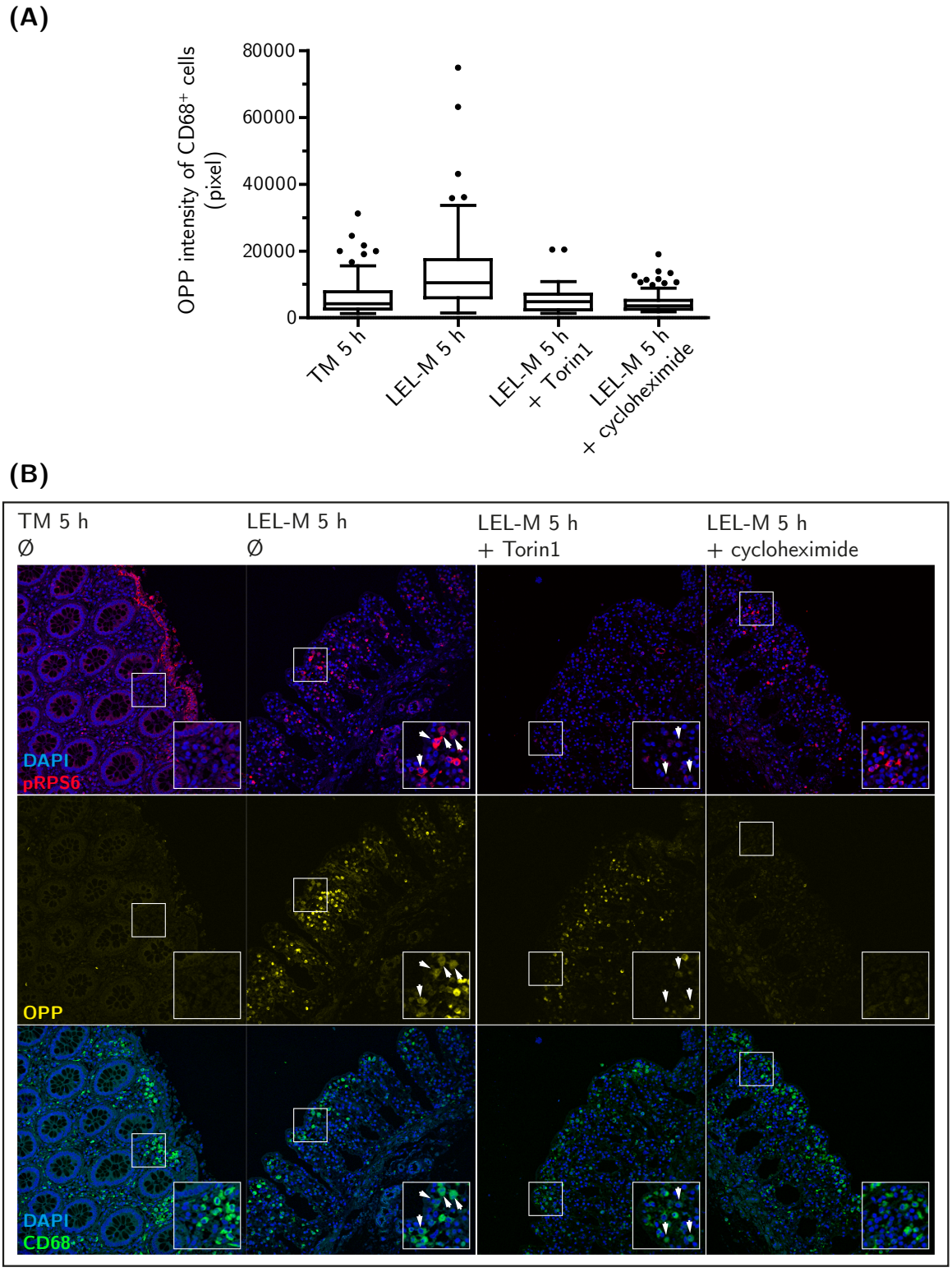

Figure 3.12.: *Association of upregulation of protein synthesis with RPS6$^{Ser235/236}$ phosphorylation in the LEL model.* Rate of protein synthesis was determined via OPP Click-It® technology). Specified inhibitors (250 nM Torin1 and 100 μg/ml cycloheximide) were present at all times. Results shown are from one representative experiment out of three independent experiments. (A) Semi-quantification of OPP intensity in CD68$^+$ macrophages shown as a Tukey boxplot. On average, 827 ($\pm$ 194) cells were analyzed per time point. (B) Immunofluorescent images used for semi-quantification.

3.9. mTORC downstream targets are upregulated in myeloid cells following their emigration out of the lamina propria

In the recent sections, the impact of mTOR on the upregulation of protein synthesis in LP cells including macrophages after the onset of inflammation was demonstrated *in situ*. Mahida *et al.* [1997] showed that the loss of the epithelial layer is associated with a massive emigration of macrophages, eosinophils, B cells as well as T cells out of the LP. In addition, previous work from our group was able to show, that in the LEL model, these emigrated cells show the induction of inflammatory markers [Szikszai *et al.*, 2015]. In this section, the activation state of the mTOR pathway in mononuclear cells that emigrated out of the LP (LPMCs) during the 12 h organ culture following LEL (LEL-M 5 - 17 h) was analyzed.

To this end, the phosphorylation levels of these emigrated intestinal LPMCs for the downstream targets RPS6$^{Ser235/236}$ (mTORC1), 4E-BP1$^{Thr37/46}$ (mTORC1) and AKT^{Ser473} (mTORC2) as well as mTOR^{Ser2448} itself were investigated. Due to the previously described methodological inability to isolate LPMCs from total mucosa samples without their activation, nonstimulated allogeneic PBMCs were utilized to define a basal phosphorylation level of the investigated targets (Figure 3.13).

Of the investigated CD45$^+$ cell populations, LP myeloid cells (CD33$^+$HLA-DR$^+$) showed the highest expression levels for phospho-mTOR^{Ser2448} as well as mTORC1 downstream targets. Notably, CD14$^-$ vs. CD14$^+$ expression levels within the myeloid cell population were slightly higher for both mTORC1 downstream targets, while they were decreased for phospho-AKT^{Ser473} expression (Figure 3.13).
CD19$^+$CD20$^+$ B cells did show an intermediate expression for phospho-mTOR^{Ser2448} as well as mTORC1 downstream targets, while CD3$^+$ T cells showed the lowest expression for all targets investigated. LP B cells did on average express the highest levels of

mTORC2 target phospho-AKT^{Ser473} among investigated cell populations (Figure 3.13).

In comparison to PBMCs, the LPMCs expression levels of the investigated targets showed differences based on cell population (Figure 3.13):
In CD33$^+$HLA-DR$^+$CD14$^+$ myeloid cells, the expression of phospho-RPS6$^{Ser235/236}$ was on average nearly five fold higher in LPMCs compared to PBMCs, while phospho-AKT^{Ser473} expression was increased nearly three fold on average.
In CD19$^+$CD20$^+$ B cells, phospho-RPS6$^{Ser235/236}$ expression was four fold higher in LPMCs vs. PBMCs, while 4E-BP1$^{Thr37/46}$ phosphorylation was three fold higher. Remarkably, phospho-AKT^{Ser473} was expressed seven fold higher in CD19$^+$CD20$^+$ LPMCs than PBMCs. There was no evident difference regarding the expression of phospho-mTOR^{Ser2448} based on cell origin.
Notably, there were no reproducible differences between PBMCs and LPMCs phosphorylation levels in CD3$^+$ T cells for any of the targets investigated.

In summary, the observed phosphorylation levels of mTORC downstream targets in LPMCs vs. PBMCs indicated the activation of the mTOR pathway in myeloid as well as B cells, while this was not evident for T cells. Note, however, that there are several distinct phosphorylation sites for the investigated targets which were not investigated.

To determine the responsiveness of the different LP cell populations towards mTOR inhibition, the phosphorylation state of the downstream targets after the constant presence of 250 nM or 1 μM Torin1 throughout the LEL model was investigated (Figure 3.14). As in *in situ* experiments, cycloheximide was used as a control; however, given the longer presence of the inhibitors compared to previous experiments, 10 μg/ml instead of 100 μg/ml cycloheximide were employed to prevent the induction of apoptosis. Please note, that 10 μg/ml were still sufficient to suppress protein synthesis at LEL-M 5 h *in situ* (data not shown).
Expression of the phosphorylation state of mTOR downstream targets as well as mTOR itself was investigated as in Figure 3.13. As can be seen in Figure 3.14, the lower dose of Torin1 (250 nM) was already within the saturation area, as the higher dose could not

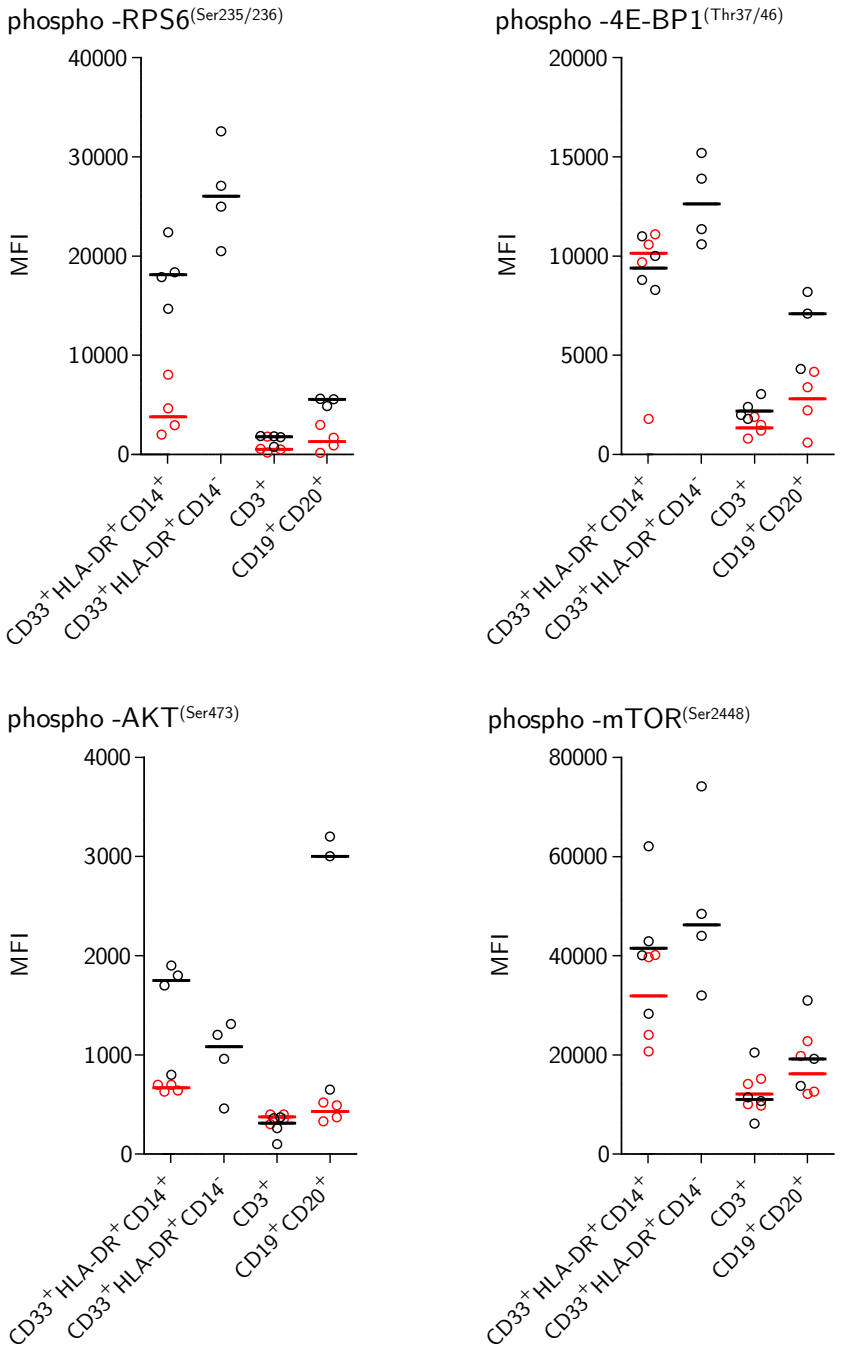

Figure 3.13.: *Expression of mTOR downstream targets in emigrated LPMCs in the LEL model.* LPMCs were isolated at LEL-M 17 h. As a comparison, allogeneic PBMCs from healthy donors were stained for same markers as LPMCs (red). $CD19^{+}CD20^{+}$ cells were identified using a common fluorochrome channel. Shown are the results of four independent experiments. The line indicates the median of the replicates.

increase the effects seen on any of the investigated downstream targets. The calculated percentages below are therefore referring to the effects of the lower dose. Note, that there was no reproducible effect of Torin1 on phospho-mTOR^{Ser2448} expression in any of the investigated cell populations.

CD33^{+}HLA-DR^{+} myeloid cells were the cell population which was most responsive towards Torin1 mediated mTOR inhibition: Phospho-RPS6$^{Ser235/236}$ expression was decreased by an average of 80 %, while the expression of phospho-4E-BP1$^{Thr37/46}$ was even reduced by 90 % in the presence of Torin1. While there was no difference in responsiveness in the investigated myeloid subpopulations towards mTORC1 downstream targets, phospho-AKT^{Ser473} expression was decreased by 47 % in CD14^{+}, but by only 35 % in CD14^{-} myeloid cells.

In CD19^{+}CD20^{+} B cells, the expression of the two investigated mTORC1 targets showed a similar decrease of 68-69 % on average. The reduction of phospho-AKT^{Ser473} expression in the presence of Torin1 varied to some extent with an average decrease of 40 %.

Finally, CD3^{+} T cells did show the lowest response towards Torin1 mediated mTORC1 inhibition with a 25 % decrease of phospho-RPS6$^{Ser235/236}$ expression, although Torin1 was able to decrease the expression of phospho-4E-BP1$^{Thr37/46}$ by 77 %. Phospho-AKT^{Ser473} expression in this cell population was not affected by Torin1.

Taken together, the results showed that Torin1 mediated inhibition had most impact on mTORC1 targets and that the myeloid cell population overall was the cell population most affected by this inhibition. These findings were in line with the ability of Torin1 to suppress overall phospho-RPS6$^{Ser235/236}$ expression *in situ*. Furthermore, the high responsiveness of the myeloid cell compartment in comparison to the other investigated cell populations stands in accordance with the high expression of mTOR solely in CD68^{+} cells *in situ*.

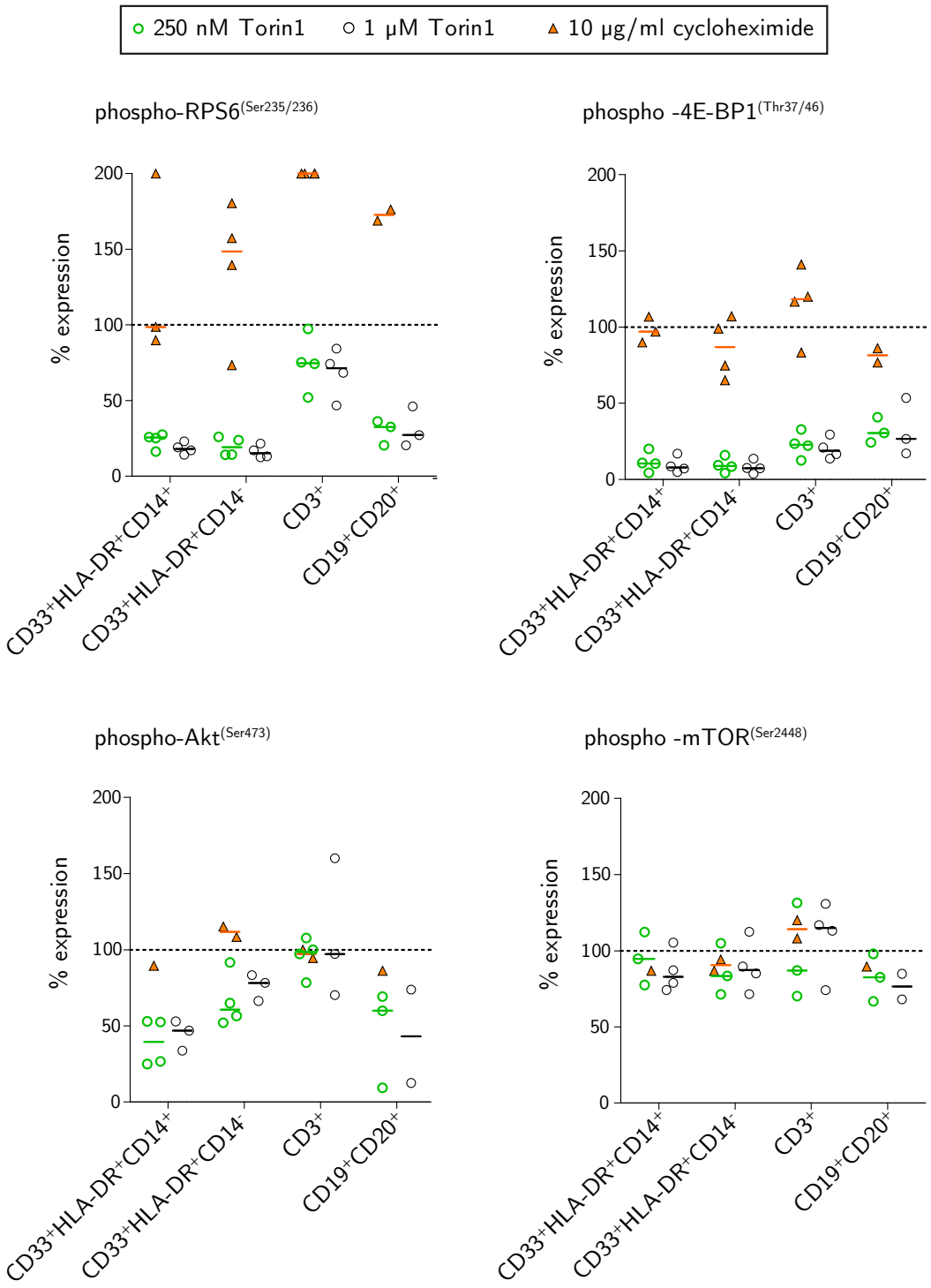

Figure 3.14.: *Effect of mTOR inhibition on emigrated LPMCs in the LEL model.* LPMCs were isolated at LEL-M 17 h. Indicated inhibitors were present at all times during the performance of the LEL model. $CD19^+CD20^+$ cells were identified using a common fluorochrome channel. Shown are the results of four independent experiments. Absolute MFI expression values of LPMCs in the absence of an inhibitor of the same experiments are shown in Figure 3.13 and were set as 100 % expression in this figure. The line indicates the median of the replicates.

3.10. mTOR differentially regulates the secretion of inflammatory mediators during the initiation of an inflammatory response in the LEL model

Finally, to determine the functional impact of mTOR pathway activity on inflammtory effector functions of LP cells, the effect of Torin1 exposure on secretion of inflammatory cytokines and chemokines was analyzed. For this purpose, the LEL model was performed in the absence or presence of 250 nM Torin1 or 10 μg/ml cycloheximide. Supernatants were collected after 12 h of organ culture (LEL-M 17 h) and subjected to Luminex® multiplex analysis. Cytokines were selected for analysis based on the upregulation of corresponding genes in the LEL model. In addition, the secretion levels of IL-18 and MIF, cytokines constitutively expressed in the LP and secreted upon stimulation, were investigated. As shown in Figure 3.15, Torin1 treatment resulted in a 26 % - 58 % inhibition of all chemokines investigated except for IL-8, which together with the cytokines IL-6, IL-1β and ICAM-1 provided inconclusive results. IL-18 and VEGF secretion levels were both decreased by approx. 50 % upon Torin1 treatment. In contrast, M-CSF and MIF secretion levels were upregulated by 10 % and 30% , respectively, after exposure to Torin1. The mTOR inhibitor did not affect the secretion levels of CD14, CD163 and MMP12 (see page A-21 in the appendix).

In summary, these results demonstrate that mTOR controls the secretion of chemokines during the initiation of the inflammatory response in the LEL model. However, the upregulation of two pro-inflammatory cytokines after Torin1 treatment suggest that the mTOR pathway has an bidirectional role in the mediation of the inflammatory response in the LEL model.

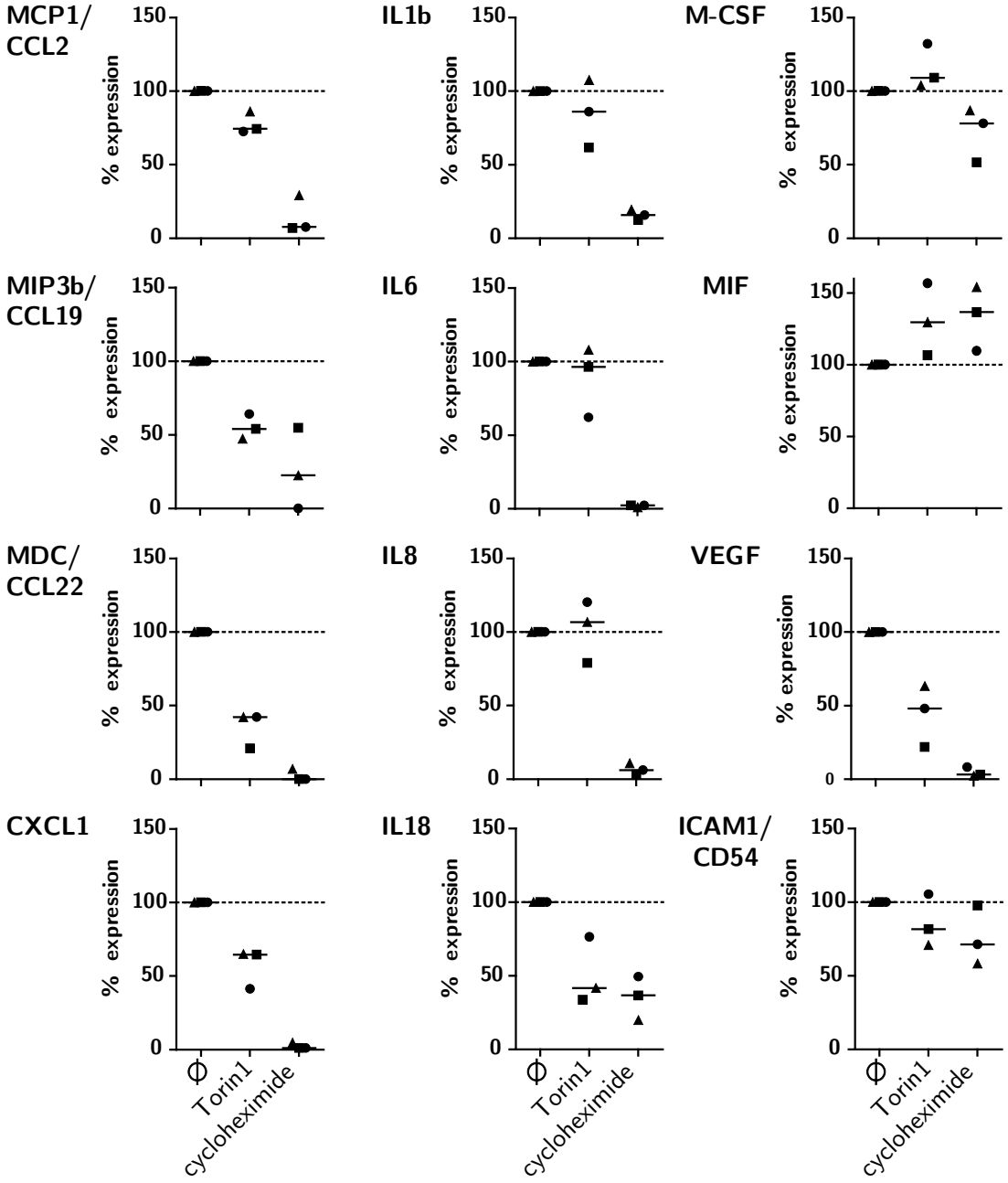

Figure 3.15.: *Impact of mTOR on the secretion of soluble factors after the onset of intestinal inflammation in the LEL model.* At LEL-M 5 h, defined tissue punches were incubated for 12 hours. Supernatants were then subjected to Luminex® multiplex analysis. Graphs show relative expression values with LEL-M 17 h without inhibitor set to 100 %. Inhibitors (250 nM Torin1, 10 μg/ml cycloheximide) were present throughout the model. The line indicates the median of the replicates. The corresponding absolute expression values can be found on page A-20 in the appendix.)

4. Discussion

Inflammation is commonly defined as an adaptive response to infection or tissue damage and is thought of having evolved in order to ultimately restore homeostasis [Medzhitov, 2008]. However, if this acute inflammatory response is not able to eliminate the initial cause of inflammation, i.e. because of genetic variants in the host or the severity of inflammation, the initially controlled inflammation persists in a then uncontrolled, pathological and chronic manner. In order to deepen our understanding of chronic inflammatory diseases such as IBD, it is essential to understand the mechanisms of the inflammatory response at its early time points as well as the reasons why in some individuals the acute inflammatory response fails to restore homeostasis and thus becomes chronic. In the intestine, where immune cells such as myeloid cells are known to be hyporesponsive under homeostatic conditions, appropriate experimental models for studying early inflammatory events in these cells are limited and thus little is known as to why and how these cells undergo activation.

In this thesis, I sought to understand the early molecular mechanisms underlying the activation of lamina propria (LP) cells, in particular immune cells, in an acute intestinal inflammation. To address this, first, the LEL model was validated as a physiological appropriate and relevant acute inflammation model by global gene expression analysis in comparison to existing IBD patient data. Second, the inflammatory response as initiated by the LEL model was characterized by the identification of canonical pathways, biological functions and potential upstream regulators by means of Ingenuity Pathway Analysis. Third, a rapid increase in protein synthesis was identified as an initial inflammatory process in LP immune cells and it was shown that this phenomenon was associated with the upregulation of the mTOR pathway. Fourth, by employing functional studies, it was demonstrated that the increased protein synthesis was partially

mediated by an upregulation of the mTOR pathway in LP cells, in particular myeloid cells. Finally, the investigation of the contribution of the mTOR pathway to the induction of the inflammatory response in these cells led to the observation of a bifunctional role of mTOR with both pro- and anti-inflammatory aspects.

4.1. The LEL model as a tool to study initial intestinal inflammation

Currently, the regulation of intestinal inflammatory events is mostly studied employing murine models. Models in the murine system possess a common genetic and environmental background between subjects and offer a broad spectrum of experimental approaches. Yet, the immune systems of mouse and man are clearly dissimilar, both in general and particular with regard to the intestine [Gibbons and Spencer, 2011; Mestas and Hughes, 2004; Zschaler *et al.*, 2014]. Human studies are often limited to first isolating cells and then stimulating them *ex vivo*, which takes these cells out of their natural environment. In this thesis, a human organ culture model, the LEL model, was characterized as a tool to study the process of early acute inflammation in LP (immune) cells of the human intestinal mucosa.

To investigate, whether earlier results of our group regarding the upregulation of pro-inflammatory cytokines in the LEL model reflected the initation of a global inflammatory response, first, global gene expression analysis from LP cells isolated by laser-capture microdissection (LMD) was performed. The data generated represents the first global gene expression analysis of LP samples existing under homeostatic (and uninflamed) conditions *in situ*. All published gene expression data of intestinal cells so far were either derived from total mucosa or LPMCs isolated not only by enzymatic digestion but also release of epithelial cells by EDTA treatment [Rogler *et al.*, 1998]. In line with the results of this thesis, LPMCs isolated by the former protocol from healthy mucosa express inflammation-associated molecules (e.g. CD14, CD86), which are not expressed by these cells under homeostatic conditions *in situ* (Rugtveit *et al.* [1997] and unpublished data). These findings indicate that these cells do not remain in a resting

state upon using such isolation methods.

The induction of a global intestinal inflammatory response in the LEL model

The global gene expression analysis in accordance with the markers investigated previously, showed the induction of a global inflammatory response after loss of the epithelial layer (LEL-M 5 h and 17 h), evident by the following findings:

(1) Pro-inflammatory genes were upregulated, i.e. *IL6*, *IL8*, *ATF3* (Activating Transcription Factor 3), *CXCL2*, *CCL21* and *CSF3* [Gruys *et al.*, 2005].

(2) Many pro-inflammatory pathways and functions were predicted to be activated (pathways: 'IL-1 Signaling', 'IL-6 Signaling', 'IL-8 Signaling', 'Acute Phase Response Signaling', 'Leukocyte Extravasation Signaling', 'B Cell Activating Factor Signaling' and 'LPS/IL-1 Mediated Inhibition of RXR Function',...; Biological Functions: 'function of blood cells', 'stimulation of cells', 'function of leukocytes','adhesion of blood cells', 'invasion of cells', 'chemotaxis', 'function of antigen presenting cells',...).

(3) Pro-inflammatory cytokines among predicted upstream regulators were predicted to be activated, while anti-inflammatory cytokines such as IL1RN and IL10 were predicted to be inhibited.

The inflammatory response as observed in the LEL model was very similar between observations (Obs.1: LEL-M 5 h vs. TM 0 h; Obs.2: LEL-M 17 h vs. TM 0 h; Obs.3: LEL-M 17 h vs. LEL-M 5 h), although there also existed differences: Genes, whose expression was highly upregulated for Obs.1, but to a lower extent for Obs.2, mainly included early response mediators as the IFN-γ regulator *IRF7* (known to be repressed by nonphosphorlyated 4E-BP1, [Colina *et al.*, 2008]) and *NR4A1*(nuclear receptor subfamily 4, Group A, Member 1). *NR4A1* (also known as NUR77) encodes a protein involved in TLR-IL1R signalling by interacting with TRAF6. Variants of the *NR4A1* gene resulting in lower protein expression are associated with a higher risk for IBD. Accordingly, deficiency in NUR77/NR4A1 expression increases the susceptibility of

mice to DSS-colitis [Wu *et al.*, 2016].

In contrast, several anti-inflammatory mediators were upregulated solely for Obs.2, one of which is the IL1 receptor antagonist *IL1RN* (also known as *IL1RA*). The importance of the anti-inflammatory role of *IL1RN* has been indicated in intestinal inflammation by the spontaneous development of colitis in $Rag2^{-/-}Il1rn^{-/-}$ mice [Akitsu *et al.*, 2014]. The role of IL1RN, which was upregulated in the UC vs. NC dataset of Granlund *et al.* [2013], in human chronic intestinal inflammation is less clear, as several studies came to contradicting conclusions regarding the association of *IL1RN* mutations with IBD depending on the ethnic background in the group investigated [Craggs *et al.*, 2001; Daryani *et al.*, 2015; Lopez-Hernandez *et al.*, 2015; Mittal *et al.*, 2005]. Remarkably, IL1RN was predicted to be an inhibited upstream regulator by IPA, indicating potential posttranscriptional regulation of its expression.

The physiological relevance of the LEL model

The comparison of the gene expression data as obtained in the LEL model with the Granlund *et al.* [2013] analysis of gene expression data from UC vs. NC mucosa revealed a significant overlap (adj.P.Val < 0.001) between both data sets and thus supports the physiological relevance of the LEL model (see Figure 3.7 on page 49).
A complete overlap could not be expected, due to the following reasons:

(1) The LEL model reflects the earliest stages of acute intestinal inflammation, whereas UC mucosa usually represents chronic stages.

(2) UC patients receive anti-inflammatory treatment that affects their gene expression levels.

(3) The UC vs. NC datasets are based on gene expression profiling of biopsies consisting of total mucosa, but not on the compartment-specific analysis of LP.

(4) Recruitment of immune cells from the peripheral blood to the LP cannot occur in the LEL model.

(5) The inflammatory response in UC patients may be dysregulated due to genetic variants identified to be linked to IBD by GWAS studies [Jostins *et al.*, 2012].

The clinical relevance of genes observed to be differentially regulated in the LEL model vs. UC needs to be further explored, in particular with regard to initial mucosal inflammatory processes. Notably, a potential involvement of some of these genes in human intestinal inflammation *in vivo* is suggested by the fact that they have been prioritized as key genes linked to IBD susceptibility loci as identified by a GWAS [Jostins *et al.*, 2012]. One of these genes, which has not been characterized in UC before and may hence be interesting for further investigations is *FOSL1*, a member of the AP1 family of transcription factors. Its overexpression in mice was shown to have a beneficial effect on DSS-induced colitis [Karin *et al.*, 1997; Takada *et al.*, 2010].

Additional evidence for the physiological relevance of the LEL model exists since many of the upregulated pathways observed here are also associated with IBD pathogenesis such as 'IL-8 signaling', 'HMGB1 Signaling', 'Wnt/Ca^+ pathway' [Mazzucchelli *et al.*, 1994; Hu *et al.*, 2015; Serafino *et al.*, 2014].

Reflection on the potential of the LEL model to study intestinal inflammation

The potential of the LEL model lies within its possibility to study molecular mechanisms underlying the initiation of an inflammatory response in human LP cells during the very first hours. In particular, it allows to study the switch from a hyporesponsive to an inflammatory state in resident LP cells.

While the initiation of inflammation with the treatment of EDTA is obviously artificial, the duration of the EDTA treatment itself is short (3x 30 min with intermittent washing) and inflammation is initiated rapidly.

EDTA as a calcium chelator leads to the detachment of the epithelial layer by removing the tight junctions of the epithelium. Thus, in contrast to DSS-induced colitis, where epithelial cells undergo necrosis, the epithelial cells themselves remain intact. As they are removed by washing steps in between EDTA treatments and because of the high volume/tissue ratio of the employed solutions, the influence of potential secreted factors

by the epithelium on LP cells is limited. Analysis of epithelial cells, isolated prior to and after detachment, did not reveal major changes in gene expression levels (nCounter Assay, data not shown), providing further evidence speaking against their impact on the induction of the intestinal inflammation as observed in the LEL model. Studies regarding the protein expression levels of the epithelium in the LEL model should be undertaken in the future.

The possibility of EDTA causing the inflammatory response in the LEL model cannot be completely ruled out. However, the treatment of PBMCs with EDTA does not lead to increased levels of investigated cytokines *IL6*, *IL8*, *IL1B* and *IL23A* [Schröder-Braunstein *et al.*, 2014]. Additionally, protein synthesis, as detected via OPP Click-It® technology, was not increased in EDTA treated PBMCs vs. HBSS treated PBMCs (see Figure A.12 on page A-16 in the appendix). Also, being a calcium chelator, EDTA rather leads to a decreased inflammatory response as calcium is needed for the activation of many inflammatory pathways i.e. the complement system.

Difficulties of the LEL model consist - as in all human models - of variances between individuals based on different genetic and environmental backgrounds, as well as age differences. Furthermore, in comparison to murine models, the possibilities of performing functional studies in the LEL model are limited, although possible, as was shown in this thesis.

Importantly, as the LEL model is an *ex vivo* organ culture model, investigations are focused on resident LP cells, since a recruitment of cells from the circulation is not possible. There is an ongoing debate, whether resident LP cells are capable of mounting an inflammatory response or if this event is mediated completely by the recruitment of circulatory immune cells [Mowat and Agace, 2014]. Utilizing the LEL model, here it was demonstrated that a vigorous inflammatory response indeed can be initiated in human resident LP cells. This finding was not totally unexpected, given that these cells function as the first line of defense.

Experimental and bioinformatic challenges and considerations

During LMD sample collection, the RNA in the LP samples was partially degraded as indicated by a RNA integrity number (RIN) < 7. LMD is a time consuming process, a factor that negatively affects RNA integrity. Even RNA isolation of whole tissue sections immediately after their preparation without prior LMD did not result in enhanced RNA quality (data not shown), leading to the conclusion that the RNA in the tissue was already degraded prior to sectioning. LP consists of loose tissue, making it more vulnerable to RNA degradation by extracellular RNases in comparison to the epithelium, where the RIN remained above 7 even after LMD (data not shown). Alternatively, the observed RNA degradation could represent side-effects of surgery. To my knowledge, there are no publications available that specifically address LP RNA quality, although two recent publications showed the tendency to RNA degradation in total colonic mucosa tissue even if mucosal samples were flash frozen immediately after resection [Heumuller-Klug *et al.*, 2015; Bao *et al.*, 2013].
Fortunately, the low RNA quality had no effect on the reliability of the WG-DASL Assay, as this assay allows the analysis of partially degraded RNA and is even compatible with RNA isolated from FFPE tissue, which is undergoing a much more severe degradation than the flash frozen samples used in this thesis.

Among the top downregulated genes in the WG-DASL and nCounter Assay, there were also known epithelium associated genes as KRT20 and PIGR [Uhlen *et al.*, 2015], indicating epithelial contamination in the LP samples. This was most likely caused by morphologically not distinguishable layers of evolving crypts beneath the microdissected LP. The downregulated genes were still included in the pathway analysis of IPA in order to gain a broader spectrum of potentially involved pathways and an indication towards their activation state. As many genes are expressed in both epithelium and LP, it was not possible to filter out epithelium-specific genes.

Regarding the robustness of the predicted results of the pathway analysis, a main limitation in general is that the prediction is limited to known pathways and the extent

of findings in the background database. Pathways involving hotspot research areas as cancer - filtered out in my analysis - have a higher chance of being detected in contrast to research areas that do not receive such broad attention or are difficult to access due to i.e. methodological reasons. Finally, if pathways involved in similar biological processes regulate overlapping sets of genes, they will both be detected and thus can lead to 'false-positive' conclusions. Finally, IPA is based on transcription levels only and remains a bioinformatic analysis.

4.2. The rapid upregulation of protein synthesis in the LEL model

In line with the high level of upregulation of gene expression at the onset of inflammation in the LEL model, the majority of predicted transcription factors known to positively regulate transcription, were predicted to be activated.

Interestingly, among upregulated genes, not many were explicitly associated with active translation. However, many of the predicted pathways, functions and upstream regulators were in some way or other associated with upregulated protein synthesis, thus indicating potential regulation of translation factors on a post-transcriptional level. For pathways, these were 'HMGB1 Signaling', 'FGF Signaling', 'PI3K/AKT Signaling'. Functions relying on anabolic events predicted to be activated were 'cell survival' and 'proliferation of cells', while functions involved in catabolism as 'oxidation of fatty acid' and 'oxidation of lipid' were predicted to be inhibited. In line with these results, miRNAs among predicted upstream regulators were uniformly presumed to be inhibited. Additionally, the only predicted translation factor, EIF4E, was presumed to be activated. Furthermore, many of the kinases predicted to be activated are actually involved in protein synthesis and 'phosphorylation of protein' was predicted as an activated function for Obs.2.

In accordance with this indicated potential regulation of protein synthesis on a post-transcriptional level, preliminary mass spectrometry results of LMD LP samples showed an enrichment in proteins which have RNA binding capacity (data not shown).

In this study, it was shown for the first time that - under the experimental conditions employed - constitutive protein synthesis in both LP and epithelium in total human colonic mucosa is low under homeostatic conditions by utilizing OPP Click-It® technology. In comparison, PBMCs showed a high level of constitutive protein synthesis without prior stimulation in the same experimental setting (see Figure A.12 on page A-16 in the appendix). In contrast, the observed ability of resident LP cells to rapidly upregulate protein synthesis after LEL demonstrated that these cells despite their anergic state under homeostatic conditions, are able to rapidly mount a vigorous response at the onset of inflammation.

In humans, protein synthesis under inflammatory conditions in the human intestine has so far only been investigated in total mucosa of IBD patients, but not specifically in the LP and under acute inflammatory conditions. Recently, Liu *et al.* [2012] introduced the in this thesis utilized OPP Click-It® technology. In accordance with the findings observed in this thesis, Liu *et al.* [2012] found no active protein synthesis in the LP in the small intestine of rats under homeostatic conditions. In contrast to the findings of this thesis, the group found positively stained OPP Click-It® positive cells in the same intestinal region within crypts and at the base of intestinal villi. However, in addition to investigating a different intestinal region in a different organism, they injected 100 μl of 20 mM OPP intraperitoneally and incubated for 1 h before tissue harvesting, whereas here, a 1000 fold lower dose (20 μM) was employed with an incubation period of only 30 min. It is therefore possible that ongoing protein synthesis in the epithelium in human TM samples investigated in this thesis was below the detection limit. The inability to detect protein synthesis in the epithelium in the conducted experiments, despite the known high turnover rates in this compartment [Lipkin *et al.*, 1963], sets the relative level of initiated protein synthesis in the LP after LEL into a new perspective. In accordance with the observation of this thesis, Liu *et al.* [2012] after investigating protein expression in rat liver, kidney and spleen, found the highest expression in hepatocytes and spleen, whereas protein synthesis in the homeostatic small intestine was comparatively low.

The possibility of several other factors being responsible for both lack of protein synthesis under homeostatic conditions as well as its induction after LEL by EDTA treatment were ruled out by a series of control experiments.

(1) The positive correlation between the observed OPP Click-It® signal and level of protein synthesis was demonstrated by the ability of the translation elongation inhibitor cycloheximide to almost completely suppress it.

(2) Side-effects of surgery were ruled out by the absence of detectable protein synthesis in biopsies taken from healthy individuals undergoing a routine endoscopic procedure.

(3) 'Starvation-nutrition' induced protein synthesis, caused by the necessary soberness of patients before medical procedure and the subsequent presence of nutrition during OPP treatment performed in RPMI medium, were excluded by the following control experiments: On the one hand, TM punches failed to exhibit an OPP Click-It® signal after incubation in either HBSS or RPMI medium for 3 h. On the other hand, an induction of protein synthesis was detectable, even if OPP treatment of the sample at LEL-M 5 h was performed in HBSS instead of RPMI medium. Accordingly, previous studies have shown that the intestine is not very sensitive to short term starvation [Adegoke *et al.*, 1999].

(4) EDTA itself as the inducer of protein synthesis rather than the LEL caused by the EDTA treatment was ruled out by the lack of significant difference in the achieved OPP Click-It® signal in PBMCs following their incubation in either EDTA/HBSS, HBSS or RPMI medium, respectively.

4.3. The mTOR pathway

mTOR is known to represent a master regulator of both transcription and translation. Whereas the pathway itself with an activation z-score of 1.3 for Obs.2 was not among the predicted activated pathways in IPA and the majority of its known members

not differentially regulated in the LEL model, there was substantial evidence for an involvement of the mTOR pathway in the LEL model on the level of gene expression: mTOR is known to phosphorylate and inactivate translation inhibitor 4E-BP1 upon its activation. Accordingly, 4E-BP1 target *IRF7* was among the top 50 upregulated genes for Obs.1 in the LEL model [Colina *et al.*, 2008]. Furthermore, expression of translation initiator EIF4E, known to bind to and be inhibited by hypophosphorylated 4E-BP1, was induced after the onset of inflammation and among predicted activated upstream regulators.
Finally, *RERGL*, a paralog of *RHEB* and the only gene significant for Obs.1, but not Obs.2 among the top 50 upregulated genes, encodes a protein that is required for mTORC1 activation on the lysosomal membrane [Kim *et al.*, 2008].

Furthermore, the induction of the mTOR pathway in the LEL model was suggested by the predicted activation of (1) mTOR activating upstream pathways 'PI3K/AKT', 'Protein Kinase A', 'HMGB1' and 'iNOS' signaling [Nobukuni *et al.*, 2005; de Joussineau *et al.*, 2014; Yang *et al.*, 2012; Lopez-Rivera *et al.*, 2014] and (2) positively regulated mTOR downstream pathways such as 'FGF' and 'WNT' signaling [Matsuo *et al.*, 2007; Inoki *et al.*, 2006].
Finally, the serine kinase IKBKB, a major downstream target of the TNF-α signaling pathway and activator of mTOR signaling kinase activity (through suppression of the mTOR inhibitor TSC1 [Lee *et al.*, 2007]), is the predicted top upstream regulator among the group kinases for both Obs.1 and Obs.2.

4.3.1. The activation of the mTOR pathway in the LEL model

$CD68^+$ macrophages - under the employed conditions - exclusively and strongly express mTOR throughout the LEL model. This is in line with the results of Latella *et al.* [2013], who showed the expression of total mTOR at the apical border of the murine colonic LP in healthy control mice, an area almost exclusively populated by macrophages, thus confirming my results both regarding cell type specificity and constitutive expression of mTOR. Accordingly, the importance of mTOR signaling in myeloid cells in inflamma-

tory processes has been shown by several studies [Schmitz *et al.*, 2008; Weichhart *et al.*, 2008; Byles *et al.*, 2013].

mTOR localization in macrophages

The subcellular localization of mTOR has been tightly associated with its activity, with a lysosomal localization being required for its activation by phosphorylation [Betz and Hall, 2013]. Interestingly, immunohistological analysis demonstrated that mTOR as well as phospho-mTOR^{Ser2448} are concentrated in granular structures in LP cells, in particular CD68^{+} macrophages, under homeostatic conditions (TM 0 h). Following LEL, mTOR remained localized in granular structures, although a distinct reduction of these structures was observed, while phospho-mTOR^{Ser2448} revealed a more diffuse, cytoplasmic staining pattern. In line with this finding, mTOR, after phosphorylation on the lysosomal membrane, has been shown to translocate to the cytoplasm where it apparently retains activity [Rosner and Hengstschläger, 2012; Zhou *et al.*, 2015; Betz and Hall, 2013]. Ser2448 represents one of four currently known phosphorylation sites of mTOR, whose exact function still remains to be defined [Chiang and Abraham, 2005; Acosta-Jaquez *et al.*, 2009]. Phosphorylation of mTOR^{Ser2448} has been shown to be mediated by the p70S6 kinase, a downstream target of mTOR. However, mTOR^{Ser2448} phosphorylation in emigrated LPMCs was not significantly inhibited in the presence of the mTORC1/2 inhibitor Torin1, suggesting that it may be regulated independently of mTOR activity. Further studies are needed to fully characterize the mTOR subcellular localization in LP cells in the LEL model, which may provide crucial information on the regulation of mTOR activation and function under homeostatic and inflamed conditions in these cells.

Upregulation of the mTOR pathway in myeloid cells

An upregulation of the mTORC1 complex at the onset of inflammation in the LEL model was indicated by an increased phosphorylation of the mTORC1 downstream

target RPS6$^{Ser235/236}$ in both Obs.1 and Obs.2. This upregulation of RPS6 phosphorylation was almost completely inhibited in the presence of the mTORC1/2 inhibitor Torin1, clearly indicating that this phosphorylation event is controlled by mTOR in LP cells. Among phospho-RPS6^{+} cells, as observed in LEL-M tissue *in situ*, were also CD68^{+} macrophages. In line with this result, RPS6$^{Ser235/236}$ phosphorylation levels were also increased in emigrated macrophages when compared to PBMC. Both findings consistently point toward the activation of the mTOR pathway during the initiation of an inflammatory response in this cell population. Importantly, many macrophages revealed a simultaneous upregulation of phospho-RPS6$^{Ser235/236}$ and protein synthesis at LEL-M 5 h and 17 h when compared to TM 0 h. The participation of the mTOR pathway activation in the upregulation of protein synthesis in this cell population was demonstrated by Torin1 treatment, which not only almost completely prevented the upregulation of RPS6$^{Ser235/236}$ phosphorylation in macrophages *in situ* and following emigration out of the LP, but also partially inhibited protein synthesis *in situ*.

Although flow cytometric analysis showed that the mTORC1 downstream target 4E-BP1$^{Thr37/46}$ phosphorylation, especially in myeloid cells, was sensitive to Torin1 inhibition, it also revealed the similarity of 4E-BP1$^{Thr37/46}$ phosphorylation levels between emigrated LPMCs and PBMCs. This finding stands in contrast with the increase in RPS6$^{Ser235/236}$ phosphorylation in emigrated LPMCs vs. PBMCs. The phosphorylation state of 4E-BP1$^{Thr37/46}$ could not be investigated *in situ* due to the inability to detect a specific signal in neither FFPE nor cryo sections, which might - besides the lack of a suitable antibody for this technique - be due to the kinetics of 4E-BP1$^{Thr37/46}$ phosphorylation. As therefore the expression of phospho-4E-BP1$^{Thr37/46}$ levels in resting LPMCs *in situ* are currently unknown, they may or may not correspond to the detected phosphorylation levels in PBMCs. A finding in favor of the latter is the detected constitutive protein synthesis in resting PBMCs in contrast to its lack in resting LP cells. Furthermore, the strong upregulation of *IRF7* expression, known to be repressed by active, non-phosphorylated 4E-BP1 in mice [Colina *et al.*, 2008], indicated the induction of 4E-BP1 phosphorylation at the onset of inflammation in the LEL model.

In line with an activation of the mTORC2 complex in LP macrophages during the initiation of an intestinal inflammatory response, phosphorylation of AKT^{Ser473} was increased in the latter cell population *in situ* as well as in emigrated HLA-$DR^+CD33^+CD14^+$ LPMCs vs. PBMCs. Further experiments are necessary to understand the observed differences of sensitivity towards Torin1 mediated AKT^{Ser473} dephosphorylation in $CD14^+$ vs. $CD14^-$ cells.

The mTOR pathway is upregulated in B Cells, but not in T cells in the LEL model

Previous experiments from our group and others already showed that resident LP T cells are hardly activated in both the LEL model or intestinal inflammation [Sido *et al.*, 2008, 2000; Qiao *et al.*, 1991, 1993; Pirzer *et al.*, 1990; De Maria *et al.*, 1993]. In line with these results, none of the investigated mTOR downstream targets were highly expressed in emigrated $CD3^+$ LPMCs or upregulated in comparison to $CD3^+$ PBMCs, suggesting that the mTOR pathway is not upregulated in this cell population at the onset of inflammation under the conditions employed.

Although the IgA^+ cell population showed the strongest induction of protein synthesis at the onset of inflammation and B cells have been implicated in mTOR dependent activation [Limon and Fruman, 2012], $CD19^+CD20^+$ emigrated LPMCs vs. PBMCs did, in comparison to macrophages, only show a moderate upregulation of either of the two mTORC1 downstream targets investigated. It has at this point to be taken into consideration that this cell population was identified using one common fluorescence channel for both $CD19^+$ and $CD20^+$. The indicated activation of the mTORC2 pathway by the induction of AKT^{Ser473} phosphorylation has to be further investigated due to the heterogeneity of results. Interestingly, although $RPS6^{Ser235/236}$ phosphorylation was efficiently decreased by Torin1 both in emigrated $CD19^+CD20^+$ LPMCs as well as in IgA^+ cells *in situ* (the latter cell type was identified based on morphology), protein synthesis was only efficiently (and still incompletely) inhibited in $CD68^+$ cells, but not

in IgA$^+$ cells. These results suggest that the observed protein synthesis in IgA$^+$ cells are controlled by a mTOR independent mechanism.
The upregulation of protein synthesis and mTORC1 downstream targets in both B and T lymphocytes *in situ* at the onset of inflammation are currently under investigation.

mTOR independent regulation of protein synthesis

As described above, Torin1 was not able to completely inhibit protein synthesis in macrophages and not at all in IgA$^+$ cells. This was not based on a dose dependent effect, as an increased inhibitor dose was unable to enhance any of the seen mTOR downstream target inhibition effects in any of the investigated cell populations. The findings therefore suggest the presence of other mTOR-independent control mechanisms of protein synthesis at the onset of inflammation in the LEL model.
Publications regarding mTOR independent translation are scarce and many mTOR independent pathways through other mechanisms are still dependent on the phosphorylation of the RPS6 upstream regulator S6K. However, some studies suggest mTOR-S6K independent translation via PKCβII-RACK1 interaction, PRR16/Largen, or direct activation of EIF4G [Grosso *et al.*, 2008; Yamamoto *et al.*, 2014; Norton and Layman, 2006]. In accordance, PKCs were among the upstream regulators predicted to be highly activated in IPA analysis for both observations. However, further investigations are necessary to positively identify these Torin1 independent mechanisms of translational control in macrophages, IgA$^+$ cells and possibly other cell populations in the LEL model.

Taken together, these findings indicate that mTOR pathway activity is upregulated during the initiation of an inflammatory response in LP macrophages. Furthermore, evidence is provided that the mTOR pathway is also activated in LP cells of the B cell lineage.

4.3.2. The mTOR mediated control of the inflammatory response

In order to define the contribution of mTOR pathway activation to the induction of inflammatory effector functions in LP cells, the impact of Torin1 on the secretion of a panel of inflammatory mediators, which were shown to be upregulated during the onset of inflammation in the LEL model, were investigated.

Despite the presence of Torin1 throughout the performance of the model, the influence of the inhibitor on almost all studied parameters was only detectable at time point LEL-M 17 h. One reason for this phenomenon could simply be the low mediator concentrations that were detected for most parameters at LEL-M 5 h (data not shown), where the supernatant was collected after 1 h, whereas for time point LEL-M 17 h, the supernatant was collected after 12 h. Overall, there were high quantitative variances between the different patient samples regarding total expression levels and response to inhibitor treatment - a characteristic feature of studies performed in the human system. Remarkably, among parameters analyzed, the investigated chemokines were the group that was most sensitive towards Torin1 mediated mTOR inhibition. Apart from chemokine ligand 19 (CCL19), which was only moderately upregulated at LEL-M 17 h vs. TM 0 h, all tested chemokines were strongly upregulated after 17 h culture without inhibitor and inhibited in the presence of Torin1.

The control of chemokine secretion by mTOR

Chemokines are important mediators in early inflammation and known to attract leukocytes towards the site of injury/inflammation, a process that has been shown to be important in the intestinal inflammatory response [MacDermott *et al.*, 1998].

The monocyte chemoattractant protein-1 (MCP-1)/CCL2 is known to recruit monocytes, memory T cells, and dendritic cells to the site of inflammation. MCP-1 has been found to be highly expressed in LP macrophages of IBD patients and its secretion from monocytes has recently been shown to be sensitive towards mTOR inhibition by rapamycin [Grimm *et al.*, 1996; Lin *et al.*, 2014].

CCL19 together with its receptor CCR7, are highly upregulated on gene expression level in the LEL model both *in situ* (CCL19: Obs.2 only, CCR7: Obs.1 and Obs.2) as well as in emigrated myeloid cells vs. myeloid PBMCs (unpublished microarray and qRT-PCR data). It has been implicated to be expressed via intestinal DCs in CD patients, where it is thought to promote the development of autoreactive T cells [Middel *et al.*, 2006]. The sensitivity of CCL19 secretion in primary cells towards mTOR inhibition is shown in this thesis for the first time.

CCL22, also known as macrophage-derived chemokine (MDC) is mainly expressed by macrophages, mast cells and DCs [Yamashita and Kuroda, 2002]. The importance of CCL22 in barrier-defect mediated inflammation was indicated by Hashimoto *et al.* [2006], who showed that CCL22 production by monocyte derived DC reflects the disease activity of patients with atopic dermatitis.
CCL22 was upregulated on gene expression level in the LEL model both *in situ* (nCounter Assay, both observations) as well as in emigrated myeloid cells vs. PBMCs (unpublished microarray data). In line with these results, Guenaltay *et al.* [2015] were able to show increased CCL22 gene expression levels in the colon of patients with microscopic colitis. In contrast, CCL2 was not among upregulated genes in the UC patient datasets from Granlund *et al.* [2013]. Its upregulation in LP cells on protein level in the context of intestinal inflammation as well as its regulation by mTOR is shown in this thesis for the first time.

Finally, CXCL1, a chemoattractant for neutrophils, which so far had no known association with mTOR and was not considered to be involved in the pathogenesis of IBD, was also upregulated in the LEL model on mRNA level *in situ*. Interestingly, murine *Cxcl1* expression is strongly upregulated in whole colon samples of mice following *Clostridium difficile* infection [McDermott *et al.*, 2016].

In summary, I was able to show that the mTOR pathway controls the secretion of several chemokines at the onset of inflammation as observed in the LEL model. If this

observation reflects a mTOR pathway mediated control of the recruitment of leukocytes *in vivo*, remains to be examined in appropriate animal models.

The mTOR mediated decrease of IL-18 and VEGF secretion

In addition to its effect on chemokine secretion, Torin1 treatment did also increase the levels of inflammasome controlled cytokine IL-18 and the angiogenetic molecule VEGF in the LEL model.

Elevated IL-18 levels [Williams *et al.*, 2015] as well as SNP loci in IL-18 or IL-18 related molecules in IBD patiens [Jostins *et al.*, 2012] have suggested a role for IL-18 in the pathology of IBD. Accordingly, it has been recently discussed as a potential target for IBD treatment [Kanai *et al.*, 2013]. In line with my results, Ko *et al.* [2008] were able to decrease LPS-induced IL-18 secretion levels in rat DCs via rapamycin. In this thesis, I was able to establish a link between the mTOR pathway and IL-18 secretion in intestinal inflammation for the first time.

mTOR mediated inhibition of the secretion of pro-inflammatory cytokines

In contrast to the above described inhibition of the secretion of several inflammatory mediators, Torin1 treatment did increase MIF as well as M-CSF secretion levels.

The pro-inflammatory macrophage migration factor (MIF) is known to be constitutively expressed in homeostatic epithelial cells, macrophages as well as various other cell types that reside in the LP [Maaser *et al.*, 2002; Yang *et al.*, 2015; Calandra *et al.*, 1994]. MIF polymorphisms have been associated with IBD susceptibility and MIF levels have been shown to be increased in UC, but not CD patients [Yang *et al.*, 2015; Murakami *et al.*, 2001]. Although MIF secretion levels are reduced at LEL-M 5 h vs. TM 0 h in the LEL model, this might be related to the absence of epithelium after LEL or a depletion of MIF pools immediately after onset of inflammation (LEL-M 3 h) and has to be investigated further. However, MIF has been indicated to act upstream of mTOR by activating the mTOR inhibitor AMPK in fibroblasts in the ischaemic heart [Miller *et al.*, 2008] - a finding that together with the demonstrated mTOR activation in the LEL model is in line with the observed decrease of MIF secretion at LEL-M 5 h vs. TM 0 h. The

increased MIF secretion levels in the presence of Torin1 indicated a negative control by the mTOR pathway. However, whether MIF is also a downstream target of mTOR or controlled through feedback mechanisms, has to be further investigated. The results indicate that mTOR also displays an anti-inflammatory role in the induction of the inflammatory response by repression of pro-inflammatory cytokines at least in the LEL model.

4.3.3. Reflections on potential other effector functions controlled by the mTOR pathway during the initiation of intestinal inflammation: Tissue remodelling

Macrophages represent the first line of defense in the intestinal LP and as such play an important part in mediating inflammatory responses. Importantly, in the context of inflammation, macrophages are known to be crucial regulators of tissue remodeling including fibrogenesis [Kühl *et al.*, 2015] - a process involved in wound healing as well as tissue remodelling and known to be regulated by mTOR through TGF-β [Gao *et al.*, 2013]. Several lines of evidence support the notion that this process is rapidly induced by LP cells during the initiation of an inflammatory reponse in the LEL model:

(1) MMPs 1, 2, 3, 10 and 12 were extensively upregulated on gene expression level. They are known regulators of tissue remodelling processes by breakdown of excessive ECM and suggested to be involved in the pathogenesis of IBD [Kirkegaard *et al.*, 2004; Kofla-Dlubacz *et al.*, 2012; Wiercinska-Drapalo *et al.*, 2003]. In line with this finding, preliminary mass spectrometry results indicated an enrichment of ECM proteins after onset of inflammation.

(2) Both *TGFB1* and *TGFB2* were upregulated on gene expression level during the whole time course of the model.

(3) TGF-β has been shown to induce the differentiation of human lung fibroblasts into myofibroblasts [Kulkarni *et al.*, 2011], a process known to be suppressed by PPAR-γ signaling (a pathway predicted to be inhibited by IPA in the LEL model), while TGF-β itself activates PI3K/AKT signaling (predicted to be activated by IPA),

ultimately inducing AKT^{Ser473} phosphorylation. AKT^{Ser473} phosphorylation is increased in macrophages both *in situ* as well as in emigrated CD33^{+}HLA-DR^{+}CD14^{+} cells following the initiation of the inflammatory response. Importantly, another research group indicated that TGF-β mediated fibrogenesis in these cells could be inhibited by rapamycin [Gao *et al.*, 2013].

(4) Further signs of tissue remodeling and fibrogenesis in the LEL model included the upregulation of angiogenetic factors such as VEGF on both mRNA and protein level. In accordance with regulation of fibrogenesis by mTOR, VEGF was among the molecules that were inhibited by Torin1.

4.4. Clinical aspects of the findings

A limited number of studies employing mTOR inhibitors for the treatment of IBD have shown mixed results: In a pediatric IBD study with 11 UC and 3 CD patients, the use of the mTOR inhibitor sirolimus (rapamycin) did lead to clinical remission of 45% (5) of UC (with additional 18 % (2) showing clinical response) and all CD patients (3). Mucosal healing was achieved in 45 % (5) of UC and 67% (2) of CD patients [Mutalib *et al.*, 2014]. Additionally, in two different case studies, two CD patients had a marked improvement after treatment with sirolimus or everolimus, respectively [Massey *et al.*, 2008; Dumortier *et al.*, 2008]. In contrast, in a different CD study, mTOR inhibition by everolimus failed to show any clinical benefit of this drug regarding maintenance of steroid-free remission when compared to standard azathioprine therapy or placebo [Reinisch *et al.*, 2008]. Similarly, murine studies analyzing the effect of mTOR inhibition on intestinal inflammation showed contradicting results, ranging from repression of epithelial cell regeneration to amelioration of inflammation [Guan *et al.*, 2015; Yin *et al.*, 2013; Sun *et al.*, 2012].

These heterogeneous observations suggest that effects of mTOR inhibition in IBD might be essentially depending on the degree of inflammation, the concentration of the inhibitor administered, the genetic background, etc.. Notably, when interpreting these results regarding the role of mTOR in intestinal inflammation, one has to keep

in mind that all described studies use rapamycin, which is unable to inhibit mTORC1 completely and is insensitive towards mTORC2 inhibition.

Interestingly, many of the predicted key genes linked to SNPs that are associated with IBD by GWAS are involved in the IP3 pathway [Jostins *et al.*, 2012]. These key genes mainly encode phosphatases, which mediate the degradation of IP3, thus regulating the activity of the PI3K-mTOR axis. Genetic variants leading to an alteration of the mTOR pathway may not unlikely contribute to the development of IBD through dysregulation of i.e. leukocyte recruitment. Furthermore, genetically determined overactivation of mTOR activity during inflammation may potentially predispose to the development of fibrosis, which represents a common complication of IBD [Rieder and Fiocchi, 2008; Gordon *et al.*, 2014].
In order to collect evidence for a contribution of the mTOR pathway to the induction of tissue remodeling and fibrogenesis during the initiation of an inflammatory response and - hence - potentially to fibrosis in chronic inflammation, the effect of mTOR inhibitors on the expression of mediators promoting these molecular processes will be tested in the LEL model in the future. Importantly, a causal relationship between these processes would support a potential benefit of mTOR inhibitors for the treatment of fibrotic events in IBD; such a therapeutic option has been discussed but neither preclinically nor clinically tested yet [Siegmund, 2015].

4.5. Conclusions and proposed model

Taken together, in this thesis, the LEL model was established as a physiologically relevant system to study the initiation of an inflammatory response in human LP cells. Global gene expression showed the induction of a strong inflammatory response in this cell population and that this inflammatory response has a significant overlap with UC patient data. For the first time it was shown here that the mTOR pathway at least in part mediates this initial inflammatory process by controlling the upregulation of translation. Furthermore, this mTOR controlled process is predominantly mediated by macrophage activity. Finally, the induction of chemokine secretion in LP cells could

be linked to mTOR activity. The findings of this thesis thus adds a number of novel aspects to our still limited understanding of initial events in intestinal inflammation and indentify the mTOR signaling pathway as a potential therapeutic target for IBD.

Based on the present findings and data published by others, the following potential model is proposed (Figure 4.1): a mucosal barrier defect - as caused by epithelial layer damage - leads to the rapid induction of a pro-inflammatory response in resident LP cells including macrophages. This event is associated with the upregulation of mRNA and protein synthesis, a process partially regulated by mTOR. mTOR controlled pro-inflammatory chemokine secretion as well as angiogenesis lead to the recruitment and subsequent infiltration of circulating leukocytes into the LP. In parallel, fibrogenesis, a process known to be regulated by mTOR, is induced to limit both area and time of exposure of LP cells to luminal microbiota. After resolution of the inflammation, homeostasis is restored. Dysregulation of the mTOR pathway - i.e. by genetic alterations - might lead to a perseverance of the inflammatory response and the manifestation of chronic inflammation and fibrosis as seen in IBD.

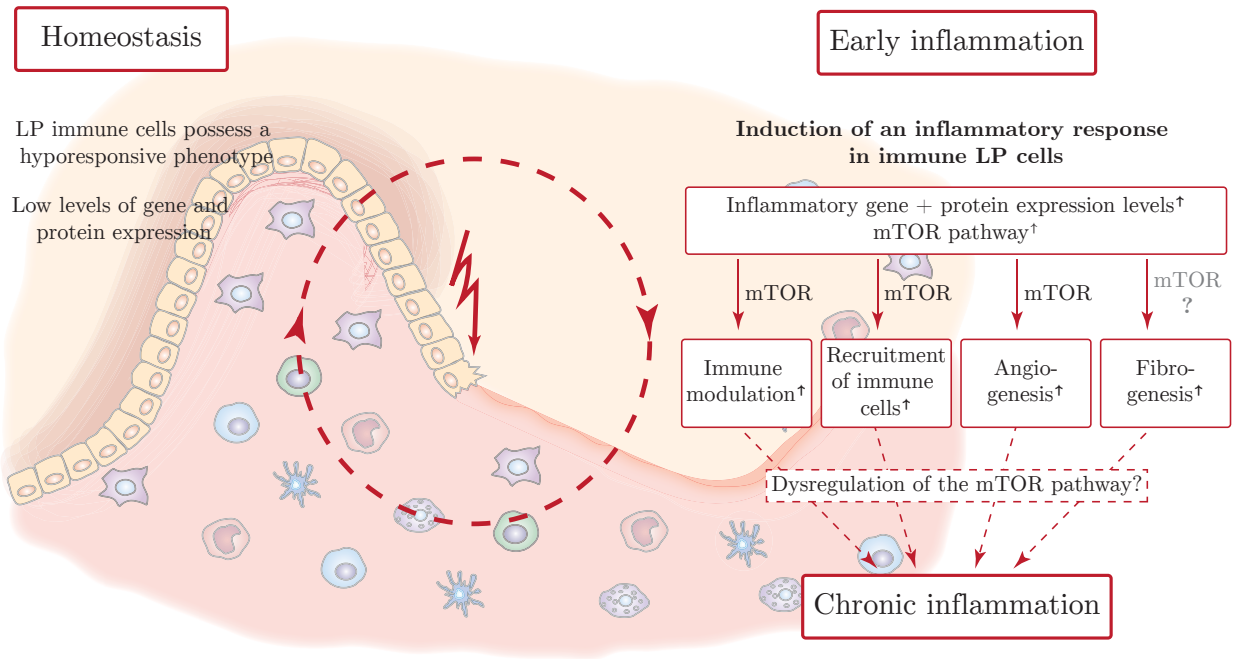

Figure 4.1.: *Proposed model.*

References

Acosta-Jaquez, H. A.; Keller, J. A.; Foster, K. G.; Ekim, B.; Soliman, G. A.; *et al.* (2009). Site-Specific mTOR Phosphorylation Promotes mTORC1-Mediated Signaling and Cell Growth. *Molecular and Cellular Biology*, 29(15):4308–4324.

Adegoke, O. A.; McBurney, M. I.; Samuels, S. E.; and Baracos, V. E. (1999). Luminal amino acids acutely decrease intestinal mucosal protein synthesis and protease mRNA in piglets. *J Nutr*, 129(10):1871–8.

Akitsu, A.; Kakuta, S.; Saijo, S.; and Iwakura, Y. (2014). Rag2-deficient IL-1 Receptor Antagonist-deficient Mice Are a Novel Colitis Model in Which Innate Lymphoid Cell-derived IL-17 Is Involved in the Pathogenesis. *Exp Anim*, 63(2):235–46.

April, C.; Klotzle, B.; Royce, T.; Wickham-Garcia, E.; Boyaniwsky, T.; *et al.* (2009). Whole-genome gene expression profiling of formalin-fixed, paraffin-embedded tissue samples. *PLoS One*, 4(12):e8162.

Autschbach, F.; Giese, T.; Gassler, N.; Sido, B.; Heuschen, G.; *et al.* (2002). Cytokine/chemokine messenger-RNA expression profiles in ulcerative colitis and Crohn's disease. *Virchows Arch*, 441(5):500–13.

Baert, F. J.; D'Haens, G. R.; Peeters, M.; Hiele, M. I.; Schaible, T. F.; *et al.* (1999). Tumor necrosis factor alpha antibody (infliximab) therapy profoundly down-regulates the inflammation in Crohn's ileocolitis. *Gastroenterology*, 116(1):22–8.

Bailey, J. R.; Bland, P. W.; Tarlton, J. F.; Peters, I.; Moorghen, M.; *et al.* (2012). IL-13 promotes collagen accumulation in Crohn's disease fibrosis by down-regulation of fibroblast MMP synthesis: a role for innate lymphoid cells? *PLoS One*, 7(12):e52332.

Bain, C. C.; Bravo-Blas, A.; Scott, C. L.; Gomez Perdiguero, E.; Geissmann, F.; *et al.* (2014). Constant replenishment from circulating monocytes maintains the macrophage pool in the intestine of adult mice. *Nat Immunol*, 15(10):929–37.

Bao, W. G.; Zhang, X.; Zhang, J. G.; Zhou, W. J.; Bi, T. N.; *et al.* (2013). Biobanking of fresh-frozen human colon tissues: impact of tissue ex-vivo ischemia times and storage periods on RNA quality. *Ann Surg Oncol*, 20(5):1737–44.

Belkaid, Y. and Hand, T. W. (2014). Role of the microbiota in immunity and inflammation. *Cell*, 157(1):121–41.

Benjamini, Y. and Hochberg, Y. (1995). Controlling the False Discovery Rate: A Practical and Powerful Approach to Multiple Testing. *Journal of the Royal Statistical Society. Series B (Methodological)*, 57(1):289–300.

Betz, C. and Hall, M. N. (2013). Where is mTOR and what is it doing there? *J Cell Biol*, 203(4):563–74.

Boirivant, M.; Fuss, I.; Fiocchi, C.; Klein, J. S.; Strong, S. A.; *et al.* (1996). Hypoproliferative human lamina propria T cells retain the capacity to secrete lymphokines when stimulated via CD2/CD28 pathways. *Proc Assoc Am Physicians*, 108(1):55–67.

Brandtzaeg, P. and Johansen, F. E. (2005). Mucosal B cells: phenotypic characteristics, transcriptional regulation, and homing properties. *Immunol Rev*, 206:32–63.

Braunstein, J.; Autschbach, F.; Giese, T.; Lasitschka, F.; Heidtmann, A.; *et al.* (2008). Up-regulation of the phosphoinositide 3-kinase pathway in human lamina propria T lymphocytes. *Clin Exp Immunol*, 151(3):496–504.

Byles, V.; Covarrubias, A. J.; Ben-Sahra, I.; Lamming, D. W.; Sabatini, D. M.; *et al.* (2013). The TSC-mTOR pathway regulates macrophage polarization. *Nat Commun*, 4:2834.

Calandra, T.; Bernhagen, J.; Mitchell, R. A.; and Bucala, R. (1994). The macrophage is an important and previously unrecognized source of macrophage migration inhibitory factor. *J Exp Med*, 179(6):1895–902.

Carpenter, S.; Ricci, E. P.; Mercier, B. C.; Moore, M. J.; and Fitzgerald, K. A. (2014). Post-transcriptional regulation of gene expression in innate immunity. *Nat Rev Immunol*, 14(6):361–376.

Chang, J. Y.; Sehgal, S. N.; and Bansbach, C. C. (1991). FK506 and rapamycin: novel pharmacological probes of the immune response. *Trends Pharmacol Sci*, 12(6):218–23.

Chen, H. (2012). VennDiagram: Generate high-resolution Venn and Euler plots. *R package version*, 113.

Chiang, G. G. and Abraham, R. T. (2005). Phosphorylation of mammalian target of rapamycin (mTOR) at Ser-2448 is mediated by p70S6 kinase. *J Biol Chem*, 280(27):25485–90.

Colina, R.; Costa-Mattioli, M.; Dowling, R. J.; Jaramillo, M.; Tai, L. H.; *et al.* (2008). Translational control of the innate immune response through IRF-7. *Nature*, 452(7185):323–8.

Cosin-Roger, J.; Ortiz-Masia, D.; Calatayud, S.; Hernandez, C.; Alvarez, A.; *et al.* (2013). M2 macrophages activate WNT signaling pathway in epithelial cells: relevance in ulcerative colitis. *PLoS One*, 8(10):e78128.

Craggs, A.; West, S.; Curtis, A.; Welfare, M.; Hudson, M.; *et al.* (2001). Absence of a genetic association between IL-1RN and IL-1B gene polymorphisms in ulcerative colitis and Crohn disease in multiple populations from northeast England. *Scand J Gastroenterol*, 36(11):1173–8.

Darwich, A. S.; Aslam, U.; Ashcroft, D. M.; and Rostami-Hodjegan, A. (2014). Meta-analysis of the turnover of intestinal epithelia in preclinical animal species and humans. *Drug Metab Dispos*, 42(12):2016–22.

Daryani, N. E.; Sadr, M.; Moossavi, S.; Shahkarami, S.; Soltani, S.; *et al.* (2015). Significance of IL-1RA Polymorphism in Iranian Patients with Inflammatory Bowel Disease. *Dig Dis Sci*, 60(5):1389–95.

de Joussineau, C.; Sahut-Barnola, I.; Tissier, F.; Dumontet, T.; Drelon, C.; *et al.* (2014). mTOR pathway is activated by PKA in adrenocortical cells and participates in vivo to apoptosis resistance in primary pigmented nodular adrenocortical disease (PPNAD). *Human Molecular Genetics*, 23(20):5418–5428.

De Maria, R.; Fais, S.; Silvestri, M.; Frati, L.; Pallone, F.; *et al.* (1993). Continuous in vivo activation and transient hyporesponsiveness to TCR/CD3 triggering of human gut lamina propria lymphocytes. *Eur J Immunol*, 23(12):3104–8.

Denning, T. L.; Norris, B. A.; Medina-Contreras, O.; Manicassamy, S.; Geem, D.; *et al.* (2011). Functional specializations of intestinal dendritic cell and macrophage subsets that control Th17 and regulatory T cell responses are dependent on the T cell/APC ratio, source of mouse strain, and regional localization. *J Immunol*, 187(2):733–47.

Diamond, J. M. (1977). Twenty-first Bowditch lecture. The epithelial junction: bridge, gate, and fence. *Physiologist*, 20(1):10–8.

Dowle, M.; Srinivasan, A.; Short, T.; with contributions from R Saporta, S. L.; and Antonyan, E. (2015). *data.table: Extension of Data.frame*.

Du, P.; Kibbe, W. A.; and Lin, S. M. (2008). lumi: a pipeline for processing Illumina microarray. *Bioinformatics*, 24(13):1547–8.

Dumortier, J.; Lapalus, M. G.; Guillaud, O.; Poncet, G.; Gagnieu, M. C.; *et al.* (2008). Everolimus for refractory Crohn's disease: a case report. *Inflamm Bowel Dis*, 14(6):874–7.

Feldman, M. E.; Apsel, B.; Uotila, A.; Loewith, R.; Knight, Z. A.; *et al.* (2009). Active-site inhibitors of mTOR target rapamycin-resistant outputs of mTORC1 and mTORC2. *PLoS Biol*, 7(2):e38.

Floyd, K.; Suter, P.; and Lutz, H. (1983). Granules of blood eosinophils are stained directly by anti-immunoglobulin fluorescein isothiocyanate conjugates. *American journal of veterinary research*, 44(11):2060–2063.

Gao, Y.; Xu, X.; Ding, K.; Liang, Y.; Jiang, D.; *et al.* (2013). Rapamycin inhibits transforming growth factor beta1-induced fibrogenesis in primary human lung fibroblasts. *Yonsei Med J*, 54(2):437–44.

Gibbons, D. L. and Spencer, J. (2011). Mouse and human intestinal immunity: same ballpark, different players; different rules, same score. *Mucosal Immunol*, 4(2):148–157.

Gordon, I. O.; Agrawal, N.; Goldblum, J. R.; Fiocchi, C.; and Rieder, F. (2014). Fibrosis in ulcerative colitis: mechanisms, features, and consequences of a neglected problem. *Inflamm Bowel Dis*, 20(11):2198–206.

Granlund, A.; Flatberg, A.; Ostvik, A. E.; Drozdov, I.; Gustafsson, B. I.; *et al.* (2013). Whole genome gene expression meta-analysis of inflammatory bowel disease colon mucosa demonstrates lack of major differences between Crohn's disease and ulcerative colitis. *PLoS One*, 8(2):e56818.

Grimm, M. C.; Elsbury, S. K.; Pavli, P.; and Doe, W. F. (1996). Enhanced expression and production of monocyte chemoattractant protein-1 in inflammatory bowel disease mucosa. *J Leukoc Biol*, 59(6):804–12.

Grosso, S.; Volta, V.; Sala, L. A.; Vietri, M.; Marchisio, P. C.; *et al.* (2008). PKCβII modulates translation independently from mTOR and through RACK1. *Biochem J*, 415(1):77–85.

Groth, C. G.; Backman, L.; Morales, J. M.; Calne, R.; Kreis, H.; *et al.* (1999). Sirolimus (rapamycin)-based therapy in human renal transplantation: similar efficacy and different toxicity compared with cyclosporine. Sirolimus European Renal Transplant Study Group. *Transplantation*, 67(7):1036–42.

Gruys, E.; Toussaint, M. J. M.; Niewold, T. A.; and Koopmans, S. J. (2005). Acute phase reaction and acute phase proteins. *Journal of Zhejiang University. Science. B*, 6(11):1045–1056.

Guan, Y.; Zhang, L.; Li, X.; Zhang, X.; Liu, S.; *et al.* (2015). Repression of Mammalian Target of Rapamycin Complex 1 Inhibits Intestinal Regeneration in Acute Inflammatory Bowel Disease Models. *J Immunol*, 195(1):339–46.

Guenaltay, S.; Kumawat, A. K.; Nyhlin, N.; Bohr, J.; Tysk, C.; *et al.* (2015). Enhanced levels of chemokines and their receptors in the colon of microscopic colitis patients indicate mixed immune cell recruitment. *Mediators Inflamm*, 2015:132458.

Gustafsson, J. K.; Ermund, A.; Johansson, M. E. V.; SchÃ¼tte, A.; Hansson, G. C.; *et al.* (2012). An ex vivo method for studying mucus formation, properties, and thickness in human colonic biopsies and mouse small and large intestinal explants. *American Journal of Physiology - Gastrointestinal and Liver Physiology*, 302(4):G430–G438.

Gwinn, D. M.; Shackelford, D. B.; Egan, D. F.; Mihaylova, M. M.; Mery, A.; *et al.* (2008). AMPK phosphorylation of raptor mediates a metabolic checkpoint. *Mol Cell*, 30(2):214–26.

Hahn-Windgassen, A.; Nogueira, V.; Chen, C. C.; Skeen, J. E.; Sonenberg, N.; *et al.* (2005). Akt activates the mammalian target of rapamycin by regulating cellular ATP level and AMPK activity. *J Biol Chem*, 280(37):32081–9.

Hashimoto, S.; Nakamura, K.; Oyama, N.; Kaneko, F.; Tsunemi, Y.; *et al.* (2006). Macrophage-derived chemokine (MDC)/CCL22 produced by monocyte derived dendritic cells reflects the disease activity in patients with atopic dermatitis. *J Dermatol Sci*, 44(2):93–9.

Hausmann, M.; Kiessling, S.; Mestermann, S.; Webb, G.; Spottl, T.; *et al.* (2002). Toll-like receptors 2 and 4 are up-regulated during intestinal inflammation. *Gastroenterology*, 122(7):1987–2000.

Hendrickson, B. A.; Gokhale, R.; and Cho, J. H. (2002). Clinical Aspects and Pathophysiology of Inflammatory Bowel Disease. *Clinical Microbiology Reviews*, 15(1):79–94.

Heumuller-Klug, S.; Sticht, C.; Kaiser, K.; Wink, E.; Hagl, C.; *et al.* (2015). Degradation of intestinal mRNA: a matter of treatment. *World J Gastroenterol*, 21(12):3499–508.

Heys, S. D.; Park, K. G.; McNurlan, M. A.; Keenan, R. A.; Miller, J. D.; *et al.* (1992). Protein synthesis rates in colon and liver: stimulation by gastrointestinal pathologies. *Gut*, 33(7):976–81.

Hu, Z.; Wang, X.; Gong, L.; Wu, G.; Peng, X.; *et al.* (2015). Role of high-mobility group box 1 protein in inflammatory bowel disease. *Inflamm Res*, 64(8):557–63.

Huber, W.; Carey, V. J.; Gentleman, R.; Anders, S.; Carlson, M.; *et al.* (2015). Orchestrating high-throughput genomic analysis with Bioconductor. *Nat Meth*, 12(2):115–121.

Hunig, T.; Tiefenthaler, G.; Meyer zum Buschenfelde, K. H.; and Meuer, S. C. (1987). Alternative pathway activation of T cells by binding of CD2 to its cell-surface ligand. *Nature*, 326(6110):298–301.

Inoki, K.; Ouyang, H.; Zhu, T.; Lindvall, C.; Wang, Y.; *et al.* (2006). TSC2 integrates Wnt and energy signals via a coordinated phosphorylation by AMPK and GSK3 to regulate cell growth. *Cell*, 126(5):955–68.

Ivanov, S. S. and Roy, C. R. (2013). Pathogen signatures activate a ubiquitination pathway that modulates the function of the metabolic checkpoint kinase mTOR. *Nat Immunol*, 14(12):1219–1228.

Jacinto, E. and Hall, M. N. (2003). Tor signalling in bugs, brain and brawn. *Nat Rev Mol Cell Biol*, 4(2):117–26.

Jenkins, S. J.; Ruckerl, D.; Cook, P. C.; Jones, L. H.; Finkelman, F. D.; *et al.* (2011). Local macrophage proliferation, rather than recruitment from the blood, is a signature of TH2 inflammation. *Science*, 332(6035):1284–8.

Johansson, M. E.; Sjovall, H.; and Hansson, G. C. (2013). The gastrointestinal mucus system in health and disease. *Nat Rev Gastroenterol Hepatol*, 10(6):352–61.

Jostins, L.; Ripke, S.; Weersma, R. K.; Duerr, R. H.; McGovern, D. P.; *et al.* (2012). Host-microbe interactions have shaped the genetic architecture of inflammatory bowel disease. *Nature*, 491(7422):119–24.

Kanai, T.; Kamada, N.; and Hisamatsu, T. (2013). Clinical strategies for the blockade of IL-18 in inflammatory bowel diseases. *Curr Drug Targets*, 14(12):1392–9.

Karin, M.; Liu, Z.; and Zandi, E. (1997). AP-1 function and regulation. *Curr Opin Cell Biol*, 9(2):240–6.

Kim, E.; Goraksha-Hicks, P.; Li, L.; Neufeld, T. P.; and Guan, K. L. (2008). Regulation of TORC1 by Rag GTPases in nutrient response. *Nat Cell Biol*, 10(8):935–45.

Kirkegaard, T.; Hansen, A.; Bruun, E.; and Brynskov, J. (2004). Expression and localisation of matrix metalloproteinases and their natural inhibitors in fistulae of patients with Crohn's disease. *Gut*, 53(5):701–9.

Ko, H.; Hambly, B. D.; Eris, J. M.; Levidiotis, V.; Wyburn, K.; *et al.* (2008). Dentritic cell derived IL-18 production is inhibited by rapamycin and sanglifehrin A, but not cyclosporine A. *Transpl Immunol*, 20(1-2):99–105.

Kofla-Dlubacz, A.; Matusiewicz, M.; Krzystek-Korpacka, M.; and Iwanczak, B. (2012). Correlation of MMP-3 and MMP-9 with Crohn's disease activity in children. *Dig Dis Sci*, 57(3):706–12.

Kühl, A. A.hl, A. A.; Erben, U.; Kredel, L. I.; and Siegmund, B. (2015). Diversity of Intestinal Macrophages in Inflammatory Bowel Diseases. *Front Immunol*, 6:613.

Kulkarni, A. A.; Thatcher, T. H.; Olsen, K. C.; Maggirwar, S. B.; Phipps, R. P.; *et al.* (2011). PPAR-gamma ligands repress TGFbeta-induced myofibroblast differentiation by targeting the PI3K/Akt pathway: implications for therapy of fibrosis. *PLoS One*, 6(1):e15909.

Lamps, L. W. (2015). Update on infectious enterocolitides and the diseases that they mimic. *Histopathology*, 66(1):3–14.

Laplante, M. and Sabatini, D. M. (2012). mTOR signaling in growth control and disease. *Cell*, 149(2):274–93.

Latella, G.; Vetuschi, A.; Sferra, R.; Speca, S.; and Gaudio, E. (2013). Localization of alphanubeta6 integrin-TGF-beta1/Smad3, mTOR and PPARgamma in experimental colorectal fibrosis. *Eur J Histochem*, 57(4):e40.

Lee, D. F.; Kuo, H. P.; Chen, C. T.; Hsu, J. M.; Chou, C. K.; *et al.* (2007). IKK beta suppression of TSC1 links inflammation and tumor angiogenesis via the mTOR pathway. *Cell*, 130(3):440–55.

Lee, S. H.; Starkey, P. M.; and Gordon, S. (1985). Quantitative analysis of total macrophage content in adult mouse tissues. Immunochemical studies with monoclonal antibody F4/80. *J Exp Med*, 161(3):475–89.

Lelouard, H.; Schmidt, E. K.; Camosseto, V.; Clavarino, G.; Ceppi, M.; *et al.* (2007). Regulation of translation is required for dendritic cell function and survival during activation. *J Cell Biol*, 179(7):1427–39.

Li, H.; Limenitakis, J. P.; Fuhrer, T.; Geuking, M. B.; Lawson, M. A.; *et al.* (2015). The outer mucus layer hosts a distinct intestinal microbial niche. *Nature Communications*, 6:8292.

Limon, J. J. and Fruman, D. A. (2012). Akt and mTOR in B Cell Activation and Differentiation. *Front Immunol*, 3:228.

Lin, H. Y.; Chang, K. T.; Hung, C. C.; Kuo, C. H.; Hwang, S. J.; *et al.* (2014). Effects of the mTOR inhibitor rapamycin on monocyte-secreted chemokines. *BMC Immunol*, 15:37.

Lipkin, M.; Bell, B.; and Sherlock, P. (1963). Cell Proliferation Kinetics in the Gastrointestinal Tract of Man. I. Cell Renewal in Colon and Rectum. *J Clin Invest*, 42(6):767–76.

Liu, J.; Xu, Y.; Stoleru, D.; and Salic, A. (2012). Imaging protein synthesis in cells and tissues with an alkyne analog of puromycin. *Proceedings of the National Academy of Sciences of the United States of America*, 109(2):413–418.

Liu, Z.; Geboes, K.; Hellings, P.; Maerten, P.; Heremans, H.; *et al.* (2001). B7 interactions with CD28 and CTLA-4 control tolerance or induction of mucosal inflammation in chronic experimental colitis. *J Immunol*, 167(3):1830–8.

Loeuillard, E.; Bertrand, J.; Herranen, A.; Melchior, C.; Guerin, C.; *et al.* (2014). 2,4,6-trinitrobenzene sulfonic acid-induced chronic colitis with fibrosis and modulation of TGF-beta1 signaling. *World J Gastroenterol*, 20(48):18207–15.

Lopez-Hernandez, R.; Valdes, M.; Campillo, J. A.; Martinez-Garcia, P.; Salama, H.; *et al.* (2015). Pro- and anti-inflammatory cytokine gene single-nucleotide polymorphisms in inflammatory bowel disease. *Int J Immunogenet*, 42(1):38–45.

Lopez-Rivera, E.; Jayaraman, P.; Parikh, F.; Davies, M. A.; Ekmekcioglu, S.; *et al.* (2014). Inducible nitric oxide synthase (iNOS) drives mTOR pathway activation and proliferation of human melanoma by reversible nitrosylation of TSC2. *Cancer research*, 74(4):1067–1078.

Ma, X. M. and Blenis, J. (2009). Molecular mechanisms of mTOR-mediated translational control. *Nat Rev Mol Cell Biol*, 10(5):307–18.

Maaser, C.; Eckmann, L.; Paesold, G.; Kim, H. S.; and Kagnoff, M. F. (2002). Ubiquitous production of macrophage migration inhibitory factor by human gastric and intestinal epithelium. *Gastroenterology*, 122(3):667–680.

MacDermott, R. P.; Sanderson, I. R.; and Reinecker, H. C. (1998). The central role of chemokines (chemotactic cytokines) in the immunopathogenesis of ulcerative colitis and Crohn's disease. *Inflamm Bowel Dis*, 4(1):54–67.

Mahida, Y. R.; Galvin, A. M.; Gray, T.; Makh, S.; McAlindon, M. E.; *et al.* (1997). Migration of human intestinal lamina propria lymphocytes, macrophages and eosinophils following the loss of surface epithelial cells. *Clin Exp Immunol*, 109(2):377–86.

Mahida, Y. R.; Patel, S.; Gionchetti, P.; Vaux, D.; and Jewell, D. P. (1989). Macrophage subpopulations in lamina propria of normal and inflamed colon and terminal ileum. *Gut*, 30(6):826–34.

Mark, A.; Thompson, R.; and Wu, C. (2014). *mygene: Access MyGene.Info*$_s$*ervices.*

Martinez, F. O.; Helming, L.; Milde, R.; Varin, A.; Melgert, B. N.; *et al.* (2013). Genetic programs expressed in resting and IL-4 alternatively activated mouse and human macrophages: similarities and differences. *Blood*, 121(9):e57–69.

Massey, D. C.; Bredin, F.; and Parkes, M. (2008). Use of sirolimus (rapamycin) to treat refractory Crohn's disease. *Gut*, 57(9):1294–6.

Matsuo, M.; Yamada, S.; Koizumi, K.; Sakurai, H.; and Saiki, I. (2007). Tumour-derived fibroblast growth factor-2 exerts lymphangiogenic effects through Akt/mTOR/p70S6kinase pathway in rat lymphatic endothelial cells. *European Journal of Cancer*, 43(11):1748–1754.

Mazumder, B.; Li, X.; and Barik, S. (2010). Translation Control: A Multifaceted Regulator of Inflammatory Response. *Journal of immunology (Baltimore, Md. : 1950)*, 184(7):3311–3319.

Mazzucchelli, L.; Hauser, C.; Zgraggen, K.; Wagner, H.; Hess, M.; *et al.* (1994). Expression of interleukin-8 gene in inflammatory bowel disease is related to the histological grade of active inflammation. *Am J Pathol*, 144(5):997–1007.

McDermott, A. J.; Falkowski, N. R.; McDonald, R. A.; Pandit, C. R.; Young, V. B.; *et al.* (2016). Interleukin-23 (IL-23), independent of IL-17 and IL-22, drives neutrophil recruitment and innate inflammation during Clostridium difficile colitis in mice. *Immunology*, 147(1):114–24.

McNurlan, M. A.; Tomkins, A. M.; and Garlick, P. J. (1979). The effect of starvation on the rate of protein synthesis in rat liver and small intestine. *Biochem J*, 178(2):373–9.

Medzhitov, R. (2008). Origin and physiological roles of inflammation. *Nature*, 454(7203):428–35.

Mestas, J. and Hughes, C. C. (2004). Of mice and not men: differences between mouse and human immunology. *J Immunol*, 172(5):2731–8.

Meuer, S. C.; Hussey, R. E.; Fabbi, M.; Fox, D.; Acuto, O.; *et al.* (1984). An alternative pathway of T-cell activation: a functional role for the 50 kd T11 sheep erythrocyte receptor protein. *Cell*, 36(4):897–906.

Middel, P.; Raddatz, D.; Gunawan, B.; Haller, F.; and Radzun, H. J. (2006). Increased number of mature dendritic cells in Crohn's disease: evidence for a chemokine mediated retention mechanism. *Gut*, 55(2):220–7.

Miller, E. J.; Li, J.; Leng, L.; McDonald, C.; Atsumi, T.; *et al.* (2008). Macrophage migration inhibitory factor stimulates AMP-activated protein kinase in the ischaemic heart. *Nature*, 451(7178):578–582.

Mittal, R. D.; Bid, H. K.; and Ghoshal, U. C. (2005). IL-1 receptor antagonist (IL-1Ra) gene polymorphism in patients with inflammatory bowel disease in India. *Scand J Gastroenterol*, 40(7):827–31.

Mizoguchi, A.; Takeuchi, T.; Himuro, H.; Okada, T.; and Mizoguchi, E. (2016). Genetically engineered mouse models for studying inflammatory bowel disease. *J Pathol*, 238(2):205–19.

Mowat, A. M. and Agace, W. W. (2014). Regional specialization within the intestinal immune system. *Nat Rev Immunol*, 14(10):667–85.

Murakami, H.; Akbar, S. M.; Matsui, H.; and Onji, M. (2001). Macrophage migration inhibitory factor in the sera and at the colonic mucosa in patients with ulcerative colitis: clinical implications and pathogenic significance. *Eur J Clin Invest*, 31(4):337–43.

Mutalib, M.; Borrelli, O.; Blackstock, S.; Kiparissi, F.; Elawad, M.; *et al.* (2014). The use of sirolimus (rapamycin) in the management of refractory inflammatory bowel disease in children. *J Crohns Colitis*, 8(12):1730–4.

Nagashima, R.; Maeda, K.; Imai, Y.; and Takahashi, T. (1996). Lamina propria macrophages in the human gastrointestinal mucosa: their distribution, immunohistological phenotype, and function. *J Histochem Cytochem*, 44(7):721–31.

Nandagopal, N. and Roux, P. P. (2015). Regulation of global and specific mRNA translation by the mTOR signaling pathway. *Translation (Austin)*, 3(1):e983402.

Neurath, M.; Fuss, I.; and Strober, W. (2000). TNBS-Colitis. *International Reviews of Immunology*, 19(1):51–62.

Nobukuni, T.; Joaquin, M.; Roccio, M.; Dann, S. G.; Kim, S. Y.; *et al.* (2005). Amino acids mediate mTOR/raptor signaling through activation of class 3 phosphatidylinositol 3OH-kinase. *Proc Natl Acad Sci U S A*, 102(40):14238–43.

Norton, L. E. and Layman, D. K. (2006). Leucine regulates translation initiation of protein synthesis in skeletal muscle after exercise. *J Nutr*, 136(2):533s–537s.

Okayasu, I.; Hatakeyama, S.; Yamada, M.; Ohkusa, T.; Inagaki, Y.; *et al.* (1990). A novel method in the induction of reliable experimental acute and chronic ulcerative colitis in mice. *Gastroenterology*, 98(3):694–702.

Pastorelli, L.; De Salvo, C.; Mercado, J. R.; Vecchi, M.; and Pizarro, T. T. (2013). Central Role of the Gut Epithelial Barrier in the Pathogenesis of Chronic Intestinal Inflammation: Lessons Learned from Animal Models and Human Genetics. *Front Immunol*, 4:280.

Patterson, S.; Gross, J.; and Webster, A. (1989). DNA probes bind non-specifically to eosinophils during in situ hybridization: carbol chromotrope blocks binding to eosinophils but does not inhibit hybridization to specific nucleotide sequences. *Journal of virological methods*, 23(2):105–109.

Pestova, T. V.; Kolupaeva, V. G.; Lomakin, I. B.; Pilipenko, E. V.; Shatsky, I. N.; *et al.* (2001). Molecular mechanisms of translation initiation in eukaryotes. *Proceedings of the National Academy of Sciences*, 98(13):7029–7036.

Peterson, L. W. and Artis, D. (2014). Intestinal epithelial cells: regulators of barrier function and immune homeostasis. *Nat Rev Immunol*, 14(3):141–153.

Pirzer, U. C.; Schurmann, G.; Post, S.; Betzler, M.; and Meuer, S. C. (1990). Differential responsiveness to CD3-Ti vs. CD2-dependent activation of human intestinal T lymphocytes. *Eur J Immunol*, 20(10):2339–42.

Ploner, A. (2012). Heatplus: Heatmaps with row and/or column covariates and colored clusters. *R package version*, 2(0).

Qiao, L.; Braunstein, J.; Golling, M.; Schurmann, G.; Autschbach, F.; *et al.* (1996). Differential regulation of human T cell responsiveness by mucosal versus blood monocytes. *Eur J Immunol*, 26(4):922–7.

Qiao, L.; Schurmann, G.; Autschbach, F.; Wallich, R.; and Meuer, S. C. (1993). Human intestinal mucosa alters T-cell reactivities. *Gastroenterology*, 105(3):814–9.

Qiao, L.; Schurmann, G.; Betzler, M.; and Meuer, S. C. (1991). Activation and signaling status of human lamina propria T lymphocytes. *Gastroenterology*, 101(6):1529–36.

R Core Team (2015). *R: A Language and Environment for Statistical Computing*. R Foundation for Statistical Computing, Vienna, Austria.

Reinisch, W.; Panes, J.; Lemann, M.; Schreiber, S.; Feagan, B.; *et al.* (2008). A multicenter, randomized, double-blind trial of everolimus versus azathioprine and placebo to maintain steroid-induced remission in patients with moderate-to-severe active Crohn's disease. *Am J Gastroenterol*, 103(9):2284–92.

Reis, P. P.; Waldron, L.; Goswami, R. S.; Xu, W.; Xuan, Y.; *et al.* (2011). mRNA transcript quantification in archival samples using multiplexed, color-coded probes. *BMC Biotechnology*, 11(1):1–10.

Rieder, F. and Fiocchi, C. (2008). Intestinal fibrosis in inflammatory bowel disease - Current knowledge and future perspectives. *Journal of Crohn's and Colitis*, 2(4):279–290.

Riegler, M.; Sedivy, R.; Pothoulakis, C.; Hamilton, G.; Zacherl, J.; *et al.* (1995). Clostridium difficile toxin B is more potent than toxin A in damaging human colonic epithelium in vitro. *J Clin Invest*, 95(5):2004–11.

Ritchie, M. E.; Phipson, B.; Wu, D.; Hu, Y.; Law, C. W.; *et al.* (2015). limma powers differential expression analyses for RNA-sequencing and microarray studies. *Nucleic acids research*, page gkv007.

Rodrigues, R.; Grosso, A. R.; and Moita, L. (2013). Genome-wide analysis of alternative splicing during dendritic cell response to a bacterial challenge. *PLoS One*, 8(4):e61975.

Rogler, G.; Hausmann, M.; Vogl, D.; Aschenbrenner, E.; Andus, T.; *et al.* (1998). Isolation and phenotypic characterization of colonic macrophages. *Clinical and Experimental Immunology*, 112(2):205–215.

Rongvaux, A.; Willinger, T.; Martinek, J.; Strowig, T.; Gearty, S. V.; *et al.* (2014). Development and function of human innate immune cells in a humanized mouse model. *Nat Biotech*, 32(4):364–372.

Rosner, M. and Hengstschläger, M. (2012). Detection of cytoplasmic and nuclear functions of mTOR by fractionation. *Methods Mol Biol*, 821:105–24.

Rugtveit, J.; Bakka, A.; and Brandtzaeg, P. (1997). Differential distribution of B7.1 (CD80) and B7.2 (CD86) costimulatory molecules on mucosal macrophage subsets in human inflammatory bowel disease (IBD). *Clinical and Experimental Immunology*, 110(1):104–113.

Sandberg, R.; Neilson, J. R.; Sarma, A.; Sharp, P. A.; and Burge, C. B. (2008). Proliferating cells express mRNAs with shortened 3' untranslated regions and fewer microRNA target sites. *Science*, 320(5883):1643–7.

Schenk, M.; Bouchon, A.; Seibold, F.; and Mueller, C. (2007). TREM-1–expressing intestinal macrophages crucially amplify chronic inflammation in experimental colitis and inflammatory bowel diseases. *J Clin Invest*, 117(10):3097–106.

Schmitz, F.; Heit, A.; Dreher, S.; Eisenächer, K.; Mages, J.; *et al.* (2008). Mammalian target of rapamycin (mTOR) orchestrates the defense program of innate immune cells. *European Journal of Immunology*, 38(11):2981–2992.

Schröder-Braunstein, J.; Gras, J.; Brors, B.; Schwarz, S.; Szikszai, T.; *et al.* (2014). Initiation of an Inflammatory Response in Resident Intestinal Lamina Propria Cells -Use of a Human Organ Culture Model. *PLoS ONE*, 9(5):e97780.

Schroeder, A.; Mueller, O.; Stocker, S.; Salowsky, R.; Leiber, M.; *et al.* (2006). The RIN: an RNA integrity number for assigning integrity values to RNA measurements. *BMC Molecular Biology*, 7(1):1–14.

Scott, F. I. and Lichtenstein, G. R. (2016). Advances in Therapeutic Drug Monitoring of Biologic Therapies in Inflammatory Bowel Disease: 2015 in Review. *Curr Treat Options Gastroenterol.*

Sekirov, I.; Russell, S. L.; Antunes, L. C.; and Finlay, B. B. (2010). Gut microbiota in health and disease. *Physiol Rev*, 90(3):859–904.

Serafino, A.; Moroni, N.; Zonfrillo, M.; Andreola, F.; Mercuri, L.; *et al.* (2014). WNT-pathway components as predictive markers useful for diagnosis, prevention and therapy in inflammatory bowel disease and sporadic colorectal cancer. *Oncotarget*, 5(4):978–92.

Shaw, R. J. and Cantley, L. C. (2006). Ras, PI(3)K and mTOR signalling controls tumour cell growth. *Nature*, 441(7092):424–30.

Sido, B.; Braunstein, J.; Breitkreutz, R.; Herfarth, C.; and Meuer, S. C. (2000). Thiol-mediated redox regulation of intestinal lamina propria T lymphocytes. *J Exp Med*, 192(6):907–12.

Sido, B.; Lasitschka, F.; Giese, T.; Gassler, N.; Funke, B.; *et al.* (2008). A prominent role for mucosal cystine/cysteine metabolism in intestinal immunoregulation. *Gastroenterology*, 134(1):179–91.

Siegmund, B. (2015). Medical Therapy of Fibrostenotic Crohn's Disease. *Viszeralmedizin*, 31(4):259–64.

Smythies, L. E.; Maheshwari, A.; Clements, R.; Eckhoff, D.; Novak, L.; *et al.* (2006). Mucosal IL-8 and TGF-beta recruit blood monocytes: evidence for cross-talk between the lamina propria stroma and myeloid cells. *J Leukoc Biol*, 80(3):492–9.

Smythies, L. E.; Sellers, M.; Clements, R. H.; Mosteller-Barnum, M.; Meng, G.; *et al.* (2005). Human intestinal macrophages display profound inflammatory anergy despite avid phagocytic and bacteriocidal activity. *J Clin Invest*, 115(1):66–75.

Smythies, L. E.; Shen, R.; Bimczok, D.; Novak, L.; Clements, R. H.; *et al.* (2010). Inflammation anergy in human intestinal macrophages is due to Smad-induced IkappaBalpha expression and NF-kappaB inactivation. *J Biol Chem*, 285(25):19593–604.

Sousa, J. E.; Costa, M. A.; Abizaid, A.; Abizaid, A. S.; Feres, F.; *et al.* (2001). Lack of neointimal proliferation after implantation of sirolimus-coated stents in human coronary arteries: a quantitative coronary angiography and three-dimensional intravascular ultrasound study. *Circulation*, 103(2):192–5.

Sousa, J. E.; Costa, M. A.; Abizaid, A.; Feres, F.; Seixas, A. C.; *et al.* (2005). Four-year angiographic and intravascular ultrasound follow-up of patients treated with sirolimus-eluting stents. *Circulation*, 111(18):2326–9.

Sun, X.; Threadgill, D.; and Jobin, C. (2012). Campylobacter jejuni induces colitis through activation of mammalian target of rapamycin signaling. *Gastroenterology*, 142(1):86–95.e5.

Szikszai, T.; Lasitschka, F.; Giese, T.; Greulich, M.; Lee, Y. S.; *et al.* (2015). Standardization of a human organ culture model of intestinal inflammation and its application for drug testing. *J Immunol Methods*, 421:96–103.

Takada, Y.; Ray, N.; Ikeda, E.; Kawaguchi, T.; Kuwahara, M.; *et al.* (2010). Fos proteins suppress dextran sulfate sodium-induced colitis through inhibition of NF-kappaB. *J Immunol*, 184(2):1014–21.

Thiesen, S.; Janciauskiene, S.; Uronen-Hansson, H.; Agace, W.; Hogerkorp, C. M.; *et al.* (2014). CD14(hi)HLA-DR(dim) macrophages, with a resemblance to classical blood monocytes, dominate inflamed mucosa in Crohn's disease. *J Leukoc Biol*, 95(3):531–41.

Thoreen, C. C.; Chantranupong, L.; Keys, H. R.; Wang, T.; Gray, N. S.; *et al.* (2012). A unifying model for mTORC1-mediated regulation of mRNA translation. *Nature*, 485(7396):109–13.

Thoreen, C. C.; Kang, S. A.; Chang, J. W.; Liu, Q.; Zhang, J.; *et al.* (2009). An ATP-competitive mammalian target of rapamycin inhibitor reveals rapamycin-resistant functions of mTORC1. *J Biol Chem*, 284(12):8023–32.

Turner, J. R. (2009). Intestinal mucosal barrier function in health and disease. *Nat Rev Immunol*, 9(11):799–809.

Uhlen, M.; Fagerberg, L.; Hallstrom, B. M.; Lindskog, C.; Oksvold, P.; *et al.* (2015). Proteomics. Tissue-based map of the human proteome. *Science*, 347(6220):1260419.

Van der Sluis, M.; De Koning, B. A.; De Bruijn, A. C.; Velcich, A.; Meijerink, J. P.; *et al.* (2006). Muc2-deficient mice spontaneously develop colitis, indicating that MUC2 is critical for colonic protection. *Gastroenterology*, 131(1):117–29.

Veldman-Jones, M. H.; Brant, R.; Rooney, C.; Geh, C.; Emery, H.; *et al.* (2015). Evaluating Robustness and Sensitivity of the NanoString Technologies nCounter Platform to Enable Multiplexed Gene Expression Analysis of Clinical Samples. *Cancer Res*, 75(13):2587–93.

Waggott, D.; Chu, K.; Yin, S.; Wouters, B. G.; Liu, F.-F.; *et al.* (2012). NanoStringNorm: an extensible R package for the pre-processing of NanoString mRNA and miRNA data. *Bioinformatics*, 28(11):1546–1548.

Weichhart, T.; Costantino, G.; Poglitsch, M.; Rosner, M.; Zeyda, M.; *et al.* (2008). The TSC-mTOR Signaling Pathway Regulates the Innate Inflammatory Response. *Immunity*, 29(4):565–577.

Wickham, H. (2009). *ggplot2: Elegant Graphics for Data Analysis*. Springer-Verlag New York.

Wickham, H. and Francois, R. (2015). *dplyr: A Grammar of Data Manipulation*.

Wiercinska-Drapalo, A.; Jaroszewicz, J.; Flisiak, R.; and Prokopowicz, D. (2003). Plasma matrix metalloproteinase-1 and tissue inhibitor of metalloproteinase-1 as biomarkers of ulcerative colitis activity. *World J Gastroenterol*, 9(12):2843–5.

Williams, T. M.; Leeth, R. A.; Rothschild, D. E.; Coutermarsh-Ott, S. L.; McDaniel, D. K.; *et al.* (2015). The NLRP1 inflammasome attenuates colitis and colitis-associated tumorigenesis. *J Immunol*, 194(7):3369–80.

Wu, H.; Li, X. M.; Wang, J. R.; Gan, W. J.; Jiang, F. Q.; *et al.* (2016). NUR77 exerts a protective effect against inflammatory bowel disease by negatively regulating the TRAF6/TLR-IL-1R signalling axis. *J Pathol*, 238(3):457–69.

Xu, J. and Gordon, J. I. (2003). Honor thy symbionts. *Proc Natl Acad Sci U S A*, 100(18):10452–9.

Xue, J.; Schmidt, S. V.; Sander, J.; Draffehn, A.; Krebs, W.; *et al.* (2014). Transcriptome-based network analysis reveals a spectrum model of human macrophage activation. *Immunity*, 40(2):274–88.

Yamamoto, K.; Gandin, V.; Sasaki, M.; McCracken, S.; Li, W.; *et al.* (2014). Largen: a molecular regulator of mammalian cell size control. *Mol Cell*, 53(6):904–15.

Yamashita, U. and Kuroda, E. (2002). Regulation of macrophage-derived chemokine (MDC, CCL22) production. *Crit Rev Immunol*, 22(2):105–14.

Yang, J.; Li, Y.; and Zhang, X. (2015). Meta-analysis of macrophage migration inhibitory factor (MIF) gene -173G/C polymorphism and inflammatory bowel disease (IBD) risk. *Int J Clin Exp Med*, 8(6):9570–4.

Yang, L.; Yu, Y.; Kang, R.; Yang, M.; Xie, M.; *et al.* (2012). Up-regulated autophagy by endogenous high mobility group box-1 promotes chemoresistance in leukemia cells. *Leuk Lymphoma*, 53(2):315–22.

Yin, H.; Li, X.; Zhang, B.; Liu, T.; Yuan, B.; *et al.* (2013). Sirolimus ameliorates inflammatory responses by switching the regulatory T/T helper type 17 profile in murine colitis. *Immunology*, 139(4):494–502.

Zhou, X.; Clister, T. L.; Lowry, P. R.; Seldin, M. M.; Wong, G. . W.; *et al.* (2015). Dynamic Visualization of mTORC1 Activity in Living Cells. *Cell Reports*, 10(10):1767–1777.

Zschaler, J.; Schlorke, D.; and Arnhold, J. (2014). Differences in innate immune response between man and mouse. *Crit Rev Immunol*, 34(5):433–54.

Declaration of Authorship

I herewith declare, that I have composed and written this thesis myself without the prohibited assistance of third parties and without making use of aids other than those specified; notions taken over directly or indirectly from other sources have been identified as such.

This paper has not previously been presented in identical or similar form to any other German or foreign examination board.

I declare that I have not undertaken any previous unsuccessful doctorate proceedings.

I declare that I recognize the doctorate regulations of the Friedrich Schiller University Jena.

Jena, September 11, 2016

Judith Gras

Curriculum Vitae

Personal Data

Judith Gras
Steinhofweg 100
69123 Heidelberg
Phone: (06221)7253511
Email: Judith.Gras@gmail.com

born 14.12.1986 in Lahnstein
German, Danish

Dissertation

06/2012 - today "Molecular Mechanisms Driving the Initiation of an Inflammatory Response in Human Lamina Propria Cells − Impact of mTOR Pathway Activation"

Meuer/Schröder-Braunstein group, Institute for Immunology, University Hospital, Heidelberg. Doctoral supervisor: Prof. Dr. Axel Brakhage, Friedrich Schiller University, Jena

Academic Education

10/07 - 04/12 Biology, Friedrich Schiller University, Jena
Major: Biochemistry; Minors: Immunology, Genetics
Degree: Diplom-Biologie (equiv. to M.Sc.)

04/11 - 04/12 **Thesis** at the Hospital for Sick Children, Toronto, Canada:
"The role of uPAR and CFH in Neutrophil Adhesion − Relevance for aHUS Pathogenesis". Supervisor: Prof. Dr. Christoph Licht

Projects

08/10 - 09/10 "Expression of Eya1 mutants" (Imhof group, CMB, Jena)

06/10 - 07/10 "Rheumatoid arthritis and regulatory T cells" (Kamradt group, University Hospital, Jena)

04/10 - 06/10 "Heme and Heme degradation products" (Imhof group, CMB, Jena)

02/10 - 04/10 "Mechanisms of thyroid hormone induced cellular senescence in N2a cells" (Baniahmad group, University Hospital, Jena)

Voluntary Year of Social Service

09/06 - 09/07 Emergency Medical Technician (German Red Cross)

Education

03/2006 GCE A-levels ("Allg. Hochschulreife"), Kant-Gymnasium, Boppard

Scholarship

2011 DAAD (PROMOS)

Publications

Paper J. Schröder-Braunstein, J. Gras, B. Brors *et al.* (2014). Initiation of an inflammatory response in resident intestinal lamina propria cells − use of a human organ culture model. PLoS ONE, 9(5):e97780.

Poster (1^{st} author) J. Gras, A. Heninger, S. Wentrup *et al.* Rapid activation of the mTOR pathway in human resident lamina propria macrophages during the initiation of intestinal inflammation. 4th European Congress of Immunology (ECI). Vienna, 09/2015

J. Gras, Y.-S. Lee, B. Brors *et al.* Activation of the unfolded protein response in resident lamina propria cells during the initiation of intestinal inflammation. 17th International Congress of Mucosal Immunology (ICMI). Berlin, 07/2015.

J. Gras, M. Paparella, B. Brors *et al.* Activation and differentiation of human lamina propria (myeloid) cells during the initiation of intestinal inflammation. 9th European Mucosal Immunology Group (EMIG) Meeting. Glasgow, 10/2014.

J. Gras, M. Paparella, B. Brors *et al.* Activation and differentiation of human lamina propria (myeloid) cells during the intiation of intestinal inflammation. European Macrophage and Dendritic Cell Society Meeting (EMDS). Vienna, 10/2014.

J. Gras, B. Brors, M. AlSaeedi *et al.* A human intestinal organ culture model for early events in inflammation. 44th Annual Meeting of the German Society for Immunology (DGFI). Bonn, 09/2014

J. Gras, B. Brors, M. AlSaeedi *et al.* A human intestinal organ culture model for the analysis of pathways in early inflammation. School for Translational Immunology (STI). Tallinn, 04/2014.

J. Gras, B. Brors, M. AlSaeedi *et al.* A human intestinal organ culture model for the analysis of pathways in early inflammation. 43th Annual Meeting of the German Society for Immunology (DGFI). Mainz, 09/2013

J. Gras, S. Schiessling, J. Ilse *et al.* Activation of Human Resident Lamina Propria Cells in Response to Epithelial Layer Damage. 6th Seeon Conference. Seeon, 06/2013.

J. Gras, F.G. Pluthero and C. Licht. "Die Bedeutung von uPAR und CFH in der Adhäsion von Neutrophilen Granulozyten - Relevanz für aHUS?". 43. Jahrestagung der Gesellschaft für Pädiatrische Nephrologie (GPN). Heidelberg, 03/2012

September 11, 2016

Acknowledgements

I would like to give special thanks to the following people for their contribution and help during this thesis:

First of all, Prof. Dr. Axel Brakhage and Prof. Dr. Stefan Meuer for giving me the opportunity to study this fascinating topic and the supervision of this thesis.

Dr. Jutta Schroeder-Braunstein for her guidance and support, for always having an open ear, the countless scientific discussions that sometimes made both of us forget time and her great ideas regarding future experiments. Her fascination for science has been an inspiration.

Antje Heidtmann for her excellent eye for experimental details and for making all these late night lab sessions so much more entertaining. Sabine Wentrup for her aid in experiments. Dr. Anne Heninger and Dr. Serin Schiessling for everything ranging from (scientific) advice to much needed comical relief. Anne, I want you to know that I am really totally into genetics! Stefan Kurzhals for all help and geeky conversations.

Dr. Felix Lasitschka for his advice regarding pathological questions and for allowing me to perform the LMD experiments in his lab. Jutta Scheuerer for all her assistance and for being such an optimist.

Prof. Benedikt Brors and Maria Dinkelacker for their support regarding bioinformatic analyses and Maria for motivating me to learn R.

All physicians and staff of the collaborating hospitals and the Institute of Pathology for their assistance in obtaining tissue samples.
The patients for giving their consent to participate in this study although facing a difficult situation in life.

My family for their continuous support. My godson Anton, who always helps me slow down and see the little things. Especially my parents, for always having my back, their love and never-ending trust.
My friends for encouragement as well as understanding.

Most importantly of all, Fabian, for being there for me, always. You are my 42.

A. Appendix

List of Figures in Appendix

List of Tables in Appendix

Digital Contents

1. WG-DASL Assay, logFC data (All)
2. nCounter Assay, logFC data (All)
3. Ingenuity Pathway Analysis (All)
    a) Canonical Pathways
    b) Functions
    c) Upstream Regulators
4. Macro for quantification of immunofluorescent images: JuQuant.ijm

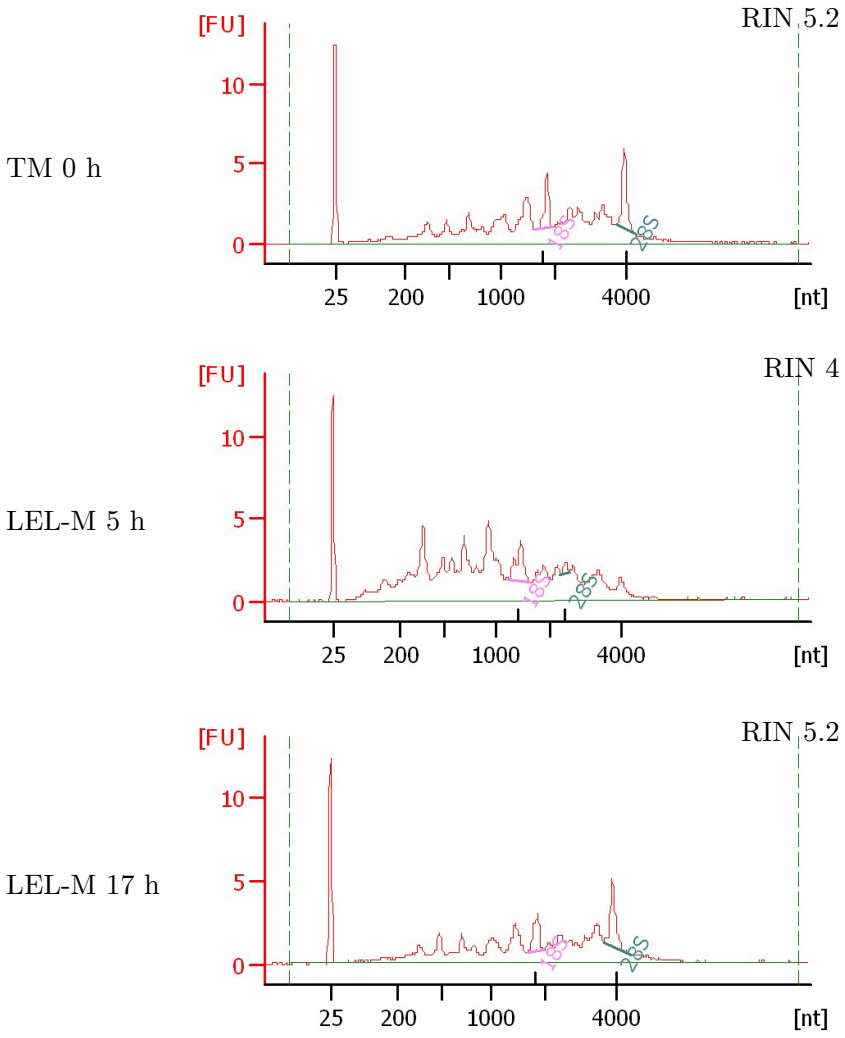

Figure A.1.: RNA integrity in the LEL model. Representative RNA electropherograms derived from tissue samples of one patient, produced by Agilent Bioanalyzer. Analyzed RNA was isolated from LMD LP samples at different time points during the LEL model. RIN: RNA Integrity Number.

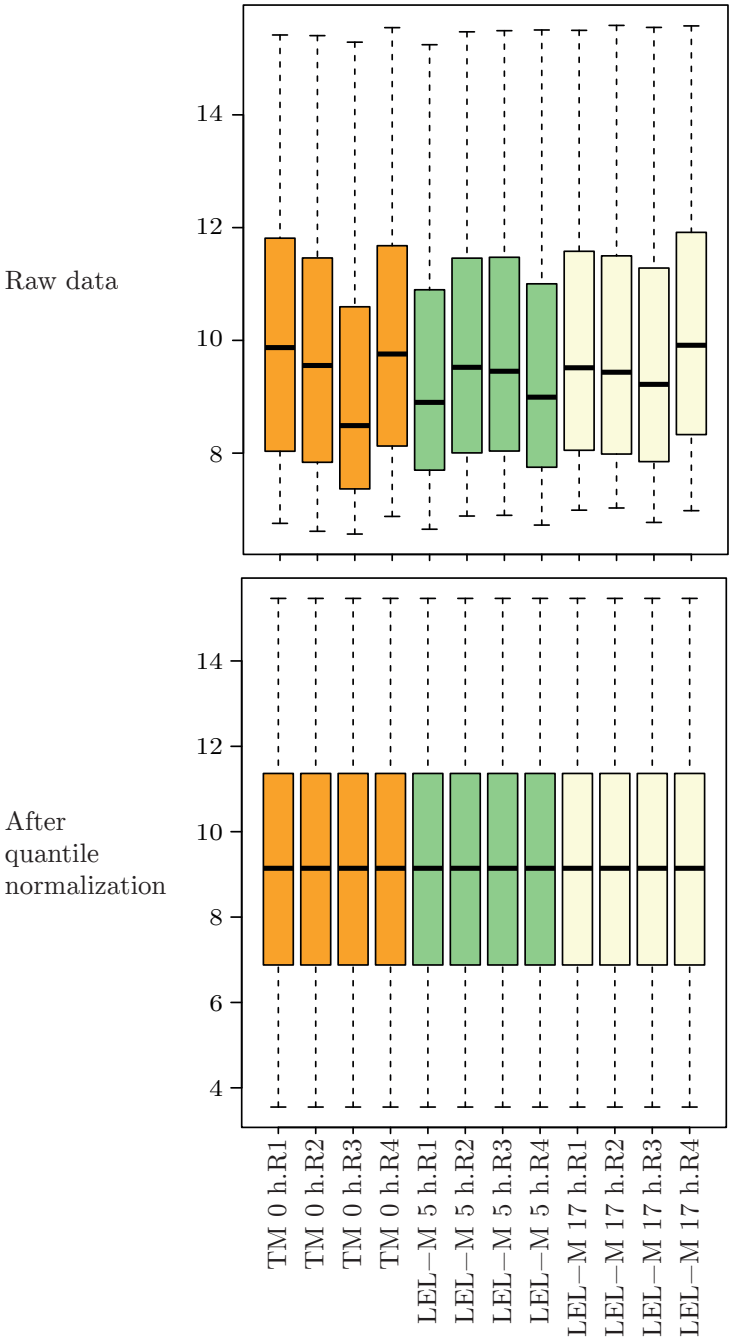

Figure A.2.: WG-DASL gene expression boxplots (raw and quantile normalized). For more details to normalization, see subsection 2.5.1 on page 25.

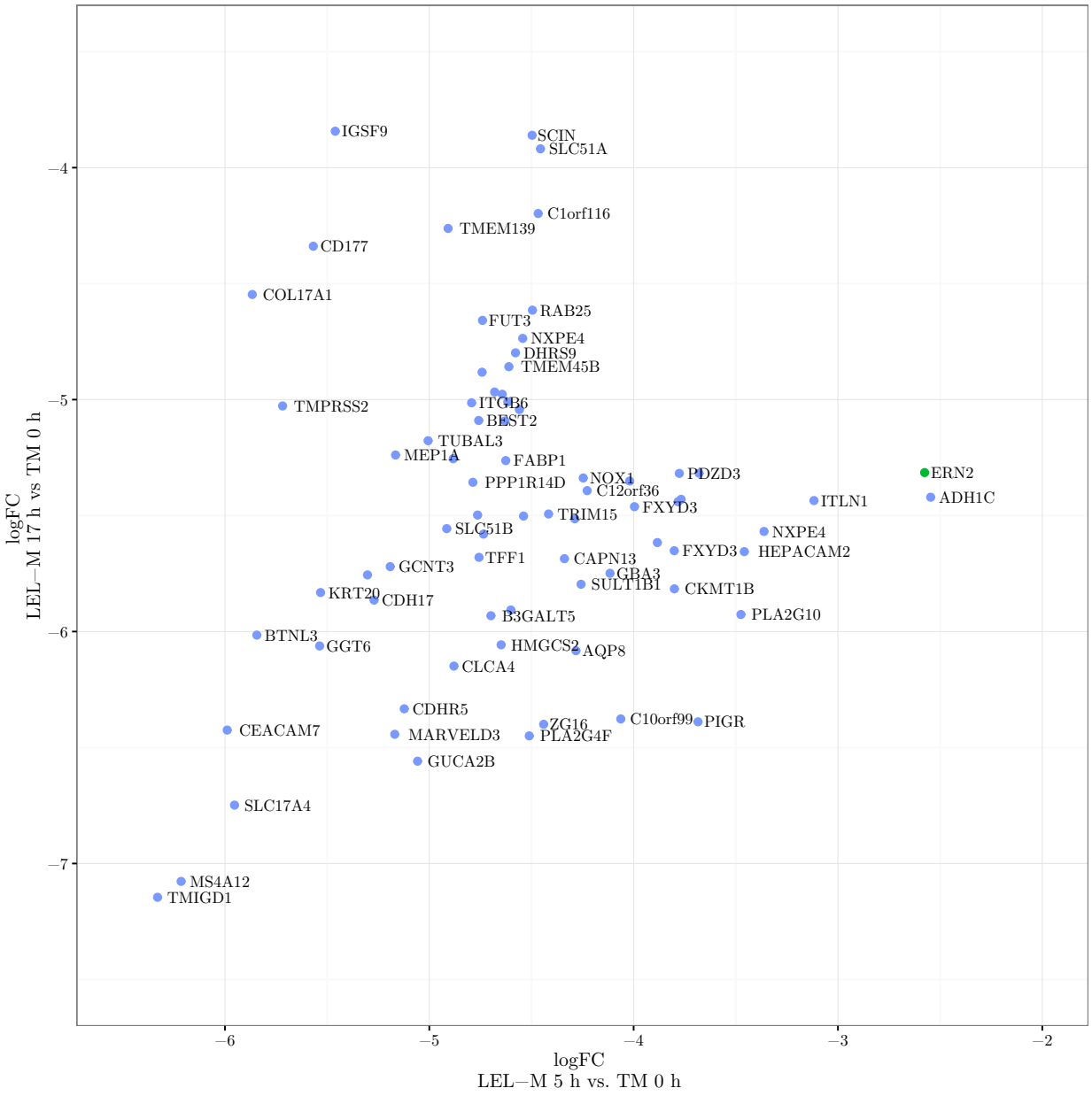

Figure A.3.: WG-DASL Assay Top 50 downregulated genes for observations LEL-M 5 h vs. TM 0 h (Obs.1) and LEL-M 17 h vs. 0 h (Obs.2). Blue dots indicate prediction of the transcription factor was significant (adj.P.Val < 0.05) for both observations, while red dots indicate significance of prediction for Obs.1 and green dots for Obs.2 only, respectively. Where logFC values were to close to each other to produce readable names, only one gene name is given at random.

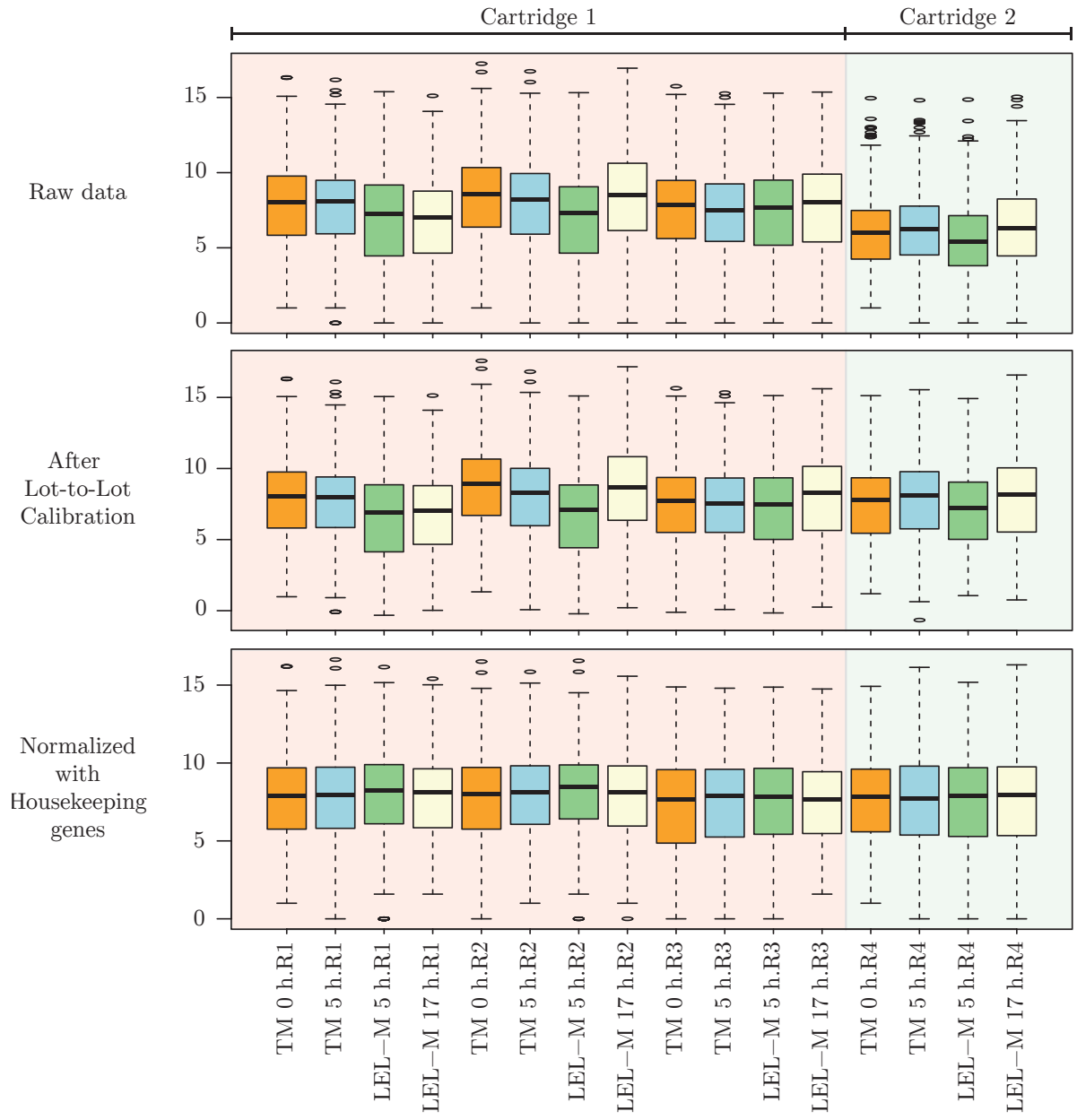

Figure A.4.: nCounter Assay gene expression boxplots (raw, calibrated and normalized). Top boxplots show log2 counter values of raw data, boxplots in the middle show values after Lot-to-Lot calibration of Cartridge 2, boxplots at the bottom show log2FC calibrated data after normalization with housekeeping genes. For more details to normalization, see subsection 2.5.2 on page 25.

```
rename("All");
selectWindow("All");
run("Set Scale...", "distance=0 known=0 pixel=1 unit=pixel");
run("Make Composite");
run("Duplicate...", "duplicate");
setTool("polygon");
waitForUser("Select lamina propria, then press ok!")
run("Clear Outside");
run("Split Channels");
selectWindow("C2-All-1");
run("Duplicate...", " ");
run("Threshold...");
setThreshold(410, 4095);
// Change to appropriate threshold, if necessary!
waitForUser("Threshold ok?")
run("Convert to Mask");
run("Watershed");
run("Set Measurements...", "area mean min integrated redirect=None decimal=3");
run("Analyze Particles...", "size=10-200 exclude add");
selectWindow("C2-All-1");
roiManager("Show None");
roiManager("Show All");
roiManager("Measure");
selectWindow("C1-All-1");
run("Grays");
run("Find Maxima...", "noise=450 output=[Point Selection] exclude");
run("Find Maxima...", "noise=450 output=Count exclude");
String.copyResults();
//displays histogram:
//run("Distribution...", "parameter=RawIntDen or=10 and=0-0");
waitForUser("Ready to close everything?")
while (nImages>0) {
          selectImage(nImages);
          close();
      }
selectWindow("Results");
run("Close");
selectWindow("ROI Manager");
run("Close");
```

Figure A.5.: Script for ImageJ macro used for semi-quantitative analysis of protein synthesis in the LEL model. Macro was written in the IJ1 macro language. For further details, see subsection 2.7.5 on page 31.

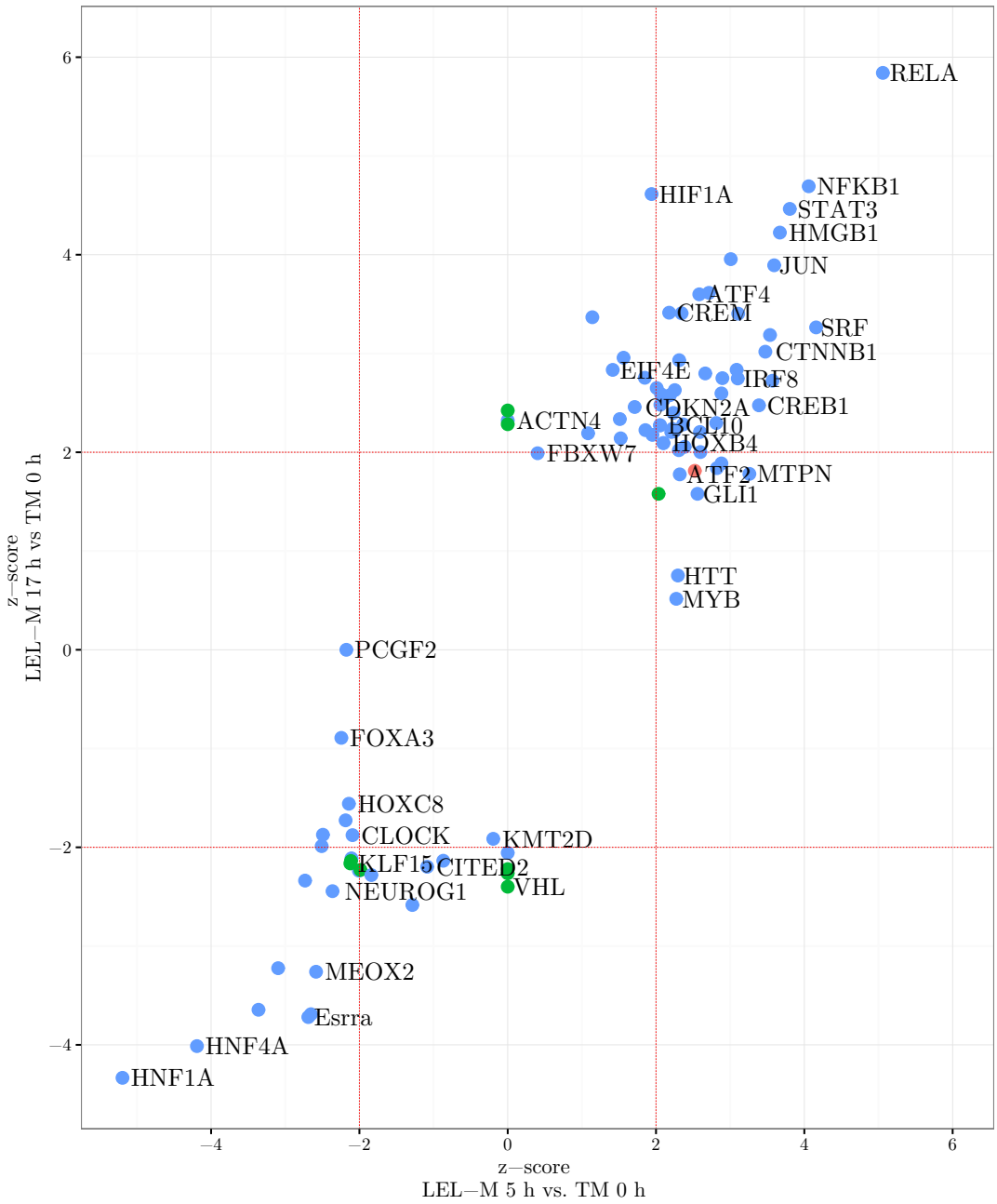

Figure A.6.: Activation of upstream transcription and translation factors in the LEL model as predicted by IPA. The only significant translation regulator was EIF4E. Blue dots indicate prediction of the transcription factor was significant (adj.P.Val < 0.05) for both observations, while red dots indicate significance of prediction for LEL-M 5 h vs. TM 0 h (Obs.1) and green dots for LEL-M 17 h vs. TM 0 h (Obs.2) only, respectively. Where z-score values were to close to each other to produce a readable name, only one name is given at random.

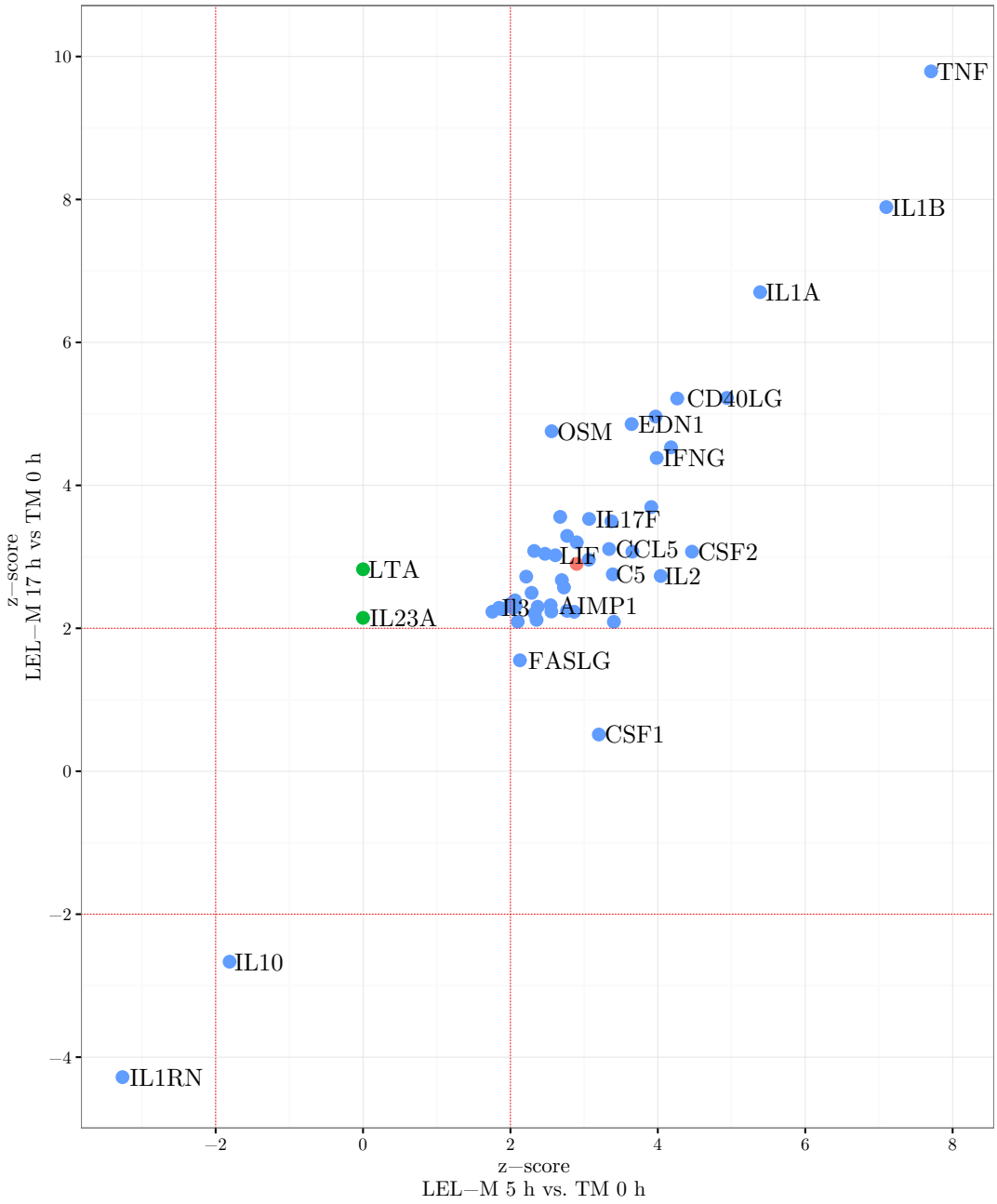

Figure A.7.: Activation of upstream regulator cytokines in the LEL model as predicted by IPA. Blue dots indicate that prediction of cytokine was significant (adj.P.Val < 0.05) for both observations, while red dots indicate significance of prediction for LEL-M 5 h vs. TM 0 h (Obs.1) and green dots for LEL-M 17 h vs. TM 0 h (Obs.2) only, respectively. Where z-score values were to close to each other to produce a readable name, only one name is given at random.

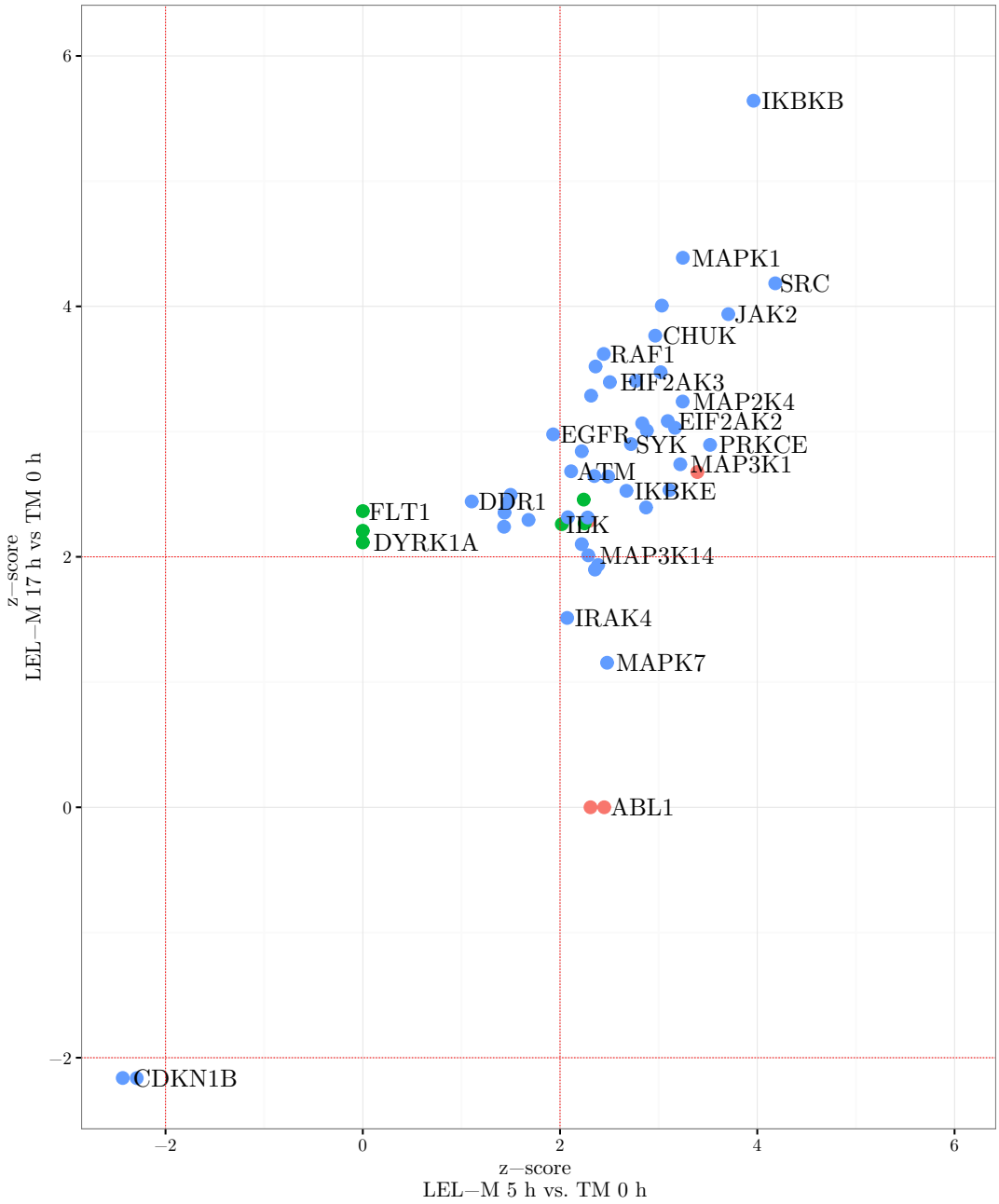

Figure A.8.: Activation of upstream regulator kinases in the LEL model as predicted by IPA. Blue dots indicate prediction of the kinase was significant (adj.P.Val $<$ 0.05) for both observations, while red dots indicate significance of prediction for LEL-M 5 h vs. TM 0 h (Obs.1) and green dots for LEL-M 17 h vs. TM 0 h (Obs.2) only, respectively. Where z-score values were to close to each other to produce a readable name, only one name is given at random.

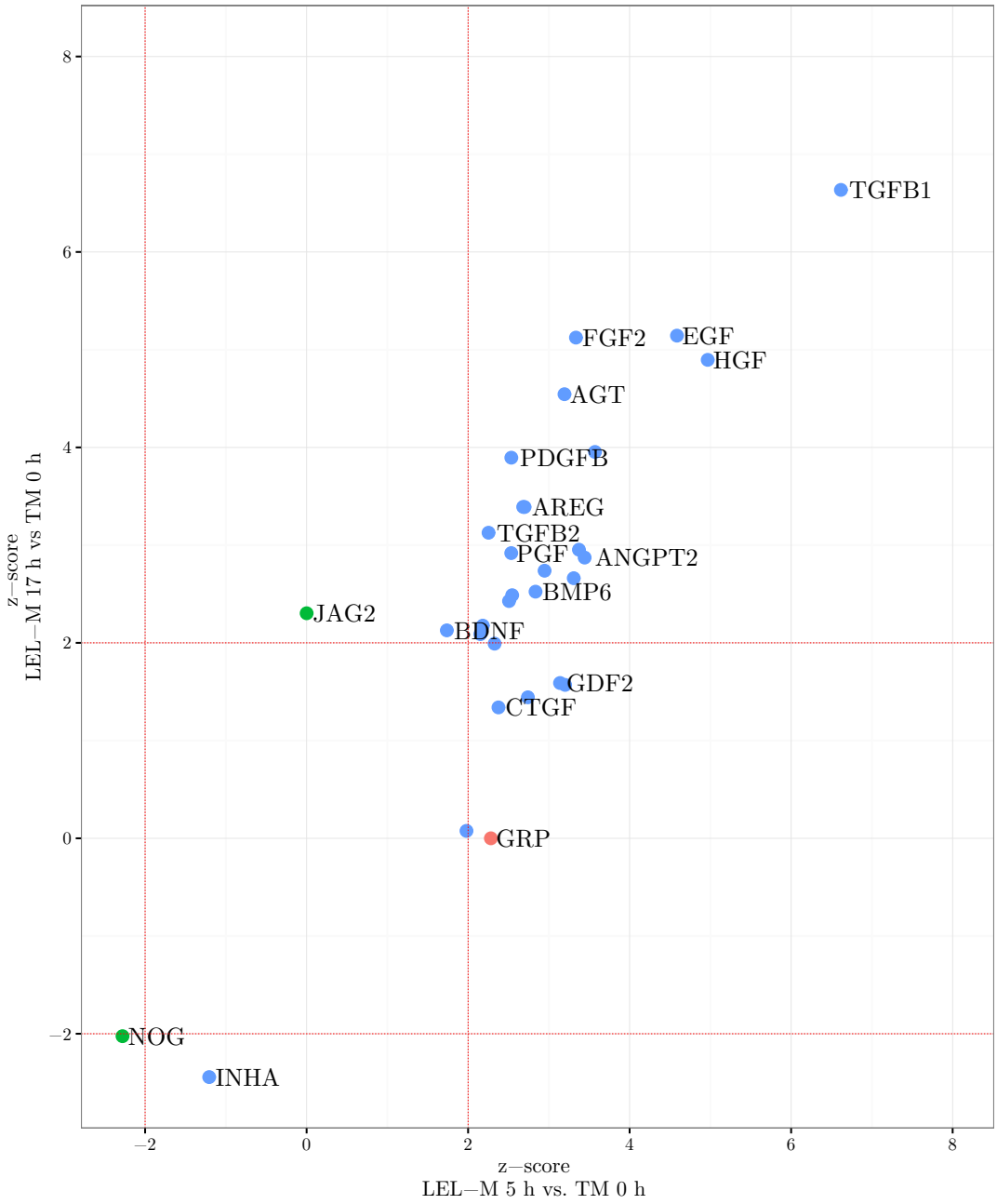

Figure A.9.: Activation of upstream regulator growth factors in the LEL model as predicted. Blue dots indicate prediction of the growth factor was significant (adj.P.Val < 0.05) for both observations, while red dots indicate significance of prediction for LEL-M 5 h vs. TM 0 h (Obs.1) and green dots for LEL-M 17 h vs. TM 0 h (Obs.2) only, respectively . Where z-score values were to close to each other to produce a readable name, only one name is given at random.

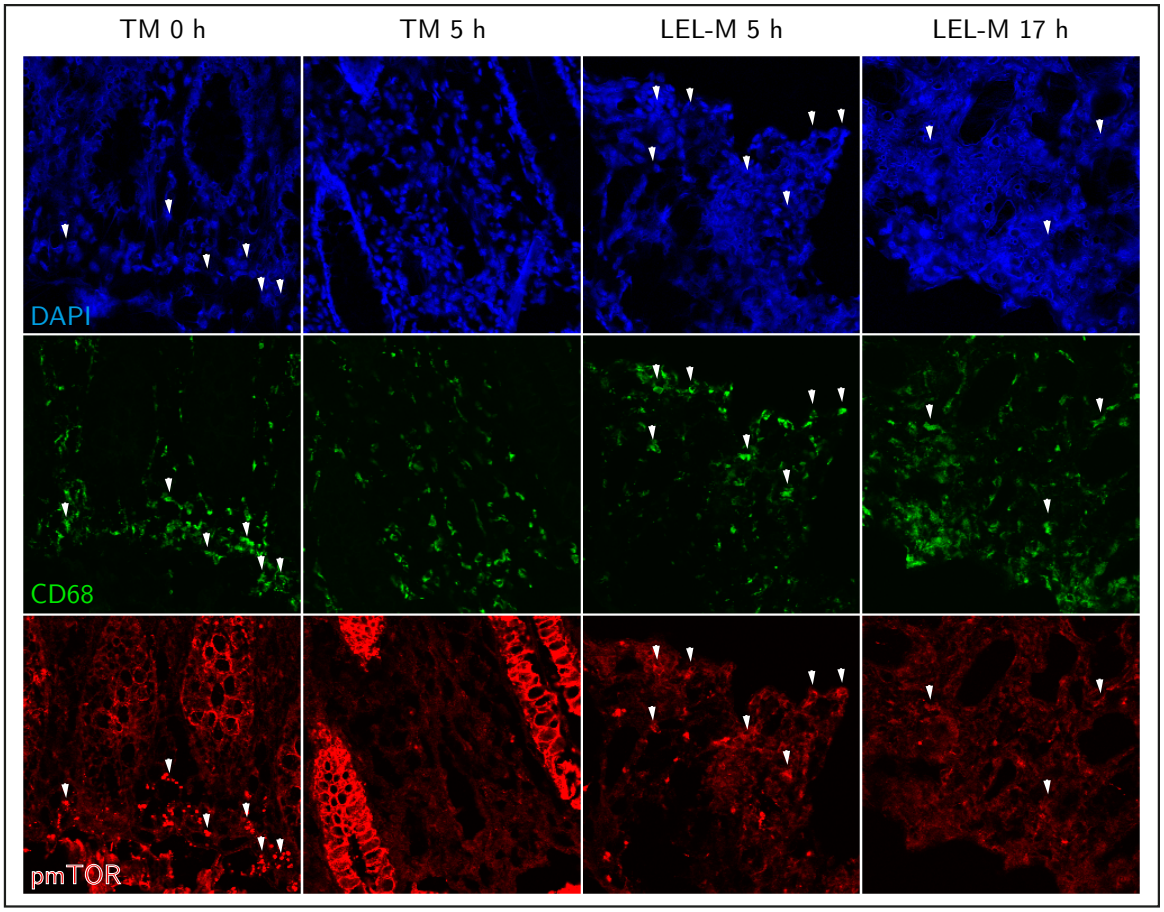

Figure A.10.: Phospho-mTOR^{Ser2448} expression in the LEL model. Immunofluorescent staining was performed using frozen sections. White arrows indicate phospho-mTOR^{+}CD68^{+} macrophages. For staining procedure, see subsection 2.7.3 on page 30.

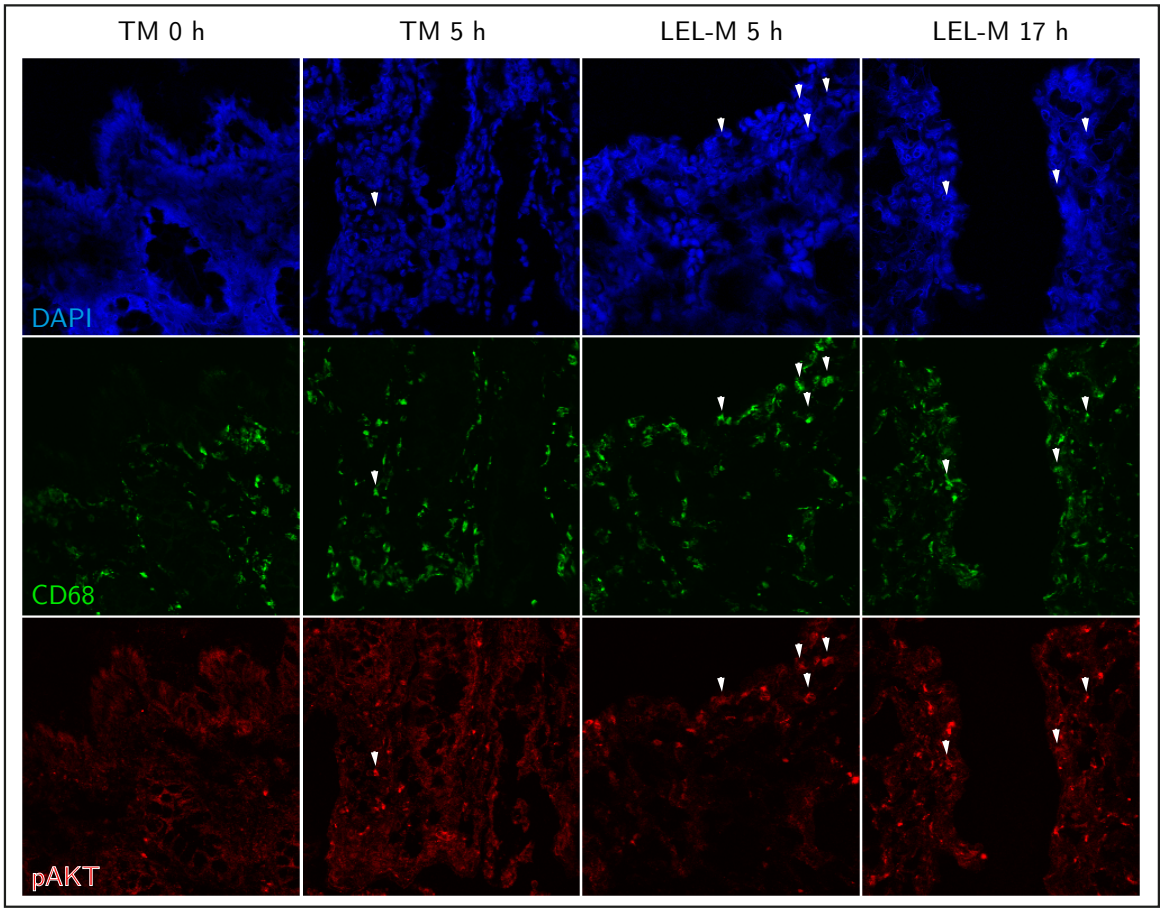

Figure A.11.: Phospho-AKT^{Ser473} expression in the LEL model. Immunofluorescent staining was performed using frozen sections. White arrows indicate phospho-AKT^{+}CD68^{+} macrophages. For staining procedure, see subsection 2.7.3 on page 30.

(A)

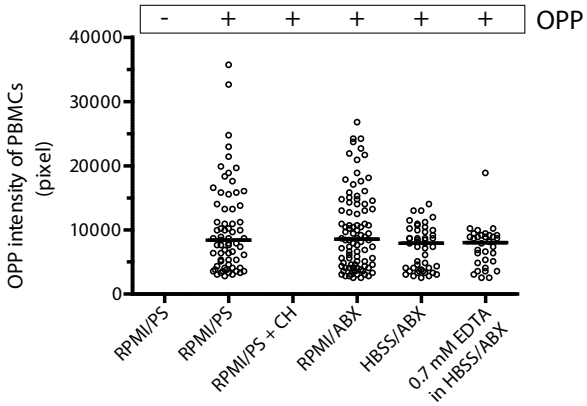
- + + + + + OPP
OPP intensity of PBMCs (pixel)
40000
30000
20000
10000
0
RPMI/PS
RPMI/PS
RPMI/PS + CH
RPMI/ABX
HBSS/ABX
0.7 mM EDTA in HBSS/ABX

(B)

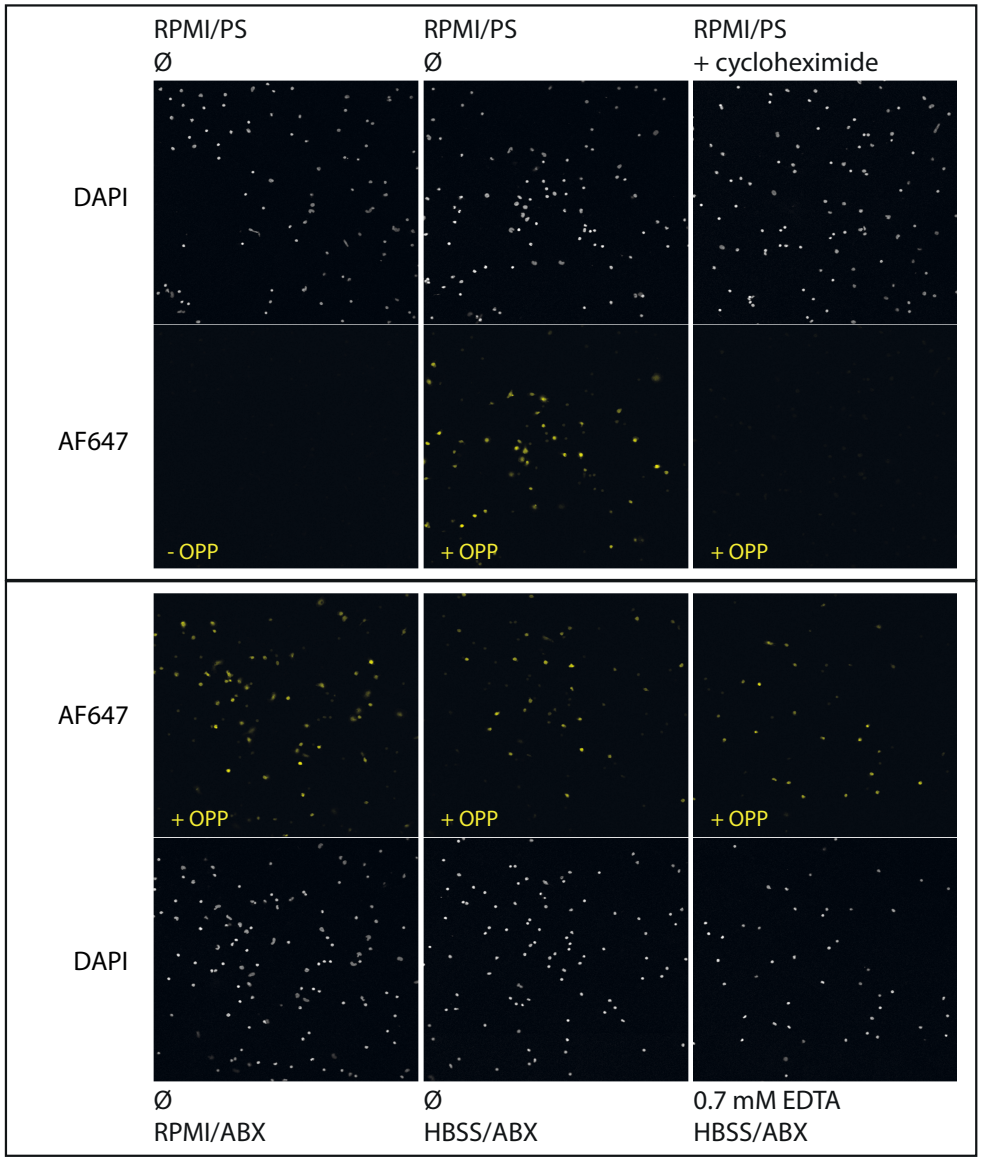
RPMI/PS Ø
RPMI/PS Ø
RPMI/PS + cycloheximide
DAPI
AF647
- OPP
+ OPP
+ OPP
AF647
+ OPP
+ OPP
+ OPP
DAPI
Ø RPMI/ABX
Ø HBSS/ABX
0.7 mM EDTA HBSS/ABX

Figure A.12. *(preceding page)*: Constitutive protein synthesis in PBMC evaluated by Click-It® technology. For details to procedure, see subsection 2.7.4 on page 31. Briefly, PBMC were obtained by Ficoll-Hypaque density gradient centrifugation. Cells were transferred to Poly-L-Lysin coated LapTek chamber slides and allow to adhere and regain resting conditions for 24 h at 37°C. 30 min prior to assessment of protein synthesis by OPP treatment (30 min, 20 μM), the medium in two wells was exchanged for HBSS/ABX and 0.7 mM EDTA in HBSS/ABX, respectively, while 100 μg/ml cycloheximide was added to a third well as a negative control for protein synthesis. (A) Semi-quantitative analysis of protein synthesis. For details to procedure, see section 2.7.5 on page 31 (B) Immunofluorescent images used for quantification. CH: cycloheximide; RPMI/PS: RPMI medium containing only Penicilin/Streptomycin; HBSS/ABX: HBSS with several antibiotics as used in LEL model (see table 2.1 on page 19)

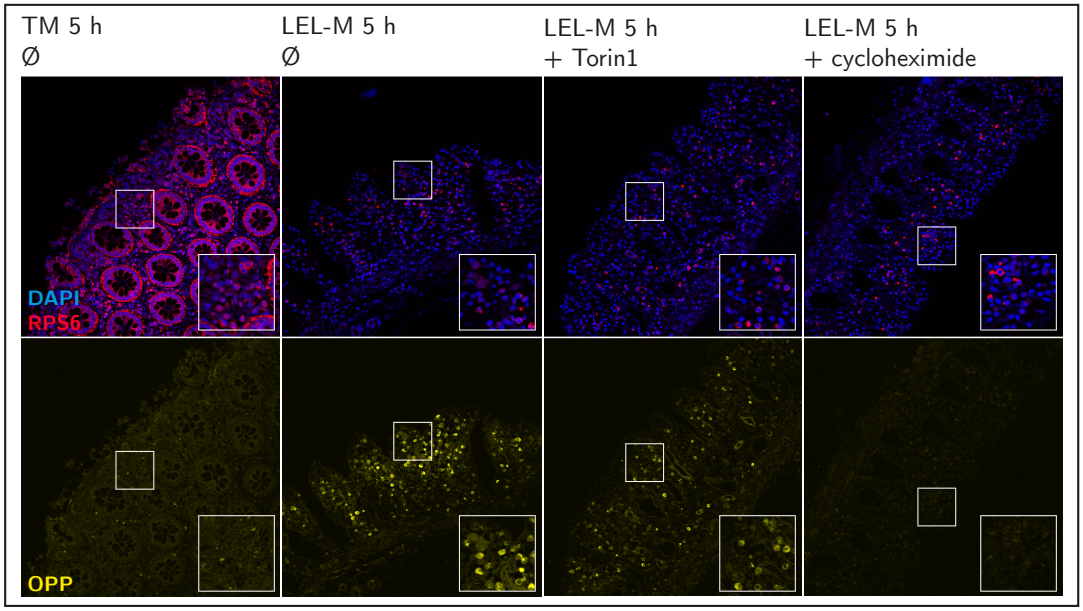

Figure A.13.: RPS6 expression in the LEL model in presence/absence of inhibitors. Rate of protein synthesis was determined via OPP Click-It® technology. Specified inhibitors (250 nM Torin-1 and 100 μg/ml cycloheximide) were present at all times during the performance of the LEL model. Results shown are from one representative experiment out of three independent experiments.

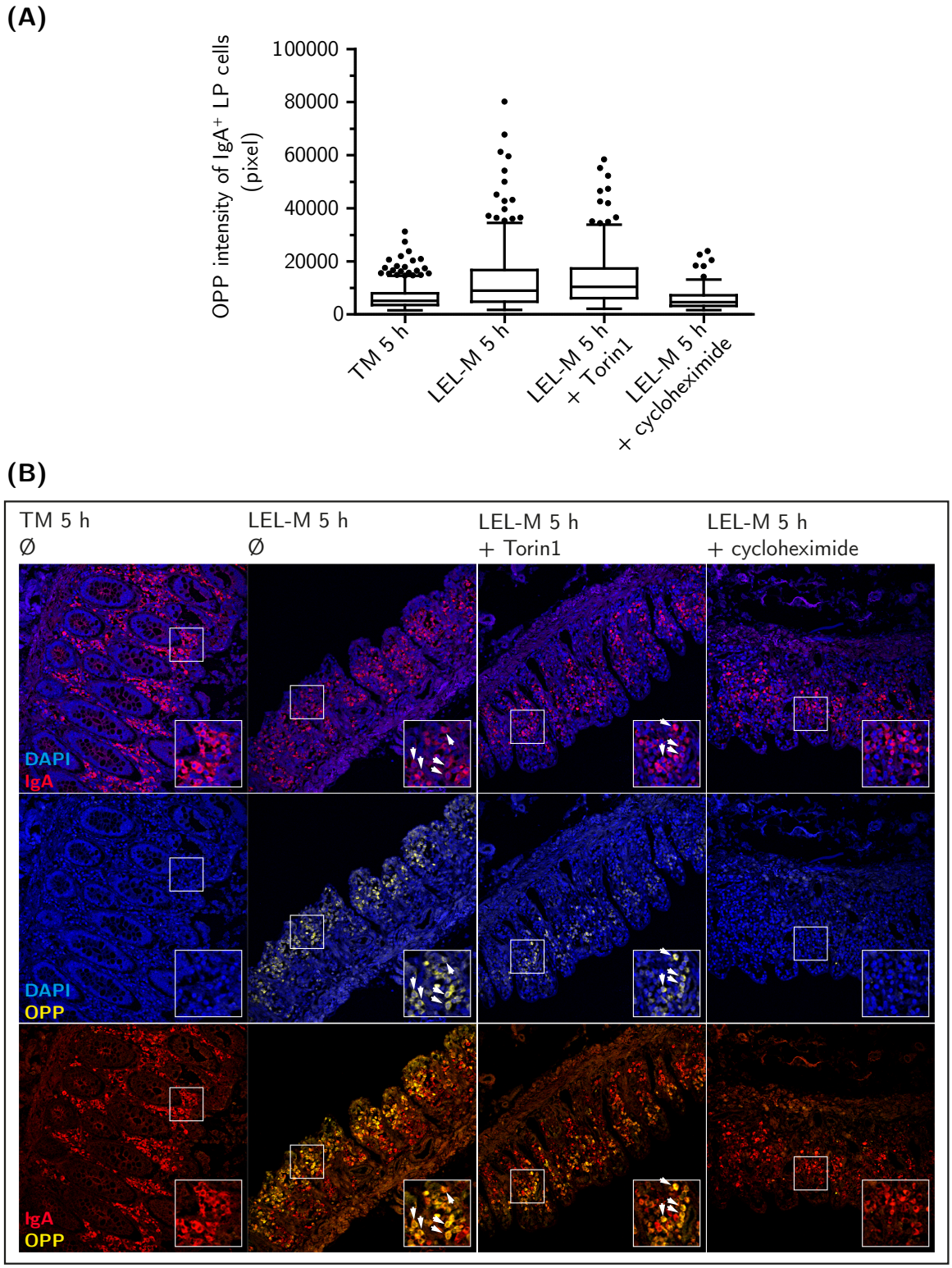

Figure A.14.: Protein synthesis in IgA$^+$ cells in the LEL model. Rate of protein synthesis was determined via OPP Click-It® technology. Specified inhibitors (250 nM Torin1 and 100 μg/ml cycloheximide) were present at all times during the performance of the LEL model. Results shown are from one representative experiment out of three independent experiments. (A) Semi-quantification of OPP intensity in IgA$^+$ macrophages shown as a Tukey boxplot (see page 31). 2100 ± 531 cells were analyzed per time point. (B) One of two immunofluorescent images used for quantification.

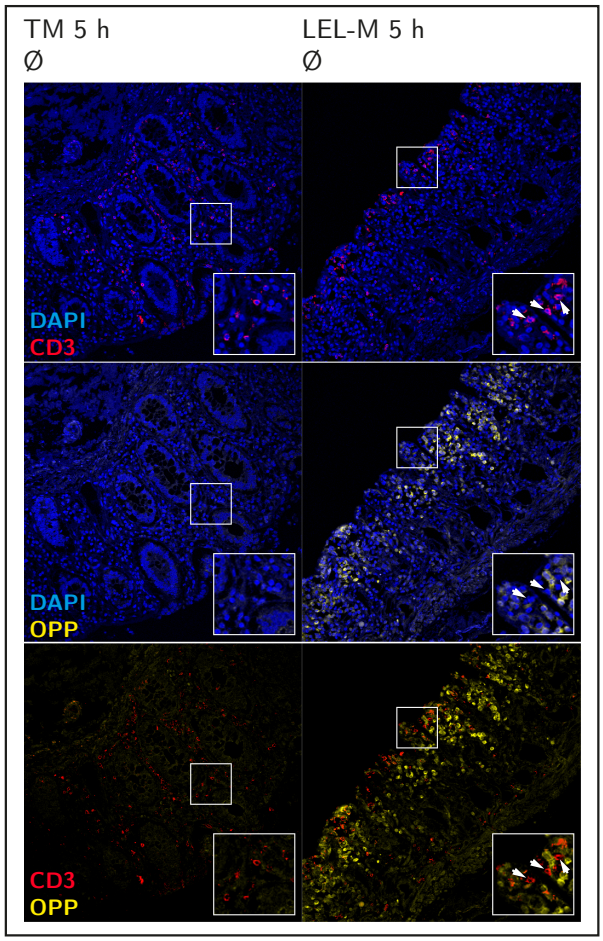

Figure A.15.: Protein synthesis in CD3$^+$ T cells in the LEL model. Rate of protein synthesis was determined via OPP Click-It® technology). Results shown are from one representative experiment out of two independent experiments.

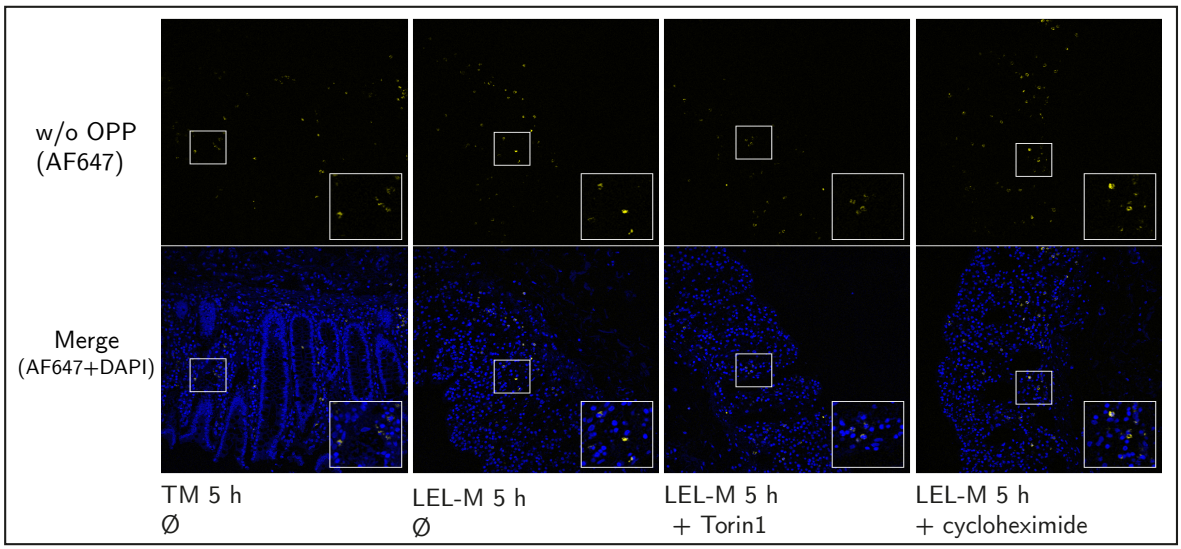

Figure A.16.: *Impact of mTOR on regulation of protein synthesis in the LEL model: Negative controls.* Rate of protein synthesis was determined via OPP Click-It® technology. Specified inhibitors (250 nM Torin1 and 100 μg/ml cycloheximide) were present at all times during the performance of the LEL model. The results represent one of three independent experiments. As a small percentage of cells was false-positive (as indicated by negative controls w/o OPP), this percentage was subtracted as background. On average, 1690 ($\pm$ 297) cells were analyzed per time point. Shown are the immunofluorescent images of negative controls used for quantification (one of two analyzed images is shown per time point). The corresponding images in the presence of OPP can be found in Figure 3.11 on page 62.

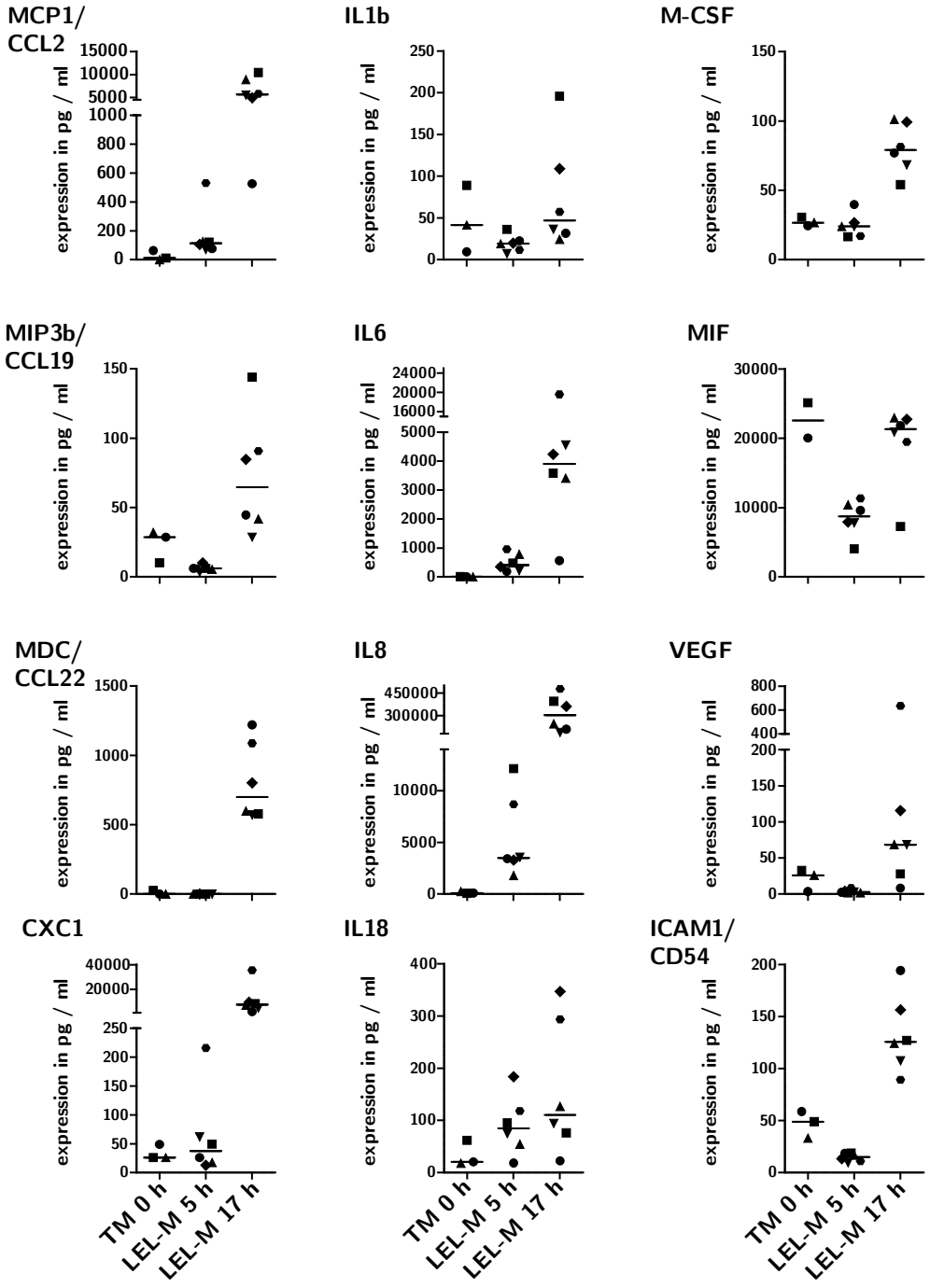

Figure A.17.: Secretion of inflammatory mediators in the LEL model I. At indicated time points, size standardized tissue punches were incubated in RPMI/ABX medium for 1 h (12 h for LEL-M 17 h). Supernatants were then subjected to Luminex® multiplex analysis. Inhibitors (250 nM Torin1, 10 μg/ml cycloheximide) were present throughout the performance of the LEL model.

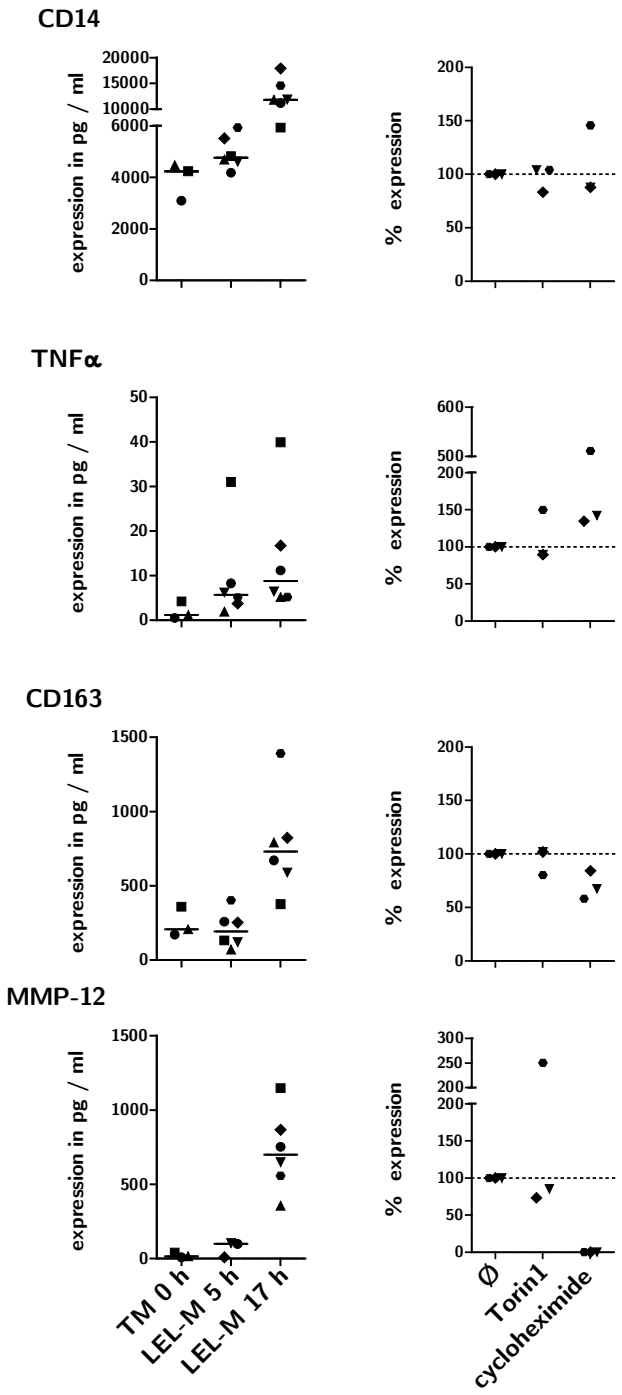

Figure A.18.: Secretion of inflammatory mediators in the LEL model II. At indicated time points, size standardized tissue punches were incubated in RPMI/ABX medium for 1 h (12 h for LEL-M 17 h). Supernatants were then subjected to Luminex® multiplex analysis. Graphs show relative expression values with LEL-M 17 h without inhibitor set to 100 %. Inhibitors (250 nM Torin1, 10 μg/ml cycloheximide) were present throughout the performance of the LEL model.

Table A.1.: WG-DASL Assay: Top 200 significantly upregulated genes for observation LEL-M 5 h vs. TM 0 h. Adj.P.Val $<$ 0.05 (Benjamini-Hochberg corrected); logFC $\geq |1|$.

	Gene	logFC	adj.P.Val
1	*CSF3*	6.52	1.0E-04
2	*IL6*	5.85	1.8E-04
3	*CSF3*	5.62	1.1E-03
4	*FAM71A*	5.62	2.1E-04
5	*MAFA*	5.45	2.0E-03
6	*RND1*	5.39	9.3E-05
7	*SERPINA3*	4.88	5.9E-04
8	*MAFF*	4.81	4.3E-04
9	*ADAMTS4*	4.71	8.1E-04
10	*EGR3*	4.70	1.1E-04
11	*AMPD3*	4.66	1.6E-03
12	*EGR3*	4.62	6.4E-05
13	*MOB4*	4.58	9.8E-05
14	*IL8*	4.57	1.6E-03
15	*CALCA*	4.44	2.0E-04
16	*CXCL2*	4.39	1.1E-04
17	*ARC*	4.37	8.3E-04
18	*IRF7*	4.34	1.1E-03
19	*TNFSF9*	4.33	9.8E-05
20	*HAS1*	4.30	3.7E-03
21	*GAP43*	4.29	5.8E-03
22	*C2CD4B*	4.26	1.1E-04
23	*ATF3*	4.25	1.4E-03
24	*DES*	4.21	1.0E-03
25	*UBC*	4.18	1.4E-03
26	*ULBP2*	4.17	1.6E-04
27	*MIR212*	4.14	5.4E-04
28	*ICAM4*	4.12	2.0E-04
29	*FOSL1*	4.12	1.2E-04
30	*SLC8A2*	4.11	1.1E-03
31	*ICAM4*	4.10	2.3E-04
32	*ABL2*	4.06	7.3E-04
33	*CCL21*	4.06	8.3E-04
34	*PCOLCE2*	4.05	2.6E-02
35	*MT1A*	4.02	3.7E-02
36	*GFPT2*	4.00	1.2E-04
37	*DNAAF1*	3.96	4.3E-04
38	*SFRP2*	3.96	1.8E-02
39	*GEM*	3.93	1.8E-03
40	*MAFF*	3.93	9.9E-04
41	*NFKB2*	3.93	1.0E-03
42	*KRT24*	3.89	8.2E-04
43	*PPP2R4*	3.87	9.7E-04
44	*NR4A1*	3.86	9.7E-03
45	*RRAD*	3.85	1.1E-04
46	*RERGL*	3.82	3.8E-02
47	*MIR132*	3.79	5.0E-03
48	*C2orf40*	3.79	5.4E-04
49	*PI16*	3.78	2.4E-02
50	*RRAD*	3.76	8.9E-04
51	*ATF3*	3.75	1.6E-03
52	*SOCS3*	3.75	1.1E-04
53	*CHRDL1*	3.74	3.7E-02
54	*MAFF*	3.66	2.1E-03
55	*RGS16*	3.65	5.0E-04
56	*PCDH10*	3.64	2.0E-04
57	*RELT*	3.59	8.4E-03
58	*NR4A2*	3.58	2.1E-03
59	*CSF3*	3.57	7.7E-03
60	*NR4A1*	3.53	3.7E-04
61	*PTGIS*	3.52	5.1E-04
62	*MIR320A*	3.52	7.3E-04
63	*PMAIP1*	3.49	4.4E-04
64	*NR4A3*	3.47	1.3E-03
65	*PEG10*	3.46	3.9E-04
66	*SLC2A14*	3.45	2.6E-04
67	*SELE*	3.44	6.2E-03
68	*NANOS1*	3.44	3.5E-03
69	*UPP1*	3.43	5.4E-03
70	*FGF18*	3.42	4.7E-04
71	*CDH16*	3.41	1.8E-02
72	*LOC440570*	3.41	9.9E-04
73	*IL1B*	3.37	2.2E-04
74	*SPHK1*	3.37	7.0E-03
75	*CDK16*	3.36	1.7E-03
76	*DDIT3*	3.35	5.3E-04

Continued...

Continued...

Table A.1.: WG-DASL Assay: Top 200 significantly upregulated genes for observation LEL-M 5 h vs. TM 0 h. Adj.P.Val $<$ 0.05 (Benjamini-Hochberg corrected); logFC $\geq |1|$. *Continued from previous page.*

	Gene	logFC	adj.P.Val
77	*MIR636*	3.35	5.4E-04
78	*MIR24-2*	3.34	1.6E-04
79	*TEX14*	3.33	8.9E-03
80	*G0S2*	3.32	2.2E-03
81	*NFKBIZ*	3.31	4.7E-03
82	*TNFRSF10D*	3.27	1.3E-03
83	*JPH2*	3.26	3.7E-03
84	*NR4A3*	3.23	1.6E-03
85	*SCN3B*	3.22	1.0E-03
86	*SLCO4A1*	3.22	1.1E-03
87	*CDH10*	3.22	1.9E-03
88	*SYT4*	3.20	1.8E-02
89	*MAFF*	3.18	4.1E-04
90	*CHRDL2*	3.18	1.1E-03
91	*UCN2*	3.15	3.9E-04
92	*SFRP1*	3.14	1.4E-02
93	*TSPYL2*	3.13	3.0E-03
94	*GREM1*	3.12	1.0E-02
95	*CD83*	3.11	7.4E-04
96	*KDM6B*	3.09	6.7E-03
97	*SOX17*	3.08	3.2E-03
98	*BDKRB1*	3.08	1.4E-02
99	*SFRP4*	3.07	3.0E-03
100	*GREM1*	3.06	5.3E-03
101	*MYC*	3.03	1.0E-02
102	*SBSPON*	3.02	2.4E-02
103	*S100A13*	3.02	3.3E-03
104	*MIR770*	3.00	3.7E-04
105	*ICAM1*	3.00	1.1E-03
106	*ING1*	3.00	6.0E-03
107	*NEFL*	2.99	1.7E-02
108	*RELN*	2.99	8.1E-03
109	*EIF4E*	2.99	3.1E-03
110	*MMP19*	2.97	8.9E-04
111	*NFKB2*	2.97	4.3E-04
112	*NPAS4*	2.96	2.0E-03
113	*TNFAIP6*	2.95	3.1E-03
114	*PNRC1*	2.95	1.7E-03
115	*MMP19*	2.94	1.0E-03
116	*VASN*	2.93	1.9E-03
117	*HSPB8*	2.92	1.2E-02
118	*PI15*	2.92	9.8E-03
119	*IL8*	2.92	9.5E-04
120	*SPHK1*	2.91	4.9E-03
121	*SERPINE1*	2.91	3.7E-04
122	*CPXM2*	2.90	2.0E-03
123	*P2RX2*	2.90	2.9E-02
124	*NR4A3*	2.90	2.2E-04
125	*VIP*	2.90	1.4E-02
126	*CCL3*	2.89	1.4E-03
127	*DHDH*	2.89	3.3E-03
128	*CD83*	2.89	3.2E-04
129	*ULBP1*	2.89	6.3E-03
130	*C9orf47*	2.88	1.5E-03
131	*CCBE1*	2.87	1.9E-03
132	*NFATC1*	2.86	1.6E-03
133	*LSMEM1*	2.86	1.3E-03
134	*TUBB3*	2.84	1.2E-03
135	*PRRX1*	2.83	1.3E-02
136	*SMOC2*	2.83	2.0E-02
137	*DLL4*	2.83	5.0E-03
138	*AKAP12*	2.82	2.2E-04
139	*LINC00152*	2.81	1.5E-03
140	*CDKN1A*	2.80	1.2E-02
141	*TSPYL2*	2.80	1.0E-02
142	*CCDC19*	2.79	3.5E-03
143	*IL23A*	2.78	1.5E-03
144	*ARL4D*	2.78	1.1E-02
145	*RGAG4*	2.78	1.2E-03
146	*MIR92B*	2.76	2.1E-03
147	*DGKB*	2.75	2.2E-02
148	*IL1A*	2.74	3.4E-03
149	*NFATC1*	2.73	1.1E-03
150	*FAM222A*	2.73	4.6E-03
151	*DYRK3*	2.72	3.4E-03

Continued...

Continued...

Table A.1.: WG-DASL Assay: Top 200 significantly upregulated genes for observation LEL-M 5 h vs. TM 0 h. Adj.P.Val $<$ 0.05 (Benjamini-Hochberg corrected); logFC $\geq$ |1|. *Continued from previous page.*

	Gene	logFC	adj.P.Val
152	*PLAUR*	2.71	1.1E-03
153	*APCDD1L*	2.71	3.3E-03
154	*SOX2*	2.70	2.5E-03
155	*PRKAR1A*	2.70	6.6E-03
156	*TGFB1*	2.70	8.9E-04
157	*KIF1A*	2.70	9.7E-03
158	*MSX1*	2.70	1.3E-02
159	*SLC41A1*	2.70	7.5E-03
160	*ARID5A*	2.69	3.1E-03
161	*WISP2*	2.69	4.0E-03
162	*NCS1*	2.69	4.8E-03
163	*MAP1A*	2.69	1.2E-02
164	*DPP6*	2.68	3.4E-02
165	*CSF2*	2.66	9.0E-03
166	*HSPA2*	2.64	9.8E-03
167	*WTAP*	2.64	3.1E-03
168	*MMP16*	2.63	3.7E-03
169	*CADM3*	2.63	6.3E-03
170	*ACAN*	2.62	9.0E-04
171	*FDCSP*	2.62	6.9E-03
172	*FAXC*	2.62	2.2E-03
173	*GCH1*	2.62	7.7E-03
174	*PTPDC1*	2.62	1.6E-02
175	*PCDHA7*	2.61	8.5E-03
176	*NR4A3*	2.61	1.0E-03
177	*TNFSF14*	2.61	4.3E-02
178	*HAPLN3*	2.60	1.7E-02
179	*MEDAG*	2.60	2.4E-02
180	*C2orf66*	2.60	1.2E-03
181	*TNFRSF12A*	2.59	1.0E-02
182	*GRIK1*	2.59	3.3E-03
183	*RGMA*	2.58	8.4E-03
184	*PDLIM7*	2.57	1.9E-03
185	*SORBS1*	2.56	1.3E-02
186	*RPL13P5*	2.56	1.9E-02
187	*FLT4*	2.56	6.4E-03
188	*HIST3H2A*	2.55	3.9E-03
189	*DUSP4*	2.55	2.3E-02
190	*PNCK*	2.54	8.0E-03
191	*CILP*	2.54	4.6E-02
192	*CYB5D1*	2.53	1.4E-03
193	*OSM*	2.53	1.2E-02
194	*MOGAT1*	2.52	1.1E-03
195	*FAP*	2.52	1.7E-02
196	*GPM6B*	2.52	1.1E-02
197	*PRPH*	2.52	3.2E-02
198	*C10orf10*	2.51	1.1E-03
199	*MIR645*	2.51	2.1E-02
200	*TUBB2B*	2.50	3.3E-03

Continued...

Table A.2.: WG-DASL Assay: Top 200 significantly downregulated genes for observation LEL-M 5 h vs. TM 0 h. Adj.P.Val $<$ 0.05 (Benjamini-Hochberg corrected); logFC $\geq |1|$.

	Gene	logFC	adj.P.Val
1	*TMIGD1*	-6.33	1.8E-03
2	*MS4A12*	-6.21	1.3E-03
3	*CEACAM7*	-5.99	1.9E-03
4	*SLC17A4*	-5.95	6.4E-05
5	*COL17A1*	-5.87	6.4E-05
6	*BTNL3*	-5.84	2.9E-04
7	*TMPRSS2*	-5.72	4.3E-03
8	*CD177*	-5.57	1.6E-04
9	*GGT6*	-5.54	2.2E-04
10	*KRT20*	-5.53	2.3E-04
11	*IGSF9*	-5.46	6.4E-05
12	*EDN3*	-5.30	3.1E-03
13	*CDH17*	-5.27	1.1E-04
14	*GCNT3*	-5.19	1.9E-03
15	*MARVELD3*	-5.17	4.3E-04
16	*MEP1A*	-5.17	1.1E-04
17	*CDHR5*	-5.12	2.5E-04
18	*GUCA2B*	-5.06	1.9E-03
19	*TUBAL3*	-5.01	9.8E-04
20	*SLC51B*	-4.91	3.1E-04
21	*TMEM139*	-4.91	1.3E-04
22	*UGT2A3*	-4.88	1.2E-04
23	*CLCA4*	-4.88	3.3E-03
24	*ITGB6*	-4.79	2.0E-03
25	*PPP1R14D*	-4.79	1.1E-03
26	*B3GALT5*	-4.76	1.4E-04
27	*BEST2*	-4.76	1.2E-04
28	*TFF1*	-4.76	1.2E-04
29	*C1orf210*	-4.74	2.3E-04
30	*FUT3*	-4.74	3.8E-04
31	*CLRN3*	-4.73	1.0E-03
32	*B3GALT5*	-4.70	1.2E-04
33	*A1CF*	-4.68	8.2E-03
34	*HMGCS2*	-4.65	4.3E-03
35	*LRRC19*	-4.64	1.2E-03
36	*GBA3*	-4.63	5.7E-04
37	*FABP1*	-4.63	7.6E-04
38	*BCAS1*	-4.62	2.6E-04
39	*TMEM45B*	-4.61	2.2E-04
40	*CDHR5*	-4.60	7.6E-04
41	*DHRS9*	-4.58	1.2E-04
42	*CDHR2*	-4.56	2.1E-03
43	*NXPE4*	-4.54	4.3E-04
44	*EFNA2*	-4.54	2.3E-04
45	*PLA2G4F*	-4.51	1.7E-04
46	*SCIN*	-4.50	2.4E-04
47	*RAB25*	-4.50	1.1E-04
48	*C1orf116*	-4.47	1.4E-03
49	*SLC51A*	-4.46	5.3E-03
50	*ZG16*	-4.44	1.3E-03
51	*CLDN8*	-4.43	5.9E-04
52	*GPR128*	-4.42	1.3E-04
53	*TRIM15*	-4.42	9.6E-03
54	*OTOP2*	-4.39	2.1E-03
55	*ANKS4B*	-4.39	2.2E-04
56	*C1orf210*	-4.37	7.6E-04
57	*PPP1R14C*	-4.36	7.6E-04
58	*CAPN13*	-4.34	6.3E-04
59	*CA7*	-4.34	1.4E-03
60	*TM4SF5*	-4.29	5.3E-03
61	*AQP8*	-4.28	1.1E-03
62	*CBLC*	-4.28	3.4E-04
63	*F2RL1*	-4.27	1.2E-04
64	*CEACAM6*	-4.27	4.6E-04
65	*CA1*	-4.27	2.4E-04
66	*LOC389332*	-4.26	1.6E-04
67	*F2RL1*	-4.26	1.2E-04
68	*SULT1B1*	-4.26	4.7E-04
69	*NOX1*	-4.25	3.5E-03
70	*GDA*	-4.23	1.3E-04
71	*C12orf36*	-4.23	1.8E-02
72	*NAT2*	-4.22	1.2E-04
73	*CLDN8*	-4.22	1.9E-04
74	*CTSE*	-4.21	3.9E-03
75	*LRRC31*	-4.19	4.1E-03
76	*NR1I2*	-4.19	4.3E-04

Continued...

Continued...

Table A.2.: WG-DASL Assay: Top 200 significantly downregulated genes for observation LEL-M 5 h vs. TM 0 h. Adj.P.Val $<$ 0.05 (Benjamini-Hochberg corrected); logFC $\geq |1|$. *Continued from previous page.*

	Gene	logFC	adj.P.Val
77	*ISX*	-4.17	1.9E-03
78	*CRB3*	-4.15	1.2E-04
79	*CD177*	-4.14	6.3E-04
80	*CEACAM5*	-4.14	2.9E-03
81	*C1orf106*	-4.14	6.5E-03
82	*BCL2L15*	-4.13	1.1E-03
83	*PDE6A*	-4.12	7.8E-04
84	*GBA3*	-4.12	4.6E-04
85	*SRI*	-4.11	3.2E-04
86	*BCAS1*	-4.11	1.1E-04
87	*CYP4F2*	-4.10	1.2E-03
88	*MT1H*	-4.09	1.2E-04
89	*KRT19*	-4.08	7.8E-04
90	*SLC13A2*	-4.08	1.3E-03
91	*DEFB1*	-4.08	1.1E-03
92	*METTL7B*	-4.08	1.6E-04
93	*SHD*	-4.06	2.3E-03
94	*C10orf99*	-4.06	8.1E-03
95	*SI*	-4.03	5.0E-04
96	*DSG2*	-4.02	3.7E-04
97	*MYO1A*	-4.02	1.6E-03
98	*FXYD3*	-4.00	7.6E-04
99	*LOC100124692*	-3.98	3.7E-04
100	*A1CF*	-3.98	4.5E-04
101	*MARVELD3*	-3.97	7.7E-03
102	*FOXA1*	-3.97	3.1E-04
103	*UGT1A6*	-3.97	4.1E-03
104	*PLS1*	-3.95	1.1E-03
105	*KRTAP13-2*	-3.95	2.5E-04
106	*FAM83E*	-3.94	8.8E-03
107	*CLDN7*	-3.94	2.1E-03
108	*PTK6*	-3.93	2.7E-04
109	*MYO5B*	-3.93	8.6E-04
110	*TJP3*	-3.92	5.2E-03
111	*LRRC26*	-3.92	1.4E-03
112	*FFAR4*	-3.92	1.5E-03
113	*GPA33*	-3.90	3.8E-04
114	*HSD11B2*	-3.88	2.9E-03
115	*SERINC2*	-3.87	2.3E-03
116	*MB*	-3.86	1.1E-04
117	*COL17A1*	-3.86	1.1E-04
118	*HKDC1*	-3.85	3.1E-03
119	*CEACAM1*	-3.85	2.7E-04
120	*PTGDR*	-3.84	4.2E-03
121	*CDH1*	-3.84	6.2E-04
122	*NOX1*	-3.82	1.2E-02
123	*SGK2*	-3.82	2.2E-04
124	*MS4A8*	-3.81	4.5E-03
125	*PLS1*	-3.81	4.7E-04
126	*FXYD3*	-3.80	2.7E-03
127	*CKMT1B*	-3.80	1.9E-03
128	*SPDEF*	-3.78	5.9E-03
129	*NXPE1*	-3.78	2.4E-03
130	*PDZD3*	-3.78	2.2E-04
131	*CDX2*	-3.77	1.2E-03
132	*TMC5*	-3.77	3.1E-04
133	*TSPAN8*	-3.76	6.0E-04
134	*EPB41L4B*	-3.76	1.1E-03
135	*ARL14*	-3.75	3.1E-03
136	*TMEM236*	-3.73	3.2E-04
137	*EPS8L3*	-3.72	8.8E-03
138	*TMEM171*	-3.72	3.3E-03
139	*BARX2*	-3.72	3.2E-04
140	*PTPRR*	-3.72	2.1E-04
141	*MYO7B*	-3.71	8.8E-03
142	*HHLA2*	-3.71	7.5E-04
143	*C9orf152*	-3.71	1.1E-03
144	*MYH14*	-3.70	1.8E-04
145	*REG4*	-3.70	1.3E-02
146	*HNF1B*	-3.70	2.7E-03
147	*SLC35G1*	-3.69	7.1E-04
148	*PIGR*	-3.68	1.0E-02
149	*ATP2C2*	-3.68	3.4E-03
150	*ESRP1*	-3.68	9.4E-04
151	*TBX10*	-3.68	1.7E-03

Continued...

Continued...

Table A.2.: WG-DASL Assay: Top 200 significantly downregulated genes for observation LEL-M 5 h vs. TM 0 h. Adj.P.Val $<$ 0.05 (Benjamini-Hochberg corrected); logFC $\geq$ |1|. *Continued from previous page.*

	Gene	logFC	adj.P.Val
152	*GUCY2C*	-3.68	2.2E-03
153	*PRAP1*	-3.66	1.1E-02
154	*SPINK1*	-3.66	1.4E-02
155	*EDN3*	-3.65	1.1E-04
156	*OVOL2*	-3.65	1.2E-03
157	*DHRS11*	-3.65	1.0E-03
158	*AP1M2*	-3.64	5.6E-04
159	*UGT1A8*	-3.63	4.5E-03
160	*ATOH1*	-3.63	1.8E-03
161	*AOC1*	-3.62	2.0E-03
162	*GPT*	-3.62	1.6E-03
163	*HRCT1*	-3.62	9.2E-03
164	*MT1H*	-3.61	3.8E-04
165	*LGALS4*	-3.61	3.8E-03
166	*WDR72*	-3.61	3.4E-03
167	*UGT1A7*	-3.60	1.8E-03
168	*TTLL6*	-3.59	9.2E-04
169	*PDZK1IP1*	-3.58	2.1E-03
170	*SCGB2A1*	-3.58	1.2E-04
171	*BCMO1*	-3.58	1.4E-03
172	*DSC2*	-3.58	2.0E-04
173	*ITPKA*	-3.57	2.3E-03
174	*PTK6*	-3.56	1.8E-02
175	*TRIM15*	-3.55	1.1E-02
176	*MUC13*	-3.53	1.0E-02
177	*CA2*	-3.53	3.4E-03
178	*BTNL3*	-3.52	8.9E-03
179	*DMBT1*	-3.51	4.6E-04
180	*PRSS3*	-3.50	1.4E-03
181	*GUCA2A*	-3.50	1.4E-03
182	*MUC2*	-3.49	4.2E-03
183	*FABP2*	-3.48	1.6E-03
184	*AKR1B10*	-3.48	5.8E-03
185	*PLA2G10*	-3.47	7.7E-03
186	*NR1I2*	-3.47	5.5E-04
187	*STX19*	-3.47	2.0E-03
188	*HEPACAM2*	-3.46	3.1E-02
189	*ALPI*	-3.45	8.8E-03
190	*SDCBP2*	-3.44	1.1E-02
191	*AGR3*	-3.44	1.6E-03
192	*CLIC5*	-3.42	1.2E-04
193	*XK*	-3.42	2.2E-04
194	*TRIM31*	-3.42	1.8E-03
195	*SLC4A4*	-3.42	2.3E-02
196	*MYOM3*	-3.41	5.4E-03
197	*CAPN9*	-3.41	5.9E-03
198	*NXPE4*	-3.41	2.0E-03
199	*MARVELD3*	-3.40	8.0E-03
200	*NGEF*	-3.40	2.4E-03

Continued...

Table A.3.: WG-DASL Assay: Top 200 significantly upregulated genes for observation LEL-M 17 h vs. TM 0 h. Adj.P.Val $<$ 0.05 (Benjamini-Hochberg corrected); logFC $\geq |1|$.

	Gene	logFC	adj.P.Val
1	*CSF3*	7.26	4.4E-07
2	*KIAA1199*	7.07	2.5E-05
3	*MMP10*	6.94	3.1E-06
4	*CSF3*	6.68	3.1E-06
5	*IL6*	6.35	4.4E-06
6	*IL8*	5.78	9.3E-05
7	*AMPD3*	5.57	2.0E-05
8	*IL24*	5.21	4.9E-04
9	*ADAMTS4*	5.20	4.4E-05
10	*SERPINA3*	4.93	1.4E-04
11	*NPTX1*	4.92	2.0E-05
12	*SLC8A2*	4.89	3.0E-05
13	*CXCL2*	4.85	3.6E-06
14	*MMP1*	4.85	2.3E-05
15	*MOB4*	4.84	6.4E-04
16	*IL1RN*	4.83	1.3E-04
17	*IL11*	4.79	6.2E-05
18	*MME*	4.75	2.6E-04
19	*MME*	4.72	7.1E-04
20	*FOSL1*	4.69	6.5E-06
21	*MMP3*	4.68	1.9E-04
22	*RND1*	4.62	3.4E-05
23	*NPTX1*	4.60	1.8E-03
24	*DKFZp451A211*	4.53	3.5E-05
25	*CALCA*	4.48	6.4E-04
26	*IL22*	4.47	1.4E-05
27	*PALM2*	4.40	5.3E-05
28	*MEDAG*	4.39	2.2E-05
29	*PALM2*	4.39	2.2E-05
30	*DPYSL4*	4.38	2.1E-04
31	*CSF3*	4.28	5.0E-04
32	*IL22*	4.27	1.7E-05
33	*C12orf50*	4.24	3.6E-05
34	*GEM*	4.20	2.9E-04
35	*SERPINB2*	4.20	2.1E-03
36	*MAFF*	4.18	2.2E-05
37	*BDKRB1*	4.18	2.2E-04
38	*CRYM*	4.17	1.5E-05
39	*IL1RN*	4.17	2.5E-03
40	*INHBA*	4.14	1.7E-05
41	*SPHK1*	4.13	5.1E-04
42	*SERPINE1*	4.12	1.1E-05
43	*P2RX2*	4.11	6.7E-05
44	*THBS2*	4.06	2.0E-04
45	*PRRX1*	4.06	2.5E-04
46	*MAFF*	4.06	8.9E-04
47	*MME*	4.05	1.8E-04
48	*ABL2*	4.05	3.1E-04
49	*C2CD4B*	4.03	2.3E-05
50	*AKAP2*	4.03	1.8E-04
51	*ANO3*	4.01	4.8E-03
52	*IL1RL1*	3.98	5.1E-05
53	*DYRK3*	3.96	1.9E-04
54	*SPHK1*	3.94	1.3E-03
55	*CSF2*	3.93	3.4E-05
56	*PRRX1*	3.90	2.8E-05
57	*CXCL5*	3.88	3.6E-03
58	*EGR3*	3.87	2.7E-05
59	*SLC2A14*	3.87	6.7E-05
60	*CRLF2*	3.86	1.6E-04
61	*G0S2*	3.86	3.1E-04
62	*HAS1*	3.85	2.1E-03
63	*KRT17*	3.84	1.6E-03
64	*UCN2*	3.83	8.0E-05
65	*ARC*	3.82	2.6E-05
66	*MIR210*	3.82	9.3E-03
67	*PTGIS*	3.81	7.1E-05
68	*CA9*	3.81	2.7E-04
69	*ATF3*	3.79	2.2E-03
70	*SPP1*	3.77	5.3E-05
71	*LRFN5*	3.77	2.7E-04
72	*SGIP1*	3.77	4.7E-04
73	*FGF5*	3.71	4.0E-05
74	*STC2*	3.71	2.6E-04
75	*NR4A2*	3.69	1.0E-03
76	*SOCS3*	3.68	2.2E-05

Continued...

Continued...

Table A.3.: WG-DASL Assay: Top 200 significantly upregulated genes for observation LEL-M 17 h vs. TM 0 h. Adj.P.Val $<$ 0.05 (Benjamini-Hochberg corrected); logFC $\geq$ |1|. *Continued from previous page.*

	Gene	logFC	adj.P.Val
77	*PTGS2*	3.67	4.5E-05
78	*PDLIM4*	3.67	4.0E-04
79	*CCL21*	3.67	2.6E-03
80	*DYRK3*	3.65	5.1E-05
81	*NFKB2*	3.64	1.7E-03
82	*RGS16*	3.62	1.3E-04
83	*TNFRSF11B*	3.61	1.1E-03
84	*UPP1*	3.61	1.5E-03
85	*FAM180A*	3.58	1.2E-04
86	*SLCO4A1*	3.57	6.7E-05
87	*IL13RA2*	3.55	1.2E-03
88	*GREM1*	3.53	2.1E-04
89	*MAFA*	3.52	1.4E-02
90	*TMEFF1*	3.50	2.6E-04
91	*IL1RL1*	3.49	1.7E-04
92	*TRIML2*	3.49	6.8E-03
93	*IL1A*	3.48	3.6E-04
94	*ICAM4*	3.47	3.2E-04
95	*GDF15*	3.46	2.6E-04
96	*GREM1*	3.46	3.4E-04
97	*PMAIP1*	3.46	4.9E-04
98	*IL8*	3.45	7.1E-05
99	*MT1A*	3.45	2.4E-03
100	*ATF3*	3.45	2.6E-03
101	*UBD*	3.44	5.7E-04
102	*MAFF*	3.43	4.3E-05
103	*NOG*	3.42	9.5E-04
104	*ANGPT2*	3.41	3.0E-03
105	*LOC440570*	3.40	4.4E-04
106	*PDPN*	3.37	2.2E-04
107	*C1orf100*	3.36	3.7E-04
108	*TNFRSF12A*	3.35	1.1E-03
109	*SERPINB2*	3.35	2.2E-02
110	*EFCAB3*	3.34	1.3E-03
111	*CBLN2*	3.33	1.6E-03
112	*MYC*	3.33	2.3E-03
113	*CHRDL1*	3.33	4.3E-03
114	*MURC*	3.31	6.4E-05
115	*RRAD*	3.30	1.7E-04
116	*ZBTB1*	3.30	2.3E-02
117	*RPL23AP82*	3.29	6.8E-04
118	*TNFRSF9*	3.28	2.0E-04
119	*GFPT2*	3.26	1.1E-04
120	*GEM*	3.25	3.7E-05
121	*ICAM4*	3.23	7.1E-04
122	*MIR212*	3.20	1.8E-03
123	*VEGFA*	3.20	1.9E-03
124	*NEURL3*	3.19	1.7E-02
125	*FDCSP*	3.15	9.2E-04
126	*LIF*	3.15	1.0E-03
127	*FGF2*	3.14	3.4E-04
128	*EGR3*	3.14	2.0E-03
129	*FAM71A*	3.14	2.3E-03
130	*PRG2*	3.13	2.5E-04
131	*BAALC*	3.13	3.0E-04
132	*RRAD*	3.11	7.7E-05
133	*MME*	3.11	1.8E-03
134	*MIR199A1*	3.08	7.9E-05
135	*SELE*	3.08	2.2E-03
136	*STC1*	3.05	2.3E-04
137	*APCDD1L*	3.04	6.4E-05
138	*ARG2*	3.03	9.3E-05
139	*PTGES*	3.03	3.2E-04
140	*AK4*	3.03	4.4E-03
141	*PCOLCE2*	3.03	1.8E-02
142	*SLC7A11*	3.02	8.6E-04
143	*KCNN2*	3.02	1.5E-02
144	*SLC11A1*	3.02	3.9E-02
145	*TNFSF9*	3.00	5.8E-04
146	*TNFSF15*	2.99	2.7E-05
147	*ZNF385D*	2.99	7.9E-05
148	*ESM1*	2.99	1.3E-02
149	*TNFAIP6*	2.98	7.2E-05
150	*TAC1*	2.98	3.0E-03
151	*GAP43*	2.96	1.8E-02

Continued...

Continued...

Table A.3.: WG-DASL Assay: Top 200 significantly upregulated genes for observation LEL-M 17 h vs. TM 0 h. Adj.P.Val < 0.05 (Benjamini-Hochberg corrected); logFC ≥ |1|. *Continued from previous page.*

	Gene	logFC	adj.P.Val
152	*FJX1*	2.94	4.0E-03
153	*CHRDL2*	2.93	1.5E-03
154	*NR1D1*	2.90	1.3E-04
155	*PFKFB4*	2.90	1.9E-04
156	*NCS1*	2.90	1.4E-03
157	*POU5F1*	2.90	4.8E-03
158	*IRX3*	2.88	1.4E-03
159	*P2RX2*	2.87	8.9E-03
160	*DES*	2.87	1.3E-02
161	*DDIT3*	2.86	5.7E-04
162	*DHDH*	2.86	1.9E-03
163	*KDM6B*	2.86	7.9E-03
164	*ULBP2*	2.84	5.9E-04
165	*HGF*	2.84	1.3E-03
166	*SLC41A1*	2.83	4.2E-03
167	*LYPD5*	2.82	2.8E-04
168	*PRDM16*	2.82	2.8E-03
169	*NR4A1*	2.82	3.9E-02
170	*CCRN4L*	2.81	6.4E-05
171	*ARL13B*	2.81	7.1E-05
172	*LYPD5*	2.81	7.3E-05
173	*TRPC4*	2.81	9.6E-05
174	*TCEAL7*	2.81	6.4E-04
175	*TAC1*	2.81	2.5E-03
176	*SPP1*	2.80	2.6E-04
177	*IGFN1*	2.80	3.4E-02
178	*TMEM132A*	2.79	8.2E-05
179	*NR4A1*	2.79	1.4E-03
180	*MAFF*	2.77	1.1E-02
181	*TGIF1*	2.76	2.0E-03
182	*DOK5*	2.75	6.7E-05
183	*OSMR*	2.75	1.5E-04
184	*NRIP3*	2.75	3.4E-04
185	*NEK10*	2.75	6.4E-04
186	*MYCN*	2.75	9.3E-04
187	*TGIF1*	2.75	1.6E-02
188	*NAV2*	2.74	3.9E-04
189	*BNIP3*	2.74	4.0E-04
190	*PI16*	2.74	1.9E-03
191	*IL33*	2.74	3.1E-03
192	*KCNF1*	2.74	4.3E-03
193	*PPP2R4*	2.74	2.2E-02
194	*IL24*	2.73	2.3E-04
195	*ULBP1*	2.73	3.7E-04
196	*UBC*	2.73	1.7E-03
197	*MIR645*	2.73	8.7E-03
198	*HAPLN3*	2.73	1.1E-02
199	*MMP19*	2.72	1.3E-03
200	*MMP19*	2.72	1.4E-03

Continued...

Table A.4.: WG-DASL Assay: Top 200 significantly downregulated genes for observation LEL-M 17 h vs. TM 0 h. Adj.P.Val $<$ 0.05 (Benjamini-Hochberg corrected); logFC $\geq |1|$.

	Gene	logFC	adj.P.Val
1	*TMIGD1*	-7.15	7.1E-06
2	*MS4A12*	-7.08	3.0E-06
3	*SLC17A4*	-6.75	3.1E-06
4	*GUCA2B*	-6.56	5.9E-05
5	*PLA2G4F*	-6.45	9.7E-05
6	*MARVELD3*	-6.44	2.2E-05
7	*CEACAM7*	-6.42	1.4E-05
8	*ZG16*	-6.40	1.4E-05
9	*PIGR*	-6.39	7.4E-05
10	*C10orf99*	-6.38	6.7E-05
11	*CDHR5*	-6.33	3.0E-06
12	*CLCA4*	-6.15	2.3E-05
13	*AQP8*	-6.08	2.1E-05
14	*GGT6*	-6.06	3.1E-06
15	*HMGCS2*	-6.06	1.7E-05
16	*BTNL3*	-6.02	6.7E-06
17	*B3GALT5*	-5.93	4.4E-06
18	*PLA2G10*	-5.93	3.3E-06
19	*CDHR5*	-5.91	2.2E-05
20	*CDH17*	-5.86	1.0E-04
21	*KRT20*	-5.83	2.8E-05
22	*CKMT1B*	-5.82	5.1E-05
23	*SULT1B1*	-5.80	2.2E-05
24	*EDN3*	-5.76	2.2E-05
25	*GBA3*	-5.75	3.1E-05
26	*GCNT3*	-5.72	9.8E-05
27	*CAPN13*	-5.69	1.3E-05
28	*TFF1*	-5.68	8.5E-03
29	*HEPACAM2*	-5.66	1.0E-05
30	*FXYD3*	-5.65	2.0E-04
31	*HSD11B2*	-5.62	2.6E-05
32	*CLRN3*	-5.58	3.1E-06
33	*NXPE4*	-5.57	1.2E-05
34	*SLC51B*	-5.56	1.1E-05
35	*TM4SF5*	-5.51	2.0E-04
36	*EFNA2*	-5.50	1.3E-05
37	*B3GALT5*	-5.50	1.2E-05
38	*TRIM15*	-5.49	9.1E-04
39	*FXYD3*	-5.46	3.6E-05
40	*NXPE1*	-5.44	1.3E-05
41	*ITLN1*	-5.44	9.7E-05
42	*CDX2*	-5.43	1.1E-05
43	*ADH1C*	-5.42	1.6E-04
44	*C12orf36*	-5.39	2.3E-05
45	*PPP1R14D*	-5.36	5.9E-05
46	*MYO1A*	-5.35	1.5E-05
47	*NOX1*	-5.34	1.1E-04
48	*PDZD3*	-5.32	1.2E-05
49	*TBX10*	-5.32	3.5E-05
50	*ERN2*	-5.31	9.1E-05
51	*CAPN9*	-5.31	1.1E-05
52	*CLDN8*	-5.27	1.3E-04
53	*FABP1*	-5.26	6.4E-05
54	*UGT2A3*	-5.25	9.3E-06
55	*MEP1A*	-5.24	3.8E-05
56	*FAM83E*	-5.23	2.9E-04
57	*ANKS4B*	-5.23	1.4E-05
58	*MUC4*	-5.21	2.4E-04
59	*TUBAL3*	-5.18	6.7E-05
60	*METTL7B*	-5.16	1.4E-05
61	*SRI*	-5.11	2.1E-04
62	*NR1I2*	-5.11	1.7E-04
63	*NOX1*	-5.10	5.1E-05
64	*GBA3*	-5.09	5.1E-05
65	*BEST2*	-5.09	9.7E-05
66	*TSPAN8*	-5.08	6.4E-05
67	*LRRC26*	-5.08	1.4E-05
68	*LGALS4*	-5.06	2.3E-04
69	*CDHR2*	-5.04	4.4E-06
70	*EPS8L3*	-5.03	4.3E-05
71	*TMPRSS2*	-5.03	1.7E-04
72	*GUCA2A*	-5.02	1.1E-05
73	*ITGB6*	-5.01	8.1E-05
74	*MUC2*	-5.01	3.6E-04
75	*BCAS1*	-5.01	1.5E-05
76	*SLC26A3*	-5.01	2.1E-04

Continued...

Continued...

Table A.4.: WG-DASL Assay: Top 200 significantly downregulated genes for observation LEL-M 17 h vs. TM 0 h. Adj.P.Val $<$ 0.05 (Benjamini-Hochberg corrected); logFC $\geq |1|$. *Continued from previous page.*

	Gene	logFC	adj.P.Val
77	*CLDN8*	-5.00	2.1E-04
78	*CD207*	-4.99	3.5E-05
79	*LRRC19*	-4.98	1.8E-04
80	*A1CF*	-4.97	1.1E-03
81	*YBX2*	-4.97	9.7E-05
82	*CLCA1*	-4.94	7.1E-06
83	*USH1C*	-4.94	2.2E-05
84	*GUCY2C*	-4.91	8.0E-05
85	*GPA33*	-4.91	9.9E-06
86	*LRRC26*	-4.88	2.3E-05
87	*C1orf210*	-4.88	2.3E-05
88	*EPS8L3*	-4.87	1.3E-04
89	*AGR3*	-4.86	4.4E-06
90	*SLC13A2*	-4.86	2.9E-04
91	*TMEM45B*	-4.86	7.8E-05
92	*AOC1*	-4.85	2.2E-05
93	*SCGB2A1*	-4.84	8.1E-06
94	*MYH14*	-4.84	2.2E-05
95	*RPL10L*	-4.81	3.0E-05
96	*DHRS9*	-4.80	1.4E-05
97	*STX19*	-4.78	2.3E-05
98	*ISX*	-4.75	4.4E-06
99	*DHRS9*	-4.74	4.8E-05
100	*NXPE4*	-4.74	4.3E-05
101	*BCL2L15*	-4.73	4.1E-04
102	*BCAS1*	-4.71	4.3E-05
103	*CA7*	-4.70	1.6E-04
104	*HRCT1*	-4.69	5.6E-04
105	*MARVELD3*	-4.68	1.4E-05
106	*FUT3*	-4.66	1.6E-04
107	*CA1*	-4.66	1.7E-04
108	*ARL14*	-4.65	3.6E-03
109	*VIL1*	-4.64	6.3E-05
110	*MT1H*	-4.62	7.5E-05
111	*RAB25*	-4.61	2.0E-05
112	*TRPM6*	-4.61	9.4E-06
113	*OVOL2*	-4.60	4.4E-04
114	*CEACAM5*	-4.59	3.4E-03
115	*PTK6*	-4.58	1.1E-05
116	*HNF4A*	-4.57	8.0E-05
117	*EPB41L4B*	-4.56	2.2E-04
118	*TTLL6*	-4.55	1.7E-05
119	*MUC13*	-4.55	1.8E-03
120	*COL17A1*	-4.55	8.2E-04
121	*DDC*	-4.54	2.0E-05
122	*SLC44A4*	-4.54	3.8E-05
123	*NXPE4*	-4.53	1.4E-05
124	*WNK4*	-4.52	5.6E-04
125	*FAM3D*	-4.52	1.1E-05
126	*ATP2C2*	-4.51	3.2E-04
127	*BCMO1*	-4.50	2.5E-04
128	*LRRC31*	-4.50	7.5E-04
129	*UGT1A8*	-4.47	1.6E-03
130	*SLC5A1*	-4.45	2.1E-04
131	*MUC17*	-4.45	3.8E-04
132	*CLEC10A*	-4.44	8.2E-04
133	*PTPRR*	-4.44	1.6E-04
134	*FOXA1*	-4.43	6.7E-05
135	*SCNN1A*	-4.43	9.8E-05
136	*CAPN9*	-4.41	7.2E-05
137	*ESRP1*	-4.40	9.7E-05
138	*PPP1R14C*	-4.38	1.5E-04
139	*NAT8B*	-4.37	2.6E-05
140	*GDA*	-4.37	7.5E-05
141	*CDX1*	-4.37	1.1E-04
142	*CYP2J2*	-4.37	5.2E-05
143	*SHROOM3*	-4.35	2.3E-04
144	*SHD*	-4.35	9.7E-05
145	*CD177*	-4.34	2.6E-04
146	*EDN3*	-4.32	2.0E-05
147	*C1orf106*	-4.31	4.3E-04
148	*ATOH1*	-4.31	1.8E-04
149	*SLC39A5*	-4.31	1.6E-05
150	*PDE6A*	-4.31	1.6E-04
151	*NAT2*	-4.30	3.6E-05

Continued...

Continued...

Table A.4.: WG-DASL Assay: Top 200 significantly downregulated genes for observation LEL-M 17 h vs. TM 0 h. Adj.P.Val $<$ 0.05 (Benjamini-Hochberg corrected); logFC $\geq$ |1|. *Continued from previous page.*

	Gene	logFC	adj.P.Val
152	*TFCP2L1*	-4.29	5.3E-05
153	*DNAJC22*	-4.29	1.0E-03
154	*FCGBP*	-4.29	5.2E-05
155	*TMEM171*	-4.28	1.1E-03
156	*ACSL5*	-4.27	1.4E-05
157	*TMEM139*	-4.26	7.1E-05
158	*CEACAM6*	-4.26	5.4E-03
159	*EPCAM*	-4.24	3.4E-04
160	*CBLC*	-4.23	8.1E-05
161	*ESPN*	-4.23	1.1E-05
162	*CHP2*	-4.23	2.3E-05
163	*PTK6*	-4.22	2.3E-04
164	*AXDND1*	-4.22	2.5E-03
165	*TJP3*	-4.21	2.1E-03
166	*GPX2*	-4.20	5.6E-04
167	*C1orf116*	-4.20	7.2E-03
168	*LOC389332*	-4.19	2.1E-05
169	*ELF3*	-4.18	2.9E-03
170	*TRIM31*	-4.18	2.8E-05
171	*AGR2*	-4.17	1.4E-02
172	*BEST4*	-4.16	1.1E-02
173	*FOXA2*	-4.16	2.0E-04
174	*LOC100124692*	-4.15	2.3E-05
175	*MB*	-4.15	3.1E-05
176	*CLDN7*	-4.15	1.1E-03
177	*PLS1*	-4.15	1.2E-04
178	*PPP1R1B*	-4.15	1.1E-04
179	*A1CF*	-4.14	2.2E-05
180	*AP1M2*	-4.14	3.0E-05
181	*EPHA10*	-4.13	5.4E-05
182	*CD177*	-4.13	2.6E-04
183	*HHLA2*	-4.12	1.1E-04
184	*VAV3*	-4.11	1.0E-03
185	*TMEM37*	-4.11	1.5E-05
186	*LGALS9B*	-4.10	1.1E-04
187	*OTOP2*	-4.10	1.7E-03
188	*PLEKHH1*	-4.08	6.7E-05
189	*RNF43*	-4.08	1.6E-03
190	*C1orf210*	-4.07	3.4E-04
191	*LIPH*	-4.06	7.3E-05
192	*TST*	-4.05	3.4E-04
193	*CTSE*	-4.03	2.7E-04
194	*EPCAM*	-4.02	7.3E-04
195	*KRT20*	-4.02	1.7E-04
196	*CRB3*	-4.01	1.5E-04
197	*FMO5*	-4.00	1.9E-04
198	*KRT19*	-4.00	9.8E-05
199	*SLC4A4*	-4.00	9.3E-05
200	*DEFB1*	-4.00	2.8E-04

Continued...

Table A.5.: WG-DASL Assay: Significantly upregulated genes for observation LEL-M 17 h vs. LEL-M 5 h. Adj.P.Val $<$ 0.05 (Benjamini-Hochberg corrected); logFC $\geq |1|$.

	Gene	logFC	adj.P.Val
1	*KIAA1199*	6.38	6.0E-03
2	*MMP10*	4.54	1.5E-02
3	*MME*	4.28	1.7E-02
4	*IL11*	4.25	6.0E-03
5	*MMP1*	4.21	2.0E-02
6	*CDCP1*	4.19	4.7E-03
7	*CDCP1*	4.11	1.5E-02
8	*AGXT*	3.88	4.8E-02
9	*MME*	3.77	1.8E-02
10	*CXCL5*	3.77	4.3E-02
11	*MME*	3.77	2.8E-02
12	*TNFRSF11B*	3.75	1.6E-02
13	*CDCP1*	3.47	1.5E-02
14	*MIR126*	3.32	2.0E-02
15	*CDCP1*	3.30	1.5E-02
16	*CA9*	3.29	1.5E-02
17	*RPL23AP82*	3.27	2.3E-02
18	*C12orf50*	3.27	1.2E-02
19	*SGIP1*	3.22	1.2E-02
20	*IL13RA2*	3.20	2.8E-02
21	*TMEM132A*	3.19	1.2E-02
22	*EFCAB3*	3.08	2.2E-02
23	*PFKFB4*	3.04	2.7E-02
24	*VLDLR*	3.02	1.2E-02
25	*FGF11*	3.01	1.5E-02
26	*CBLN2*	3.00	1.5E-02
27	*C12orf50*	3.00	4.0E-02
28	*IL24*	2.98	1.8E-02
29	*IL22*	2.94	1.5E-02
30	*HK2*	2.84	1.2E-02
31	*C1orf100*	2.83	1.8E-02
32	*MMP12*	2.77	4.6E-02
33	*IL22*	2.74	2.0E-02
34	*TMEFF1*	2.73	2.7E-02
35	*HMGN2P46*	2.71	3.0E-02
36	*NPTX1*	2.66	1.6E-02
37	*AK4*	2.63	1.8E-02
38	*MYCN*	2.59	2.7E-02
39	*PPIAL4G*	2.56	4.0E-02
40	*C4orf3*	2.55	1.8E-02
41	*ADCY8*	2.50	1.2E-02
42	*AKAP2*	2.49	1.8E-02
43	*KCNE2*	2.44	1.6E-02
44	*ITGA2*	2.43	1.2E-02
45	*PDLIM4*	2.41	1.8E-02
46	*RAB33A*	2.41	3.7E-02
47	*PANX2*	2.41	4.3E-02
48	*NAV2*	2.39	3.4E-02
49	*B3GNT4*	2.38	2.0E-02
50	*TFR2*	2.38	2.7E-02
51	*CLMP*	2.36	2.5E-02
52	*MURC*	2.35	1.2E-02
53	*INSIG2*	2.30	1.8E-02
54	*FOXD1*	2.29	1.6E-02
55	*TNFSF15*	2.24	4.0E-02
56	*NEK10*	2.24	1.9E-02
57	*HS3ST3A1*	2.23	2.7E-02
58	*VEGFA*	2.23	1.5E-02
59	*SLC8A3*	2.20	3.7E-02
60	*SLC41A3*	2.20	4.3E-02
61	*HMGA2*	2.18	2.7E-02
62	*ZNF160*	2.18	1.5E-02
63	*FAM162A*	2.18	2.7E-02
64	*IKBIP*	2.17	1.5E-02
65	*ZNF470*	2.17	4.6E-02
66	*TBX3*	2.15	3.6E-02
67	*PGK1*	2.14	4.0E-02
68	*BNIP3*	2.13	2.7E-02
69	*C4orf47*	2.07	1.8E-02
70	*PALM2*	2.06	4.1E-02
71	*PPFIA4*	2.04	1.5E-02
72	*KCNK1*	2.04	1.5E-02
73	*NEURL3*	2.01	2.8E-02
74	*EFCAB13*	2.01	2.3E-02
75	*WISP1*	2.01	1.9E-02
76	*EML5*	1.98	4.6E-02

Continued...

Continued...

Table A.5.: WG-DASL Assay: Significantly upregulated genes for observation LEL-M 17 h vs. LEL-M 5 h. Adj.P.Val $<$ 0.05 (Benjamini-Hochberg corrected); logFC $\geq |1|$. *Continued from previous page.*

	Gene	logFC	adj.P.Val
77	*GPR174*	1.98	2.3E-02
78	*SNX33*	1.98	2.3E-02
79	*RUNDC1*	1.93	1.5E-02
80	*MIR30D*	1.92	4.2E-02
81	*EFTUD1*	1.90	2.8E-02
82	*FUT11*	1.86	2.7E-02
83	*TBX3*	1.84	4.2E-02
84	*PRG2*	1.83	4.3E-02
85	*N4BP3*	1.81	1.8E-02
86	*HERC4*	1.80	5.0E-02
87	*OXTR*	1.80	4.0E-02
88	*SIGLEC15*	1.80	3.3E-02
89	*ZSWIM4*	1.79	2.0E-02
90	*FAM117B*	1.79	4.2E-02
91	*EFTUD1*	1.74	3.7E-02
92	*ZNF654*	1.73	2.7E-02
93	*CLDN14*	1.73	4.8E-02
94	*RSPH10B*	1.70	4.2E-02
95	*MXI1*	1.70	2.8E-02
96	*UPF3B*	1.68	2.7E-02
97	*IZUMO4*	1.68	5.0E-02
98	*TMEM194A*	1.66	1.6E-02
99	*AGPAT5*	1.65	4.7E-02
100	*MTFP1*	1.63	2.7E-02
101	*PGAM1*	1.62	3.3E-02
102	*KIAA0930*	1.59	3.8E-02
103	*EFTUD1*	1.56	4.2E-02
104	*THAP2*	1.55	4.8E-02
105	*DNHD1*	1.53	2.7E-02
106	*CLEC2D*	1.50	2.7E-02
107	*ZNF84*	1.49	4.6E-02
108	*JAK3*	1.48	4.8E-02
109	*GAD1*	1.45	5.0E-02
110	*AK2*	1.44	4.2E-02

Table A.6.: WG-DASL Assay: Significantly downregulated genes for observation LEL-M 17 h vs. LEL-M 5 h. Adj.P.Val $<$ 0.05 (Benjamini-Hochberg corrected); logFC $\geq$ |1|.

	Gene	logFC	adj.P.Val
1	*IGSF21*	-3.23	2.7E-02
2	*SIGLEC1*	-3.09	2.7E-02
3	*PRND*	-2.98	1.8E-02
4	*CD163*	-2.96	1.5E-02
5	*CLEC10A*	-2.92	3.4E-02
6	*RAB7B*	-2.75	4.8E-02
7	*FMO2*	-2.69	4.9E-02
8	*CLEC10A*	-2.57	2.7E-02
9	*WNT11*	-2.56	1.2E-02
10	*ENHO*	-2.43	1.8E-02
11	*FOLR2*	-2.40	1.5E-02
12	*GSTM5*	-2.33	4.6E-02
13	*SSPO*	-2.32	4.6E-02
14	*MYO7A*	-2.31	1.5E-02
15	*C2orf66*	-2.30	3.6E-02
16	*PADI4*	-2.24	4.0E-02
17	*CDH23*	-2.23	1.5E-02
18	*SRPK3*	-2.23	2.7E-02
19	*ISLR*	-2.23	1.5E-02
20	*GALNT16*	-2.22	1.5E-02
21	*TMEM37*	-2.21	1.8E-02
22	*REM1*	-2.20	2.7E-02
23	*C20orf166-AS1*	-2.19	2.8E-02
24	*ANO1*	-2.19	1.8E-02
25	*OXER1*	-2.19	4.8E-02
26	*H1FX-AS1*	-2.15	2.7E-02
27	*CRISPLD1*	-2.14	1.6E-02
28	*OBSCN*	-2.12	1.5E-02
29	*ACCS*	-2.12	3.7E-02
30	*REEP2*	-2.05	4.0E-02
31	*FGFR4*	-2.04	2.8E-02
32	*CC2D2A*	-2.03	4.3E-02
33	*ANO1*	-2.02	1.8E-02
34	*COL4A5*	-2.02	3.7E-02
35	*EGFLAM*	-1.98	1.6E-02
36	*CYP11A1*	-1.92	4.3E-02
37	*VIPR1*	-1.92	2.7E-02
38	*MEI1*	-1.90	2.7E-02
39	*RTN1*	-1.90	4.9E-02
40	*NOSTRIN*	-1.89	3.7E-02
41	*CAND2*	-1.88	2.7E-02
42	*C17orf82*	-1.87	2.0E-02
43	*PDLIM7*	-1.87	3.8E-02
44	*IL11RA*	-1.85	4.9E-02
45	*MROH7*	-1.85	1.8E-02
46	*LTC4S*	-1.84	4.6E-02
47	*MS4A6A*	-1.84	2.7E-02
48	*CD1C*	-1.78	4.2E-02
49	*FCER1A*	-1.78	4.2E-02
50	*FBLN1*	-1.73	2.7E-02
51	*LILRB5*	-1.69	2.7E-02
52	*CD34*	-1.69	4.8E-02
53	*FGGY*	-1.68	4.8E-02
54	*TENC1*	-1.67	3.4E-02
55	*FAM181B*	-1.67	2.7E-02
56	*MAPK10*	-1.66	4.2E-02
57	*EXOC3L1*	-1.64	4.9E-02
58	*ZBTB16*	-1.62	3.7E-02
59	*STAP1*	-1.61	4.0E-02
60	*ZNF488*	-1.59	2.7E-02
61	*MS4A6A*	-1.54	2.7E-02
62	*C1QA*	-1.53	4.2E-02
63	*THY1*	-1.52	4.7E-02
64	*ETV1*	-1.49	4.3E-02
65	*MAPK10*	-1.48	4.0E-02
66	*FRAT1*	-1.38	4.8E-02
67	*ULBP2*	-1.33	4.0E-02
68	*GRASP*	-1.31	4.2E-02

Continued...

Table A.7.: nCounter Assay: Significantly upregulated genes for observation LEL-M 5 h vs. TM 0 h. Adj.P.Val < 0.05 (Benjamini-Hochberg corrected); logFC $\geq |1|$.

	Gene	logFC	adj.P.Val
1	*CXCL2*	7.25	1.3E-05
2	*IL6*	6.54	5.1E-05
3	*IL8*	6.27	1.4E-04
4	*SELE*	6.06	8.9E-05
5	*ICAM4*	5.92	4.9E-07
6	*SOCS3*	5.27	5.6E-05
7	*ICAM1*	4.98	1.3E-05
8	*IL1A*	4.57	1.1E-03
9	*IL1B*	4.55	1.3E-04
10	*CD83*	4.37	1.3E-05
11	*EGR1*	4.08	4.0E-04
12	*CCR7*	4.00	6.9E-04
13	*NFKBIZ*	3.99	4.4E-05
14	*IRF1*	3.83	1.3E-05
15	*PTGS2*	3.76	1.3E-04
16	*IL23A*	3.65	2.3E-05
17	*ICAM5*	3.57	6.2E-05
18	*TNFAIP3*	3.26	4.7E-05
19	*CXCL1*	3.19	1.6E-03
20	*RELB*	3.17	6.2E-05
21	*TRAF1*	3.14	9.6E-04
22	*CCL4*	3.13	2.3E-05
23	*TNFRSF9*	3.08	3.4E-04
24	*CCL20*	2.91	1.6E-03
25	*DUSP4*	2.89	1.4E-03
26	*NFATC1*	2.72	3.1E-04
27	*CCL3*	2.69	2.9E-03
28	*IRAK2*	2.65	7.3E-05
29	*TNFRSF4*	2.62	2.8E-04
30	*CSF2*	2.57	1.6E-03
31	*C7*	2.51	1.3E-03
32	*STAT4*	2.48	3.1E-04
33	*IL1RN*	2.31	1.8E-02
34	*TNFAIP6*	2.29	1.3E-04
35	*NFATC2*	2.28	3.0E-04
36	*CD274*	2.27	1.2E-03
37	*C3*	2.22	3.7E-02
38	*BATF*	2.20	1.6E-03
39	*POLR2A*	2.16	5.3E-05
40	*IRF7*	2.16	2.1E-04
41	*BCL3*	2.09	2.0E-03
42	*NFKB1*	2.09	1.7E-04
43	*CCL2*	2.08	1.8E-02
44	*TNF*	2.06	2.9E-03
45	*CD40*	2.03	7.1E-04
46	*NFIL3*	1.99	3.4E-04
47	*BCL6*	1.97	1.6E-04
48	*ICOSLG*	1.96	2.6E-04
49	*CCRL2*	1.92	1.6E-03
50	*CDKN1A*	1.90	1.4E-03
51	*IL22*	1.84	2.7E-02
52	*C9*	1.84	3.8E-02
53	*LIF*	1.78	1.6E-02
54	*PLAUR*	1.76	4.0E-03
55	*CD70*	1.74	9.0E-03
56	*CD44*	1.69	6.0E-04
57	*C8A*	1.58	2.2E-02
58	*IFIH1*	1.57	1.6E-03
59	*FYN*	1.57	2.0E-03
60	*MARCO*	1.57	3.6E-02
61	*TGFB1*	1.55	3.0E-04
62	*ITLN2*	1.49	2.4E-02
63	*ITGA5*	1.49	2.0E-03
64	*IFI16*	1.47	6.0E-04
65	*EGR2*	1.45	1.2E-02
66	*SMAD3*	1.45	1.9E-03
67	*PLAU*	1.42	2.5E-03
68	*NOTCH1*	1.40	2.6E-03
69	*CEBPB*	1.40	8.0E-04
70	*TRAF3*	1.37	1.6E-03
71	*CCL26*	1.37	1.1E-02
72	*ARG2*	1.36	1.7E-02
73	*IL13*	1.33	1.8E-02
74	*MX1*	1.31	1.4E-02
75	*STAT5A*	1.30	1.2E-03
76	*IFNB1*	1.29	1.1E-02

Continued...

Continued...

Table A.7.: nCounter Assay: Significantly upregulated genes for observation LEL-M 5 h vs. TM 0 h. Adj.P.Val < 0.05 (Benjamini-Hochberg corrected); logFC $\geq |1|$. *Continued from previous page.*

	Gene	logFC	adj.P.Val
77	*ICOS*	1.29	2.4E-02
78	*SKI*	1.29	1.3E-03
79	*TBK1*	1.28	3.4E-03
80	*MAP4K4*	1.27	1.5E-03
81	*CX3CL1*	1.23	1.8E-02
82	*TNFSF15*	1.19	1.3E-02
83	*GBP1*	1.19	2.0E-02
84	*TNFRSF10C*	1.13	2.7E-02
85	*JAK1*	1.09	4.8E-03
86	*CDH5*	1.06	5.9E-03
87	*CXCR4*	1.05	2.0E-02
88	*CD7*	1.04	2.8E-02
89	*CD80*	1.04	4.1E-02
90	*VCAM1*	1.03	4.6E-02
91	*ADA*	1.03	6.9E-03
92	*MAPKAPK2*	1.03	4.3E-03
93	*CLU*	1.02	4.2E-02

Table A.8.: nCounter Assay: Significantly downregulated genes for observation LEL-M 5 h vs. TM 0 h. Adj.P.Val < 0.05 (Benjamini-Hochberg corrected); logFC $\geq |1|$.

	Gene	logFC	adj.P.Val
1	*PIGR*	-8.27	8.9E-05
2	*CEACAM6*	-6.20	1.3E-05
3	*ITLN1*	-5.68	1.3E-05
4	*CD24*	-5.21	3.8E-06
5	*CEACAM1*	-4.91	1.3E-05
6	*PLA2G2A*	-3.87	4.1E-03
7	*MUC1*	-3.69	4.8E-06
8	*CCR2*	-3.66	1.5E-04
9	*GZMA*	-3.34	6.3E-04
10	*CD164*	-3.14	3.6E-04
11	*CD3D*	-3.07	4.1E-04
12	*CLEC7A*	-2.83	7.3E-05
13	*HLA-DPA1*	-2.82	1.5E-03
14	*C1QB*	-2.80	2.9E-04
15	*CD40LG*	-2.74	6.8E-04
16	*MRC1*	-2.61	7.1E-04
17	*TNFRSF17*	-2.60	1.2E-04
18	*FCGR3A/B*	-2.58	2.1E-03
19	*TNFRSF11A*	-2.54	1.5E-04
20	*HLA-DMB*	-2.51	3.4E-04
21	*HAVCR2*	-2.43	4.5E-03
22	*MYD88*	-2.41	4.1E-05
23	*ITGAE*	-2.41	3.6E-04
24	*C1QA*	-2.30	1.6E-03
25	*TLR8*	-2.30	7.3E-04
26	*CCL24*	-2.28	2.4E-04
27	*MSR1*	-2.28	1.1E-04
28	*FCGR2B*	-2.28	8.9E-04
29	*CCL15*	-2.27	1.6E-04
30	*IL18*	-2.26	6.6E-05
31	*SLAMF6*	-2.26	8.7E-04
32	*CD27*	-2.24	6.6E-04
33	*BTLA*	-2.19	1.2E-02
34	*HLA-DRB1*	-2.13	2.8E-02
35	*CD9*	-2.11	1.2E-03
36	*CCL8*	-2.11	8.9E-04
37	*KLRC3*	-2.08	1.0E-03
38	*FCER1G*	-2.08	1.9E-03
39	*XCR1*	-2.08	9.4E-03
40	*KLRC1*	-2.05	2.1E-02
41	*ITGA6*	-2.02	3.1E-04
42	*CD3E*	-2.01	1.0E-03
43	*CD163*	-2.00	1.2E-03
44	*CD209*	-1.99	4.0E-03
45	*CCR1*	-1.99	2.9E-03
46	*KLRC4*	-1.98	5.8E-03
47	*PSMB5*	-1.96	1.8E-03
48	*CD1D*	-1.94	1.2E-03
49	*KLRD1*	-1.93	5.7E-03
50	*LEF1*	-1.93	5.7E-03
51	*PPARG*	-1.90	4.2E-04
52	*CD1A*	-1.90	2.2E-03
53	*SYK*	-1.89	5.0E-04
54	*CTSS*	-1.84	1.8E-03
55	*MR1*	-1.83	9.9E-03
56	*SIGIRR*	-1.82	3.5E-03
57	*PRF1*	-1.80	2.0E-04
58	*FCER1A*	-1.79	5.9E-03
59	*CASP1*	-1.78	2.8E-04
60	*HLA-DPB1*	-1.78	2.9E-03
61	*TLR7*	-1.76	1.6E-03
62	*LCK*	-1.76	4.3E-03
63	*PTPN6*	-1.76	2.5E-04
64	*TNFSF13B*	-1.75	9.6E-03
65	*LY96*	-1.74	2.9E-03
66	*CMKLR1*	-1.72	3.0E-04
67	*CD4*	-1.72	1.3E-03
68	*C1QBP*	-1.71	1.2E-03
69	*RORC*	-1.71	3.2E-03
70	*FCGRT*	-1.69	1.8E-04
71	*LAIR1*	-1.69	1.6E-03
72	*CSF1R*	-1.67	2.1E-02
73	*CXCR6*	-1.66	2.4E-03
74	*HFE*	-1.66	6.4E-04
75	*GZMB*	-1.65	5.7E-03
76	*IL23R*	-1.65	1.8E-03

Continued...

Continued...

Table A.8.: nCounter Assay: Significantly downregulated genes for observation LEL-M 5 h vs. TM 0 h. Adj.P.Val $<$ 0.05 (Benjamini-Hochberg corrected); logFC $\geq$ |1|. *Continued from previous page.*

	Gene	logFC	adj.P.Val
77	*ARHGDIB*	-1.64	4.7E-03
78	*IL16*	-1.63	6.1E-04
79	*CD53*	-1.63	1.4E-03
80	*EDNRB*	-1.62	4.1E-03
81	*LILRA6*	-1.60	5.9E-03
82	*CTSC*	-1.59	2.9E-03
83	*ITGAL*	-1.58	4.1E-03
84	*ITGA4*	-1.57	4.9E-04
85	*IFITM1*	-1.57	2.1E-02
86	*CD74*	-1.57	2.4E-03
87	*KLRC2*	-1.57	2.3E-02
88	*GZMK*	-1.56	1.1E-02
89	*MIF*	-1.54	2.4E-03
90	*B2M*	-1.54	7.6E-03
91	*HLA-DRA*	-1.54	1.1E-02
92	*CD2*	-1.54	5.6E-03
93	*UBE2L3*	-1.52	2.4E-03
94	*PYCARD*	-1.52	1.6E-03
95	*CCR5*	-1.50	1.4E-03
96	*PSMB10*	-1.50	6.6E-04
97	*FCGR2A/C*	-1.49	1.9E-02
98	*CD86*	-1.49	3.8E-02
99	*CD160*	-1.48	5.0E-02
100	*CD14*	-1.46	3.2E-02
101	*TLR5*	-1.43	4.7E-03
102	*FCGR2A*	-1.42	2.2E-03
103	*OAZ1*	-1.41	6.9E-03
104	*ITGB2*	-1.40	2.0E-03
105	*GAPDH*	-1.39	4.0E-03
106	*KIR2DL1*	-1.39	5.2E-03
107	*CIITA*	-1.39	1.3E-02
108	*TLR3*	-1.38	1.5E-02
109	*LILRA4*	-1.38	5.7E-03
110	*TIRAP*	-1.37	5.2E-03
111	*BTK*	-1.35	8.8E-04
112	*HLA-DOB*	-1.35	3.7E-03
113	*KLRF1*	-1.34	2.5E-02
114	*TUBB*	-1.33	1.6E-02
115	*TNFSF8*	-1.33	9.3E-03
116	*KLRB1*	-1.32	3.7E-02
117	*PSMB8*	-1.32	3.1E-03
118	*BAX*	-1.31	8.8E-04
119	*CASP10*	-1.27	9.9E-03
120	*PTPN22*	-1.26	5.4E-03
121	*IKBKE*	-1.24	3.4E-03
122	*LTB4R2*	-1.23	9.0E-03
123	*ITGA2B*	-1.22	4.5E-02
124	*LILRB4*	-1.22	3.8E-02
125	*KLRAP1*	-1.22	6.2E-03
126	*CX3CR1*	-1.22	2.4E-02
127	*HLA-DMA*	-1.21	2.9E-03
128	*PPIA*	-1.20	6.3E-03
129	*PSMB9*	-1.19	3.5E-03
130	*DPP4*	-1.19	2.0E-02
131	*CUL9*	-1.18	9.5E-03
132	*GFI1*	-1.17	7.9E-03
133	*IL7*	-1.17	4.8E-03
134	*IL1R2*	-1.16	4.5E-03
135	*CCL5*	-1.16	4.0E-02
136	*GPI*	-1.16	1.5E-03
137	*ATG16L1*	-1.16	2.0E-03
138	*CYBB*	-1.14	1.1E-02
139	*FADD*	-1.12	9.4E-03
140	*CLEC4A*	-1.12	2.4E-02
141	*SH2D1A*	-1.10	2.2E-02
142	*BCL10*	-1.10	6.9E-03
143	*PSMB7*	-1.09	8.7E-03
144	*BCAP31*	-1.08	2.7E-03
145	*CD45R0*	-1.08	2.7E-02
146	*TAL1*	-1.08	5.7E-03
147	*CR1*	-1.06	4.0E-02
148	*MAP4K1*	-1.05	2.1E-02
149	*PSMC2*	-1.05	4.0E-03
150	*ITGAM*	-1.03	3.7E-03
151	*DEFB1*	-1.03	3.2E-02

Continued...

Table A.8.: nCounter Assay: Significantly downregulated genes for observation LEL-M 5 h vs. TM 0 h. Adj.P.Val < 0.05 (Benjamini-Hochberg corrected); logFC $\geq |1|$. *Continued from previous page.*

	Gene	logFC	adj.P.Val
152	*SMAD5*	-1.02	8.0E-03
153	*CARD9*	-1.02	1.8E-02
154	*NFATC3*	-1.02	1.3E-02
155	*LILRB5*	-1.02	3.7E-02

Table A.9.: nCounter Assay: Significantly upregulated genes for observation LEL-M 17 h vs. TM 0 h. Adj.P.Val < 0.05 (Benjamini-Hochberg corrected); logFC $\geq |1|$.

	Gene	logFC	adj.P.Val
1	*IL8*	8.55	1.4E-05
2	*CXCL2*	7.48	1.4E-05
3	*IL6*	6.42	4.2E-04
4	*LIF*	5.84	1.7E-05
5	*SOCS3*	5.37	2.6E-04
6	*CXCL1*	4.89	1.4E-05
7	*IL1A*	4.85	6.5E-04
8	*PTGS2*	4.82	3.1E-05
9	*ICAM4*	4.66	5.4E-05
10	*PLAU*	4.62	3.4E-05
11	*TNFSF15*	4.44	5.9E-05
12	*SELE*	4.32	1.3E-03
13	*ICAM1*	4.24	5.9E-05
14	*TNFRSF9*	3.92	5.9E-05
15	*IL1RL1*	3.80	1.5E-04
16	*IRF1*	3.70	1.6E-04
17	*IL22*	3.65	8.3E-03
18	*IL1RN*	3.35	6.6E-04
19	*IRAK2*	3.33	1.4E-05
20	*CD274*	3.21	6.6E-04
21	*IL1B*	3.20	8.1E-05
22	*TRAF1*	3.20	1.3E-03
23	*EGR1*	3.19	4.0E-03
24	*CCR7*	3.09	1.8E-03
25	*MME*	3.03	4.6E-02
26	*BCL6*	2.98	1.0E-04
27	*TNFAIP3*	2.95	1.6E-04
28	*SPP1*	2.94	6.4E-04
29	*CSF2*	2.94	1.8E-03
30	*NFKBIZ*	2.89	4.2E-04
31	*C9*	2.78	1.2E-02
32	*CD83*	2.72	4.2E-04
33	*ICAM5*	2.41	5.7E-04
34	*CD70*	2.41	3.0E-03
35	*CCL20*	2.32	9.9E-03
36	*CCL2*	2.29	1.2E-02
37	*TNFAIP6*	2.23	7.7E-04
38	*ITGA5*	2.23	1.8E-04
39	*GBP1*	2.21	2.4E-02
40	*IL23A*	2.21	1.3E-03
41	*NFIL3*	2.20	4.8E-04
42	*RELB*	2.19	4.4E-04
43	*TNFRSF4*	2.15	1.6E-03
44	*CEBPB*	2.15	9.1E-05
45	*IDO1*	2.09	1.1E-02
46	*BCL3*	2.08	3.4E-03
47	*C3*	2.02	4.7E-02
48	*SLC2A1*	1.97	7.1E-04
49	*IFI16*	1.96	2.2E-03
50	*SMAD3*	1.95	4.0E-04
51	*DEFB103B*	1.86	9.5E-03
52	*MAPKAPK2*	1.85	1.4E-03
53	*STAT5A*	1.83	1.7E-03
54	*CCL22*	1.80	1.2E-02
55	*ARG2*	1.78	1.1E-02
56	*MAP4K4*	1.70	4.0E-04
57	*ETS1*	1.69	1.1E-03
58	*RUNX1*	1.67	4.4E-03
59	*ZEB1*	1.67	5.0E-04
60	*PLAUR*	1.66	6.3E-03
61	*TAP1*	1.65	2.2E-02
62	*NFKB1*	1.65	1.6E-03
63	*NFATC1*	1.64	1.0E-03
64	*CD59*	1.64	1.3E-03
65	*IL1RL2*	1.59	8.3E-03
66	*CDKN1A*	1.57	3.4E-03
67	*IL1R1*	1.55	1.3E-03
68	*IRF7*	1.51	4.9E-03
69	*CD44*	1.49	2.7E-03
70	*CCL19*	1.45	4.3E-02
71	*CD40*	1.37	1.6E-03
72	*DUSP4*	1.35	4.7E-02
73	*CD80*	1.32	4.1E-02
74	*IL2RA*	1.32	3.8E-03
75	*TBX21*	1.32	7.3E-03
76	*BATF3*	1.30	4.2E-02

Continued...

Continued...

Table A.9.: nCounter Assay: Significantly upregulated genes for observation LEL-M 17 h vs. TM 0 h. Adj.P.Val < 0.05 (Benjamini-Hochberg corrected); logFC $\geq |1|$. *Continued from previous page.*

	Gene	logFC	adj.P.Val
77	*STAT3*	1.28	4.4E-03
78	*NOD2*	1.27	7.5E-03
79	*RELA*	1.26	5.7E-03
80	*IL18R1*	1.25	8.3E-03
81	*IFIH1*	1.21	3.5E-02
82	*FYN*	1.20	7.9E-03
83	*GNLY*	1.20	1.5E-02
84	*EGR2*	1.19	2.0E-02
85	*SKI*	1.19	6.7E-03
86	*CD22*	1.18	9.4E-03
87	*JAK1*	1.17	2.2E-03
88	*BATF*	1.14	4.9E-02
89	*POLR2A*	1.14	4.4E-03
90	*ICOSLG*	1.13	6.3E-03
91	*TNFRSF13B*	1.12	1.3E-02
92	*MCL1*	1.11	2.2E-02
93	*FOXP3*	1.10	2.0E-02
94	*TBK1*	1.03	6.6E-03
95	*ICOS*	1.03	3.8E-02

Table A.10.: nCounter Assay: Significantly downregulated genes for observation LEL-M 17 h vs. TM 0 h. Adj.P.Val $<$ 0.05 (Benjamini-Hochberg corrected); logFC $\geq |1|$.

	Gene	logFC	adj.P.Val
1	*PIGR*	-8.57	4.2E-04
2	*CEACAM6*	-6.32	1.5E-05
3	*ITLN1*	-6.25	2.3E-05
4	*CD24*	-5.83	1.5E-05
5	*CEACAM1*	-4.82	2.3E-05
6	*PLA2G2A*	-4.59	4.2E-04
7	*CD163*	-4.42	7.2E-04
8	*C1QB*	-4.33	6.4E-04
9	*CCL24*	-4.09	4.2E-04
10	*MRC1*	-3.99	1.8E-04
11	*C1QA*	-3.88	8.6E-04
12	*MUC1*	-3.82	1.7E-05
13	*IL18*	-3.55	1.8E-05
14	*MSR1*	-3.38	4.4E-04
15	*HLA-DPA1*	-3.36	6.6E-04
16	*CMKLR1*	-3.28	4.2E-04
17	*FCER1A*	-3.17	6.6E-04
18	*HLA-DMB*	-3.16	4.8E-04
19	*CCR2*	-3.07	6.6E-04
20	*HLA-DRB1*	-3.02	2.1E-02
21	*GZMA*	-2.93	4.2E-04
22	*CYBB*	-2.89	2.2E-03
23	*FCGR3A/B*	-2.84	2.2E-03
24	*CLEC7A*	-2.83	2.7E-03
25	*CD209*	-2.80	9.1E-03
26	*LILRB5*	-2.73	7.1E-04
27	*CD74*	-2.72	7.7E-04
28	*CSF1R*	-2.71	7.0E-03
29	*TLR8*	-2.68	4.2E-04
30	*HLA-DPB1*	-2.60	6.4E-04
31	*HLA-DRB3*	-2.59	6.6E-04
32	*PYCARD*	-2.55	1.9E-03
33	*CCL18*	-2.54	4.4E-03
34	*FCGRT*	-2.47	1.2E-04
35	*PPARG*	-2.47	4.2E-04
36	*CTSG*	-2.45	3.1E-03
37	*HLA-DRA*	-2.40	2.3E-03
38	*CCL8*	-2.35	6.6E-04
39	*CSF3R*	-2.34	1.8E-03
40	*TLR5*	-2.34	1.1E-04
41	*FKBP5*	-2.30	6.6E-03
42	*CD4*	-2.29	1.2E-03
43	*LAIR1*	-2.28	6.5E-04
44	*CCL13*	-2.25	4.4E-03
45	*CD36*	-2.25	8.0E-04
46	*IL1R2*	-2.24	4.4E-04
47	*CD40LG*	-2.24	1.7E-03
48	*LILRA4*	-2.23	1.3E-03
49	*HLA-DMA*	-2.21	1.2E-04
50	*FCER1G*	-2.18	7.9E-03
51	*CXCR2*	-2.18	8.7E-03
52	*CCL15*	-2.14	4.2E-04
53	*CD9*	-2.09	7.1E-04
54	*ITGA6*	-2.07	4.2E-04
55	*CCR1*	-2.05	4.8E-03
56	*HAVCR2*	-2.04	1.1E-02
57	*ITGB2*	-2.02	7.2E-04
58	*GZMK*	-2.02	1.8E-03
59	*CD14*	-2.00	3.1E-02
60	*TNFRSF17*	-1.98	4.4E-03
61	*ITGAM*	-1.90	7.4E-04
62	*SIGIRR*	-1.89	5.3E-03
63	*TNFRSF11A*	-1.89	4.2E-04
64	*GUSB*	-1.88	4.9E-04
65	*ARHGDIB*	-1.87	5.6E-03
66	*RORC*	-1.87	1.2E-03
67	*DEFB1*	-1.84	1.7E-03
68	*CLEC6A*	-1.84	2.3E-03
69	*CARD9*	-1.82	1.7E-03
70	*TLR7*	-1.82	2.3E-03
71	*XCR1*	-1.81	4.6E-03
72	*CD164*	-1.81	6.4E-04
73	*MYD88*	-1.78	2.6E-04
74	*TLR4*	-1.78	9.0E-03
75	*C5*	-1.77	3.6E-03
76	*CTSC*	-1.75	1.4E-03

Continued...

Continued...

Table A.10.: nCounter Assay: Significantly downregulated genes for observation LEL-M 17 h vs. TM 0 h. Adj.P.Val $<$ 0.05 (Benjamini-Hochberg corrected); logFC $\geq$ |1|. *Continued from previous page.*

	Gene	logFC	adj.P.Val
77	*CXCR3*	-1.66	3.9E-03
78	*ITGAE*	-1.66	2.2E-03
79	*HFE*	-1.66	5.5E-03
80	*KLRF1*	-1.63	8.0E-04
81	*TLR3*	-1.61	2.3E-03
82	*NCF4*	-1.58	7.0E-03
83	*ABCB1*	-1.57	1.6E-02
84	*IL7*	-1.56	2.4E-02
85	*CX3CR1*	-1.52	3.2E-02
86	*PTPN6*	-1.51	2.5E-03
87	*SYK*	-1.50	1.6E-02
88	*LILRA6*	-1.48	1.5E-02
89	*TNFSF8*	-1.46	1.6E-02
90	*CD34*	-1.44	2.0E-02
91	*PLA2G2E*	-1.43	3.3E-02
92	*CD1D*	-1.41	4.6E-02
93	*LILRA2*	-1.40	7.5E-03
94	*SELL*	-1.39	1.7E-03
95	*CCBP2*	-1.39	2.4E-02
96	*NLRP3*	-1.38	7.3E-03
97	*BST1*	-1.37	5.5E-03
98	*CCND3*	-1.37	6.6E-03
99	*CD160*	-1.32	2.1E-02
100	*CASP10*	-1.31	2.0E-03
101	*PTGER4*	-1.30	3.7E-03
102	*CD1A*	-1.29	1.1E-02
103	*TLR2*	-1.27	4.9E-02
104	*CD27*	-1.27	2.1E-02
105	*KLRF2*	-1.27	2.7E-02
106	*LEF1*	-1.23	1.1E-02
107	*IL11RA*	-1.23	4.4E-02
108	*ENTPD1*	-1.23	3.0E-02
109	*CLEC4E*	-1.21	2.5E-02
110	*CTSS*	-1.19	4.5E-02
111	*IL12RB1*	-1.18	3.2E-02
112	*KLRC1*	-1.16	2.9E-02
113	*IFNGR1*	-1.15	7.2E-03
114	*CCR6*	-1.14	3.2E-02
115	*IL10*	-1.13	1.1E-02
116	*CD55*	-1.13	1.1E-02
117	*ATG16L1*	-1.13	5.2E-03
118	*PTAFR*	-1.12	1.4E-02
119	*LILRA1*	-1.11	7.5E-03
120	*LILRB3*	-1.07	4.8E-02
121	*TLR1*	-1.07	3.7E-02
122	*TNFSF12*	-1.05	1.3E-02
123	*MR1*	-1.05	4.6E-02
124	*KIR2DS1*	-1.04	4.9E-02
125	*C1QBP*	-1.04	7.2E-03
126	*BCAP31*	-1.04	7.4E-03
127	*CR2*	-1.03	2.0E-02
128	*PSMB5*	-1.02	3.8E-02
129	*SLAMF6*	-1.02	3.4E-02
130	*PRF1*	-1.00	4.7E-03

Continued...

Table A.11.: nCounter Assay: Significantly upregulated genes for observation LEL-M 17 h vs. LEL-M 5 h. Adj.P.Val < 0.05 (Benjamini-Hochberg corrected); logFC $\geq |1|$.

	Gene	logFC	adj.P.Val
1	*LIF*	4.07	1.1E-03
2	*TNFSF15*	3.25	3.0E-03
3	*PLAU*	3.19	1.6E-03
4	*IL1RL1*	3.06	2.1E-03
5	*GZMB*	2.69	2.8E-02
6	*SLC2A1*	2.46	1.1E-03
7	*MIF*	2.32	1.6E-03
8	*IL8*	2.29	2.3E-02
9	*IDO1*	2.20	2.4E-02
10	*SPP1*	2.16	1.3E-02
11	*CD3D*	2.11	2.4E-02
12	*GPI*	2.01	1.1E-03
13	*CCL22*	1.87	3.7E-02
14	*GAPDH*	1.87	3.0E-03
15	*LCK*	1.84	1.6E-02
16	*TNFRSF13B*	1.84	1.1E-03
17	*ETS1*	1.82	3.6E-03
18	*CXCL1*	1.70	4.8E-02
19	*CASP1*	1.67	1.2E-02
20	*PSMB9*	1.64	1.3E-02
21	*EDNRB*	1.63	2.8E-02
22	*CXCR6*	1.59	1.7E-02
23	*PSMB8*	1.48	2.8E-02
24	*GFI1*	1.47	7.6E-03
25	*TIGIT*	1.44	2.7E-02
26	*GNLY*	1.38	2.4E-02
27	*CLEC4A*	1.34	3.5E-02
28	*ITGAL*	1.33	2.0E-02
29	*IKZF3*	1.30	1.6E-02
30	*SLAMF6*	1.24	2.4E-02
31	*PDCD1LG2*	1.20	4.9E-02
32	*TAL1*	1.19	2.4E-02
33	*ZEB1*	1.18	1.6E-02
34	*IL1R1*	1.16	2.9E-02
35	*CD59*	1.12	3.6E-02
36	*RELA*	1.11	2.4E-02
37	*RUNX1*	1.10	4.8E-02
38	*TBX21*	1.08	4.6E-02
39	*LTA*	1.08	2.8E-02
40	*SMAD5*	1.07	2.6E-02
41	*PAX5*	1.06	4.1E-02
42	*CD53*	1.06	3.8E-02
43	*BAX*	1.06	2.0E-02
44	*IL23R*	1.04	4.8E-02
45	*CASP8*	1.03	2.8E-02
46	*JAK3*	1.02	3.6E-02
47	*BCL6*	1.01	5.0E-02

Continued...

Table A.12.: nCounter Assay: Significantly downregulated genes for observation LEL-M 17 h vs. LEL-M 5 h. Adj.P.Val < 0.05 (Benjamini-Hochberg corrected); logFC $\geq |1|$.

	Gene	logFC	adj.P.Val
1	*CCL4*	-2.99	1.2E-02
2	*CXCR2*	-2.43	3.7E-02
3	*CCL3*	-2.42	3.5E-02
4	*CD163*	-2.42	3.4E-02
5	*HLA-DRB3*	-2.26	5.3E-03
6	*CCRL2*	-2.14	1.0E-02
7	*CTSG*	-2.03	2.8E-02
8	*CSF3R*	-1.95	2.8E-02
9	*CLEC4E*	-1.94	1.0E-02
10	*NFATC2*	-1.84	2.0E-02
11	*NLRP3*	-1.81	6.6E-03
12	*CCL24*	-1.81	4.8E-02
13	*CD34*	-1.76	2.5E-02
14	*CYBB*	-1.76	5.0E-02
15	*CLEC6A*	-1.72	2.8E-02
16	*LILRB5*	-1.72	2.9E-02
17	*STAT4*	-1.68	6.3E-03
18	*CD83*	-1.65	6.3E-03
19	*PLA2G2E*	-1.58	3.0E-02
20	*CMKLR1*	-1.55	3.9E-02
21	*DUSP4*	-1.53	1.7E-02
22	*GP1BB*	-1.46	2.0E-02
23	*IL23A*	-1.45	3.7E-02
24	*KIR2DS1*	-1.42	3.4E-02
25	*TNF*	-1.40	4.7E-02
26	*IRAK3*	-1.39	3.6E-02
27	*FCER1A*	-1.39	3.4E-02
28	*CCL13*	-1.31	3.3E-02
29	*IL18*	-1.29	1.7E-02
30	*CD36*	-1.27	3.6E-02
31	*SELL*	-1.23	2.7E-02
32	*ICAM5*	-1.16	3.3E-02
33	*NFKBIZ*	-1.10	2.8E-02
34	*IL10RA*	-1.09	3.6E-02
35	*CCR10*	-1.08	4.2E-02
36	*IL1R2*	-1.07	3.6E-02
37	*TGFB1*	-1.03	2.8E-02
38	*CD55*	-1.02	4.5E-02
39	*POLR2A*	-1.02	2.8E-02
40	*HLA-DMA*	-1.00	3.3E-02

Continued...

Table A.13.: nCounter Assay: Significantly upregulated genes for observation LEL-M 5 h vs. TM 5 h. Adj.P.Val < 0.05 (Benjamini-Hochberg corrected); logFC $\geq |1|$.

	Gene	logFC	adj.P.Val
1	*ICAM4*	5.88	3.2E-07
2	*CXCL2*	4.62	1.1E-03
3	*ICAM5*	4.41	1.1E-03
4	*IL6*	4.11	1.6E-03
5	*SELE*	3.87	2.0E-03
6	*IL1A*	3.76	8.6E-03
7	*IL1B*	3.62	6.2E-03
8	*CCR7*	3.47	4.3E-03
9	*ICAM1*	3.47	8.0E-05
10	*IRF1*	3.23	1.2E-04
11	*IL8*	3.07	1.3E-02
12	*SOCS3*	2.80	1.0E-03
13	*IL23A*	2.74	1.7E-03
14	*TRAF1*	2.70	2.9E-03
15	*NFATC1*	2.63	9.8E-04
16	*RELB*	2.58	2.7E-04
17	*EGR1*	2.51	2.1E-03
18	*NFKBIZ*	2.46	7.3E-04
19	*CD83*	2.45	1.7E-03
20	*C7*	2.39	1.7E-03
21	*CXCL1*	2.32	3.6E-02
22	*IFNB1*	2.28	1.8E-03
23	*NFATC2*	2.25	1.2E-03
24	*IRAK2*	2.24	1.1E-03
25	*STAT4*	2.18	1.1E-03
26	*DUSP4*	2.12	7.9E-03
27	*TNF*	2.10	3.2E-02
28	*TNFAIP6*	2.09	7.3E-04
29	*POLR2A*	2.05	2.6E-04
30	*CCRL2*	2.04	1.7E-03
31	*CD40*	1.94	1.7E-03
32	*ICOSLG*	1.92	3.2E-04
33	*IRF7*	1.91	1.1E-03
34	*CXCR2*	1.88	4.0E-02
35	*BATF*	1.80	2.8E-02
36	*TNFSF15*	1.79	5.3E-03
37	*CD274*	1.75	7.1E-03
38	*TNFRSF4*	1.73	5.6E-03
39	*PTGS2*	1.63	1.8E-02
40	*CDKN1A*	1.60	4.1E-03
41	*BCL6*	1.59	1.4E-03
42	*NFKB1*	1.58	1.4E-03
43	*CCL4*	1.55	3.7E-02
44	*TGFB1*	1.54	9.5E-04
45	*ITLN2*	1.51	2.9E-02
46	*NOTCH1*	1.51	1.6E-03
47	*C8A*	1.48	3.7E-03
48	*STAT5A*	1.48	1.9E-03
49	*TRAF3*	1.47	1.9E-03
50	*CD80*	1.41	8.0E-03
51	*MX1*	1.41	1.3E-02
52	*SKI*	1.41	1.4E-03
53	*MARCO*	1.39	4.9E-02
54	*IRAK3*	1.37	2.5E-02
55	*BCL3*	1.36	1.7E-03
56	*CD44*	1.35	3.5E-03
57	*ITGA5*	1.34	4.8E-03
58	*TBK1*	1.33	3.7E-03
59	*BCL2*	1.32	1.8E-02
60	*GP1BB*	1.32	4.6E-03
61	*CSF2*	1.32	2.2E-02
62	*MBL2*	1.30	1.2E-02
63	*IFI16*	1.29	1.9E-03
64	*NFIL3*	1.29	6.2E-03
65	*PLA2G2E*	1.25	1.1E-02
66	*MAP4K4*	1.23	3.3E-03
67	*CLEC4E*	1.20	2.8E-02
68	*FYN*	1.18	9.6E-03
69	*TNFAIP3*	1.18	2.8E-02
70	*TNFRSF10C*	1.15	4.2E-02
71	*EBI3*	1.14	8.7E-03
72	*ARG2*	1.13	5.0E-03
73	*SMAD3*	1.12	7.9E-03
74	*IFIH1*	1.11	2.1E-02
75	*CDH5*	1.05	8.7E-03
76	*IL18R1*	1.04	8.6E-03

Continued...

Continued...

Table A.13.: nCounter Assay: Significantly upregulated genes for observation LEL-M 5 h vs. TM 5 h. Adj.P.Val < 0.05 (Benjamini-Hochberg corrected); logFC $\geq |1|$. *Continued from previous page.*

	Gene	logFC	adj.P.Val
77	*PLAUR*	1.02	1.5E-02
78	*IL4R*	1.02	1.3E-02

Table A.14.: nCounter Assay: Significantly downregulated genes for observation LEL-M 5 h vs. TM 5 h. Adj.P.Val $<$ 0.05 (Benjamini-Hochberg corrected); logFC $\geq |1|$.

	Gene	logFC	adj.P.Val
1	*PIGR*	-8.17	4.6E-04
2	*ITLN1*	-5.46	9.2E-04
3	*CEACAM6*	-5.41	2.1E-04
4	*PLA2G2A*	-4.86	1.7E-03
5	*CD24*	-4.60	4.6E-05
6	*CEACAM1*	-3.68	6.1E-04
7	*MUC1*	-3.63	2.6E-04
8	*GZMA*	-3.57	2.7E-03
9	*CD3D*	-3.39	1.1E-03
10	*CCR2*	-3.19	5.2E-04
11	*CD40LG*	-2.95	1.9E-03
12	*CD164*	-2.77	1.9E-03
13	*CD3E*	-2.72	1.2E-03
14	*IFNG*	-2.68	1.2E-02
15	*TNFRSF17*	-2.67	1.2E-04
16	*CCL8*	-2.62	1.1E-03
17	*GZMB*	-2.62	3.6E-03
18	*KLRC3*	-2.55	4.3E-03
19	*HLA-DPA1*	-2.51	3.7E-03
20	*ITGAE*	-2.49	4.6E-04
21	*KLRD1*	-2.44	4.6E-03
22	*KLRB1*	-2.39	5.5E-03
23	*CCL5*	-2.39	8.6E-03
24	*KLRC1*	-2.36	1.4E-02
25	*CCL15*	-2.31	4.2E-03
26	*HLA-DMB*	-2.30	2.4E-03
27	*MRC1*	-2.30	1.7E-03
28	*TNFRSF11A*	-2.29	4.3E-03
29	*SH2D1A*	-2.29	2.2E-03
30	*BTLA*	-2.28	1.8E-02
31	*CD27*	-2.26	1.1E-03
32	*CD160*	-2.26	1.3E-02
33	*KLRC4*	-2.24	1.2E-02
34	*CLEC7A*	-2.23	4.0E-03
35	*LCK*	-2.22	8.5E-03
36	*GZMK*	-2.19	2.2E-02
37	*SLAMF6*	-2.16	2.7E-03
38	*C1QBP*	-2.16	1.4E-03
39	*XCR1*	-2.14	1.8E-02
40	*C1QB*	-2.13	9.1E-03
41	*MIF*	-2.04	9.5E-04
42	*SIGIRR*	-2.02	2.2E-03
43	*FCGR2B*	-2.00	1.7E-03
44	*PRF1*	-1.98	4.8E-03
45	*KLRC2*	-1.97	1.1E-02
46	*PSMB5*	-1.93	1.9E-03
47	*FCER1A*	-1.92	2.8E-03
48	*ARHGDIB*	-1.91	1.9E-03
49	*GAPDH*	-1.86	1.2E-03
50	*CD9*	-1.86	1.1E-02
51	*B2M*	-1.84	1.9E-03
52	*KLRK1*	-1.83	2.9E-02
53	*MYD88*	-1.82	9.5E-04
54	*ITGA6*	-1.82	1.4E-03
55	*LEF1*	-1.82	9.7E-03
56	*CD53*	-1.80	1.2E-03
57	*FCGR3A/B*	-1.79	3.6E-02
58	*PTPN6*	-1.78	9.5E-04
59	*IFITM1*	-1.78	9.1E-03
60	*CXCR6*	-1.78	9.8E-03
61	*TNFSF13B*	-1.77	1.2E-02
62	*CTSS*	-1.75	1.4E-03
63	*HAVCR2*	-1.74	4.9E-02
64	*IL16*	-1.74	3.5E-03
65	*CASP1*	-1.74	1.5E-03
66	*SYK*	-1.74	1.6E-03
67	*C1QA*	-1.72	1.3E-02
68	*KIR2DL3*	-1.71	1.2E-02
69	*CD1A*	-1.71	7.9E-03
70	*GPR183*	-1.70	9.1E-03
71	*ITGAL*	-1.70	1.5E-02
72	*CTSC*	-1.70	1.8E-03
73	*EEF1G*	-1.66	3.3E-03
74	*IL23R*	-1.65	3.8E-03
75	*CD79A*	-1.63	3.0E-03
76	*LY96*	-1.61	7.8E-03

Continued...

Continued...

Table A.14.: nCounter Assay: Significantly downregulated genes for observation LEL-M 5 h vs. TM 5 h. Adj.P.Val $<$ 0.05 (Benjamini-Hochberg corrected); logFC $\geq$ |1|. *Continued from previous page.*

	Gene	logFC	adj.P.Val
77	*PSMB10*	-1.60	1.3E-03
78	*IL18*	-1.59	1.7E-03
79	*TUBB*	-1.59	6.2E-03
80	*ITGA4*	-1.58	1.7E-03
81	*PPARG*	-1.58	1.7E-03
82	*FCER1G*	-1.57	1.7E-02
83	*RORC*	-1.57	7.0E-03
84	*KLRF1*	-1.55	2.0E-02
85	*CD2*	-1.51	3.7E-02
86	*TIGIT*	-1.51	1.1E-02
87	*UBE2L3*	-1.49	5.0E-03
88	*RARRES3*	-1.47	2.5E-02
89	*PSMB9*	-1.45	5.6E-03
90	*OAZ1*	-1.44	4.4E-03
91	*PYCARD*	-1.43	3.6E-03
92	*CD45R0*	-1.43	1.4E-02
93	*PSMB8*	-1.42	4.5E-03
94	*TLR7*	-1.41	4.4E-03
95	*PTPN22*	-1.41	1.8E-02
96	*DPP4*	-1.39	7.1E-03
97	*GPI*	-1.38	1.8E-03
98	*CCR5*	-1.38	4.8E-02
99	*IL1R2*	-1.37	7.0E-03
100	*CD4*	-1.37	1.2E-02
101	*HLA-DRA*	-1.37	2.2E-02
102	*HLA-DPB1*	-1.36	2.8E-02
103	*KIT*	-1.35	9.0E-03
104	*IL2RG*	-1.35	5.0E-03
105	*CD1D*	-1.35	1.5E-02
106	*MSR1*	-1.33	1.6E-02
107	*FCGR2A/C*	-1.31	3.8E-02
108	*HLA-DOB*	-1.31	5.7E-03
109	*BTK*	-1.26	2.5E-03
110	*EDNRB*	-1.26	2.8E-02
111	*KIR2DS1*	-1.21	3.6E-02
112	*KLRG1*	-1.20	2.2E-02
113	*GFI1*	-1.20	1.1E-02
114	*ICAM3*	-1.19	6.2E-03
115	*CD163*	-1.19	1.7E-02
116	*PSMB7*	-1.18	7.8E-03
117	*ATG10*	-1.18	7.9E-03
118	*BAX*	-1.17	3.4E-03
119	*PDCD1LG2*	-1.16	1.7E-02
120	*LILRA6*	-1.15	8.5E-03
121	*MAP4K1*	-1.13	2.9E-02
122	*PSMC2*	-1.12	4.4E-03
123	*PTPRC$_a$ll*	-1.11	1.7E-02
124	*PPIA*	-1.11	1.4E-02
125	*CD74*	-1.11	1.5E-02
126	*LAIR1*	-1.10	2.8E-02
127	*FCGRT*	-1.09	7.1E-03
128	*TNFSF10*	-1.09	1.3E-02
129	*CIITA*	-1.08	2.6E-02
130	*IL7*	-1.08	1.3E-02
131	*CXCR4*	-1.07	2.2E-02
132	*CD19*	-1.07	2.8E-02
133	*TNFSF8*	-1.07	1.2E-02
134	*SMAD5*	-1.06	8.0E-03
135	*CCL13*	-1.06	4.4E-02
136	*ITGB2*	-1.03	4.1E-02
137	*TLR5*	-1.03	2.8E-02
138	*HFE*	-1.02	8.6E-03
139	*CD45RB*	-1.02	4.8E-02
140	*NFATC3*	-1.01	1.6E-02
141	*LTB4R2*	-1.01	1.9E-02

Continued...

Obs.1: LEL-M 5 h vs. TM 0 h (↑)			Obs.2: LEL-M 17 h vs. TM 0 h(↑)		
ARG2	*IL23A*	*TNFRSF9*	*ARG2*	*ICAM5*	*NFIL3*
BCL6	*IL6*	*TRAF1*	*BCL6*	*IDO1*	*NFKB1*
C3	*IL8*		*C3*	*IFI16*	*NFKBIZ*
C7	*IRAK2*		*CCL19*	*IL1A*	*PLAU*
CCL2	*IRF1*		*CCL2*	*IL1B*	*PLAUR*
CCL3	*IRF7*		*CCL20*	*IL1R1*	*PTGS2*
CD274	*NFATC1*		*CD274*	*IL1RL1*	*RELA*
CD40	*NFATC2*		*CD40*	*IL1RL2*	*RELB*
CD83	*NFIL3*		*CD59*	*IL1RN*	*RUNX1*
CDKN1A	*NFKB1*		*CD70*	*IL22*	*SELE*
CSF2	*NFKBIZ*		*CD80*	*IL23A*	*SKI*
CXCL1	*PLAUR*		*CD83*	*IL2RA*	*SLC2A1*
CXCL2	*PTGS2*		*CDKN1A*	*IL6*	*SOCS3*
DUSP4	*RELB*		*CSF2*	*IL8*	*SPP1*
EGR1	*SELE*		*CXCL1*	*IRAK2*	*STAT3*
FYN	*SOCS3*		*CXCL2*	*IRF1*	*TNFAIP3*
GBP1	*STAT4*		*DUSP4*	*IRF7*	*TNFAIP6*
ICAM1	*TGFB1*		*EGR1*	*LIF*	*TNFRSF9*
ICAM4	*TNFAIP3*		*EGR2*	*MAP4K4*	*TNFSF15*
ICAM5	*TNFAIP6*		*GBP1*	*MCL1*	*TRAF1*
IL1A	*TNFRSF10C*		*ICAM1*	*MME*	*ZEB1*
IL1B	*TNFRSF4*		*ICAM4*	*NFATC1*	

Table A.15.: List of common upregulated genes in WG-DASL and nCounter Assay. Genes shown in red were unique for the specified observation. Genes were defined as upregulated for specified time point vs. TM = 0 h by showing a logFC ≥ 1 and an adj.P.Val < 0.05. ↑: upregulated

Obs.1: LEL-M 5 h vs. TM 0 h (↓)			Obs.2: LEL-M 17 h vs. TM 0 h(↓)		
ARG2	*EGR1*	*PTGS2*	*ABCB1*	*CEACAM6*	
C7	*FYN*	*PYCARD*	*C1QA*	*CLEC7A*	*LILRA6*
CCL24	*GBP1*	*RELB*	*C1QB*	*CMKLR1*	*LILRB5*
CCR2	*GZMA*	*SELE*	*C5*	*CSF1R*	*MRC1*
CD1D	*HLA-DPB1*	*SLAMF6*	*CARD9*	*CSF3R*	*MSR1*
CD24	*IL18*	*STAT4*	*CCL13*	*CTSG*	*MUC1*
CD40	*IL23R*	*TLR7*	*CCL24*	*CX3CR1*	*NCF4*
CDKN1A	*IRF1*	*TLR8*	*CCL8*	*DEFB1*	*PIGR*
CEACAM1	*ITLN1*	*TNFRSF10C*	*CCR2*	*FCER1A*	*PLA2G2A*
CEACAM6	*KLRC4*	*TNFRSF4*	*CD160*	*GZMA*	*PPARG*
CIITA	*KLRD1*	*TNFRSF9*	*CD163*	*HLA-DMB*	*PYCARD*
CLEC7A	*MUC1*	*TRAF1*	*CD209*	*HLA-DPB1*	*RORC*
CSF2	*NFATC2*		*CD24*	*IL11RA*	*TLR3*
CX3CR1	*NFIL3*		*CD36*	*IL18*	*TLR4*
CXCR6	*NFKB1*		*CD4*	*ITGAM*	*TLR5*
DEFB1	*PIGR*		*CD74*	*ITLN1*	*TLR8*
DUSP4	*PPARG*		*CEACAM1*	*KLRF1*	*XCR1*

Table A.16.: List of common downregulated genes in WG-DASL and nCounter Assay. Genes shown in red were unique for the specified observation. Genes were defined as downregulated for specified time point vs. TM = 0 h by showing a logFC $\leq$ -1 and an adj.P.Val $<$ 0.05. ↓: downregulated

Obs. 1 & 2 (Overlap)		Obs. 1	Obs. 2		
ATF3	*IL6*	*BHLHE22*	*ACSL4*	*IRF1*	*PITPNC1*
BCL6	*LYPD5*	*C3*	*ADM*	*KRT17*	*PLAU*
C2CD4B	*MMP9*	*CCL3*	*ALDH1A2*	*KYNU*	*PRRX1*
CCL2	*NAMPT*	*NFKBIZ*	*BHLHE40*	*MME*	*PTGS2*
CD83	*NR4A2*	*PCDH17*	*CEMIP*	*MMP1*	*SERPINB8*
CXCL1	*PFKFB3*	*PDLIM7*	*CXCL5*	*MMP10*	*SGIP1*
CXCL2	*PLAUR*	*TAGLN*	*FLNC*	*MMP3*	*SLC11A1*
CXCL8	*SERPINA3*		*HIF1A*	*MTHFD2*	*SLC2A3*
EGR1	*SERPINE1*		*IDO1*	*NCOA7*	*TMEM158*
FDCSP	*SIK1*		*IER3*	*OSM*	*TNFRSF12A*
GEM	*SOD2*		*IFI16*	*PDE4B*	*TNFRSF6B*
GREM1	*TGM2*		*IL13RA2*	*PDPN*	*UBD*
IL1A	*TNFAIP6*		*IL1RN*	*PHLDA1*	
IL1B	*ZC3H12A*		*IL33*	*PIM3*	

Table A.17.: Gene expression overlap between upregulated genes in the LEL-M model (WG-DASL Assay) and the UC vs. NC dataset [Granlund *et al.*, 2013]. Obs. 1: LEL-M 5 h vs. TM 0 h, Obs. 2: LEL-M 17 h vs. TM 0 h. Columns 2 and 3 show overlap of genes detected uniquely for Obs.1 or Obs.2, respectively. Significant differential expression was defined by a logFC ≥ 1 and an adj.P.Val < 0.01. UC: ulcerative colitis, NC: normal colon

Obs. 1 & 2 (Overlap)			Obs. 1	Obs. 2	
A1CF	*ITPKA*	*SLC30A10*	*EXPH5*	*ABCG2*	*SLC4A4*
ACADS	*KRT12*	*SLC35G1*	*GPR160*	*ACAA2*	*SPIRE2*
ACOX1	*LDHD*	*SLC39A5*	*MEP1B*	*ACSF2*	*SUGCT*
ACSL5	*LRRC19*	*SLC3A1*	*MIER3*	*ADH1C*	*WDR78*
AHCYL2	*LRRC31*	*SLC51A*	*PHLPP2*	*ASAP3*	*YBX2*
AKR1B10	*MARVELD3*	*SLC51B*		*CHP2*	
AMACR	*MB*	*SLC9A2*		*CHST13*	
AQP8	*MEP1A*	*SOWAHA*		*CKB*	
BEST2	*METTL7B*	*SRI*		*CLYBL*	
BRINP3	*MPST*	*STAP2*		*CNTFR*	
C1orf115	*MS4A10*	*TEX11*		*CNTNAP2*	
CA1	*MS4A12*	*TINAG*		*CYP4F12*	
CA12	*MS4A8*	*TM4SF5*		*DDC*	
CA2	*MT1F*	*TMEM171*		*EPHX2*	
CDHR5	*MT1G*	*TMEM236*		*ERBB2*	
CDKN2B	*MT1H*	*TMEM37*		*GCNT2*	
CEACAM7	*MYO1A*	*TMEM56*		*GOLT1A*	
CES2	*MYO1D*	*TMIGD1*		*GSTA1*	
CGN	*NAT8B*	*TRPM6*		*HPGD*	
CHAD	*NXPE4*	*TUBAL3*		*HSD17B11*	
CLDN8	*OTOP2*	*UGT1A10*		*LINC01559*	
CMBL	*PDE6A*	*UGT1A7*		*MAOA*	
CYP2C18	*PDZD3*	*UGT1A8*		*MROH7*	
CYP4F2	*PLA2G12B*	*UGT2A3*		*MTMR11*	
DEFB1	*PLEKHG6*	*VIPR1*		*NPY*	
DHRS11	*PP7080*	*XK*		*OTC*	
EDN3	*PPARG*	*ZG16*		*PBLD*	
ENTPD5	*PPP1R14C*			*PCK1*	
EPB41L4B	*PROM2*			*PIGZ*	
FMO5	*PTGDR*			*PKDCC*	
FRMD1	*PTPRR*			*PKIB*	
GBA3	*RAPGEFL1*			*PRAP1*	
GUCA2A	*SATB2*			*PRKG2*	
GUCA2B	*SCIN*			*PXMP2*	
HMGCS2	*SGK2*			*RAVER2*	
HSD11B2	*SHD*			*SELENBP1*	
IGSF9	*SLC16A9*			*SEMA6A*	
IMPA2	*SLC17A4*			*SLC19A3*	
INPP5J	*SLC22A5*			*SLC22A18AS*	
ISX	*SLC26A2*			*SLC22A23*	

Table A.18.: Gene expression overlap of downregulated genes in the LEL-M model (WG-DASL Assay) and the UC vs. NC dataset [Granlund *et al.*, 2013]. Obs. 1: LEL-M 5 h vs. TM 0 h, Obs. 2: LEL-M 17 h vs. TM 0 h. Columns 2 and 3 show overlap of genes detected uniquely for Obs.1 or Obs.2, respectively. Significant differential expression was defined by a logFC $\leq$ -1 and an adj.P.Val $<$ 0.01. UC: ulcerative colitis, NC: normal colon

↓					↑
Obs.1 & 2 (Overlap)		Obs.1	Obs.2		*Obs.2*
CTSE	*S100P*	*PI3*	*AIF1*	*MNDA*	*ABCG1*
CASP5	*SLC5A1*	*SLAMF6*	*ASS1*	*OLFM4*	*HES5*
CEACAM6	*TFF1*		*CCL24*	*P2RY13*	*LAMA1*
LCN2	*TFF2*		*CD74*	*SERPINA1*	*VLDLR*
DMBT1	*XDH*		*CSF3R*	*SIGLEC10*	
MUC1			*GPX2*	*SPINK5*	
FFAR4			*HLA-DMB*	*TMEM200A*	
PDZK1IP1			*LST1*	*ZG16B*	
PLEKHS1			*MDK*		

Table A.19.: Anticorrelation of differentially regulated genes between LEL-M model (WG-DASL Assay) and the UC vs. NC dataset [Granlund *et al.*, 2013]. Obs. 1: LEL-M 5 h vs. TM 0 h, Obs. 2: LEL-M 17 h vs. TM 0 h. Shown are genes that were downregulated ↓or upregulated ↑in the WG-DASL Assay but regulated the opposite direction in the UC vs. NC data set. Significant differential expression was defined by a logFC $\geq |1|$ and an adj.P.Val < 0.01. UC: ulcerative colitis; NC: normal colon; ↑: upregulated; ↓: downregulated

Obs.1 & 2 (Overlap)		Obs.1		Obs.2	
Gene	SNP	Gene	SNP	Gene	SNP
ATF4	rs2413583	*FLRT1*	rs559928	*CXCR5*	rs630923
CD40	rs1569723	*FYN*	rs3851228	*FOSL2*	rs925255
CSF2	rs2188962	*STAT4*	rs1517352	*IL1R1*	rs917997
FOSL1	rs2231884			*IL22*	rs7134599
ICAM1	rs11879191			*IL24*	rs3024505
IL1RL1	rs917997			*LIF*	rs2412970
IL1RL2	rs917997			*PDLIM4*	rs2188962
NFIL3	rs4743820			*PFKFB4*	rs3197999
REL	rs7608910			*RELA*	rs2231884
TNFAIP3	rs6920220			*SMAD7*	rs7240004
TNFRSF9	rs35675666			*SPRY4*	rs6863411
UCN2	rs3197999			*STAT3*	rs12942547
				TNFSF15	rs4246905
				TRAF3IP2	rs3851228

Table A.20.: WG-DASL upregulated genes linked to single nucleotid polymorphisms (SNP) loci [Jostins *et al.*, 2012], which are upregulated in the LEL model but not present in the UC vs. NC dataset [Granlund *et al.*, 2013]. Obs. 1: LEL-M 5 h vs. TM 0 h, Obs. 2: LEL-M 17 h vs. TM 0 h. Column 1 contains genes that were present for both observations. Significant differential expression was defined by a logFC $\geq |1|$ and an adj.P.Val < 0.01. UC: ulcerative colitis; NC: normal colon

Table A.21.: WG-DASL Assay: Predicted Canonical Pathways (IPA). To appear in this table, at least one observation for the indicated pathway had to have a -(log P.Val) > 1.3 ($\equiv$ to a linear P.Val < 0.05). The table is sorted by -(log P.Val) (> 1.3) and subsequently z-score of LEL-M 5 h vs. TM 0 h. % OL: % overlap between differentially regulated genes in WG-DASL Assay and genes known to be involved in the specified pathway.

	Canonical Pathway	**LEL-M 5 h vs. TM 0 h**			**LEL-M 17 h vs. TM 0 h**			**LEL-M 17 h vs. 5 h**		
		z- score	% OL	-(log P.Val)	z- score	% OL	-(log P.Val)	z-score	% OL	-(log P.Val)
1	Dendritic Cell Maturation	2.86	14.1	2.33	1.77	18.5	3.04		1.7	0.96
2	IL-1 Signaling	2.84	16.5	2.20	2.84	16.0	1.17		2.1	0.91
3	HMGB1 Signaling	2.56	19.2	4.06	3.40	22.5	3.97		2.5	1.37
4	Acute Phase Response Signaling	2.45	16.0	3.28	3.29	19.9	3.69			
5	IL-6 Signaling	2.20	21.6	5.28	3.65	25.9	5.61		2.6	1.40
6	Protein Kinase A Signaling	2.14	11.7	2.05	0.47	13.6	1.49			
7	B Cell Activating Factor Signaling	2.12	22.5	2.39	2.24	15.0	0.62		2.5	0.64
8	iNOS Signaling	2.12	20.5	2.10	1.63	19.1	1.26		2.1	0.58
9	FGF Signaling	1.94	15.3	1.72	1.70	19.1	1.96		2.3	0.95
10	TNFR2 Signaling	1.89	27.6	2.77	1.41	31.0	2.65			
11	p38 MAPK Signaling	1.88	20.5	4.71	2.35	22.2	3.75			
12	PI3K/AKT Signaling	1.81	14.6	1.98	2.24	18.8	2.43		1.6	0.70
13	LPS/IL-1 Mediated Inhibition of RXR Function	1.73	15.5	3.68	2.07	23.6	7.85		1.8	1.23
14	4-1BB Signaling in T Lymphocytes	1.67	32.3	3.96	2.12	29.0	2.43		3.2	0.74
15	April Mediated Signaling	1.67	23.7	2.55	1.13	18.4	1.00		2.6	0.66
16	TNFR1 Signaling	1.67	20.4	2.27	0.33	20.4	1.53			
17	p53 Signaling	1.51	16.3	2.27	0.83	19.4	2.20			
18	Neurotrophin/TRK Signaling	1.41	14.9	1.37	0.82	11.1	0.31			
19	ATM Signaling	1.39	25.4	4.27	0.63	20.3	1.73		1.7	0.50
20	Toll-like Receptor Signaling	1.29	29.7	7.28	0.78	29.7	5.34			

Continued on next page

Table A.21.: WG-DASL Assay: Canonical Pathways (IPA). *Continued from previous page.*

	Canonical Pathway	**LEL-M 5 h vs. TM 0 h** z- score	% OL	-(log P.Val)	**LEL-M 17 h vs. TM 0 h** z- score	% OL	-(log P.Val)	**LEL-M 17 h vs. 5 h** z- score	% OL	-(log P.Val)
21	CDK5 Signaling	1.29	15.2	1.87	1.29	16.5	1.39		2.9	1.53
22	Role of PRRs in Recognition of Bacteria and Viruses	1.16	19.2	4.22	-0.24	24.0	4.91		2.4	1.32
23	Death Receptor Signaling	1.16	14.1	1.46	1.29	17.4	1.52		1.1	0.35
24	Inhibition of Angiogenesis by TSP1	1.13	23.5	2.30	0.82	15.4	0.65		5.1	1.58
25	TWEAK Signaling	1.13	20.6	1.75	0.33	26.5	2.14			
26	Cell Cycle: G2/M DNA Damage Checkpoint Regulation	1.13	16.3	1.37	1.67	20.4	1.53			
27	TREM1 Signaling	1.09	28.0	6.49	1.23	31.6	6.29			
28	Nitric Oxide Signaling in the Cardiovascular System	0.83	14.0	1.51	1.50	15.0	1.07		0.9	0.28
29	Lymphotoxin β Receptor Signaling	0.82	16.7	1.54	1.89	17.9	1.18			
30	Dopamine Receptor Signaling	0.82	14.1	1.30	0.38	14.1	0.77		1.1	0.35
31	MIF Regulation of Innate Immunity	0.63	24.4	2.88	-0.58	27.3	2.81		2.3	0.61
32	ERK/MAPK Signaling	0.63	12.3	1.52	1.37	18.3	3.09		1.1	0.46
33	TGF-β Signaling	0.58	16.1	1.99	0.26	19.5	2.06			
34	NRF2-mediated Oxidative Stress Response	0.58	13.3	1.96	0.00	13.9	1.03			
35	CD40 Signaling	0.54	23.1	3.76	1.29	24.6	3.03		3.1	1.18
36	Estrogen-mediated S-phase Entry	0.45	20.8	1.39	0.00	16.7	0.61			
37	NF-κB Signaling	0.43	14.0	2.20	0.87	20.3	3.99		1.2	0.52
38	IL-17A Signaling in Airway Cells	0.33	15.6	1.49	1.73	22.7	2.51		4.6	2.05

Continued on next page

Table A.21.: WG-DASL Assay: Canonical Pathways (IPA). *Continued from previous page.*

	Canonical Pathway	**LEL-M 5 h vs. TM 0 h** z- score	% OL	-(log P.Val)	**LEL-M 17 h vs. TM 0 h** z- score	% OL	-(log P.Val)	**LEL-M 17 h vs. 5 h** z- score	% OL	-(log P.Val)
39	STAT3 Pathway	0.28	17.8	2.26	-0.26	20.3	2.02		2.7	1.08
40	Apoptosis Signaling	0.28	14.6	1.57	-1.21	20.2	2.31			
41	Endothelin-1 Signaling	0.21	14.5	2.50	-1.46	13.4	0.89		1.1	0.47
42	BMP signaling pathway		15.8	1.72	-0.82	18.2	1.53		1.3	0.41
43	Antioxidant Action of Vitamin C	-0.26	18.2	3.02	1.41	21.9	3.29		1.0	0.31
44	MIF-mediated Glucocorticoid Regulation	-0.38	24.2	2.39	-1.16	37.1	4.52			
45	Cell Cycle: G1/S Checkpoint Regulation	-0.38	15.6	1.49	0.38	14.1	0.64			
46	IL-22 Signaling	-0.45	20.8	1.39	0.45	20.8	0.99		8.3	1.98
47	Cyclins and Cell Cycle Regulation	-0.91	16.7	2.01	-1.51	15.4	0.94			
48	Wnt/ β -catenin Signaling	-1.15	14.2	2.29	-0.69	15.9	1.70		1.2	0.52
49	Insulin Receptor Signaling	-1.50	12.9	1.41						
50	Eicosanoid Signaling	-1.63	18.8	2.31	-2.33	19.5	1.96		1.2	0.38
51	LXR/RXR Activation	-1.71	19.0	4.00	-3.16	25.8	6.07		0.8	0.25
52	Aldosterone Signaling in Epithelial Cells	-2.12	18.4	4.47	-2.12	14.2	1.06			
53	PPARα/RXRα Activation	-2.98	14.0	2.30	-4.38	16.4	2.01			
54	PPAR Signaling	-3.15	18.3	2.91	-3.67	25.8	4.60		1.1	0.34
55	IL-8 Signaling	1.21	10.3	0.78	2.27	16.0	1.86		1.1	0.46
56	Leukocyte Extravasation Signaling	2.14	10.1	0.74	2.20	16.2	2.07	1.34	3.4	3.43
57	Ceramide Signaling	1.90	12.5	0.95	2.14	17.9	1.54		1.2	0.38
58	Oncostatin M Signaling		8.8	0.28	2.12	23.5	1.65		5.9	1.69

Continued on next page

Table A.21.: WG-DASL Assay: Canonical Pathways (IPA). *Continued from previous page.*

	Canonical Pathway	**LEL-M 5 h vs. TM 0 h** z- score	% OL	-(log P.Val)	**LEL-M 17 h vs. TM 0 h** z- score	% OL	-(log P.Val)	**LEL-M 17 h vs. 5 h** z- score	% OL	-(log P.Val)
59	ILK Signaling	-0.47	11.4	1.13	1.89	17.1	2.39		1.1	0.47
60	Wnt/Ca^+ pathway	2.83	14.3	1.09	1.51	18.6	1.37			
61	Ephrin Receptor Signaling	1.16	9.2	0.47	1.41	15.8	1.72		1.1	0.50
62	Gαs Signaling	0.91	11.0	0.76	1.21	16.8	1.57		1.8	0.78
63	Role of Oct4 in Mammalian Embryonic Stem Cell Pluripotency		15.2	1.12	1.00	21.7	1.71			
64	HIPPO signaling	-0.45	9.3	0.40	0.58	19.5	2.06			
65	cAMP-mediated signaling	0.43	11.4	1.28	0.47	20.2	4.84		0.9	0.37
66	Cardiac β-adrenergic Signaling	1.16	12.0	1.14	0.24	17.0	1.91		1.4	0.64
67	Coagulation System	0.82	17.1	1.22	-0.30	31.4	3.18			
68	Regulation of Cellular Mechanics by Calpain Protease	0.00	12.3	0.75	-0.63	22.4	2.19		1.7	0.50
69	Neuregulin Signaling	-0.38	10.2	0.55	-0.83	18.3	1.78		1.1	0.34
70	PTEN Signaling	-1.60	11.9	1.01	-1.09	17.5	1.86		1.7	0.74
71	Sperm Motility	-0.58	10.7	0.74	-1.89	16.2	1.56			

Table A.22.: WG-DASL Assay: Predicted Biological Functions (IPA). To appear in this table, at least one observation for the specified function had to have values for both z-score and P.Val. General P.Val. Cut off: 0.01.

		LEL-M 5 h vs. TM 0 h		LEL-M 5 h vs. TM 0 h		LEL-M 17 h vs. 5h	
	Biological Function	z-score	P value	z-score	P value	z-score	P value
1	cell survival	3.46	6.3E-11	2.91	2.8E-17		
2	function of blood cells	3.16	4.9E-10	2.35	5.1E-19		
3	survival of organism	3.06	8.1E-15	2.04	4.6E-22		
4	function of leukocytes	3.02	2.6E-11	1.95	1.5E-19		
5	cell viability	2.98	6.3E-11	2.78	7.5E-18	2.58	9.6E-03
6	adhesion of blood cells	2.96	1.3E-06				
7	stimulation of cells	2.90	1.2E-08	2.52	9.1E-16		
8	function of phagocytes	2.68	1.3E-08	1.88	4.3E-17		
9	homeostasis of blood cells	2.40	7.0E-09	2.79	2.1E-12		
10	homeostasis of leukocytes	2.39	1.0E-08	2.72	2.9E-12		
11	cellular homeostasis	2.39	1.9E-19	3.08	1.2E-21	-0.63	1.7E-03
12	Lymphocyte homeostasis	2.39	7.3E-09	2.72	1.4E-12		
13	function of mononuclear leukocytes	2.38	3.1E-07				
14	recruitment of cells	2.38	1.3E-10	2.03	2.4E-20		
15	cell movement	2.21	1.1E-21	2.10	4.8E-39	1.03	1.3E-04
16	invasion of cells	2.01	2.0E-14	2.94	1.5E-26	1.75	4.8E-03
17	expansion of cells	1.94	2.2E-07	1.82	7.4E-10		
18	chemotaxis	1.89	6.4E-11	2.28	1.5E-20		
19	quantity of cells	1.88	9.1E-18	1.82	7.7E-33		
20	homing of cells	1.87	8.3E-12	2.25	1.1E-21		
21	activation of cells	1.83	4.9E-11	1.35	6.4E-20	0.26	5.0E-03
22	cellular infiltration	1.80	3.9E-10	0.52	6.8E-17	-0.69	7.4E-03
23	chemotaxis of cells	1.77	1.7E-10	2.08	1.2E-19		
24	migration of cells	1.75	4.3E-21	1.64	6.5E-37	1.27	4.5E-04

Continued on next page

Table A.22.: WG-DASL Assay: Predicted Biological Functions (IPA). *Continued from previous page.*

	Biological Function	LEL-M 5 h vs. TM 0 h z-score	LEL-M 5 h vs. TM 0 h P value	LEL-M 5 h vs. TM 0 h z-score	LEL-M 5 h vs. TM 0 h P value	LEL-M 17 h vs. 5h z-score	LEL-M 17 h vs. 5h P value
25	metabolism of carbohydrate	1.74	8.1E-07				
26	leukocyte migration	1.74	2.0E-15	0.98	8.8E-25	-0.15	4.0E-03
27	cell movement of muscle cells	1.74	1.4E-07	2.44	1.3E-10		
28	proliferation of cells	1.70	1.8E-24	2.11	5.4E-47	1.82	5.3E-04
29	binding of DNA	1.65	2.8E-08	2.49	3.6E-10		
30	inflammatory response	1.63	4.8E-19	0.62	3.5E-28		
31	concentration of eicosanoid	1.58	5.5E-07				
32	binding of cells	1.55	2.0E-07				
33	ion homeostasis of cells	1.49	2.6E-09	2.07	7.3E-11	-0.78	5.4E-03
34	secretion of molecule	1.48	3.7E-07				
35	synthesis of nitric oxide	1.48	1.1E-09	1.08	8.6E-10		
36	colony formation	1.40	6.5E-07	-0.32	5.6E-16		
37	cellular infiltration of cells	1.35	1.9E-10	0.45	1.5E-15		
38	metabolism of reactive oxygen species	1.21	6.4E-09	-0.18	2.0E-10		
39	cell death of liver	1.19	1.2E-07				
40	concentration of fatty acid	1.14	1.2E-06				
41	production of antibody	1.01	3.6E-07	0.42	1.3E-10		
42	quantity of metal ion	0.99	2.2E-13				
43	synthesis of reactive oxygen species	0.90	2.2E-09	0.04	1.5E-10		
44	cell-mediated response	0.89	9.9E-07				
45	quantity of metal	0.89	4.7E-12				
46	cell death of blood cells	0.77	6.9E-10	-0.17	1.7E-17		
47	transcription	0.69	7.8E-07	0.34	2.8E-12		
48	quantity of $Ca2^{+}$	0.67	2.0E-09				
49	cell death	0.66	1.9E-26	0.31	1.2E-40		

Continued on next page

Table A.22.: WG-DASL Assay: Predicted Biological Functions (IPA). *Continued from previous page.*

	Biological Function	LEL-M 5 h vs. TM 0 h z-score	LEL-M 5 h vs. TM 0 h P value	LEL-M 5 h vs. TM 0 h z-score	LEL-M 5 h vs. TM 0 h P value	LEL-M 17 h vs. 5h z-score	LEL-M 17 h vs. 5h P value
50	metabolism of prostaglandin	0.66	5.4E-07	0.90	4.5E-10		
51	production of protein	0.66	1.3E-06	-0.01	4.6E-11		
52	production of reactive oxygen species	0.66	1.4E-06				
53	necrosis	0.59	2.1E-19	0.05	2.9E-39	-0.77	4.3E-03
54	apoptosis of epithelial cells	0.58	4.3E-11	0.51	5.8E-14		
55	quantity of carbohydrate	0.44	2.2E-09				
56	cell death of epithelial cells	0.28	4.0E-09	0.97	5.8E-18		
57	size of lesion	0.25	2.6E-11	-0.29	2.6E-16	2.03	1.4E-03
58	behavior	0.23	1.2E-09	0.91	2.7E-11		
59	quantity of Na^+	0.21	3.1E-07				
60	conversion of cells	0.13	9.6E-07				
61	interphase	0.11	1.3E-07				
62	inflammation of body region	0.11	8.0E-20	0.08	4.6E-31	-1.57	2.1E-03
63	inflammation of organ	0.09	4.8E-19	0.18	1.8E-34	-1.50	6.3E-03
64	Cytosis	0.02	2.1E-07	-0.43	9.7E-15		
65	apoptosis	-0.06	4.7E-23	-0.07	4.1E-38		
66	transport of metal ion	-0.08	2.4E-08				
67	Fibrosis	-0.17	2.5E-13	-0.83	1.1E-18	-0.45	2.8E-03
68	transport of metal	-0.25	1.8E-07				
69	necrosis of epithelial tissue	-0.26	3.9E-12	0.48	1.0E-23		
70	concentration of acylglycerol	-0.31	2.7E-08	-0.37	3.2E-11		
71	transport of molecule	-0.34	2.6E-12	-0.63	9.2E-21		
72	quantity of epithelial tissue	-0.35	1.8E-07	-0.97	1.4E-12		
73	concentration of lipid	-0.39	6.2E-14	0.23	5.8E-21		
74	concentration of triacylglycerol	-0.47	3.3E-09	-0.38	4.9E-11		

Continued on next page

Table A.22.: WG-DASL Assay: Predicted Biological Functions (IPA). *Continued from previous page.*

		LEL-M 5 h vs. TM 0 h		LEL-M 5 h vs. TM 0 h		LEL-M 17 h vs. 5h	
	Biological Function	z-score	P value	z-score	P value	z-score	P value
75	cell death of endothelial cells	-0.52	1.5E-09	-0.41	9.2E-12		
76	inflammation of body cavity	-0.55	1.7E-14	-0.56	1.9E-23	-1.54	5.1E-03
77	apoptosis of endothelial cells	-0.57	1.5E-08	-0.83	2.7E-10		
78	quantity of lesion	-0.64	3.2E-07				
79	transport of inorganic cation	-0.67	9.0E-09				
80	activation-induced cell death	-0.70	9.0E-07				
81	proliferation of gastrointestinal cells	-0.76	1.3E-06				
82	quantity of steroid	-0.89	3.3E-09	0.15	2.7E-15		
83	transport of Na^+	-0.90	9.2E-07				
84	transport of cation	-0.94	7.9E-08				
85	cell-cell adhesion	-0.94	6.8E-07				
86	apoptosis of blood cells	-1.01	4.7E-11	-0.64	2.9E-16		
87	transport of monovalent inorganic cation	-1.17	3.7E-07				
88	concentration of cholesterol	-1.17	2.0E-07				
89	cell death of heart	-1.30	3.7E-08				
90	transport of ion	-1.37	3.4E-10				
91	cellular degradation	-1.48	2.0E-06				
92	degeneration of cells	-1.97	1.1E-06				
93	oxidation of lipid	-2.17	1.2E-08				
94	oxidation of fatty acid	-2.24	1.3E-07				
95	Edema	-2.86	6.8E-11	-2.66	5.1E-12		
96	morbidity or mortality	-5.30	4.3E-16	-5.30	1.4E-24		
97	organismal death	-5.73	1.6E-15	-5.52	1.4E-23		
98	organization of cytoplasm			2.73	9.9E-11		
99	organization of cytoskeleton			2.67	1.8E-10		

Continued on next page

Table A.22.: WG-DASL Assay: Predicted Biological Functions (IPA). *Continued from previous page.*

	Biological Function	LEL-M 5 h vs. TM 0 h z-score	LEL-M 5 h vs. TM 0 h P value	LEL-M 5 h vs. TM 0 h z-score	LEL-M 5 h vs. TM 0 h P value	LEL-M 17 h vs. 5h z-score	LEL-M 17 h vs. 5h P value
100	growth of plasma membrane projections			2.37	7.8E-10		
101	function of antigen presenting cells			2.25	1.8E-13		
102	phosphorylation of protein			2.22	1.6E-11		
103	adhesion of connective tissue cells			2.04	4.9E-10	0.928	5.9E-03
104	cell movement of epithelial cells			1.87	4.9E-10		
105	synthesis of lipid			1.75	4.7E-10		
106	migration of epithelial cells			1.60	5.2E-10		
107	stimulation of blood cells			1.54	1.7E-11		
108	invasion of carcinoma cell lines			1.25	1.1E-09		
109	binding of protein binding site			1.23	3.8E-11		
110	angiogenesis of lesion			1.15	1.8E-11		
111	recruitment of blood cells			1.13	1.6E-17		
112	homing of blood cells			1.08	4.6E-17		
113	cell cycle progression			1.08	5.7E-12		
114	cell movement of blood cells			1.01	6.7E-26		
115	migration of blood cells			0.97	2.2E-25	-0.451	1.7E-03
116	metabolism of terpenoid			0.80	1.0E-09		
117	transmigration of cells			0.64	2.4E-10		
118	quantity of immunoglobulin			0.48	1.0E-10		
119	Wound			0.45	2.7E-12		
120	transcription of DNA			0.44	8.0E-10		
121	colony formation of cells			0.37	7.2E-14		
122	expression of RNA			0.12	2.7E-12		
123	immune response of cells			-0.86	1.5E-10		
124	fatty acid metabolism			-0.93	1.1E-11		

Table A.23.: WG-DASL Assay: Predicted Upstream Regulators (IPA). To appear in this table, at least one observation for this pathway had to have an z-score $> |2|$ and an P.Val Overlap with target genes < 0.05). The table is sorted by molecule type and subsequently z-score of LEL-M 5 h vs. TM 0 h. l-dep NR: ligand-dependent nuclear receptor; tl. reg.: translation regulator; ts. reg.: transcription regulator.

			LEL-M 5 h vs. TM 0 h			**LEL-M 17 h vs. TM 0 h**			**LEL-M 17 h vs. 5 h**		
	Upstream Regulator	Molecule Type	logFC	z-score	P.Val Overlap	logFC	z-score	P.Val Overlap	logFC	z-score	P.Val Overlap
1	NFkB (complex)	complex		7.55	2.8E-19		7.56	1.6E-25		1.95	3.5E-02
2	LDL	complex		4.34	3.2E-08		3.16	3.1E-13			
3	Ap1	complex		4.33	1.4E-04		4.67	7.0E-09		1.55	7.0E-03
4	TCR	complex		4.15	8.2E-07		4.68	3.1E-10			
5	PDGF BB	complex		4.12	5.3E-17		5.34	1.5E-23			
6	Cg	complex		3.76	6.0E-10		4.48	1.5E-19		1.58	1.2E-03
7	PI3K (complex)	complex		3.59	7.0E-10		4.19	7.8E-15		1.39	9.1E-04
8	NfkB-RelA	complex		3.31	2.5E-06		2.50	1.9E-04			
9	Fcer1	complex		3.29	8.8E-05		3.45	5.2E-06			
10	NfkB1-RelA	complex		3.23	9.3E-06		3.55	2.0E-06			
11	Collagen type I	complex		3.21	2.6E-03		3.65	4.7E-09		1.69	3.7E-04
12	TSH	complex		2.81	2.0E-04		3.01	8.1E-04			
13	lymphotoxin-alpha1-beta2	complex		2.75	2.8E-05		3.11	1.1E-06			
14	Stat3-Stat3	complex		2.74	1.4E-03		2.51	2.8E-04			
15	Ifn gamma	complex		2.60	1.4E-03		2.40	3.1E-05			
16	Fibrinogen	complex		2.46	1.3E-04		2.08	9.1E-05			
17	Lh	complex		2.36	5.8E-05		2.62	2.9E-07			3.6E-03
18	IL17a dimer	complex		2.28	2.5E-06		2.22	2.8E-05			
19	IL-17f dimer	complex		2.12	6.4E-08		1.84	9.7E-06			

Continued on next page

Table A.23.: WG-DASL Assay: Predicted Upstream Regulators (IPA). *Continued from previous page.*

	Upstream Regulator	Molecule Type	**LEL-M 5 h vs. TM 0 h** logFC	z-score	P.Val Overlap	**LEL-M 17 h vs. TM 0 h** logFC	z-score	P.Val Overlap	**LEL-M 17 h vs. 5 h** logFC	z-score	P.Val Overlap
20	Pka	complex		2.10	5.7E-07		1.83	1.7E-09			3.5E-02
21	Pdgf (complex)	complex		2.10	1.2E-06		2.72	2.0E-07			
22	PDGF-AA	complex		2.06	6.7E-02		1.75	5.3E-04			
23	IgG2b	complex		-2.10	1.5E-04						
24	CD3	complex		-4.07	2.3E-08		-4.57	4.6E-10		-2.06	1.8E-01
25	TNF	cytokine		7.71	6.6E-32		9.79	7.1E-60		2.82	7.3E-04
26	IL1B	cytokine	3.4	7.10	1.1E-28	2.5	7.89	1.0E-48		2.12	8.9E-04
27	IL1A	cytokine	2.7	5.39	2.4E-15	3.5	6.70	6.7E-26		2.04	1.1E-03
28	IL3	cytokine		4.94	2.7E-06		5.22	1.8E-12			7.4E-03
29	CSF2	cytokine	2.7	4.46	2.6E-15	3.9	3.07	7.8E-28			
30	CD40LG	cytokine		4.26	1.3E-09		5.22	1.3E-14		1.97	4.8E-03
31	IL17A	cytokine		4.18	4.3E-06		4.53	1.0E-14		0.57	1.3E-03
32	IL2	cytokine		4.04	2.9E-09		2.73	1.1E-09			
33	IFNG	cytokine		3.98	1.0E-22		4.38	1.1E-36		0.33	4.1E-06
34	IL6	cytokine	5.9	3.97	3.4E-08	6.3	4.96	5.5E-24		1.47	1.1E-04
35	IL18	cytokine	-1.2	3.91	1.0E-04	-2.1	3.70	6.0E-05			4.5E-02
36	TNFSF13B	cytokine		3.65	4.0E-06		3.07	3.9E-06			
37	EDN1	cytokine		3.64	5.3E-05		4.86	8.0E-11			2.6E-02
38	TNFSF11	cytokine		3.40	3.8E-03		2.09	3.1E-07			3.7E-03
39	C5	cytokine		3.39	4.9E-08	-1.1	2.76	9.6E-10			
40	C5	cytokine		3.39	4.9E-08		2.53	4.2E-03			
41	SPP1	cytokine	2.5	3.37	4.9E-04	3.8	3.50	7.4E-05			

Continued on next page

Table A.23.: WG-DASL Assay: Predicted Upstream Regulators (IPA). *Continued from previous page.*

	Upstream Regulator	Molecule Type	**LEL-M 5 h vs. TM 0 h** logFC	z-score	P.Val Overlap	**LEL-M 17 h vs. TM 0 h** logFC	z-score	P.Val Overlap	**LEL-M 17 h vs. 5 h** logFC	z-score	P.Val Overlap
42	CCL5	cytokine		3.34	9.0E-09		3.11	2.6E-10			
43	CSF1	cytokine	1.4	3.20	2.8E-06		0.51	3.9E-12		-1.46	5.7E-05
44	IL17F	cytokine		3.07	2.0E-05		3.53	6.7E-10			1.2E-02
45	TNFSF12	cytokine		3.06	3.0E-03		2.96	3.8E-07			1.8E-02
46	IL15	cytokine		2.90	5.6E-07		3.20	1.6E-10			
47	IL4	cytokine		2.86	2.3E-07		2.23	8.2E-24		0.19	7.6E-07
48	EPO	cytokine		2.77	6.9E-03		3.29	5.8E-08			
49	WNT3A	cytokine		2.73	2.1E-04		2.57	2.5E-06		1.44	1.8E-03
50	TSLP	cytokine		2.70	3.0E-03		2.67	2.7E-04			
51	LIF	cytokine		2.61	1.5E-07	3.2	3.02	1.3E-14		1.04	5.7E-03
52	OSM	cytokine	2.5	2.56	5.6E-19	2.1	4.76	1.1E-20		1.92	2.8E-02
53	IL5	cytokine		2.56	9.5E-12		2.24	7.0E-11			
54	AIMP1	cytokine		2.55	4.8E-04		2.32	1.2E-02			
55	NAMPT	cytokine	2.4	2.47	1.9E-04	2.6	3.04	4.1E-07			
56	IL32	cytokine		2.37	4.5E-04		2.30	5.3E-05			
57	PF4	cytokine		2.35	3.3E-05		2.12	1.5E-03			
58	WNT5A	cytokine		2.33	1.1E-03	1.3	2.21	1.4E-06			
59	TNFSF15	cytokine		2.32	3.5E-02	3.0	3.08	3.9E-04			
60	CXCL12	cytokine		2.21	3.2E-04		2.72	1.7E-07			
61	FASLG	cytokine		2.13	8.3E-06		1.55	2.8E-06			1.5E-02
62	IL26	cytokine		2.10	1.7E-03		2.09	3.9E-04			
63	MIF	cytokine		2.06	1.7E-03		2.39	3.3E-06			

Continued on next page

Table A.23.: WG-DASL Assay: Predicted Upstream Regulators (IPA). *Continued from previous page.*

	Upstream Regulator	Molecule Type	**LEL-M 5 h vs. TM 0 h** logFC	z-score	P.Val Overlap	**LEL-M 17 h vs. TM 0 h** logFC	z-score	P.Val Overlap	**LEL-M 17 h vs. 5 h** logFC	z-score	P.Val Overlap
64	IL17B	cytokine		2.06	3.1E-05		2.05	9.2E-05			
65	IL17C	cytokine		2.00	1.3E-04		2.34	4.4E-03			
66	IL33	cytokine		1.88	2.3E-03	2.7	2.27	2.1E-04			
67	Il3	cytokine		1.85	1.3E-04		2.29	3.9E-05			
68	IL36B	cytokine		1.76	8.1E-05		2.23	1.0E-05			
69	CCL11	cytokine		1.32	1.4E-02		2.09	1.1E-06			3.8E-03
70	IL21	cytokine		0.85	5.9E-03		2.07	2.0E-04			
71	IL10	cytokine		-1.81	2.3E-08		-2.67	1.1E-13		-2.21	1.8E-02
72	IL1RN	cytokine		-3.26	4.0E-08	4.8	-4.28	6.5E-09			3.5E-02
73	TRAF6	enzyme		3.90	1.4E-07		4.17	4.5E-09			
74	FN1	enzyme		3.79	1.1E-03		4.77	3.3E-07			
75	HRAS	enzyme		3.43	5.6E-07		3.82	1.2E-13			
76	RHOA	enzyme		3.03	3.8E-03		1.99	1.9E-04			
77	PTGS2	enzyme	2.4	3.02	3.7E-05	3.7	3.09	6.5E-09		0.73	1.3E-02
78	TRAF2	enzyme		2.59	3.0E-05		2.61	8.6E-10			
79	GNA13	enzyme		2.10	1.1E-04			4.4E-05			
80	PADI2	enzyme	-1.8	2.08	2.2E-02	-2.3	1.83	2.7E-04			
81	TERT	enzyme		2.03	2.8E-02		1.97	1.1E-08			7.4E-03
82	LPL	enzyme		-1.60	6.8E-06		-2.50	4.7E-04			
83	ATG16L1	enzyme		-1.79	1.2E-05		-2.04	2.6E-06			
84	CAT	enzyme		-1.91	1.3E-04	-1.4	-2.17	1.1E-06			
85	SCD	enzyme		-2.06	1.8E-02		-1.34	5.5E-04			

Continued on next page

Table A.23.: WG-DASL Assay: Predicted Upstream Regulators (IPA). *Continued from previous page.*

	Upstream Regulator	Molecule Type	**LEL-M 5 h vs. TM 0 h** logFC	z-score	P.Val Overlap	**LEL-M 17 h vs. TM 0 h** logFC	z-score	P.Val Overlap	**LEL-M 17 h vs. 5 h** logFC	z-score	P.Val Overlap
86	ADA	enzyme		-2.09	2.4E-03		-2.71	9.8E-05			1.1E-02
87	DICER1	enzyme		-3.05	1.2E-04		-2.42	5.3E-04			
88	TNFAIP3	enzyme	2.5	-3.33	7.1E-06	2.4	-2.99	1.3E-04			
89	BRAF	enzyme			2.8E-07	1.1	2.09	3.2E-09			
90	DNMT3A	enzyme			4.9E-02		-2.08	2.4E-04			
91	TGFB1	growth factor	2.7	6.62	9.0E-27	1.5	6.64	4.7E-47		0.20	3.8E-06
92	HGF	growth factor		4.97	4.1E-13	2.8	4.90	7.3E-27		1.99	4.2E-02
93	EGF	growth factor		4.59	3.4E-09		5.14	1.7E-22		1.52	8.1E-03
94	TGFB3	growth factor		3.57	2.8E-04		3.95	4.1E-07			2.1E-02
95	ANGPT2	growth factor		3.44	1.6E-04	3.4	2.87	3.6E-08			
96	VEGFA	growth factor		3.37	3.0E-07	3.2	2.95	1.1E-16	2.2	1.31	3.1E-03
97	FGF2	growth factor		3.34	1.4E-12	3.1	5.12	2.1E-24		0.30	1.5E-02
98	LEP	growth factor		3.31	3.3E-05		2.66	1.4E-15		0.88	3.4E-02
99	GH1	growth factor		3.20	2.0E-04		1.57	8.8E-08			
100	AGT	growth factor		3.19	9.3E-09		4.54	2.8E-19		1.72	2.6E-01
101	GDF2	growth factor		3.14	1.3E-05		1.59	1.3E-06			
102	BMP2	growth factor		2.95	1.2E-06		2.74	8.7E-08			
103	BMP6	growth factor		2.84	3.2E-03		2.52	1.1E-05			1.4E-02
104	IGF1	growth factor		2.74	6.6E-13	-1.7	1.44	1.0E-16		-1.41	6.8E-03
105	AREG	growth factor		2.70	3.0E-03		3.39	2.3E-05			
106	KITLG	growth factor		2.68	1.7E-02		3.39	6.1E-08			
107	TGFA	growth factor	-3.4	2.55	2.2E-06	-2.7	2.49	2.3E-10			

Continued on next page

Table A.23.: WG-DASL Assay: Predicted Upstream Regulators (IPA). *Continued from previous page.*

	Upstream Regulator	Molecule Type	**LEL-M 5 h vs. TM 0 h** logFC	z-score	P.Val Overlap	**LEL-M 17 h vs. TM 0 h** logFC	z-score	P.Val Overlap	**LEL-M 17 h vs. 5 h** logFC	z-score	P.Val Overlap
108	PDGFB	growth factor		2.54	1.2E-06		3.90	4.1E-07			
109	PGF	growth factor		2.53	4.8E-04	1.5	2.92	2.9E-05			
110	NGF	growth factor		2.51	3.0E-07		2.43	1.2E-11			
111	CTGF	growth factor		2.38	3.0E-03		1.34	8.2E-05			
112	BTC	growth factor		2.33	1.2E-03		1.99	4.4E-05			
113	TGFB2	growth factor	1.7	2.25	7.5E-03	1.5	3.13	5.0E-06			
114	NRG1	growth factor		2.18	1.9E-04		2.18	6.6E-05			
115	BMP4	growth factor		2.15	4.9E-05	-1.7	2.09	9.5E-07		1.76	7.0E-03
116	BDNF	growth factor		1.74	6.4E-09	1.6	2.13	5.7E-06			
117	EREG	growth factor		1.32	6.7E-03		2.01	9.1E-05			
118	INHA	growth factor		-1.21	6.8E-05		-2.44	1.2E-07		-1.42	4.1E-04
119	F2R	GPCR		3.94	2.1E-06		4.06	1.6E-05			
120	CXCR4	GPCR		2.84	3.2E-04	1.7	2.52	1.0E-04			8.5E-04
121	F2RL1	GPCR	-4.3	2.69	6.3E-04	-4.0	3.35	1.2E-05			
122	S1PR2	GPCR	1.6	2.68	2.8E-05	1.7	2.46	1.3E-03			
123	PTGER2	GPCR		2.28	3.7E-06		1.78	2.2E-07			
124	IL1	group		5.36	7.7E-11		4.94	2.9E-20		1.62	7.3E-04
125	Jnk	group		5.17	2.5E-08		4.92	5.4E-12			
126	P38 MAPK	group		4.91	2.8E-12		4.97	6.3E-27		1.80	1.0E-02
127	ERK	group		4.69	3.8E-11		4.87	4.5E-13			
128	Vegf	group		4.67	4.9E-18		4.17	7.9E-32		0.46	8.0E-04
129	ERK1/2	group		3.88	4.4E-06		5.39	1.5E-16		2.51	1.7E-05

Continued on next page

Table A.23.: WG-DASL Assay: Predicted Upstream Regulators (IPA). *Continued from previous page.*

	Upstream Regulator	Molecule Type	**LEL-M 5 h vs. TM 0 h** logFC	z-score	P.Val Overlap	**LEL-M 17 h vs. TM 0 h** logFC	z-score	P.Val Overlap	**LEL-M 17 h vs. 5 h** logFC	z-score	P.Val Overlap
130	Tnf (family)	group		3.85	1.4E-06		4.06	4.2E-09			
131	Mapk	group		3.79	1.2E-08		3.35	4.0E-08			
132	Tlr	group		3.76	2.9E-05		3.62	8.1E-05			
133	Pkc(s)	group		3.57	1.2E-08		3.32	2.4E-09			
134	Nfat (family)	group		3.54	8.2E-09		3.82	4.3E-09			
135	caspase	group		2.93	6.9E-05		2.53	1.1E-02			
136	Fc gamma receptor	group		2.79	7.1E-07		2.22	3.9E-04			
137	IL-1R	group		2.74	2.4E-04		2.78	5.9E-06			9.1E-03
138	Akt	group		2.74	8.2E-11		3.20	3.8E-15			
139	Pkg	group		2.73	3.8E-06		1.71	2.0E-03			
140	Gm-csf	group		2.68	1.7E-04		2.17	4.6E-08			1.2E-03
141	SAA	group		2.68	2.0E-03		2.26	4.4E-06			
142	Pro-inflammatory Cytokine	group		2.49	6.8E-07		2.84	1.4E-06			
143	Tgf beta	group		2.43	3.1E-08		3.28	7.5E-17		-0.11	1.0E-02
144	Fgf	group		2.29	8.3E-03		2.49	6.9E-04			
145	Mek	group		2.23	2.4E-05		2.83	5.3E-07			
146	NFkB (family)	group		2.10	7.3E-04		2.34	2.5E-03			
147	TCF	group		2.10	1.2E-04		1.75	1.1E-08			
148	MAP2K1/2	group		1.94	1.5E-04		2.71	4.1E-04			

Continued on next page

Table A.23.: WG-DASL Assay: Predicted Upstream Regulators (IPA). *Continued from previous page.*

	Upstream Regulator	Molecule Type	**LEL-M 5 h vs. TM 0 h** logFC	z-score	P.Val Overlap	**LEL-M 17 h vs. TM 0 h** logFC	z-score	P.Val Overlap	**LEL-M 17 h vs. 5 h** logFC	z-score	P.Val Overlap
149	Ras	group		1.62	1.8E-08		2.46	1.5E-12		1.69	5.2E-03
150	Interferon alpha	group		1.39	1.9E-03		2.07	6.3E-07			
151	Creb	group		1.36	4.1E-03		2.07	2.4E-07		1.07	1.4E-03
152	IFN Beta	group		0.84	2.4E-03		2.19	6.2E-04			
153	SERCA	group		-2.30	1.3E-05		-2.05	1.2E-03			
154	Nr1h	group		-2.51	1.6E-07		-0.91	1.3E-05		2.18	8.9E-03
155	Alpha catenin	group		-4.76	3.4E-09		-4.07	1.1E-12			
156	ITGAV	ion channel		2.21	1.3E-03		2.76	1.2E-05			
157	CFTR	ion channel		-1.60	1.2E-04		-2.48	3.1E-06			
158	PKD1	ion channel		-3.90	8.6E-05		-4.77	4.2E-06			
159	P2RX4	ion channel	-1.8		3.0E-02		2.03	9.2E-05			
160	SRC	kinase		4.18	5.5E-06	-3.9	4.18	1.5E-10			2.9E-02
161	IKBKB	kinase		3.96	2.4E-12		5.64	1.1E-17		2.07	4.0E-03
162	JAK2	kinase		3.71	1.5E-04		3.94	4.4E-07			
163	PRKCE	kinase		3.52	3.8E-07		2.89	8.3E-04			
164	MAPK1	kinase		3.25	1.1E-07		4.39	1.3E-07			
165	MAP3K1	kinase		3.22	4.0E-03		2.74	1.8E-05			
166	MAPK3	kinase	-1.3	3.17	3.8E-05	-1.7	3.03	5.6E-07			
167	MAPK8	kinase	1.3	3.11	8.6E-05		2.53	3.3E-08			
168	EIF2AK2	kinase		3.09	6.8E-07		3.08	2.3E-06			
169	MAPK14	kinase		3.03	2.2E-06		4.01	3.5E-11			
170	FGFR1	kinase	1.8	3.02	1.9E-03	2.2	3.47	8.1E-06			

Continued on next page

Table A.23.: WG-DASL Assay: Predicted Upstream Regulators (IPA). *Continued from previous page.*

	Upstream Regulator	Molecule Type	**LEL-M 5 h vs. TM 0 h** logFC	z-score	P.Val Overlap	**LEL-M 17 h vs. TM 0 h** logFC	z-score	P.Val Overlap	**LEL-M 17 h vs. 5 h** logFC	z-score	P.Val Overlap
171	CHUK	kinase		2.97	1.1E-10		3.77	5.9E-12		1.64	2.1E-02
172	PRKCA	kinase		2.88	4.8E-05		3.01	2.9E-04			
173	MAP2K3	kinase	2.0	2.87	2.0E-02		2.39	1.1E-04			
174	TBK1	kinase		2.83	2.9E-03		3.07	3.1E-05			
175	RIPK2	kinase	1.7	2.77	1.4E-04	1.8	3.41	2.8E-04			
176	EIF2AK3	kinase		2.51	1.8E-04		3.40	7.6E-07			
177	JAK1	kinase		2.49	8.5E-04		2.64	3.6E-04			
178	RAF1	kinase		2.44	3.6E-09		3.62	1.3E-18			
179	MAP3K7	kinase		2.39	1.8E-03	1.2	1.94	8.5E-05			
180	IKBKG	kinase		2.36	3.0E-11		3.52	8.2E-09			3.6E-02
181	RET	kinase		2.35	5.8E-08		2.65	1.7E-10			1.3E-02
182	PRKCD	kinase		2.32	1.2E-06		3.29	9.3E-08			1.3E-02
183	MAP3K14	kinase		2.29	7.0E-04		2.01	9.5E-05			
184	PTK2	kinase		2.28	3.0E-04		2.31	8.2E-04			
185	MAP2K7	kinase		2.24	5.1E-02		2.46	5.0E-05			
186	MAP3K8	kinase	1.5	2.22	1.9E-04		2.84	9.3E-06			
187	TGFBR1	kinase		2.22	4.5E-03		2.10	1.6E-04			
188	ATM	kinase		2.11	1.0E-05		2.68	2.4E-04			
189	IRAK4	kinase		2.07	2.6E-10		1.51	1.2E-08			
190	ILK	kinase		2.02	1.4E-01	1.4	2.26	1.4E-04			
191	EGFR	kinase		1.93	4.6E-16		2.98	2.1E-22		0.60	2.2E-04
192	PRKCB	kinase		1.68	8.3E-05		2.30	6.5E-05			

Continued on next page

Table A.23.: WG-DASL Assay: Predicted Upstream Regulators (IPA). *Continued from previous page.*

	Upstream Regulator	Molecule Type	**LEL-M 5 h vs. TM 0 h** logFC	z-score	P.Val Overlap	**LEL-M 17 h vs. TM 0 h** logFC	z-score	P.Val Overlap	**LEL-M 17 h vs. 5 h** logFC	z-score	P.Val Overlap
193	NDRG1	kinase		1.50	2.0E-04		2.50	1.3E-07			1.6E-04
194	MET	kinase		1.47	1.6E-03		2.44	1.1E-05			
195	PIK3R1	kinase		1.44	2.1E-05		2.35	3.4E-05			
196	STK11	kinase		-2.29	5.3E-04		-2.16	1.4E-02			
197	CDKN1B	kinase		-2.43	2.4E-03		-2.16	6.2E-04			
198	NTRK1	kinase	1.7		6.7E-03		2.05	6.9E-04			
199	NR3C2	l-dep NR	-2.0	2.62	1.6E-04	-2.2	1.44	7.3E-08			
200	ESR1	l-dep NR		1.71	1.0E-06		2.13	5.2E-11		2.00	3.9E-04
201	RORC	l-dep NR		0.88	5.2E-07	-1.8	2.08	1.8E-10			1.3E-02
202	PPARG	l-dep NR	-2.0	-2.42	5.6E-11	-2.2	-2.66	2.0E-18			
203	miR-320b (and other miRNAs w/seed AAAGCUG)	mat. microrna		-2.06	9.1E-04			2.4E-02			
204	mir-373	microrna		-2.10	9.1E-04		-2.53	5.7E-06			
205	mir-515	microrna		-2.10	9.1E-04		-2.53	5.7E-06			
206	let-7	microrna	1.6	-2.31	9.6E-03	1.6	-2.20	1.8E-04			3.5E-02
207	mir-15	microrna		-2.31	5.4E-03	1.4	-0.59	2.7E-04			
208	APP	other	1.1	6.12	3.2E-12		4.46	7.5E-17		2.03	4.9E-03
209	MYD88	other		5.47	2.0E-08		5.21	3.8E-14		1.60	5.6E-02
210	TICAM1	other		4.95	9.0E-07		4.10	2.7E-08			
211	NOD2	other		4.72	5.5E-10		4.17	1.6E-08			

Continued on next page

Table A.23.: WG-DASL Assay: Predicted Upstream Regulators (IPA). *Continued from previous page.*

	Upstream Regulator	Molecule Type	**LEL-M 5 h vs. TM 0 h** logFC	z-score	P.Val Overlap	**LEL-M 17 h vs. TM 0 h** logFC	z-score	P.Val Overlap	**LEL-M 17 h vs. 5 h** logFC	z-score	P.Val Overlap
212	TRADD	other		3.75	4.8E-09		3.89	1.2E-08			
213	SELPLG	other		3.14	5.3E-04		2.46	3.8E-05			
214	TAC1	other		3.07	6.9E-03	3.0	3.50	2.5E-05			1.5E-03
215	CAMP	other		2.82	2.8E-06		2.83	1.8E-07			
216	CYR61	other		2.71	5.2E-03		3.94	1.6E-08			1.4E-03
217	H2AFB3 (includes others)	other		2.70	5.2E-07		2.50	7.5E-05			
218	RETNLB	other		2.56	1.1E-05	-3.0	1.88	1.1E-03			
219	DMP1	other		2.38	9.9E-02		3.38	6.5E-04			
220	Ins1	other		2.34	2.5E-04		1.53	7.5E-07			
221	OSCAR	other		2.30	7.3E-04		1.40	2.5E-03			
222	LUM	other		2.29	4.3E-04		2.28	1.5E-03			
223	ITGB6	other	-4.8	2.28	6.7E-03	-5.0	1.70	9.7E-06			
224	DMD	other	1.6	2.24	7.8E-05		1.69	5.7E-05			
225	LMNA	other	2.0	2.22	8.6E-04		1.99	1.2E-01			
226	C5	other		2.08	3.4E-02	-1.1	2.76	9.6E-10			
227	NOD1	other		2.08	7.3E-04		2.07	2.5E-03			
228	COCH	other		2.07	2.3E-04		1.79	7.8E-03			
229	THBS4	other		1.72	1.3E-02		3.01	7.5E-04			
230	S100A9	other		1.66	3.9E-10		2.32	9.3E-12			
231	RETN	other		1.61	1.9E-04		2.17	5.2E-04			
232	TMEM173	other		1.50	9.9E-07		2.09	2.0E-05			

Continued on next page

Table A.23.: WG-DASL Assay: Predicted Upstream Regulators (IPA). *Continued from previous page.*

	Upstream Regulator	Molecule Type	**LEL-M 5 h vs. TM 0 h** logFC	z-score	P.Val Overlap	**LEL-M 17 h vs. TM 0 h** logFC	z-score	P.Val Overlap	**LEL-M 17 h vs. 5 h** logFC	z-score	P.Val Overlap
233	TSC2	other		-0.54	1.9E-03		-2.11	2.4E-04			
234	CBX7	other		-2.03	2.9E-04		-2.25	2.4E-04			
235	ARRB2	other		-2.20	9.7E-05		-1.15	4.0E-07			
236	CDH1	other	-3.8	-2.25	3.0E-02	-3.9	-2.29	4.4E-04			
237	COL18A1	other		-2.63	2.2E-05		-4.19	4.7E-10			1.6E-02
238	COL1A1	other			9.5E-03		2.05	4.4E-05			
239	MYOC	other			2.5E-04		2.03	3.0E-05			
240	SERPINE2	other			1.8E-02		-2.08	2.1E-05			
241	F2	peptidase		6.01	2.1E-08		7.09	1.7E-15			
242	F7	peptidase		3.04	1.6E-06		3.78	9.1E-10			
243	PLG	peptidase		2.70	6.8E-03		3.00	1.6E-04			
244	C3	peptidase	2.2	2.22	8.8E-04	1.4	2.33	3.0E-03			
245	KLK5	peptidase		1.75	1.5E-03		2.25	1.5E-04			
246	ELANE	peptidase		1.68	2.4E-04		2.20	7.4E-05			
247	F10	peptidase		1.61	3.4E-05		2.04	3.3E-06			
248	PRTN3	peptidase		-2.02	4.1E-04		-2.01	1.2E-03			
249	NT5E	phosphatase		-2.05	3.7E-03		-2.51	2.7E-04			
250	DUSP5	phosphatase		-2.25	5.4E-05		-2.46	5.1E-05			
251	SOCS3	phosphatase	3.7	-2.31	8.4E-05	3.7	-1.47	4.3E-03			
252	DUSP1	phosphatase		-2.98	2.1E-06		-3.75	1.6E-06			
253	EIF4E	tl. reg	3.0	1.42	1.0E-02	2.7	2.83	7.9E-05			
254	TLR4	tm receptor		5.83	4.5E-07	-1.5	4.95	4.6E-09			

Continued on next page

Table A.23.: WG-DASL Assay: Predicted Upstream Regulators (IPA). *Continued from previous page.*

	Upstream Regulator	Molecule Type	**LEL-M 5 h vs. TM 0 h** logFC	z-score	P.Val Overlap	**LEL-M 17 h vs. TM 0 h** logFC	z-score	P.Val Overlap	**LEL-M 17 h vs. 5 h** logFC	z-score	P.Val Overlap
255	TLR7	tm receptor	-2.2	5.18	6.0E-06		5.29	1.4E-08			
256	TREM1	tm receptor		4.01	2.5E-16		4.38	2.1E-26		2.01	5.7E-03
257	TLR3	tm receptor		3.83	3.3E-03	-2.1	4.15	3.8E-04			
258	IL6R	tm receptor		3.77	1.2E-05		3.44	8.0E-10			8.8E-03
259	TLR2	tm receptor		3.50	2.2E-06		4.10	8.7E-08			
260	CD40	tm receptor	1.3	3.28	8.6E-05	1.1	4.31	4.1E-06			
261	CD14	tm receptor		3.28	1.3E-04		3.25	3.9E-05			
262	TLR5	tm receptor		3.06	2.2E-04	-2.4	3.67	5.4E-07			
263	IL1R1	tm receptor		3.02	3.1E-05	2.1	3.47	4.1E-07			
264	NCR2	tm receptor		2.76	1.3E-04		3.24	8.2E-07			
265	TYROBP	tm receptor		2.72	7.0E-04		2.90	4.1E-04			
266	FCGR2A	tm receptor		2.71	1.4E-03		2.38	2.8E-04			
267	ICAM1	tm receptor	3.0	2.46	2.8E-03	2.5	2.18	4.1E-04			2.5E-02
268	AGER	tm receptor		2.35	2.9E-08		2.93	2.3E-06			7.1E-03
269	F3	tm receptor		2.33	8.9E-03		2.27	3.9E-04			
270	IL17RA	tm receptor		2.28	1.0E-03		1.54	5.1E-05			
271	TNFRSF1B	tm receptor		2.15	2.4E-04		2.05	8.3E-07			
272	IFNGR1	tm receptor		2.13	4.6E-03		2.56	8.2E-04			
273	LY96	tm receptor		2.08	7.3E-04		1.24	2.0E-05			
274	IL1RL2	tm receptor	1.6	2.07	9.1E-04	2.2	2.31	1.6E-04			
275	CAV1	tm receptor		1.96	1.6E-03		2.25	4.4E-07			
276	CLEC7A	tm receptor	-1.8	1.83	3.5E-03	-2.5	2.27	5.3E-04			

Continued on next page

Table A.23.: WG-DASL Assay: Predicted Upstream Regulators (IPA). *Continued from previous page.*

	Upstream Regulator	Molecule Type	**LEL-M 5 h vs. TM 0 h** logFC	z-score	P.Val Overlap	**LEL-M 17 h vs. TM 0 h** logFC	z-score	P.Val Overlap	**LEL-M 17 h vs. 5 h** logFC	z-score	P.Val Overlap
277	CD28	tm receptor		-2.46	4.1E-06		-2.39	2.7E-07			
278	IL10RA	tm receptor		-4.13	1.2E-10		-4.21	8.5E-23		-2.67	2.6E-03
279	BCL2	transporter	1.8	2.46	2.4E-04		2.79	2.3E-03			
280	ITGB1BP1	transporter		2.07	9.1E-04		2.30	1.6E-04			
281	SFTPA1	transporter		-3.49	1.2E-08		-3.87	1.1E-10			
282	RELA	ts. reg.		5.06	1.1E-10	1.1	5.84	1.4E-16			5.0E-02
283	SRF	ts. reg.		4.16	4.1E-07		3.26	8.3E-10			1.9E-02
284	NFKB1	ts. reg.	1.4	4.06	7.1E-08	1.5	4.69	6.0E-12			4.2E-02
285	STAT3	ts. reg.		3.80	5.1E-09	1.7	4.46	3.1E-20		0.47	2.6E-02
286	HMGB1	ts. reg.		3.67	1.1E-04		4.22	1.6E-10			
287	JUN	ts. reg.	1.1	3.59	7.1E-10		3.89	2.9E-20		1.26	1.4E-03
288	REL	ts. reg.	1.8	3.57	2.4E-07	2.1	2.72	1.4E-08			
289	EGR1	ts. reg.	1.6	3.54	3.5E-11	1.4	3.19	2.9E-11			
290	CTNNB1	ts. reg.		3.47	9.7E-11		3.02	1.9E-14		0.66	1.2E-02
291	CREB1	ts. reg.		3.39	1.5E-12		2.48	2.9E-18		-1.48	1.3E-02
292	MTPN	ts. reg.		3.26	3.3E-04		1.78	5.6E-03			
293	SMAD2	ts. reg.		3.11	1.2E-03		3.40	8.5E-05			
294	IRF8	ts. reg.		3.10	7.7E-03		2.75	1.8E-06			
295	KLF6	ts. reg.		3.09	3.9E-07		2.84	1.1E-10			
296	STAT4	ts. reg.	1.1	3.01	1.2E-07		3.96	5.3E-07			
297	FOXO1	ts. reg.		2.88	6.1E-07		1.89	2.2E-10			
298	NFKBIA	ts. reg.		2.88	2.2E-12		2.60	1.9E-18		1.49	1.6E-04

Continued on next page

Table A.23.: WG-DASL Assay: Predicted Upstream Regulators (IPA). *Continued from previous page.*

	Upstream Regulator	Molecule Type	**LEL-M 5 h vs. TM 0 h** logFC	z-score	P.Val Overlap	**LEL-M 17 h vs. TM 0 h** logFC	z-score	P.Val Overlap	**LEL-M 17 h vs. 5 h** logFC	z-score	P.Val Overlap
299	PLAG1	ts. reg.		2.82	2.2E-03		1.84	6.7E-04			4.4E-02
300	CREBBP	ts. reg.		2.81	4.5E-06		2.30	9.2E-11			
301	NFATC2	ts. reg.	1.9	2.71	7.7E-03		3.61	1.0E-05			
302	TP63	ts. reg.		2.66	2.6E-10		2.80	1.3E-16			
303	SP1	ts. reg.		2.60	5.8E-09		2.00	5.5E-14		0.59	3.5E-03
304	IRF6	ts. reg.		2.59	3.9E-06	-1.6	2.21	4.4E-07			
305	ATF4	ts. reg.	1.6	2.58	1.9E-05	1.5	3.60	1.3E-09			5.7E-03
306	GLI1	ts. reg.		2.56	4.8E-08	-1.6	1.58	8.2E-09			
307	SMAD3	ts. reg.		2.39	7.6E-09		2.06	1.3E-11		-0.09	3.7E-02
308	FOS	ts. reg.		2.37	1.6E-10		2.28	8.2E-18		1.43	9.9E-03
309	PDX1	ts. reg.		2.35	1.8E-09		3.41	2.0E-09			
310	ATF2	ts. reg.		2.32	1.1E-04		1.78	1.8E-06			
311	IFI16	ts. reg.		2.31	1.2E-02	1.2	2.93	7.0E-05			
312	STAT1	ts. reg.		2.31	6.0E-07		2.02	5.5E-09			
313	HTT	ts. reg.		2.30	2.6E-06		0.75	3.0E-11			
314	NFKBIB	ts. reg.	2.3	2.25	2.5E-03	2.2	2.63	3.4E-05			
315	ETV5	ts. reg.		2.25	1.0E-03		2.21	7.6E-06			
316	FOXO4	ts. reg.		2.23	1.9E-04		2.40	2.7E-05			2.7E-02
317	MYOCD	ts. reg.		2.22	5.2E-05		2.24	1.3E-03			
318	POU5F1	ts. reg.		2.19	3.8E-06	2.9	2.58	3.7E-08		0.82	3.4E-02
319	CREM	ts. reg.		2.18	4.3E-04		3.41	2.6E-04			
320	DDIT3	ts. reg.	3.3	2.10	1.1E-04	2.9	2.53	3.0E-05			

Continued on next page

Table A.23.: WG-DASL Assay: Predicted Upstream Regulators (IPA). *Continued from previous page.*

	Upstream Regulator	Molecule Type	**LEL-M 5 h vs. TM 0 h** logFC	z-score	P.Val Overlap	**LEL-M 17 h vs. TM 0 h** logFC	z-score	P.Val Overlap	**LEL-M 17 h vs. 5 h** logFC	z-score	P.Val Overlap
321	TSC22D1	ts. reg.		2.10	9.1E-04		2.09	2.5E-03			
322	CARM1	ts. reg.		2.07	1.6E-03		1.48	1.8E-05			
323	ELK1	ts. reg.		2.07	4.6E-07		2.59	2.2E-07			
324	TBX5	ts. reg.		2.06	6.7E-04		2.48	2.3E-05			
325	TP53	ts. reg.		2.06	7.1E-12		0.59	4.4E-20			
326	HOXA5	ts. reg.		2.05	1.0E-03		2.27	6.9E-04			
327	Hmgb1	ts. reg.		2.02	2.8E-05		1.77	1.3E-03			
328	NOTCH1	ts. reg.		2.01	1.5E-05		2.65	6.9E-12			
329	CYLD	ts. reg.	1.6	2.00	4.4E-03	2.0	1.77	1.0E-04			
330	FOXC2	ts. reg.	2.4	1.95	2.8E-05	2.1	2.18	1.1E-06			
331	HIF1A	ts. reg.		1.94	4.6E-11	1.9	4.61	3.0E-25		2.67	4.1E-06
332	MYC	ts. reg.	3.0	1.86	7.9E-08	3.3	2.22	1.0E-13		1.94	1.0E-01
333	CDKN2A	ts. reg.		1.71	3.3E-02		2.46	3.9E-05			
334	ETS1	ts. reg.		1.56	2.2E-05		2.96	9.7E-11		0.85	2.3E-03
335	SMAD4	ts. reg.		1.52	1.4E-05		2.14	4.2E-09		1.09	2.1E-04
336	SMARCA4	ts. reg.		1.22	2.6E-04		2.03	5.4E-07			
337	EPAS1	ts. reg.		1.14	2.8E-06		3.37	4.1E-13		1.64	6.3E-03
338	HAND2	ts. reg.		1.08	8.1E-04		2.19	1.8E-04			
339	TAF4	ts. reg.		-0.87	8.5E-04		-2.14	2.3E-07			
340	CITED2	ts. reg.		-1.09	3.0E-02		-2.20	5.9E-06			4.0E-04
341	HLX	ts. reg.		-1.39	4.0E-05		-2.05	3.9E-04			
342	WDR77	ts. reg.		-1.84	1.1E-03		-2.28	1.9E-04			

Continued on next page

Table A.23.: WG-DASL Assay: Predicted Upstream Regulators (IPA). *Continued from previous page.*

	Upstream Regulator	Molecule Type	**LEL-M 5 h vs. TM 0 h** logFC	z-score	P.Val Overlap	**LEL-M 17 h vs. TM 0 h** logFC	z-score	P.Val Overlap	**LEL-M 17 h vs. 5 h** logFC	z-score	P.Val Overlap
343	ZBTB7A	ts. reg.		-2.06	8.1E-05		-1.58	8.1E-05			
344	CLOCK	ts. reg.		-2.09	2.6E-06		-1.88	7.5E-04			
345	HNF1B	ts. reg.	-3.7	-2.11	1.5E-04	-3.6	-2.11	4.1E-04			
346	PPARGC1A	ts. reg.		-2.11	5.6E-02	-2.5	-2.14	1.9E-06		0.81	3.0E-03
347	HOXC8	ts. reg.		-2.14	1.3E-03		-1.56	7.4E-05			
348	PCGF2	ts. reg.		-2.18	4.1E-04			3.3E-02			
349	LHX1	ts. reg.		-2.19	5.9E-04		-1.73	4.5E-04			
350	NEUROG1	ts. reg.		-2.36	7.0E-05		-2.44	1.1E-07			
351	DACH1	ts. reg.		-2.51	4.9E-05		-1.99	6.6E-05			
352	MEOX2	ts. reg.		-2.59	9.4E-05		-3.26	5.5E-09			
353	KLF2	ts. reg.		-2.65	5.6E-07		-3.69	1.7E-11			4.8E-02
354	Esrra	ts. reg.		-2.69	3.8E-04		-3.72	3.1E-06			
355	SMAD7	ts. reg.		-2.73	8.4E-04	1.3	-2.34	8.1E-07			
356	ZFP36	ts. reg.	2.4	-3.10	2.0E-07	1.9	-3.22	4.5E-08			
357	GFI1	ts. reg.		-3.36	9.6E-09		-3.65	7.2E-09			
358	HNF4A	ts. reg.	-3.0	-4.19	9.0E-04	-4.6	-4.01	5.9E-08			
359	HNF1A	ts. reg.	-2.2	-5.20	2.2E-12	-2.8	-4.33	1.2E-16			
360	ACTN4	ts. reg.			1.8E-02		2.32	3.9E-04			4.7E-02